

Bente Højlund Hyldegaard

Electrochemical zone for degradation of chlorinated ethenes in aquifers



ELECTROCHEMICAL ZONE FOR DEGRADATION OF CHLORINATED
ETHENES IN AQUIFERS

Bente Højlund Hyldegaard

PhD thesis
Industrial PhD project

COWI A/S

DTU

Kongens Lyngby
July 2019

SUPERVISORS

Lisbeth M. Ottosen, professor, Technical University of Denmark, Department of Civil Engineering, Denmark

Lars Nissen, business development manager, COWI A/S, Department of Waste & Contaminated Sites, Denmark

Rasmus Jakobsen, senior researcher, Geological Survey of Denmark and Greenland, Department of Geochemistry, Denmark

Niels D. Overheu, special consultant, Capital Region of Denmark, Center for Regional Development, Denmark

David B. Gent, research environmental engineer, US Army, Engineer Research and Development Centers Environmental Laboratory, USA

ASSESSMENT COMMITTEE

Massimo Rolle, associate professor, Technical University of Denmark, Department of Environmental Engineering, Denmark

John Flyvbjerg, chief consultant, Capital Region of Denmark, Center for Regional Development, Denmark

Célia Dias-Ferreira, professor auxiliar (associate professor), University Aberta, Department of Science and Technology, Portugal

Copyright © Bente Højlund Hyldegaard, 2019

Printed by DTU-Tryk

DTU, Department of Civil Engineering

PREFACE

The present thesis compiles the work of my industrial PhD research project conducted at COWI A/S, Department of Waste & Contaminated Sites, and DTU, Department of Civil Engineering, Section of Materials and Durability, in collaboration with the Capital Region of Denmark, Center for Regional Development, and US Army Corps of Engineers, Engineer Research and Development Centers Environmental Laboratory. The main supervisors were Lisbeth M. Ottosen (DTU), Lone T. Karlby (COWI, 2016), Eline B. Weeth (COWI, 2017-2019), Lars Nissen (COWI, 2019) and Rasmus Jakobsen (COWI, GEUS). Co-supervisors included Niels D. Overheu (Capital Region of Denmark) and David B. Gent (US Army). An expert reference group was associated with the project, consisting of Nancy Hamburger (the Capital Region of Denmark), Neal Durant (Geosyntec Consultants), Mogens Jakobsen (DTU Nanotech), Basil Uthuppu (DTU Nanotech) and Jan Preuthun (Kjul & Co.).

This industrial PhD project was approved by the Innovation Fund Denmark and funded by Innovation Fund Denmark (grant number 5016-00165B), COWIfonden (grant number C-131.01), the Capital Region of Denmark (grant number 14002102), COWI A/S, Department of Waste & Contaminated Sites, DTU, Department of Civil Engineering, and the Danish Ministry of Higher Education and Science (grant number 7079-00012B).

The experimental work was mainly carried out at DTU Civil Engineering and at the Innovation Garage owned by the Capital Region of Denmark. Project management and writing tasks were mainly carried out in COWI. An external research stay was completed at Northeastern University, Boston, USA, in March-July 2018, as part of the research group of Professor Akram Alshawabkeh.

The thesis is written to an audience with some knowledge of the field of contaminated sites and electrochemistry. Focus is on applied electrochemistry and undivided flow-through electrochemical systems operated at constant current for the removal of chlorinated ethenes.



Kongens Lyngby, July 2019

ACKNOWLEDGEMENTS

First, I would like to express my thankfulness to COWI A/S and DTU for giving me the opportunity to become immersed in this interesting industrial PhD research project. It has given me all the challenges, creativity outlets, problem solving insights, learning, networking and acquisition of knowledge that I was seeking. I owe the deepest respect and gratitude to my current and previous supervisors Lisbeth M. Ottosen, Lone T. Karlby, Eline B. Weeth, Lars Nissen, Rasmus Jakobsen and co-supervisors Niels D. Overheu and David B. Gent for highly professional supervision, valuable and constructive feedback, encouragement, for having faith in me and for continuous support throughout the various stages of the project. A special thanks to Lisbeth M. Ottosen for an overwhelming nomination to one of the Danish Ministry of Higher Education and Science's Elite Research Travel Grants; it is beyond words.

I would like to thank my colleagues at COWI and DTU Civil Engineering for exchange of experiences, assistance and endless cheering. The lab technicians at DTU Civil Engineering, Ebba C. Schnell, Sabrina J. Hvid and Malene E. Møller, have provided priceless support with analysis and tending of experiments. Also, a thank to Professor Akram Alshawabkeh for welcoming and hosting me in his recognized research group, where Ljiljana Rajic provided insightful supervision during my external research stay at Northeastern University. The laboratory Eurofins, Denmark was very cooperative in adapting their analytical procedures to low volume samples, which was crucial to the level of documentation in this research. Thanks to Claus Rye Schierbeck for creating very elegant illustrations of the experimental set-ups. Per Møller, DTU Mechanical Engineering and Daniel Minzari, IPU contributed with valuable inputs related to material properties.

This project would not have been realized without the financial support of Innovation Fund Denmark, COWIfonden and the Capital Region of Denmark, for what I am much obliged. Also, cast iron and sandy sediment was kindly donated by Morten S. Christensen at Velamp A/S and Hans P. Joensen at Nymølle Stenindustrier A/S, respectively.

Finally, I owe my mom Pia, dad Torben, brother Morten, and husband Søren everything for their limitless and indispensable support, tolerance, love and contagious enthusiasm. Also, I am grateful for the support provided by my family-in-law and my cousin Anders for e.g. collection of sandy sediment. My friends have been patient, understanding and supportive beyond measure. This project had not made progress if not for the infinite support and competent scientific contributions offered by my husband Søren, who have spent many weekends, evenings and nights in the lab to provide assistance and company, and to take care of me. For that, I am forever grateful.

ABSTRACT

The potential of applying electrochemistry as a means for remediation of harmful chlorinated ethene plumes in groundwater aquifers was investigated. The aim of this PhD project was to mature the method towards field-application for protection of the drinking water resource. To simulate the electrochemical concept of a field-application, two undivided flow-through column reactors and one box reactor were designed. These reactors were used for assessment of the influence of various reactor design parameters and field-realistic parameters on the tetrachloroethylene (PCE) removal performance, and induced hydrogeochemical changes. The reactor design parameters assessed included a variety of electrode materials, catalyst loadings, electrode shapes, electrode configurations, constant current intensities, reactor orientations, reactor dimensions, porous matrices and flow rates. The assessment of influence of the reactor design and induced changes in hydrogeochemistry revealed:

- In complex field-realistic systems using electrode rods, the main transformation pathway responsible for removal of PCE was indirect reduction and indirect oxidation via electrochemically generated reactants. This is promising considering field-application where installation of a transect of electrode meshes is not viable.
- Aged contamination of PCE, with degradation products in groundwater, was treated concurrently in complex field-realistic systems when establishing a redox sequence of reduction followed by oxidation, which was also the sequence affecting the surrounding hydrogeochemistry the least.
- At lab scale, significant release of electrolytically generated gases from the electrode surfaces at high current intensity, short electrode spacing, low flow rate and presence of porous matrices obscured the actual performance variation related to these parameters. This challenge would most likely not be present in *in situ* electrochemical application.
- Advantages of using iron anodes were outperformed by significant corrosion and clogging of porous matrices when applied in field-realistic systems.
- Naturally present chloride and organic matter was oxidized in a multistep reaction, forming trichloromethane, which over time decreased in concentration.

The field-parameters incorporated into the assessment of chlorinated ethene removal performance in field-realistic systems were a realistic flow rate, contaminated groundwater, sandy sediment and groundwater aquifer temperatures. Major findings are:

- Electrochemical removal of an aged contamination of PCE was highest when applied in field-realistic systems, despite of competition by complex chemistry, contrary to simplified systems of synthetic groundwater and an inert porous matrix of glass beads, which represent *state of the art* for this PhD project.
- PCE concentrations reached from at starting concentration of 50 µg/l were 7.8 ± 2.3 µg/l and the lower chlorinated ethenes were completely removed with no intermediates accumulating and insignificant volatilization.

These findings contribute with knowledge on electrochemical removal of PCE and the performance of electrochemical remediation in complex field-realistic aquifer settings. The low PCE concentrations reached after treatment and the complete removal of intermediates are encouraging in relation to upscaling the method.

RESUME

Potentialet i at anvende elektrokemi til at begrænse spredningen af forureningsfaner med de sundhedsskadelige klorerede opløsningsmidler, i grundvandsmagasiner, er blevet undersøgt. Det overordnede formål for ph.d.-projektet var at modne metoden til feltimplementering for beskyttelse af drikkevandsressourcen. Til udvikling af det elektrokemiske koncept, blev der udviklet to kolonnereaktorer samt en boksreaktor. Disse reaktorer blev brugt som led i at øge kendskabet til, hvilke parametre, der har størst betydning for den elektrokemiske nedbrydning, forårsagede ændringer i hydrogeokemi, og til at udvikle metoden til fjernelse af perklorethen (PCE) fra naturlige grundvandsressourcer. Af reaktordesigns blev forskellige elektrodematerialer, mængder af katalysatorer, elektrodeformer, elektrodekonfigurationer, intensiteter af konstant strømstyrke, orienteringer af reaktorer, reaktordimensioner, porøse materialer og flow rater undersøgt. Studiet af betydningen af reaktordesign og forårsagede ændringer i naturlig hydrogeokemi viste:

- I komplekse, realistiske rammer ved brug af stangformede elektroder, var de dominerende nedbrydningsmekanismer bag fjernelsen af PCE indirekte reduktion og indirekte oxidation. Med henblik på feltimplementering, er disse resultater lovende, da installation af et tværgående elektrodenet er en uholdbar fremgangsmåde.
- PCE og nedbrydningsprodukter i forurennet grundvand blev sideløbende fjernet i forsøg simulerende komplekse og realistiske rammer med en redoxsekvens bestående af reduktion fulgt af oxidation. Denne sekvens påvirkede også den omgivende hydrogeokemi mindst.
- På laboratorieskala påvirkede frigivelsen af elektrolytisk dannede gasser fra elektrodeoverfladerne markant ydeevnen ved høj strømstyrke, kort elektrodeafstand, lav flow rate og ved tilstedeværelse af porøst materiale. Denne udfordring antages ikke at opstå ved *in situ* rensning af grundvand med metoden.
- Fordelene ved at anvende jernanoder blev overgået af betydelig korrosion og tilstopning af porøse materialer ved anvendelse i realistiske rammer.
- Naturligt tilstedeværende kloridioner og organisk materiale blev trinvist oxideret med dannelse af triklormetan, som over tid blev nedbragt i koncentration.

De realistiske rammer inkluderet i undersøgelsen af fjernelse af klorerede opløsningsmidler var en realistisk flow rate, oppumpet forurennet grundvand, sandet sediment og temperaturer tilsvarende grundvandsmagasiner. Overordnede resultater er:

- Elektrokemisk fjernelse af en PCE-forurening med nedbrydningsprodukter var højest i realistiske rammer, trods afledte sideløbende ændringer i tilstedeværende kemi, i modsætning til simple rammer bestående af syntetisk grundvand og en inert porøs matrix af glaskugler, hvilket udgør *state of the art* for dette ph.d.-projekt.
- PCE med en startkoncentration på 50 µg/l blev fjernet ned til 7.8 ± 2.3 µg/l og de lavere klorerede ethener blev fjernet fuldstændig uden dannelse af klorerede nedbrydningsprodukter og med ubetydelig afdampning.

Disse resultater bidrager med viden om elektrokemisk fjernelse af PCE samt om ydeevnen for elektrokemisk oprensning af PCE i de komplekse rammer for grundvandsmagasiner. Den lave PCE-koncentration, som blev opnået uden dannelse af giftige mellemprodukter, er lovende i forhold til videreudvikling af metoden i fuld skala.

TABLE OF CONTENTS

Preface	iii
Acknowledgements	iv
Abstract	v
Resume	vii
List of abbreviations and symbols.....	xi
Structure of thesis.....	xii
1 Introduction	1
1.1 Chlorinated ethene contaminations	1
1.2 Electrochemical remediation	3
1.2.1 <i>Electrode materials</i>	6
1.2.2 <i>Electrochemically induced degradation pathways</i>	9
1.2.3 <i>Electrochemistry in complex settings</i>	11
2 Knowledge gaps	14
3 Research methodology	15
3.1 Framing contaminated sites – A case study.....	17
3.2 Experimental design requirements	18
3.3 The electrochemical reactors developed.....	20
4 Significance of electrochemical reactor design on performance	22
4.1 Electrochemical design parameters	22
4.1.1 <i>Electrode material</i>	22
4.1.2 <i>Catalytic coating</i>	24
4.1.3 <i>Electrode shape</i>	25
4.1.4 <i>Electrode configuration</i>	25
4.1.5 <i>Electrode spacing</i>	27
4.1.6 <i>Current intensity</i>	27
4.2 Other design parameters	29
4.2.1 <i>Reactor orientation</i>	29
4.2.2 <i>Reactor dimension</i>	30
4.2.3 <i>Porous matrix</i>	31
4.2.4 <i>Flow rate</i>	33
5 Significance of field-parameters on electrochemical performance	35
5.1 Field-realistic flow rate.....	36
5.2 Field-extracted groundwater with an aged contamination.....	36
5.3 Sandy aquifer geology	37
5.4 Groundwater aquifer temperature.....	37

5.5	Electrochemical degradation pathways in field-realistic systems	38
5.6	Electrochemically induced hydrogeochemical changes	41
5.7	Overview of electrochemical performance in field-realistic systems.....	44
6	Perspectives of electrochemical treatment of chlorinated ethene plumes	46
7	Main conclusions	50
	References	52
	Own publications (Appendix I-V).....	61
	Appendix I.....	63
	Appendix II	75
	Appendix III.....	97
	Appendix IV	113
	Appendix V	125
	Supporting note I.....	141
	Supporting note II	155
	Awards.....	165
	Elite research travel grant 2018	166
	Battelle palm pitch 2018.....	167
	Presenter award, Electrochemical Science & Technology Conference 2017.....	168
	Conference contributions.....	169
	EREM 2017 (Platform presentation).....	171
	DEF 2017 (platform presentation).....	173
	Battelle 2018 (Poster and pitch presentation).....	175
	RemTEC 2019 (Poster and pitch presentation)	177
	AquaConSoil 2019 (Platform presentation)	179

LIST OF ABBREVIATIONS AND SYMBOLS

A	Anode (+)
Al	Aluminum
BDD	Boron-doped diamond
BPE	Bipolar electrode
C	Carbon
C	Cathode (-)
cis-DCE	cis-1,2-dichloroethylene
Cl _{2(g)}	Chlorine gas
Cu	Copper
DNAPL	Dense non-aqueous phase liquid
E°	Standard electrode potential
ERD	Enhanced reductive dechlorination
Fe	Iron
H ₂	Hydrogen gas
H ₂ O ₂	Hydrogen peroxide
HCO ₃ ⁻	Bicarbonate
ISCO	<i>In situ</i> chemical oxidation
MMO	Mixed metal oxide
Ni	Nickel
O ₂	Oxygen
O ₃	Ozone
•OH	Hydroxyl radical
P&T	Pump-and-treat
PCE	Tetrachloroethylene
Pd	Palladium
Pd/Fe	Palladium coated iron electrode
PRB	Permeable reactive barrier
Pt	Platinum
SHE	Standard hydrogen electrode
SS	Stainless steel
TCE	Trichloroethylene
TCM	Trichloromethane
trans-DCE	trans-1,2-dichloroethylene
VC	Vinyl chloride
VOC	Volatile organic carbon
1,1-DCE	1,1-dichloroethylene
→	Groundwater flow direction and reactor orientation

STRUCTURE OF THESIS

The thesis is organized into two parts: the first part sets the frame of the topic and compiles the research conducted. The second part contains appended material; five journal papers, two supporting notes, three awards and five conference contributions. The first part is structured into seven chapters:

1 Introduction: The framework of the project related to drinking water, harmful contamination and challenged remediation technologies is outlined. The current knowledge on electrochemical remediation, a possible alternative method, is presented with a focus on undivided flow-through applications operated at constant current for the removal of chlorinated ethenes.

2 Knowledge gaps: Reviewing the literature pointed out some knowledge gaps within electrochemical removal of chlorinated ethenes. The key knowledge gaps in focus in the present study are described.

3 Research methodology: An overview of the research conducted is given and the correlation between appended journal papers and key knowledge gaps is presented. Common characteristics of contaminated groundwater aquifer sites and the related requirements for the experimental set-ups are framed. Finally, the developed column and box reactors are described. Details are provided in appended papers and supporting notes.

4 Significance of electrochemical reactor design on performance: The electrochemical removal performance of chlorinated ethenes is influenced by several reactor design parameters. The identified significances of such were assessed and the results are presented.

5 Significance of field-parameters on electrochemical performance: The influence of various field-realistic parameters on the electrochemically induced removal of chlorinated ethenes is discussed. Also, the effect of electrochemistry on the natural hydrogeochemistry is evaluated.

6 Perspectives of electrochemical treatment of chlorinated ethene plumes: The determination of the potential of applied electrochemical treatment of chlorinated ethene plumes in aquifers was supported by the findings of this PhD project. Advantages and current challenges are listed, and suggestions to further activities are given.

7 Main conclusions: The main conclusions from the compiled findings of this industrial PhD project are drawn up and marks the end of the first part of the thesis.

1 INTRODUCTION

Water is essential to life and with a growing population, the need for drinking water is increasing significantly. With the increase in population, materialism is intensified, wherefore the use of anthropogenic chemicals in production lines also increases. Spills, leakage, improper disposal etc. unfortunately seem to go hand in hand with handling of chemicals. History has shown, that many man-made chemicals have unintended adverse impacts on human health and/or the environment, e.g. pesticides [1,2], chlorinated ethenes [3,4], per- and polyfluoroalkyl substances [5,6]. Thus, harmful chemicals have been and probably continuously will be introduced to the environment, with contamination of groundwater used for drinking water being a prevailing risk. Consequently, the cases of life-threatening diseases may increase. At best, seen from a health perspective, the contaminated drinking water extraction areas will be closed, to protect the consumers. I.e., the combination of increasing population and contamination puts pressure on water as a scarce resource [7]. Hence, remediation of groundwater is inevitable, also for ethical considerations. In high-permeable aquifers, often located deep in the ground, contaminant plumes can be widely distributed, which challenge the remediation [8]. Therefore, optimization through research and development of existing and new remediation technologies is important.

1.1 CHLORINATED ETHENE CONTAMINATIONS

Chlorinated ethenes are examples of harmful anthropogenic chemicals that have entered the environment [9] and ultimately reach the consumers via e.g. drinking water and/or indoor air contamination. Chlorinated ethenes, commonly known as chlorinated solvents, include tetrachloroethylene (PCE) and trichloroethylene (TCE). These specific compounds were used in large quantity in the 1960'ies and 1970'ies in dry-cleaning and metal processing [10,11], but are still in use in large quantities due to growing markets in e.g. Asia and a lack of regulation [12]. PCE and TCE can be biodegraded under certain environmental conditions, by specific microbial cultures [13–16]. However, biodegradation is slow, and accumulation of the chlorinated intermediates *cis*-1,2-dichloroethylene (*cis*-DCE), *trans*-1,2-dichloroethylene (*trans*-DCE), 1,1-dichloroethylene (1,1-DCE) and vinyl chloride (VC) is often observed [17–19]. The chlorinated intermediates are more harmful than their parent components [20]. Chlorinated ethenes are classified as health and environmental hazards with exclamation and corrosion marks [20]. Severe health hazards include carcinogenicity, reproductive toxicity and organ toxicity [3,4,20].

Consequently, regulatory defined maximum contaminant levels of chlorinated ethenes in drinking water are low [21,22]. The chlorinated ethenes are dense non-aqueous phase liquids (DNAPLs), i.e. denser than water. Other inherent properties include high volatilities, low sorption, relatively low viscosities, low interfacial tension between DNAPL and water, and low absolute solubilities (high relative to the regulatory maximum contaminant levels) [11]. This combination of properties implies that within the environmental sphere, chlorinated ethene DNAPLs can penetrate deep into soil matrices, even into small fractures – also below water tables, with exceedance of the regulatory maximum contaminant levels of drinking water and possibly contamination of indoor air of buildings (Figure 1) [11,23,24].

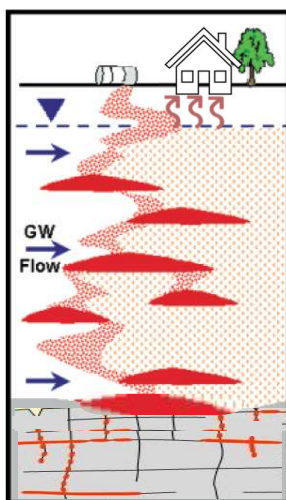


Figure 1. Conceptual model of the fate of DNAPL contamination in the subsurface.

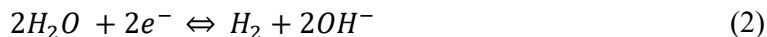
Figure modified from Parker et al. [23] and Kueper et al. [24].

Technologies applied for remediation of chlorinated ethene plumes in high-permeable aquifers include pump-and-treat (P&T) [25,26], enhanced reductive dechlorination (ERD) [11,26], *in situ* chemical oxidation (ISCO) [27,28], permeable reactive barriers (PRB) [29,30] and air-sparging [31,32]. A common challenge for ISCO, PRB and ERD is to achieve an adequate delivery of the degrading substance, e.g. permanganate, ZVI or dechlorinating microbial culture, into the contaminated zone [28,33,34]. Controlling the longevity of the reactants and directing the reactants towards transformation of chlorinated ethenes rather than naturally present substances are other challenges [28,35,36]. Air-sparging and P&T using activated carbon are non-destructive methods aiming at transferring the dissolved chlorinated ethenes to the vapor phase and solid phase, respectively [31]. I.e., a secondary waste stream that needs to be handled *ex situ* is generated. Further, P&T using activated carbon filters e.g. has a limited efficiency towards the

chlorinated intermediates [31,37]. Due to differences in complexity of contaminated sites, remediation activities are tailored to each site resulting in a graduation of technology applicability from one site to another [38]. However, as outlined, the current remediation technologies face challenges.

1.2 ELECTROCHEMICAL REMEDIATION

A potentially alternative method for *in situ* remediation of chlorinated ethene plumes, i.e. reduction of mass flux, is electrochemistry, where an electric current is applied across a saturated soil matrix. Electric currents have been used to enhance transport mechanisms for extraction of e.g. heavy metals [39,40] and delivery of reactants into primarily low-permeable soil matrices to stimulate degradation [41–43] by utilization of electrokinetic mechanisms [44]. Combinations of electrokinetics with PRB [45,46], ISCO [47] and ERD [43,48] to overcome the challenges of these technologies have also been studied. Electrochemical methods differ from the electrokinetic methods in that it rather than taking advantage of the transport processes, takes advantage of the electrode processes, resulting in establishment of different redox zones due to dissociation of water, known as water electrolysis [40]. When an electric current is applied to a set of electrodes in saturated medium, the electrodes polarize into a cathode and an anode. At the anode, which is positively polarized, water electrolysis creates an oxidizing and acidic environment (Eq. 1), while reducing and alkaline conditions establish around the negatively polarized cathode (Eq. 2) [44].



Water electrolysis (Eq. 1-2) is a fast process, which can result in pH below 2 and above 12 at the anode and cathode, respectively [44]. Reduction potentials of -600 mV vs. standard hydrogen electrode (SHE) can be achieved near the cathode, which is suitable for reduction of chlorinated ethenes [49,50].

Advantages of electrochemical remediation include a) the combination of reduction and oxidation of contaminants, b) ability of engineering the redox processes for enhancement of desired processes and thereby adaption towards site-specific characteristics, e.g. contaminant composition, c) the option to install several sequences of electrodes to cover the extent of the contamination [40,42,51]. A conceptual design example of electrochemical treatment of chlorinated ethene plumes is shown in Figure 2.

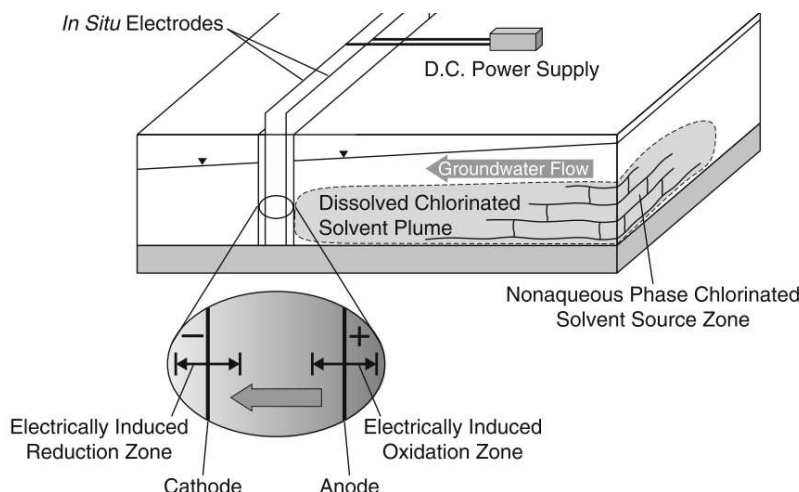


Figure 2. One example of a conceptual design applied for electrochemical remediation of chlorinated ethenes with installation of an electrode barrier intersecting the contaminant plume [52].

One field-application of electrochemical remediation of chlorinated ethene plumes has been reported; a pilot test in which an electrode mesh was installed for flow-through of the contaminant plume, demonstrating a 95% removal of TCE with application of constant voltage [51,52]. Constructing an electrode mesh across an entire contaminant plume is costly, complicated and limited to shallow aquifers [51]. More work has been done in laboratory studies to investigate the electrochemically induced processes in controlled systems. A summary of the major findings in published laboratory studies, which have focused on electrochemical removal of aqueous chlorinated ethenes in simulated groundwater systems, is shown in Table 1. In the summary are studies applying a constant current to solid electrodes in undivided flow-through reactors, as these design parameters are most suited and representative for field-scale applications.

Table 1. Summary of findings in studies on electrochemical removal of aqueous chlorinated ethenes in undivided flow-through reactors with solid electrodes operated at constant current. Updated from [53].

Experimental design ^a	Current [mA]	Findings	Ref.
Fluid: Synthetic Geology: Limestone gravel Configuration: A→C→A Anode: Cast Fe, MMO Cathode: Cu Catalyst: -	15-120	Cast iron anodes enhanced TCE removal. The three-electrode configuration further enhanced the removal. Lower flow rate enhanced removal, exceeding 82.2 %. Correlation between current density and influent concentration with upper threshold for current on removal.	[54]
Fluid: Synthetic Geology: "Glass beads" Configuration: C→C→A, A→C, C→A Anode: MMO, cast Fe Cathode: MMO, cast Fe Catalyst: Pd/C, Pd/Al pellets	30-90	Increased electrode spacing and flow rate reduced the removal efficiency. Higher surface area (foam) improved conversion of TCE. Removal rates at 60 mA exceeded those at 30 and 90 mA. C→C→A and Pd coating significantly increased removal rates and efficiencies. >99 % TCE removal was achieved.	[55]

Table 1 continued...

Experimental design ^a	Current [mA]	Findings	Ref.
Fluid: Synthetic Geology: "Glass beads" Configuration: A→C→C Anode: MMO Cathode: MMO Catalyst: Pd/Al ₂ O ₃ pellets	60	Presence of Fe(II) significantly enhanced TCE removal through Fenton reaction. Addition of sulfite improved TCE removal due to transformation into SO ₄ ²⁻ , reaching a removal efficiency of 71 %. Fouling of Pd by sulfide was assessed and found insignificant.	[56]
Fluid: Synthetic Geology: Limestone gravel, "glass beads" Configuration: C→A Anode: MMO Cathode: Fe Catalyst: Pd	60	Presence of humic substance (HS) reduced TCE removal in a linear relationship. HS influenced the electrochemical processes of the cathode. TCE degradation in limestone without HS reached 82.9 %, which was superior to that in glass beads.	[57]
Fluid: Synthetic Geology: Limestone block Configuration: Anode: Cast Fe Cathode: Cu Catalyst: -	90	Humic acids decreased TCE removal from 90% to 80 %, dichromate to 53-70 %, selenate to 76-89 %, nitrate to 81-91 %. A mixture of the latter three contaminants reduced TCE removal to around 40 %. The limestone block enhanced removal of TCE when compared to an acrylic column.	[58]
Fluid: Synthetic Geology: - Configuration: A→C, C→A Anode: MMO Cathode: MMO Catalyst: Pd/Al ₂ O ₃ pellets	30-120	C→A configuration was superior to A→C with TCE removal of 54.5 % and 34.8 %, respectively. Polarity reversal enhanced the removal to 69.3 %. Optimal design of polarity reversal for TCE removal was 15 cycles h ⁻¹ at 60 mA resulting in a power consumption of 13 W cm ⁻² .	[59]
Fluid: Synthetic Geology: - Configuration: C→A Anode: MMO Cathode: Fe, Ni, Cu, C, Al Catalyst: Pd	30-90	Highest TCE removal was obtained with foam cathodes of Ni > C > Cu > Fe ~ Al. 60 mA was most efficient. Fe foam increased removal from 43.5% to 99.8% when Pd coated, with an upper threshold for removal vs. Pd load. Coating changed cathode material performance to Fe > Cu > C > Al > Ni. Nitrate inhibited the removal.	[60]
Fluid: Synthetic Geology: - Configuration: C→A Anode: MMO Cathode: 304 SS, 316SS, 430 SS, Ni/Fe, Ni Catalyst: -	60	The amount of Ni embedded in the SS influenced the TCE removal: 430 SS < 304 SS < 316SS of 37.5%, 52.6% and 61.7%, respectively. Highest removal by pure Ni foam cathode of 68.4%.	[61]
Fluid: Synthetic Geology: - Configuration: C→A Anode: C Cathode: C Catalyst: -	60-120	Monopolar mode resulted in TCE removal of 29 %. Introducing two bipolar electrodes increased removal to 66 % due to enhanced peroxide formation. In bipolar mode, a current of 120 mA enhanced the removal, while highest current efficiency was obtained for 60 mA.	[62]
Fluid: Synthetic Geology: - Configuration: C→A Anode: BDD Cathode: BDD Catalyst: -	2-20 mA/cm ²	TCE removal > 85% by direct and indirect oxidation via OH [•] . Cl mass balance was accounted for by TCE, Cl ⁻ and ClO ₃ ⁻ . No chlorinated intermediates accumulated. TCE half life was < 3 min.	[63]

^a A: Anode. C: Cathode. →: Flow direction. MMO: Mixed metal oxide coating on titanium. SS: Stainless steel. BDD: Boron-doped diamond.

From the studies presented in Table 1, it is seen that the focus of the investigations has been on the influence of electrode composition, electrode configuration, current intensity, contaminant concentration and flow rate on the removal of TCE. High removals of >99% were demonstrated at currents of 60 mA when using palladium (Pd) coated iron (Fe) foam cathodes in a sequence of cathode followed by anode. The promising results are worth to proceed with for further development of the electrochemical method.

1.2.1 ELECTRODE MATERIALS

The use of various electrode materials for electrochemical remediation of chlorinated ethenes in flow-through reactors, outlined in Table 1, has demonstrated electrode material specific properties. The reported advantages and disadvantages of materials used as anodes, cathodes and catalysts are shown in Table 2, Table 3 and Table 4, respectively. The lists are expanded with some findings in other studies using the electrode materials reported in Table 1, e.g. in studies investigating electrochemical removal of chlorinated ethenes in static or circulated reactors.

Table 2. Reported advantages and disadvantages of anode materials used for electrochemical removal of chlorinated ethenes in undivided flow-through reactors operated at constant current.

Anode material	Advantages	Disadvantages	Ref.
Cast iron, Fe	<ul style="list-style-type: none"> • Ferrous iron is released rather than O₂ (corrosion); low VOC^a stripping • Maintains a reducing environment suitable for fast reductive dechlorination • Easily acquired and in various purities and costs 	<ul style="list-style-type: none"> • Formation of Fe complexes, i.e. possibly clogging and electrode coverage • Elevated pH downgradient the electrochemical zone due to low H⁺ formation 	[49,55, 64] [49,54, 64]
Mixed metal oxide, MMO	<ul style="list-style-type: none"> • Dimensionally stable, i.e. retains its structure; can be reused • Maintains the pH and oxidation-reduction potential of the water 	<ul style="list-style-type: none"> • Potential release of impurities embedded in the Fe • Low O₂ overpotential^b: generates oxidizing conditions, i.e. VOC stripping may increase • O₂ evolution competes with oxidation of the chlorinated ethenes 	[53,61] [49,55, 64] [54,55]
Graphite	<ul style="list-style-type: none"> • Slow decomposition of H₂O₂ generates •OH 	<ul style="list-style-type: none"> • Oxidizes chloride to chlorine gas 	[62]
Diamond (boron-doped), BDD	<ul style="list-style-type: none"> • Affinity to produce •OH 	<ul style="list-style-type: none"> • Removal of organics in competition with •OH transformation to O₂ 	[63,65]

^a VOC: Volatile organic carbon.

^b Overpotential: The difference between the theoretic and observed energy level required to drive a reaction.

Fe anodes are best suited for removal of chlorinated ethenes, reaching up to 99% TCE removal, due to release of ferrous ions instead of oxygen, which creates highly reducing conditions [49,54,64]. However, Fe complex formation may challenge the application of Fe anodes due to e.g. clogging of pores in porous matrices (Table 2).

Table 3. Reported advantages and disadvantages of cathode materials used for electrochemical removal of chlorinated ethenes in undivided flow-through reactors operated at constant current.

Cathode material	Advantages ^a	Disadvantages	Ref.
Iron, Fe	<ul style="list-style-type: none"> • Performs better than MMO for removal of chlorinated ethenes • Pd coated Fe is superior to coated Ni, Al, C, Cu 	<ul style="list-style-type: none"> • High H₂ overpotential; slower hydrodechlorination than noble metals 	[55]
Mixed metal oxide, MMO	<ul style="list-style-type: none"> • Low cost • Low cost 	<ul style="list-style-type: none"> • Interacts with H₂ on its surface, forming oxides, i.e. less H₂ for hydrodechlorination 	[60] [49,61] [49,55,64]
Carbon, C	<ul style="list-style-type: none"> • High surface area and porosity • Superior to Fe, Cu, Al in terms of chlorinated ethene removal • Low reactivity • Low cost 	<ul style="list-style-type: none"> • Fragile, i.e. not suitable in the field 	[55,60] [60] [55] [49]
Graphite	<ul style="list-style-type: none"> • Produces H₂O₂ and •OH • Cheap, safe material 	<ul style="list-style-type: none"> • Slow H₂ formation due to limited reactivity 	[62]
Copper, Cu	<ul style="list-style-type: none"> • Performs better than Fe and Al for chlorinated ethene removal • Low cost 	<ul style="list-style-type: none"> • Induces precipitation and electrode coverage • Higher H₂ evolution overpotential than noble metals; slower hydrodechlorination 	[49,64] [49,60,64]
Nickel, Ni	<ul style="list-style-type: none"> • Lower H₂ overpotential supports higher hydrodechlorination than C, Cu, Al, Fe 	<ul style="list-style-type: none"> • Accumulates H₂ bubbles on its surface 	[60]
Aluminum, Al	<ul style="list-style-type: none"> • Low cost 	<ul style="list-style-type: none"> • Corrodes with Al-complex formation • Weak bond strength with hydrogen reduces hydrodechlorination 	[60] [60]

^a Pd: Palladium. H₂O₂: Hydrogen peroxide. H₂: Hydrogen.

Nickel (Ni) has shown to be superior as cathode material for chlorinated ethene removal, with reported TCE removals of 68% [60,61]. It is the catalytic properties of Ni of lower hydrogen (H₂)

overpotential, which facilitate the enhanced removal [60]. This suggests use of catalysts on cathodes (Table 4).

Table 4. Reported advantages and disadvantages of using catalysts on cathodes for electrochemical removal of chlorinated ethenes in undivided flow-through electrochemical reactors operated at constant current.

Catalyst ^a	Advantages	Disadvantages	Ref.
Nobel metals, e.g. Ag, Pt	<ul style="list-style-type: none"> • Low H₂ overpotentials, i.e. fast reduction by hydrodechlorination 	<ul style="list-style-type: none"> • Costly 	[55,63]
Palladium, Pd	<ul style="list-style-type: none"> • Catalyzes formation of H₂O₂, i.e. oxidation of chlorinated ethenes • Improves hydro-dechlorination of Fe > Cu > C > Al > Ni and reaction rates • Higher surface area and sufficient bond strength with hydrogen 	<ul style="list-style-type: none"> • Low Pd load incapable of binding reactive hydrogen on its surface • High Pd load enhances proton reduction, i.e. competing with hydrodechlorination • Costly 	[55,60] [60] [55,64]

^a Ag: Silver. Pt: Platinum.

The catalyst Pd alters the efficiencies of cathode materials in terms of chlorinated ethene removal. With application of Pd, Fe cathodes have demonstrated TCE removals above 99% [60]. The removal efficiency obtainable is non-linearly correlated to the load of Pd on the cathode, i.e. an optimum load exist, which is suggested to be 0.76 mg Pd per cm² electrode surface area [60].

In laboratory studies, the electrode material significantly influences the chlorinated ethene removals. Thus, when designing an electrochemical remedy, (1) the electrode materials must be carefully selected. (2) another consideration for selecting cathode materials and use of catalyst is whether polarity reversal will be applied for e.g. removal of precipitates on the electrode surface, since Pd may be repelled and toxic metals, embedded in the electrode material, released during anodic polarization [66]. (3) related to electrode selection is the shape of the electrode material, e.g. rod, mesh, foam. Foams have a higher surface area, which enhances the contaminant removal [49,54,67,68]. (4) the sequence of the electrodes in flow-through reactors is determining the order of the redox zones and therefore is important. A sequence of reducing zones followed by oxidizing zones has demonstrated the highest TCE removal of up to 87% [54,55]. Extending the redox zones by applying three electrodes in sequence can increase the reaction kinetics and thereby improve the removals obtained [55]. (5) the current intensity applied also influences the removal. In literature, different optimal current intensities have been reported [54,55,62,64], which suggests

a correlation with one or several of the four other design parameters mentioned. Hence, the optimal current intensity appears to be system specific. In addition, the current intensity is found to be non-linearly correlated with the chlorinated ethene removal [55], wherefore intelligent design of the electrochemical zones is required.

1.2.2 ELECTROCHEMICALLY INDUCED DEGRADATION PATHWAYS

Chlorinated ethenes flowing through electrochemical zones are overall subject to reduction and oxidation. The dominating degradation pathways for chlorinated ethenes are shown in Figure 3. In detail, electrochemical reduction and oxidation transformation mechanisms are more complex and may include direct abiotic reduction, indirect abiotic reduction, direct abiotic oxidation and indirect abiotic oxidation [69]. Secondly, biotic reduction [50,70,71] and/or oxidation [72,73] may be stimulated if specific microbial degraders are present in the system.

Direct abiotic reduction is when the chlorinated ethenes, adsorbed to the cathode surface, receive electrons directly from the electrode [69,74–76]. Indirect abiotic reduction is when electrons are transferred via hydrogen formed from water electrolysis [69,74,75]. The specific contribution of direct and indirect abiotic reduction of chlorinated ethenes is dependent on e.g. the cathode material and current intensity applied [69]. As an example, the indirect abiotic reduction is enhanced when using metals with low H_2 overpotential, e.g. Ni or Pd (Table 3, Table 4) [69,77]. Moreover, abiotic reduction can be divided into β -elimination (Figure 3, dotted arrows from chlorinated ethenes to (chlorinated) acetylenes), hydrogenation (Figure 3, dotted arrows from (chlorinated) acetylenes to (chlorinated) ethenes), and hydrolysis (Figure 3, solid arrows and dotted arrows between (chlorinated) acetylenes) [30,78,79].

Direct abiotic oxidation is when electrons are directly transferred to the anode during transformation of the adsorbed chlorinated ethenes [69,80]. Indirect oxidation is oxidation via electrogenerated species, e.g. hydrogen peroxide (H_2O_2), hydroxyl radicals ($\bullet OH$), chlorine (Cl_2), ozone (O_3), persulfate (SO_5^{2-} , $S_2O_8^{2-}$) (Figure 3, dashed arrows) [56,69,81,82]. As for abiotic reduction, the abiotic oxidation mechanisms are dependent on the electrode material, e.g. low oxygen (O_2) overpotential and stability [69]. For example, Pd catalyzes formation of H_2O_2 (Table 4).

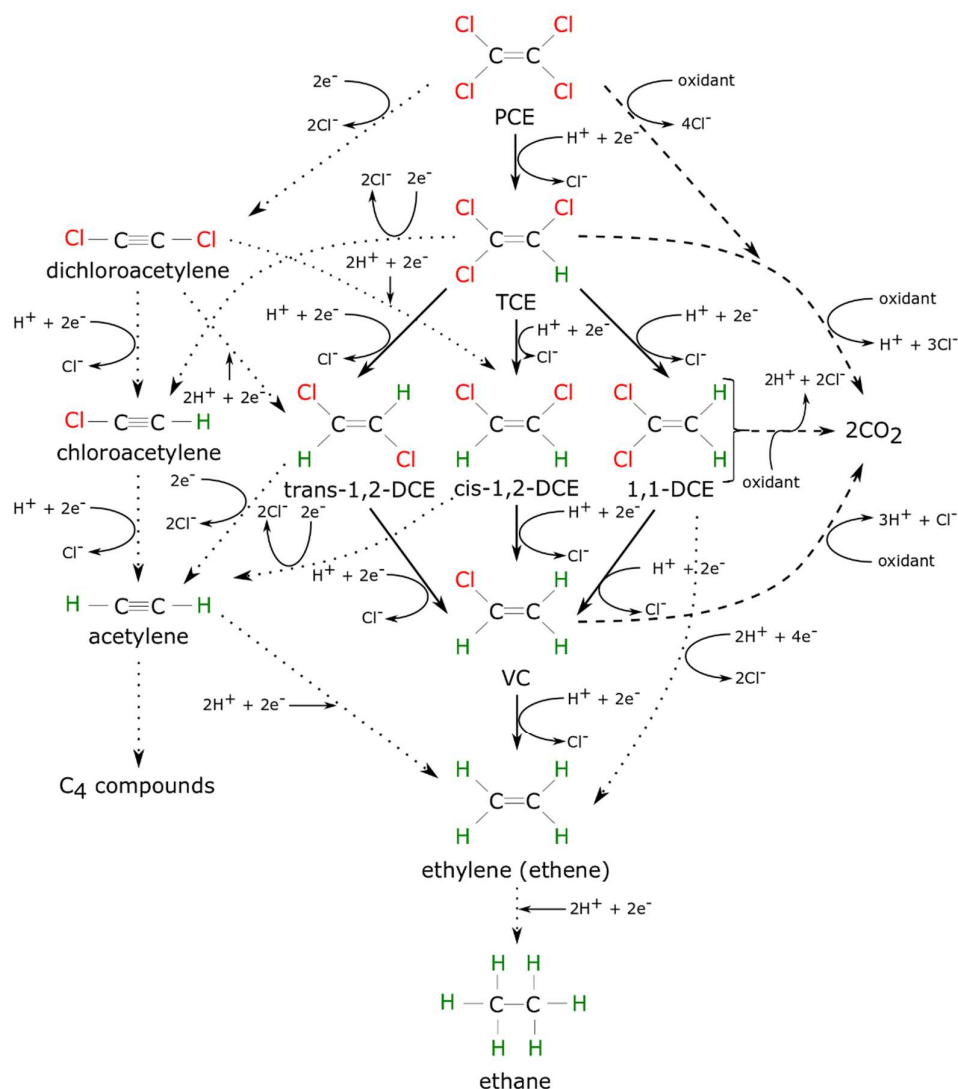


Figure 3. Possible in situ electrochemically induced degradation pathways for the chlorinated ethenes tetrachloroethylene (PCE), trichloroethylene (TCE), dichloroethylenes (DCEs) and vinyl chloride (VC); biotic reduction (solid arrows), abiotic reduction (dotted arrows) and/or abiotic oxidation (dashed arrows). Figure adapted from Ottosen *et al.* [83].

Standard electrode potentials (E°) are used as an indicator of the reaction tendency [44]. Some reported reaction potentials of the chlorinated ethenes are shown in Table 5. Reduction reactions of a given contaminant species can proceed in electrochemical zones with potentials lower than that of the contaminant species, e.g. PCE may be transformed via hydrogenolysis at potentials <0.592 V vs. SHE (Table 5). Opposite, oxidation can proceed in zones with potentials higher than that of the contaminant species, e.g. TCE may be abiotically oxidized at potentials >0.540 V vs. SHE (Table 5). The higher the reaction potential, the higher the energy yield and thereby

willingness to react [84,85]. As outlined in Table 5, the chlorinated ethenes have different tendencies of reduction and oxidation via the various abiotic and biotic pathways described. Since the reaction potentials reported differ significantly between studies, trends rather than specific figures should be extrapolated: 1) abiotic reduction of the chlorinated ethenes via β -elimination is more probable than via hydrogenolysis, 2) abiotic reduction of PCE and TCE is more likely than that of the chlorinated intermediates, 3) the chlorinated intermediates are more prone to oxidation than reduction, and 4) the chlorinated ethenes are more likely to be abiotically reduced than biotically reduced. These trends are promising for the use of electrochemical remediation of chlorinated ethenes in that both the β -elimination reduction and the oxidation pathways suggest that formation of chlorinated ethene intermediates is circumvented.

Table 5. Reduction and oxidation potentials for the chlorinated ethenes. The list is not comprehensive.

Chlorinated ethene	Abiotic reduction		Abiotic Oxidation [V vs. SHE]	Biotic reduction Hydrogenolysis [V vs. SHE]	Biotic Oxidation [V vs. SHE]
	Hydrogenolysis [V vs. SHE]	Elimination [V vs. SHE]			
PCE	0.592 [79]	0.631 [79] 0.795 [76]		0.43 [86]	
TCE	0.509-0.530 [79]	0.599 [79] 0.757 [76]	0.540 [80]	0.42 [86]	
cis-DCE	0.407 [79]	0.568 [79] 0.718 [76]		0.31 [86]	0.700 [86]
trans-DCE	0.428 [79]	0.589 [79] 0.718 [76]			0.700 [86]
1,1-DCE	0.423 [79] 0.655 [76]	Not applicable [79]			0.700 [86]
VC	0.481 [79]	Not applicable [79]		0.38 [86]	0.500 [86]

For a potential field-application of electrochemical treatment of chlorinated ethenes, the transformation mechanisms are increasingly complex compared to in controlled laboratory studies of synthetic groundwater and an inert porous matrix, as the transformation mechanisms are also influenced by the contaminant concentration, flow rate, pH, temperature, conductivity and competing reactions [55,69], which in the field furthermore are subject to variations.

1.2.3 ELECTROCHEMISTRY IN COMPLEX SETTINGS

At contaminated sites, the hydrogeochemistry is complex and the naturally present chemical species may compete with the contaminants for electrons within the electrochemical zone. Some

possible redox reactions related to the hydrogeochemistry are listed in Table 6 in reducing form. Some of these reactions will proceed as oxidation reactions in the electrochemical reactor.

Table 6. Standard potentials of possible reactions during electrochemical application in natural hydro-geochemical settings. Reactions are written as reductions despite some will be driven towards oxidation.

Species	Half reaction	E° [V]	Ref.
Al	$Al^{3+} + 3e^- \rightleftharpoons Al_{(s)}$	-1.68	[87]
	$Al(OH)_4^- + 3e^- \rightleftharpoons Al_{(s)} + 4OH^-$	-2.31	[87,88]
Ca	$Ca^{2+} + 2e^- \rightleftharpoons Ca_{(s)}$	-2.84	[87]
Cl	$Cl_{2(g)} + 2e^- \rightleftharpoons 2Cl^-$	1.36	[87,88]
	$HClO + H^+ + 2e^- \rightleftharpoons Cl^- + H_2O$	1.49	[87]
	$HClO_2 + 2H^+ + 2e^- \rightleftharpoons HClO + H_2O$	1.70	[87]
	$ClO_3^- + 3H^+ + 2e^- \rightleftharpoons HClO_2 + H_2O$	1.18	[87]
	$ClO_4^- + 2H^+ + 2e^- \rightleftharpoons ClO_3^- + H_2O$	1.20	[87]
	$CO_{2(g)} + 8H^+ + 8e^- \rightleftharpoons CH_{4(g)} + 2H_2O$	0.170	[88]
Fe	$Fe^{2+} + 2e^- \rightleftharpoons Fe_{(s)}$	-0.447	[87–89]
	$Fe^{3+} + 3e^- \rightleftharpoons Fe_{(s)}$	-0.037	[87]
	$Fe^{3+} + e^- \rightleftharpoons Fe^{2+}$	0.771	[87–89]
	$FeO_4^{2-} + 8H^+ + 3e^- \rightleftharpoons Fe^{3+} + 4H_2O$	2.20	[87]
	$Fe(OH)_3 + 3H^+ + e^- \rightleftharpoons Fe^{2+} + 3H_2O$	-0.980	[89]
H	$2H^+ + 2e^- \rightleftharpoons H_{2(g)}$	0.000	[87,88]
	$2H_2O + 2e^- \rightleftharpoons H_{2(g)} + 2OH^-$	-0.828	[87]
	$H_2O_2 + 2H^+ + 2e^- \rightleftharpoons 2H_2O$	1.76	[87,88]
	$K^+ + e^- \rightleftharpoons K_{(s)}$	-2.92	[87]
Mg	$Mg^{2+} + 2e^- \rightleftharpoons Mg_{(s)}$	-2.36	[87,88]
Mn	$Mn^{2+} + 2e^- \rightleftharpoons Mn_{(s)}$	-1.19	[87]
	$MnO_2 + 4H^+ + 2e^- \rightleftharpoons Mn^{2+} + 2H_2O$	1.22	[87,89]
	$MnO_4^- + 8H^+ + 5e^- \rightleftharpoons Mn^{2+} + 4H_2O$	1.51	[87]
Na	$Na^+ + e^- \rightleftharpoons Na_{(s)}$	-2.71	[87]
NO ₃	$NO_3^- + 10H^+ + 8e^- \rightleftharpoons NH_4 + 3H_2O$	0.880	[88]
	$NO_3^- + 2H^+ + 2e^- \rightleftharpoons NO_2^- + H_2O$	0.830	[88]
O	$O_{2(g)} + 4H^+ + 4e^- \rightleftharpoons 2H_2O_{(g)}$	1.23	[87–89]
	$O_2 + 2H^+ + 2e^- \rightleftharpoons H_2O_2$	0.695	[87]
	$O_2 + 2H_2O + 2e^- \rightleftharpoons H_2O_2 + 2OH^-$	-0.146	[87]
	$O_3 + H_2O + 2e^- \rightleftharpoons O_2 + 2OH^-$	1.25	[87,88]
S	$S_{(s)} + 2H^+ + 2e^- \rightleftharpoons H_2S$	0.142	[87,88]
	$SO_4^{2-} + 10H^+ + 8e^- \rightleftharpoons H_2S + 4H_2O$	0.340	[88]
Zn	$Zn^{2+} + 2e^- \rightleftharpoons Zn_{(s)}$	-0.762	[87,88]

Water electrolysis at the cathode has a reduction potential of -0.828 V. Of the species listed in Table 6, competitive reactions include reduction of CO_2 , Fe^{2+} , Fe^{3+} , O_2 to H_2O_2 , S and Zn^{2+} . At the anode, with a potential of -1.23 V (as the reversed reduction reaction), competing reactions include oxidation of Cl^- , HClO , HClO_2 , ClO_3^- , Fe^{2+} , Mn^{2+} and O_2 . I.e. besides dissolution and precipitation of metals, formation of the reactive species H_2O_2 , O_3 , ClO_3^- , ClO_4^- and $\text{Cl}_{2(g)}$ may be stimulated and assist in the contaminant transformation (Section 1.2.2). When comparing the reported potentials of chlorinated ethene transformation with those of ionic species (Table 5, Table 6), it is seen that abiotic and biotic chlorinated ethene transformation occur in the range of sulfate-, iron- and nitrate-reduction. This is coinciding with the electron acceptors used by anaerobic microbial dechlorination cultures [90].

Studies have shown, that presence of Fe^{2+} and S^{2-} enhance the electrochemical removal of chlorinated ethenes [56], while chromate, selenate, NO_3^- [54,58,60], HCO_3^- [91] and humic substances [57,58] inhibit the removal. Influence of natural hydrogeochemistry on electrochemically induced transformation of chlorinated ethenes makes testing in natural aquifer settings necessary for improved feasibility assessment, understanding of induced processes and thereby the ability to engineer the technology.

2 KNOWLEDGE GAPS

The overall objective of this industrial PhD project was to mature the electrochemical method towards *in situ* remediation of chlorinated ethenes in groundwater plumes and to evaluate the potential of the method. Combining the use of electrochemistry with contamination and environmental settings require multidisciplinary knowledge on material science, electrochemistry, hydrogeochemistry and contaminated sites. From the literature review in chapter 1, the major identified knowledge gaps in relation to this overall objective are:

- A. Previously published research has focused on TCE removal and thus the influence of the major electrochemical reactor design parameters (electrode material, catalyst load, electrode configuration, electrode spacing and current intensity) on chlorinated ethene removal is assessed on TCE. Since PCE is the parent component, offset should be taken in PCE to cover the full range of chlorinated ethenes detected at contaminated sites. A compilation of experiences on e.g. electrode material properties and stimulated chlorinated ethene degradation pathways is necessary.
- B. Chlorinated ethene removal has been the focus of previous studies with little attention given to electrochemically induced changes in hydrogeochemistry and the potential impact of resulting changes on the execution of electrochemical application. To optimize the method towards field-application with least changes caused in the surrounding settings, the significant influences of electrochemistry and hydrogeochemistry must be identified and studied, such as the severity of clogging of porous matrices due to corrosion of Fe anodes and precipitation of minerals, as indicated in the literature. If necessary, the electrochemical reactor design must be adapted to cope with the most significant impacts.
- C. Electrochemical zones for removal of chlorinated ethenes have previously been studied in simplified reactor systems, neglecting the complex conditions in groundwater aquifers. The influence of field-realistic aquifer parameters, i.e. a field-realistic flow rate, field-extracted groundwater, a partially degraded aged contamination, sandy sediment and temperatures of aquifers, on the chlorinated ethene removal need to be assessed for evaluation of the potential of *in situ* electrochemical treatment of chlorinated ethene plumes in high-permeable aquifers.

In Chapter 3, the research methodology is described and a correlation between research activities, appended papers, supporting notes and assessment of knowledge gaps (A-C) is outlined.

3 RESEARCH METHODOLOGY

A process diagram of the overall research methodology employed for development of electrochemical removal of aqueous chlorinated ethenes in realistic aquifer systems towards evaluation of the applied potential is presented in Figure 4. For a detailed description of methodologies used in the separate studies, please visit the relevant appendix (A) or supporting note (SN.). An overview of appended studies and their contributions to identified key knowledge gaps A, B and C (Chapter 2) is included in Table 7.

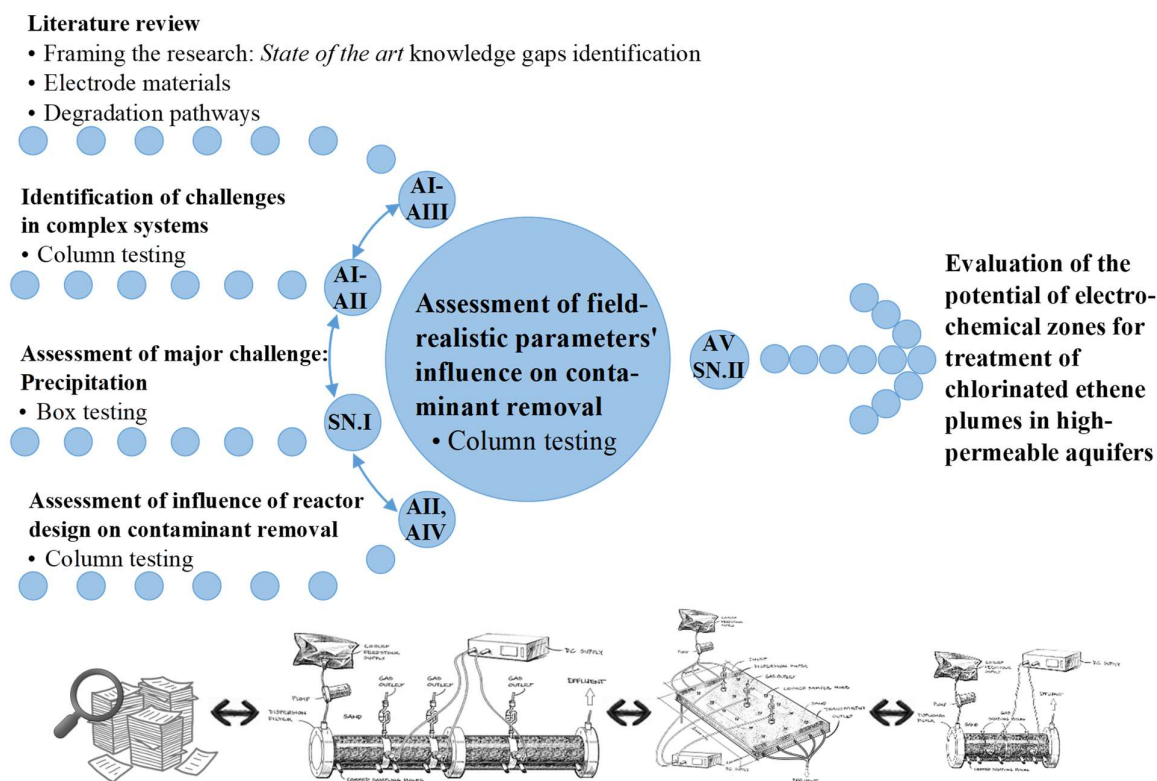


Figure 4. Research methodologies applied in the process of developing and assessing the potential of electrochemical removal of aqueous chlorinated ethenes in high-permeable aquifer settings. A description of appendices (A) and supporting notes (SN.) is given in Table 7.

For an optimal assessment and beneficial output of the research, field-representative characteristics of contaminated sites need to be identified. Section 3.1 is the description of a contaminated site used to represent the typical chlorinated ethene contaminated site. The related experimental set-up requirements are outlined in Section 3.2, while Section 3.3 is a presentation of reactors designed in this PhD project.

Table 7. Overview of appended material and the correlation with knowledge gap A, B and C (Chapter 2).

Appended material ^a	Title	Aim	Knowledge gap
AI	Challenges in electrochemical remediation of chlorinated solvents in natural groundwater aquifer settings	First part of the paper is a review used for identification of knowledge gaps within electrochemical remediation of chlorinated ethene plumes. Second part is a laboratory study on influences of field-realistic aquifer settings on the application of electrochemistry. Impacts were rated according to their relative significances. A simplified equilibrium model was defined to assist in interpretation of complex hydrogeochemical responses.	A B
AII	Selecting electrode materials and sequence for electrochemical removal of chlorinated ethenes in groundwater	This paper is a review on properties of electrode materials and catalysts. An assessment of surface characteristics of cast Fe and high-purity Fe materials was performed incl. related differences in Pd electroless plating. Deviating corrosion behaviors of Fe anodes in A-A-C and C-C-A configurations within natural hydrogeochemical settings was presented. Impact on the complex hydrogeochemistry was studied.	A B
AIII	Electrokinetics applied in remediation of subsurface soil contaminated with chlorinated ethenes – A review	A review on electrokinetics in combination with established remediation technologies was carried out with a focus on remediation of chlorinated ethenes in the low-permeable subsurface. The study includes a review on degradation pathways of the chlorinated ethenes.	A
AIV	Transformation of tetrachloroethylene in a flow-through electrochemical reactor	Influence of electrochemical reactor designs on PCE removal was studied to optimize the reactor for improved simulation of field-applied design for chlorinated ethene removal in high-permeable aquifer settings.	A
AV	Electrochemical transformation of an aged tetrachloroethylene contamination in realistic aquifer settings	This paper presents results on the influence of a typical groundwater flow rate, field-extracted groundwater, aged contamination, sandy sediment and groundwater temperatures on the performance of electrochemical removal of PCE in a flow-through reactor. The power consumption, PCE transformation mechanisms and resulting changes in hydrogeochemistry were assessed.	B C
SN.I	Electrochemically induced precipitation of groundwater species and anode composites in a flow-through box reactor	Precipitation of e.g. Fe was identified in AI as a major challenge when using Fe anodes in aquifer settings. Behavior of electrochemically induced precipitation was visually studied. Removal of an aged PCE contamination and changes in hydrochemistry were presented.	A B
SN.II	Galvanic abilities of electrodes installed in saturated sandy sediment - background reference test for electrochemical transformation of chlorinated ethenes	The aim was to conduct a reference test on e.g. background contaminant mass loss during electrochemical removal of chlorinated ethenes in field-realistic aquifer settings (AV). Data on galvanic properties, and changes in contaminant and porewater composition were presented.	B C

^a A: Appendix (journal papers). SN.: Supporting note (additional work).

3.1 FRAMING CONTAMINATED SITES – A CASE STUDY

The contaminated site of the Innovation Garage, located in Skovlunde, DK, was identified in collaboration with the Capital Region of Denmark to represent a "typical" chlorinated ethene contaminated site. The Capital Region of Denmark is a government agency responsible for the public efforts to map, investigate and remediate contaminated sites and thus has extensive knowledge on contaminated sites. At the Innovation Garage, an aged contamination of PCE has infiltrated the high-permeability zone, which is situated in a sandy sediment (Figure 5).

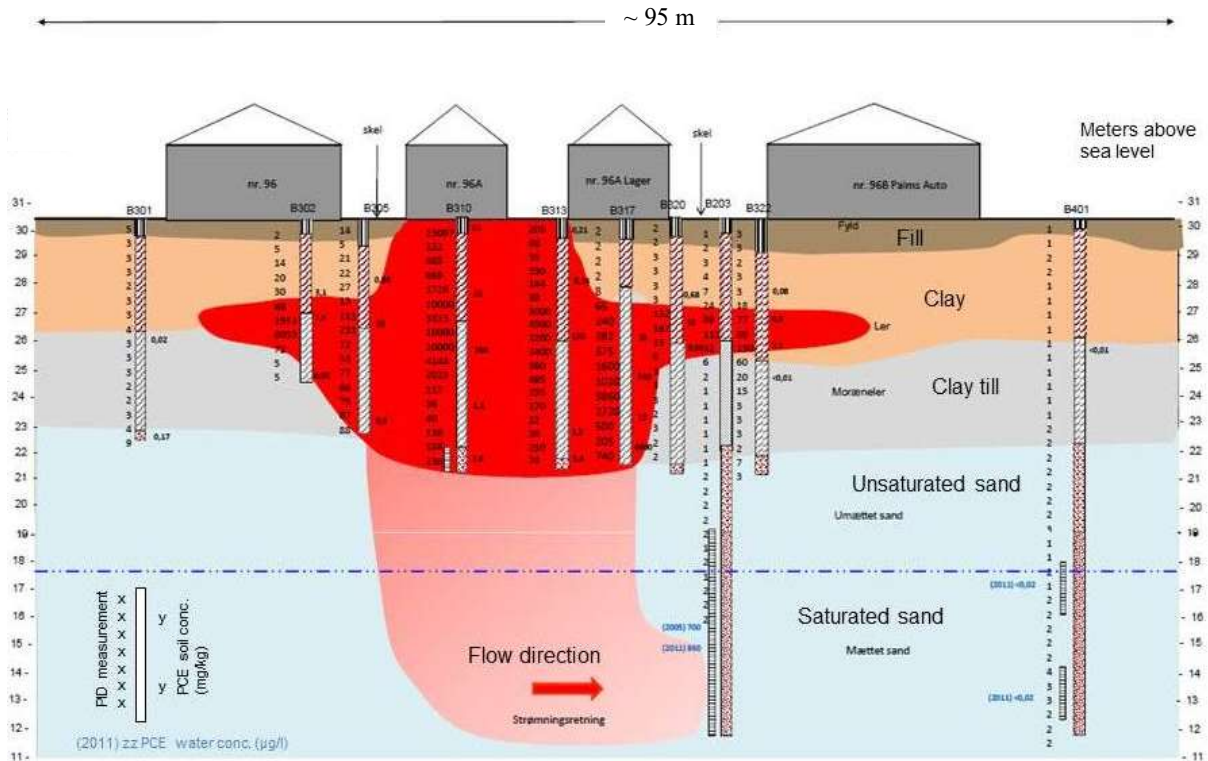


Figure 5. Conceptual model of geology and PCE contamination at the Innovation Garage, DK.

Source: The Capital Region of Denmark [92].

The major characteristics of the Innovation Garage incorporated into the experimental assessments of this project are flow rate, the groundwater, the aged contamination of PCE, sandy sediment and the groundwater temperatures:

- Flow rate: A common seepage velocity of approximately 100 m/yr was applied. For testing of the influence of flow rate, a lower and higher flow rate were also tested.
- Groundwater: Natural groundwater contains a variety of ionic species. Groundwater was extracted at this site from either a well or an on-site P&T facility.

- Aged contamination: The extracted groundwater contained an aged contamination. Major contaminant species included PCE, TCE and cis-DCE.
- Sandy sediment: Information on grain size distribution and carbon content of the sandy sediment of the high-permeable aquifer was used to identify a similar sandy sediment. Such a sandy sediment was available from a quarry in Svogerslev, DK. The sediment was used as received, i.e. not acid washed, sorted etc.
- Groundwater temperatures: At Danish sites, groundwater temperatures are in the range of 8-10 °C.

When working with field-extracted contaminated groundwater instead of a synthetic and spiked solution, natural fluctuations in concentrations between sampling rounds is a prerequisite. I.e. starting conditions for all experiments cannot be predetermined and are not constant. Characterization of the sandy sediment and field-extracted groundwater is provided in the specific appended studies (Appendix I-V, Supporting note I-II).

3.2 EXPERIMENTAL DESIGN REQUIREMENTS

Combining testing on electrochemistry with chlorinated ethenes and a porous matrix is challenging and put demands on the experimental set-up. Since, the chlorinated ethenes are volatile, the set-up must be a closed system to limit volatilization. However, venting of electrolytically generated gases is needed for equalization of pressure to hinder drainage of the reactor or in worst case cracking due to pressure build up. Thus, means of venting, which limit the mass loss of contaminants due to volatilization, must be implemented. In addition, the geological matrix increases the electrical resistivity of the system, wherefore high-capacity power supplies and rheostats, for testing of three-electrode configurations, must be acquired to be able to apply a suitable current intensity. In general, the higher the current, the more gases are formed. For application of current intensities in the range reported in literature, the resulting consumption of water due to electrolysis is significant relative to the supply of water at a field-realistic flow rate through a porous matrix (see Example 1). Consequently, drainage of the reactor is a risk.

Example 1: Water electrolysis during flow-through electrochemical application

Current intensities applied for removal of chlorinated ethenes is up to 120 mA (Table 1). At the cathode, one mole of electrons is transferred per mole of water converted (Eq. 2). The mass of water consumed due to water electrolysis can be estimated using Faraday's Law:

$$V_{H_2O} = \frac{ItM_{H_2O}}{zF\rho_{H_2O}}$$

Where V_{H_2O} is the volume of water consumed [ml], I is the current [A], t is time [s], M_{H_2O} is the molar mass of water [18.02 g/mole], z is the number of electrons transferred [-], F is Faraday's constant [96485 C/mole] and ρ_{H_2O} is the density of water [1 g/ml]. During one minute of application of 120 mA, 1.34 ml of water will be converted at the cathode, assuming that water electrolysis is the only electrode process. At the anode, the consumption of water due to electrolysis is half that of the cathode (Eq. 1), i.e. 0.67 ml.

In a column reactor ($L = 16.8$ cm, $D = 7.8$ cm) with a water-filled porosity of 38% and a seepage velocity of 150 m/yr, the resulting pumping rate and thereby supply of water is 0.5 ml/min. I.e. lower than the water consumed due to electrolysis at both the anode and cathode. This example is assuming an efficiency of water electrolysis of 100%, i.e. no competing reactions are occurring. In the presence of e.g. field-extracted groundwater, contamination and a sandy sediment, competing reactions are expected and thereby a lower consumption of water.

During sampling in flow-through reactors at field-realistic flow rates, dragging of the solution towards sampling points is another risk, which influences the execution and interpretation of data. To limit the effect of dragging of solution towards sampling points, less than 2% by volume of the solution was chosen in this study as the maximum volume to be extracted during sampling. Furthermore, with a complex chemistry, an extensive analytical program must be employed for tracking of developments over the course of reactors and time. Besides economical aspects, this implies extraction of a considerable size of liquid volume. To compensate for a large sampling scheme, the dimensions of the reactors must be large enough to allow sampling and/or analytical procedures with a minimum requirement of sample volume must be developed and/or identified.

3.3 THE ELECTROCHEMICAL REACTORS DEVELOPED

Three electrochemical reactors were designed in this project; two columns and one box reactor. The columns were kindly provided by US Army Corps of Engineers (Dr David Gent) and Northeastern University (Professor Akram Alshawabkeh). Both columns were completely redesigned to comply with the requirements described in Section 3.2, and to facilitate the investigation to fill in the knowledge gaps selected (Chapter 2). One column reactor was used mainly in the assessment of the influence of natural aquifer settings on the electrochemical execution (Figure 6, Appendix I-II). The second column was used in the studies on influences of electrochemical reactor design and of field-realistic parameters on the contaminant removal (Figure 7, Appendix IV-V, Supporting note II). The box reactor was used primarily for assessment of the major challenges related to precipitation (Figure 8, Supporting note I). Flexibility of the reactors designed enabled testing of e.g. various electrode shapes and electrode configurations, as discussed in Chapter 4.

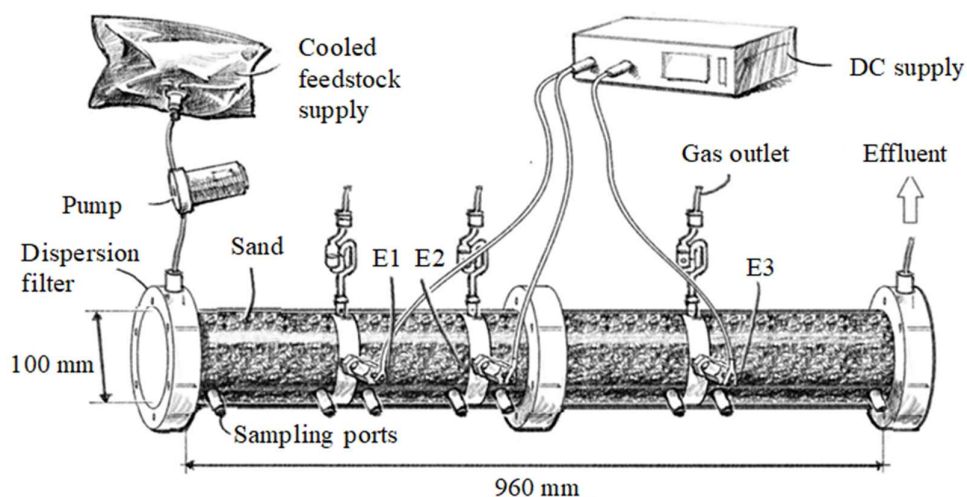


Figure 6. Illustration of one column reactor designed in this PhD project.

Each reactor contributed to the assessment with specific features. The prolonged electrode spacings of the column reactor in Figure 6 of app. 18 cm and 34 cm, compared to the literature listed in Table 1 with electrode spacings <5 cm, facilitated assessment of each electrode's specific contribution to induced changes in the natural hydrogeochemistry. The column reactor in Figure 7 favored testing on the influence of reactor design and field-realistic parameters on contaminant removal, for which many parameters are varied one at a time, because of its reduced dimensions

and thereby shortened time for flow-through of one pore volume. The additional dimension of the box reactor (Figure 8) and mounting of well screens for monitoring and installation of electrodes better replicated a field-implementation scenario. The transverse distribution of reactants generated, precipitates etc. could be assessed. With the box reactor, several parallel sequences of electrodes or two-planar electrode configurations potentially could be studied.

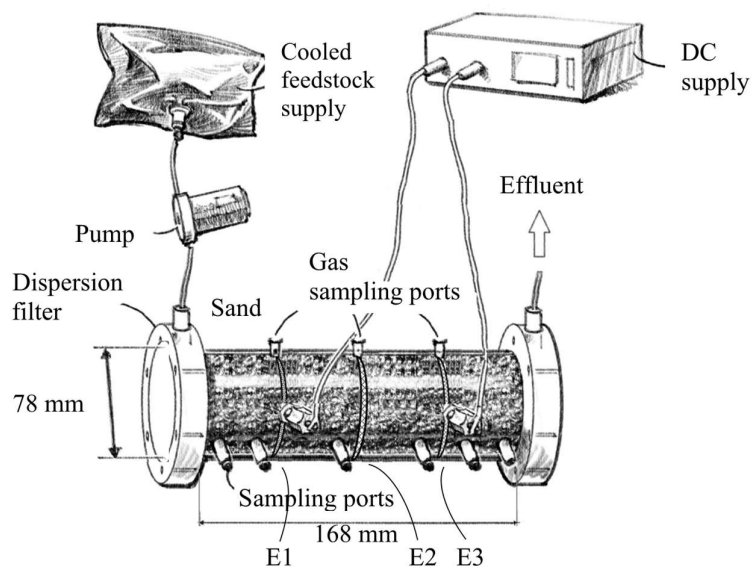


Figure 7. Illustration of the second column reactor designed in this PhD project.

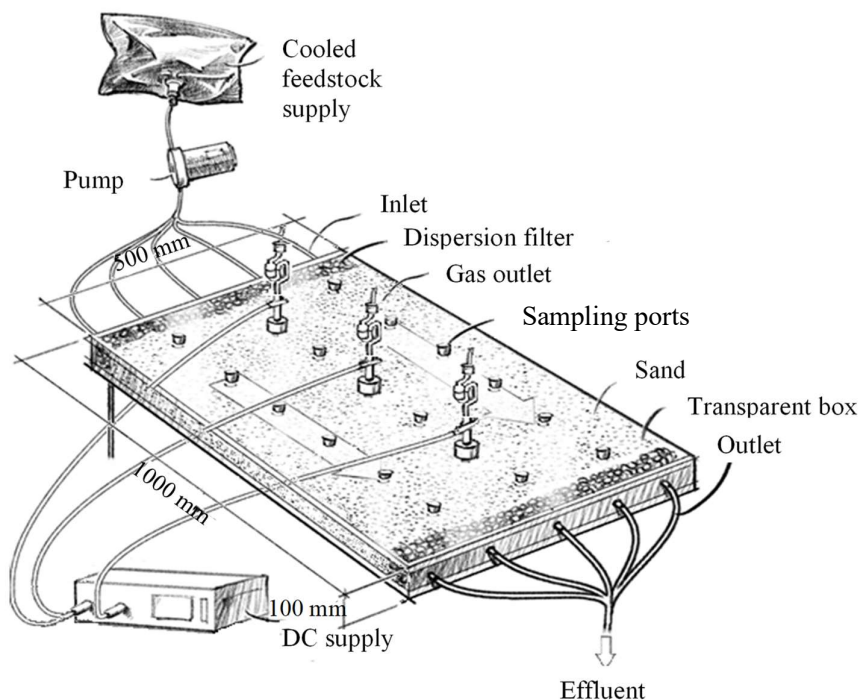


Figure 8. Illustration of the box reactor designed in this PhD project.

4 SIGNIFICANCE OF ELECTROCHEMICAL REACTOR DESIGN ON PERFORMANCE

In this chapter, an evaluation of the influence of electrochemical reactor design on the performance is presented. Section 4.1 is assessing the influence of various electrochemical design parameters, e.g. current intensity. In Section 4.2, other design parameters are discussed, e.g. influence of reactor orientation. The evaluation is based on the experimental work appended (Appendix I-V, Supporting note I-II), for which an overview of the various design parameters tested is given in Table 8. The influence of field-parameters is discussed in Chapter 5.

4.1 ELECTROCHEMICAL DESIGN PARAMETERS

Included in the assessment of electrochemical design parameters in undivided flow-through reactors operated at constant current are various electrode materials, loads of catalyst coating, electrode shapes, electrode configurations, electrode spacings and current intensities. Focus is on the contaminant removals obtained.

4.1.1 ELECTRODE MATERIAL

High removals of chlorinated ethenes have been demonstrated with use of Fe electrodes and Pd catalyst (Section 1.2.1). Therefore, Pd coated Fe and cast Fe electrodes were studied in this project. The degree of purity of Fe materials was found to influence the surface characteristics prior to and after electroless palladization (Appendix II). The Pd coated 99.95% Fe material surface was dominated by presence of Fe and Pd. With a decreasing degree of Fe purity, increasing amounts of oxides were detected. The least pure Fe material, 98+%, also had Cl adsorbed onto the surface at locations of oxide formations. The properties of electrode impurities, e.g. toxicity, is especially important for Fe materials used as anodes, since these were observed released into the groundwater concurrently with corrosion of the Fe anode (Appendix I-II, Supporting note I). The impact of Fe anode corrosion in sandy sediment was rated as a major challenge due to clogging of the porous matrix by Fe complexes (Appendix I). The distribution of Fe complexes formed depended on the electrode configuration (Appendix II). With application of an A – A – C configuration, white $\text{Fe}(\text{OH})_2$, black FeO and/or Fe_3O_4 , and red $\text{Fe}(\text{OH})_3$ complexes deposited in parallel lines upgradient the cathode. Whereas for the C – C – A configuration, the FeO and/or Fe_3O_4 complex distribution was uniform downgradient the anode (Appendix II). The challenge of anode material induced clogging was overcome by using stable MMO anodes (Appendix IV-V).

Table 8. Design parameters tested with reference to the specific experimental set-up used.

Appended material		AI	AII	AIV	AV, SI.II	SI.I
Reactor [Figure]		6	6	7	7	8
Anode, A	99.8% Fe rod		X			
	Cast Fe rod	X	X			X
	MMO mesh disc			X	X	
Bipolar, BPE	MMO			X	X	
Cathode, C	99.95% Fe rod					X
	99.8% Fe rod	X	X			
	98+% Fe rod		X			
	98% Fe foam			X	X	
	316SS mesh disc			X		
	Cast Fe rod		X			
Catalyst, Pd	0.76 mg/cm ²	X	X	X		X
	1.14 mg/cm ²			X		
	1.33 mg/cm ²				X	
Electrode configuration	C-A			X		
	C-C-A	X	X	X		X
	A-A-C		X			
	C-BPE-A			X	X	
Electrode spacing	2.5			X		
	4			X	X	
	17.6→33.6	X	X			
	27.7→32.6					X
Current	0 mA			X	X	
	12 mA	X	X			
	57 mA					X
	60 mA			X		
	120 mA			X	X	
	180 mA			X		
Electrode diameter	6.35 mm	X	X			
	12.7 mm					X
	770 mm			X	X	
Electrode width/length	1.8 mm			X	X	
	2.8 mm			X		
	4 mm			X	X	
	130 mm	X	X			X
Orientation		→	→	→; ↑	→	→
Porous matrix	Glass beads			X	X	
	Sandy sediment	X	X		X	
Porosity	31-42%	X	X	X	X	
	100%			X		X
Groundwater	Synthetic			X	X	
	Field-extracted	X	X		X	X
Seepage velocity	48 m/yr		X			
	61 m/yr	X	X			
	122 m/yr	X				X
	150 m/yr	X		X	X	
	305 m/yr					
	1204-1581 m/yr			X		
Temperature	6-10 °C				X	X
	20-22 °C	X	X	X	X	

4.1.2 CATALYTIC COATING

Use of catalysts with a lower H_2 overpotential on cathodes favor the indirect abiotic reduction pathway of chlorinated ethenes (Section 1.2.2). The significance of Pd loads of 0.76, 1.14 and 1.33 mg/cm^2 and Ni in 316SS on PCE removal was tested (Figure 9, Appendix IV-V).

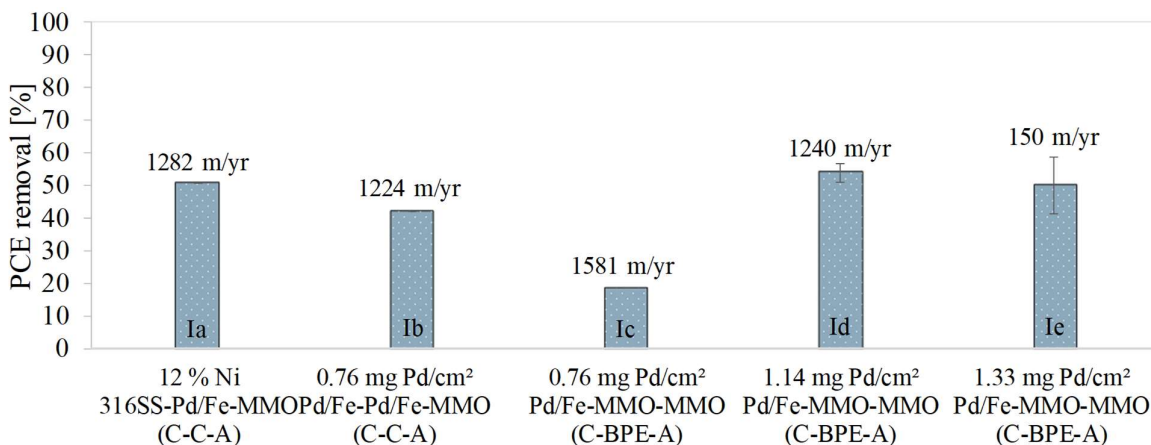


Figure 9. Influence of Pd and Ni catalysts on PCE removal in undivided flow-through reactors at 120 mA. C: cathode, BPE: bipolar electrode, A: anode. Seepage velocities are indicated above the bars. Error bars are based on duplicate testing. Figure adapted from Appendix IV-V.

With electroless plating, Pd adsorbed onto Fe in lumps (Appendix II) [60]. The findings of an inverse correlation between degree of Fe purity and level of oxide coverage after palladization (Section 4.1.1), may suggest use of materials with naturally embedded catalysts, e.g. 316SS with a high Ni content. Catalytic abilities of 316SS appeared to improve the PCE removal by 20% compared to use of Pd in a C – C – A electrode configuration (Figure 9, Ia vs. Ib). In similar studies by Rajic et al. [60,61], 316SS and Pd coated Fe cathodes were capable of removing 62% and >99% of TCE, respectively. This suggests, that by increasing the Pd load, removals superior to that by 316SS may be obtained, which is verified by trends for the C – BPE – A (BPE: bipolar electrode) configuration in Figure 9 (Ic-Ie). Insignificant differences in removal with 1.33 mg/cm^2 vs. 1.14 mg/cm^2 (Figure 9, Ie vs. Id) could be due to a non-linear correlation with the optimum Pd load being in between the tested loads [60]. The optimum Pd load of 0.76 mg/cm^2 on Fe foam in the study by Rajic et al. [60] was deficient in this set-up applied (Figure 7). The deviation could be a consequence related to dimensioning, where the ratio of electrode surface area to water volume in the reactor applied in this project was lower.

4.1.3 ELECTRODE SHAPE

Shapes of electrodes tested include rods, foams and meshes (Table 8). The MMO meshes used had larger openings than the 316SS mesh, which again were larger than the pores of the Fe foam. Advantages of foams and meshes are large surface areas, but their small pores/openings have shown to hamper the release of H_2 and O_2 gasses generated, resulting in reduced contact between the contaminants and electrodes and therefore removals [60,61,93]. This effect with smaller pores of the Fe foams than the openings in 316SS mesh may explain the PCE removal performance with Pd/Fe and 316SS of 42% and 50%, respectively (Figure 9, Ib vs. Ia, Appendix IV), where higher removals were expected with use of the Pd/Fe foams [60,61]. It indirectly may also explain the lower PCE removal of 19% in the C – BPE – A configuration for a Pd load of 0.76 mg Pd/cm^2 (Figure 9, Ic), since the current running through this Fe foam cathode was double that of the C – C – A configuration, where the current was equally split between the two Fe foam cathodes. I.e., the rate of gas formation on the cathode was higher in the C – BPE – A reactor. However, this is contradictory to the enhanced removal with increasing Pd loads observed in the C – BPE – A reactor (Figure 9, Ic-Ie, Appendix IV-V). The load of catalyst rather than gas entrapment seems to explain the different performances of the mesh and foam cathodes, where the low load of 0.76 mg Pd/cm^2 appears insufficient in adsorbing the atomic hydrogen needed for dechlorination to occur [60]. Based on visual observation of gas release from the rods, foams and meshes studied, the rods were better if the goal is to avoid entrapment of gas.

4.1.4 ELECTRODE CONFIGURATION

The electrode configurations tested were A – A – C, C – A, C – C – A and C – BPE – A in simple and/or complex hydrogeochemical settings (Table 8), where A is positively polarized, C is negatively polarized, and BPE is positively polarized on the side facing C, while negatively polarized on the side facing A. The influence of electrode configuration is assessed across the performed studies with similar test conditions (Figure 10). In simplified systems, the configuration of C – BPE – A performed better than C – A for Pd loads of 1.14 mg/cm^2 (Figure 10, IIb vs. IIa). Enhanced removal obtained with use of BPEs has been reported for use of graphite electrodes [62]. For Pd loads of 0.76 mg/cm^2 , higher PCE removal was obtained with a configuration of C – C – A than C – BPE – A (Figure 10, Ia vs. Ib). Across the Pd loads applied, higher removals were obtained with configurations of $C - BPE - A > C - C - A \geq C - A$ (Figure

10, IIb; Ia ; IIa). In Rajic et al. [55], >99% TCE removal and similar reaction rates were also observed for configurations of C – C – A and C – A.

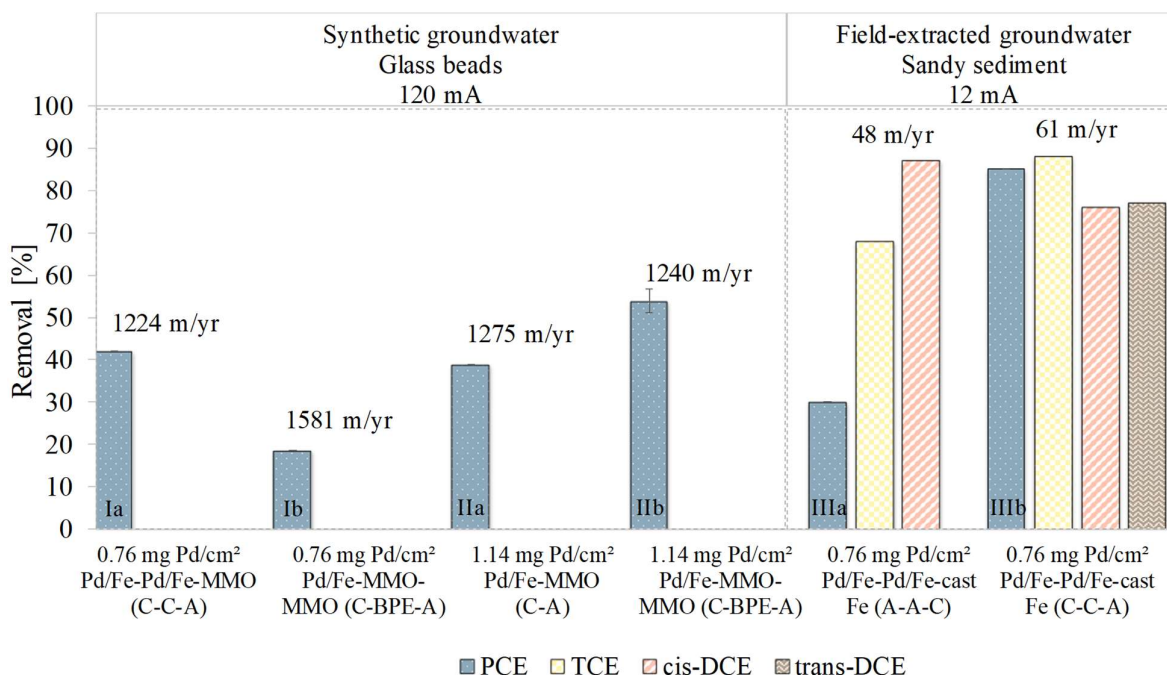


Figure 10. Influence of various electrode configurations on removal of PCE, TCE, cis-DCE and trans-DCE (if present) in undivided flow-through reactors. C: cathode, BPE: bipolar electrode, A: anode. Seepage velocities are indicated above the bars. Error bars are based on duplicate testing. Figure adapted from Appendix I-II, IV.

In complex systems, the aged contamination was treated concurrently in configurations of C – C – A and A – A – C, but with overall higher removals in the C – C – A reactor (Figure 10, IIIb vs. IIIa). Reduction by the indirect pathway (Section 1.2.2) appear dominant, since the electrodes used were rods, where a major fraction of the contamination was flowing by the electrodes without being in contact with the actual electrode surface as required for direct reduction. No VC was leaving the electrochemical zone. The redox sequence generated by the C – C – A configuration was observed to disturb the surrounding environment the least, i.e. measured downgradient the electrochemical zone and compared to pre-treatment levels, less changes in e.g. pH and porewater composition was observed (Appendix II). Reduction followed by oxidation was thus found the best redox sequence.

4.1.5 ELECTRODE SPACING

The electrode spacings tested under similar conditions were 2.5 cm and 4 cm in a configuration of C – BPE – A embedded in an inert porous matrix (Table 8, Appendix IV). PCE removals reached at 2.5 and 4 cm electrode spacings were 41% and 54±3%, respectively. I.e., an increase in removal with an increase in electrode spacing was observed. This is opposite to findings by Rajic et al. [55] in an entirely water-filled reactor, who explained the decrease in removal with increased electrode spacing by elevated electrical resistivity and thereby cell voltage, which inhibited the removal processes. The findings of the present study may be due to a) extension of the redox zones with prolonged electrode spacing, favoring contaminant transformation, and/or b) gas accumulation in the inert porous matrix. At the 2.5 cm electrode spacing, gas formed at the electrodes appeared to infiltrate the matrix rather than floating towards the gas extraction ports, maybe due to a less densely packed porous matrix. Consequently, gases covered electrode surface sites, lowering the active electrode surface area. With the 4 cm electrode spacing, gas release and extraction was improved. The removals observed suggested limited mass loss due to volatilization of PCE into the entrapped gas phase at 2.5 cm electrode spacing. These findings indicate that PCE is transformed rather than volatilized and that an extension of the established redox zones by increasing the electrode spacing may enhance the PCE removal.

4.1.6 CURRENT INTENSITY

The current intensities applied were 0 mA, 60 mA, 120 mA and 180 mA to a Pd/Fe – MMO – MMO electrode configuration (C – BPE – A when current applied, Appendix IV-V) in the column illustrated in Figure 7. Observed contaminant removals are shown in Figure 11. In the range of 0 mA – 120 mA, the contaminant removal increased with increasing current intensity (Figure 11, Ia-Ic, IIIa-IIIb, IVa-IVc), but a decrease was observed at a current of 180 mA (Figure 11, IIb vs. IIa). At 180 mA, the elevated formation of gases at the electrodes had difficulties in escaping the porous matrix, resulting in coverage of the electrodes and an increase in pressure with subsequent leaking. Similar experiences were made by Rajic et al. [55], but with the decrease observed at 90 mA.

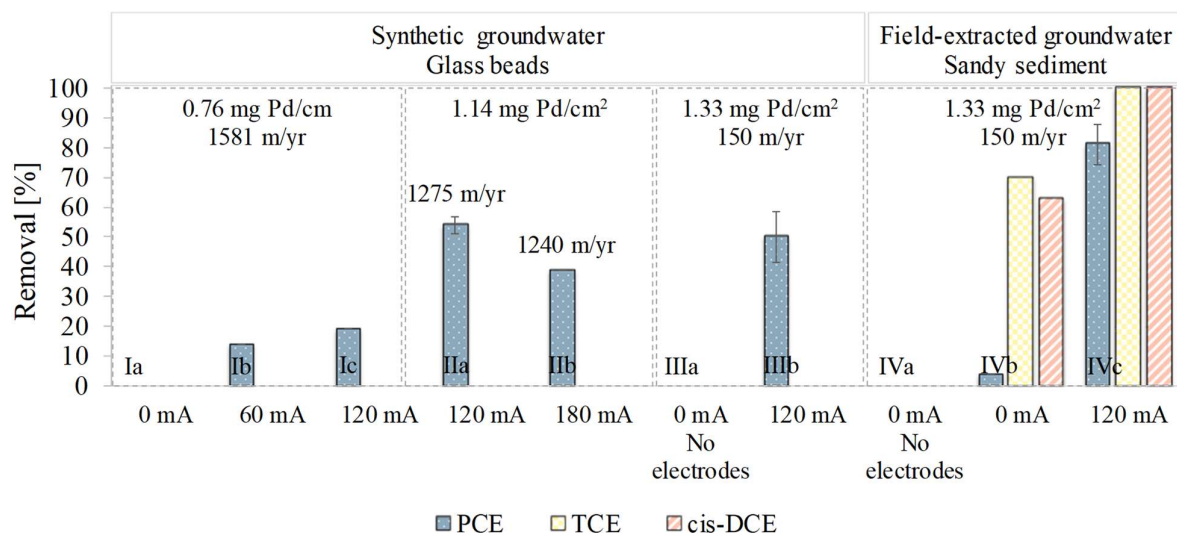


Figure 11. Influence of various current intensities on removal of PCE, TCE, cis-DCE and trans-DCE (if present) in undivided flow-through reactors with Pd/Fe – MMO – MMO electrodes in a configuration of cathode – bipolar electrode – anode when current is applied. Seepage velocities and Pd loadings are indicated. Error bars are based on duplicate testing. Figure adapted from results in Appendix IV-V and Supporting note II.

Galvanic effects were observed in the experiments with field-extracted groundwater and sandy sediment, i.e. a potential difference established between the electrodes without application of current (Figure 11, IVb, Supporting note II). The resulting potential was 0.926 ± 0.013 V only, but stimulated some chlorinated ethene removal, whether abiotic or biotic (Figure 11, IVb, Supporting note II). Without electrodes in the column, no removal was detected (Figure 11, IVa).

This comparison of findings on the influence of electrochemical design parameters on chlorinated ethene removal across studies carried out in this project and compared with literature shows, that the current intensity and the side effects from degree of gas formation is crucial for the removal under various electrode spacings, materials and shapes applied in a porous matrix. Further, that the optimal current intensity and catalyst loading is dependent on reactor dimension and electrode shape. In the following, the influence of other design parameters, e.g. reactor orientation and dimension, on the chlorinated ethene removal is examined.

4.2 OTHER DESIGN PARAMETERS

The influence of reactor orientation, porous matrix characteristics, flow rate and reactor dimension on chlorinated ethene removal is assessed in the following. It is based on the appended studies and related experiences (Appendix I-II, IV-V, Supporting note I-II).

4.2.1 REACTOR ORIENTATION

Vertical oriented, completely water-filled reactors with an upward flow conveniently facilitate a self-controlled venting for gases generated due to water electrolysis: Once gases have detached from the electrode surfaces, they float towards the top of the reactor and out with the effluent. In horizontally oriented reactors, released gasses accumulate on the upper part of the reactor, demanding means of venting. Horizontally oriented reactors were used in this project, because they better simulate the concept of a potential field-application. Hence, various means of venting were tested. The major ones included automatic venting by use of gas-liquid separation membranes, self-acting vents and fermentation locks, and manual extraction. Of the automatic venting mechanisms tested, the simple and cheap fermentation locks were most applicable. However, none of the automatic means of venting could handle the transient changes induced by the electric field (Appendix III). Manual extraction was the steadiest and least disturbing action, but required a continuous supervision throughout the duration of the test. This may explain why the *state of the art* within electrochemical remediation of chlorinated ethenes in undivided flow-through reactors operated at constant current is based on testing with vertically oriented reactors (Table 1).

For the electrochemical concept of treatment in-between electrode wells, investigated in this project, horizontally oriented reactors simulate field-implementations the best. To be able to transfer the knowledge obtained in vertically oriented reactors, testing on the influence of reactor orientation on PCE removal was carried out at a field-realistic seepage velocity of 150 m/yr and at a seepage velocity of 1314 m/yr in settings comparable to that in similar studies in the literature. The experiments were conducted without a porous matrix in the cell. At groundwater flow rates, PCE removals in the horizontal and vertical reactors were 86% and 77%, respectively. At high flow rates, the removals achieved in the horizontally and vertically oriented reactors were 30% and 14%, respectively. I.e., the horizontally oriented reactors performed better than the vertically oriented reactor. Based on observations, these results were related to the ease of gas release. In

the vertically oriented reactors, gasses accumulated on the upgradient (lower) side of the electrodes until a certain gas phase volume was reached and the gases could penetrate the perforated foam and mesh electrodes (Appendix IV) [93]. This reduced the active electrode surface area. Also, a gas phase accumulated around the effluent point until a certain volume had accumulated and was pushed out of the reactor. During accumulation of gasses, the potential difference increased. In the horizontally oriented reactors, gasses readily floated towards the extraction ports and were evacuated immediately, with no fluctuations in potential difference observed.

4.2.2 REACTOR DIMENSION

The influence of reactor dimension on chlorinated ethene removal is assessed by comparing performances of reactors of different dimensions operated under similar conditions to the extent possible. The assessment is based on appended studies and the literature. The resulting output is a comparison of column dimensions and the up-scaling from column to box reactor (Figure 12).

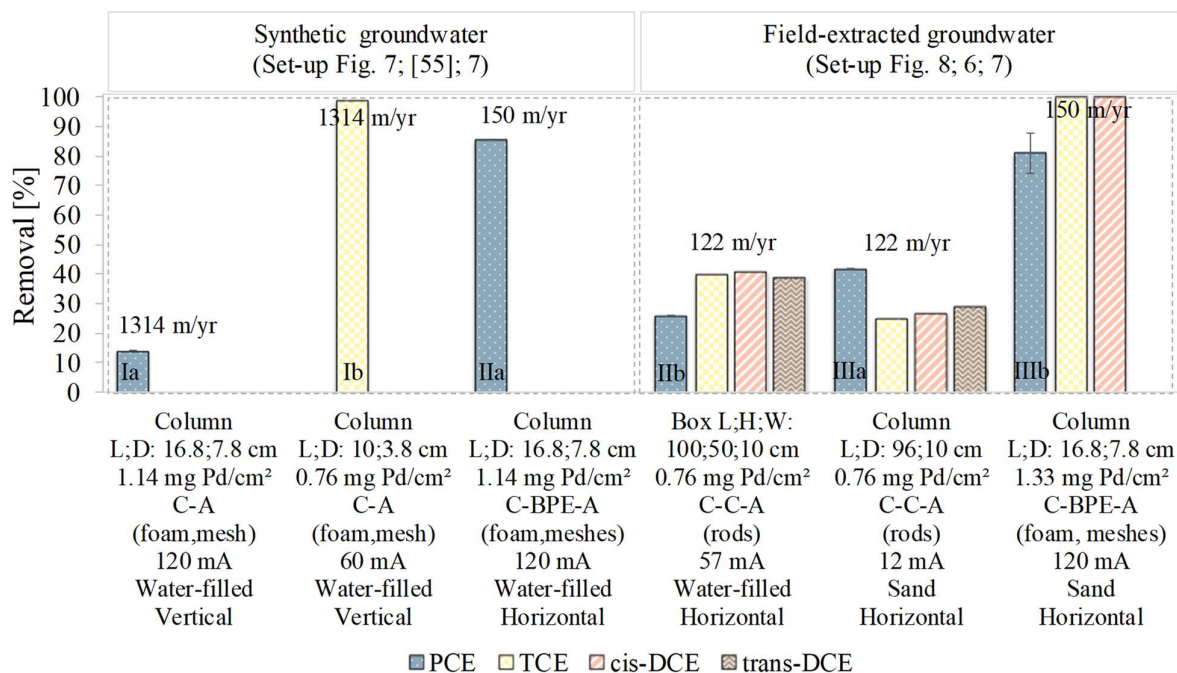


Figure 12. Influence of reactor dimensions on chlorinated ethene removal in undivided flow-through electrochemical reactors. C: cathode, BPE: bipolar electrode, A: anode. See Table 8 for elaboration on design parameters. Error bars are based on duplicate testing. Figure adapted from results in Appendix I, IV-V, Supporting note I and Rajic et al. [55](1b).

Column reactors

Besides differences in reactor dimensions, the only variables in experimental conditions applied for the studies underlying data Ia-Ib (Figure 12) was catalyst loading and current intensity. To compensate for the larger dimensions of the reactor (Ia), the current intensity and catalyst loading was elevated. Yet, chlorinated ethene removals in the larger column reactor (Ia) and smaller column reactor (Ib, [55]) of 14% and >99% were observed, respectively. More additional design parameters were varied between the studies underlying data IIIa-IIIb (Figure 12); catalyst load, current intensity, electrode configuration and electrode shape. Resulting PCE removals of 42% and $81\pm 7\%$ for IIIa and IIIb, respectively, verify that column reactors with a specific combination of dimensions has a unique set of optimum design parameters related to it.

Column vs. box reactors

Variables included catalyst loading, electrode configuration, electrode shape, current intensity and composition of groundwater solution (Figure 12, IIa-IIb). The resulting PCE removals were 86% and 26% in the column and box reactor, respectively. Considering the observed deviations in performances due to varying column reactor dimensions (Figure 12, Ia-Ib, IIIa-IIIb) and the lower catalyst load, current intensity and contact with electrodes due to the shape of electrodes applied in the box set-up (Figure 12, IIb) relative to column set-up (Figure 12, IIa), the extra dimension of the box reactor unexpectedly appears less influential. Box reactors simulate field-applications better, wherefore more studies in box reactors should be carried out.

4.2.3 *POROUS MATRIX*

An immediate influence of electrochemical testing in porous matrices (glass beads and sandy sediment) was elevated electrical resistivity and thereby potential difference at constant current (Figure 13a). The electrical resistivity for electrochemical testing in glass beads was higher than in completely water-filled reactors (Figure 13a, Ib vs. Ia, IIb vs. IIa, IVa vs. IIIa) and in sandy sediment (Figure 13a, IVa vs. IVb). The pore spaces in the homogenous glass bead matrix were larger than in the heterogeneous sandy sediment. Consequently, the electrolytically formed gases were observed to infiltrate the glass bead matrix and not the sandy sediment. A similar behavior has been observed during testing in limestone gravel [57]. Gases entrapped in the pore spaces decreased the permeability, covered the electrode surfaces and thereby elevated the electrical resistivity.

The influence of a porous matrix on the chlorinated ethene removal is assessed by comparing performances in completely water-filled reactors with that in porous matrices of glass beads (Appendix IV) and sandy sediment (Appendix I vs. Supporting note I), i.e. several design parameters are variables (Figure 13b). Considering the previously discussed findings on the influence of catalyst loading, electrode configuration, electrode spacing, current intensity and reactor dimension on the chlorinated ethene removal, and comparing with the removals obtained in Figure 13b, the observed trend in influence of a porous matrix is an enhancement of the PCE removal (Ib vs. Ia, IIIb vs. IIIa). Sorption onto the porous matrices studied was negligible (Appendix IV-V).

The degree of gas intrusion and thereby electrode coverage may explain the tendency of higher PCE removal in sandy sediment at a low flow rate compared to in glass beads (Figure 13b, IVb vs. IVa), where the smaller pore spaces in the sandy sediment hindered the gas intrusion and thereby improved the release of gases from the electrode surfaces. A more complex flow pattern with turbulent flow and thereby improved contact between the chlorinated ethenes and generated reactants for flow through a porous matrix compared to a completely water-filled reactor is suggested to explain the elevated removal observed in porous matrices. One outlier is observed for testing at a low flow rate (Figure 13b, IIb vs. IIa). The influence of groundwater flow rates is discussed in Section 4.2.4.

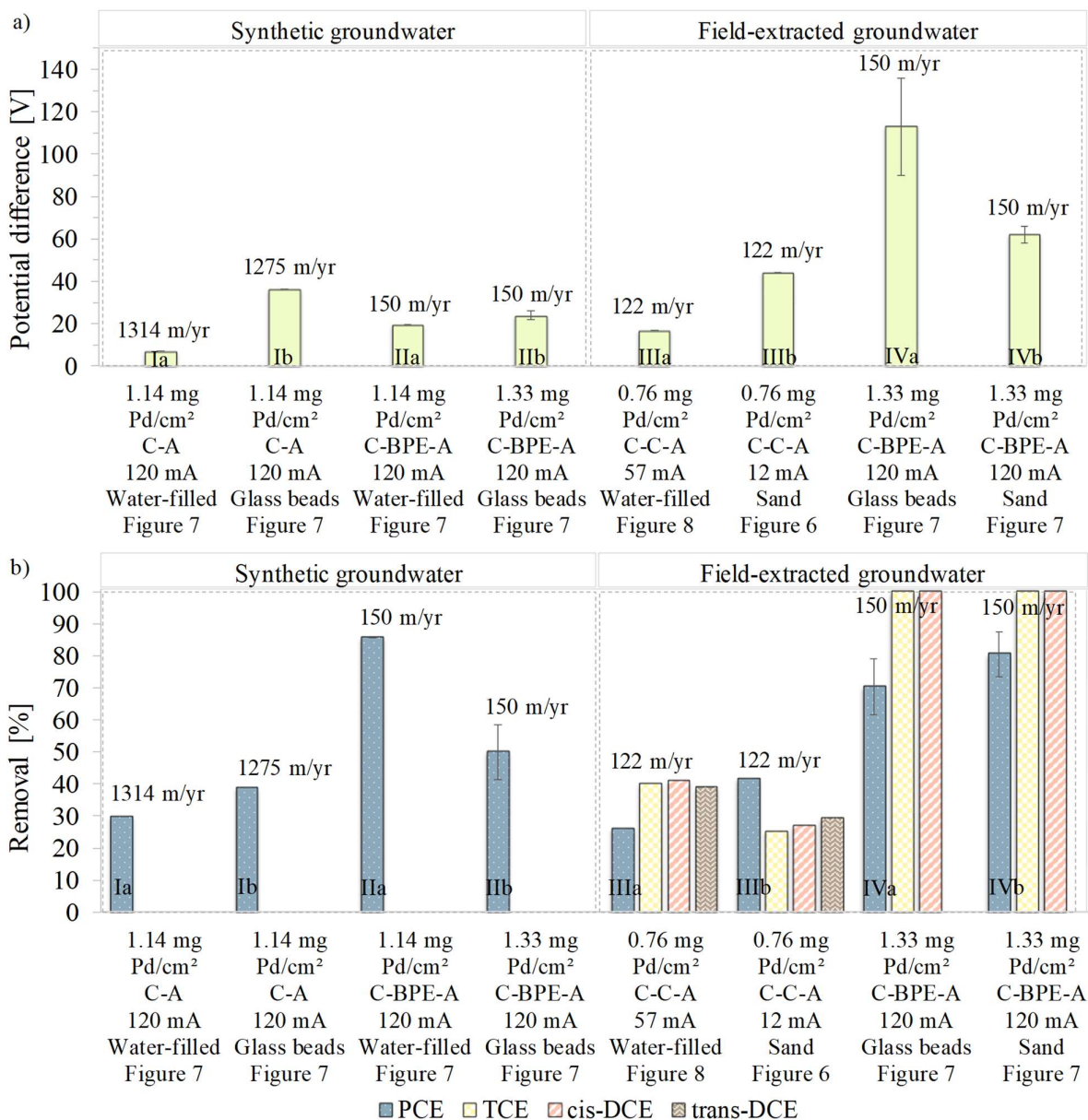


Figure 13. Influence of a porous matrix on a) potential difference and b) chlorinated ethene removal in undivided flow-through electrochemical reactors. C: cathode, BPE: bipolar electrode, A: anode.

See Table 8 for elaboration on design parameters. Error bars are based on duplicate testing.

Figure adapted from results in Appendix I, IV-V and Supporting note I.

4.2.4 FLOW RATE

The influence of groundwater flow rates on the electrochemically induced chlorinated ethene removal was studied (Appendix I). It was observed, that the higher the flow rate, the lower the resulting chlorinated ethene removal percentage. This is in line with observations made in

Appendix IV (Section 4.2.1) and by Rajic et al. [55] in completely water-filled reactors. The outlier in terms of influence of a porous matrix on electrochemical removal of PCE (Figure 13b, IIb vs. IIa) may be due to an indirect effect of flow rates: At low flow rates, gases formed at the electrodes were increasingly trapped in the interface between the electrodes and the porous matrix and grew into the matrix rather than being released from the electrode surfaces. In the completely water-filled reactor at a low flow rate, gases were better released from the electrode surfaces and facilitated a higher PCE removal at the low flow rate. Elevated flow rates appeared to assist in gas release from the foam and mesh electrodes, with the gases being pushed towards the gas extraction ports rather than intruding the porous matrix through a slow growth into the matrix. Thus, at the elevated flow rate tested, a larger active electrode surface area was maintained [93]. This effect may counteract the shortcoming of removals at high flow rates and explain the similar performances obtained at 150 m/yr and 1275 m/yr (Figure 13b, IIb vs. Ib, take into account the enhancement related to the electrode configuration of C – BPE – A) [94].

This comparison of findings on the observed influences of various electrochemical and reactor design parameters on chlorinated ethene removal illustrate the complexity of electrochemical removal. Just as contaminated site characteristics vary and require adaption of remediation strategies, each reactor design needs adjustments for optimal operating conditions. The mechanisms controlling the contaminant removal need to be studied in detail to enhance the understanding of upscaling. Further, when evaluating the performances of electrochemical reactors, it is important to evaluate the actual contaminant concentration reached downgradient the electrochemical zone, since the purpose is to comply with the regulatory maximum contaminant levels. E.g., the >99% TCE removal obtained with the reactor design by Rajic et al. [55] (Figure 12, Ib) appears better than the design resulting in a PCE removal of $81 \pm 7\%$ (Figure 12, IIIb). However, the inlet contaminant concentrations tested were different and the resulting concentrations post-treatment were app. 50 $\mu\text{g/l}$ and $7.8 \pm 2.3 \mu\text{g/l}$, respectively. Thus, based on the specific contaminant concentrations reached downgradient the electrochemical zone, the design applied in this project (Appendix V) is preferable.

5 SIGNIFICANCE OF FIELD-PARAMETERS ON ELECTROCHEMICAL PERFORMANCE

The studies on electrochemical design parameters carried out in undivided flow-through reactors with sandy sediment and/or field-extracted groundwater indicated complex changes in the hydrogeochemistry (Appendix I-II, Supporting note I). To understand the influence of field-realistic settings on electrochemical removal of chlorinated ethenes, field-parameters were stepwise added to the electrochemical reactor in Figure 7 in the order of field-realistic flow rate (Section 5.1), field-extracted groundwater containing an aged contamination of PCE (Section 5.2), sandy sediment (Section 5.3) and finally testing at temperatures similar to that in groundwater aquifers (Section 5.4) (Appendix V). This stepwise approach of increased realism is illustrated in Figure 14.

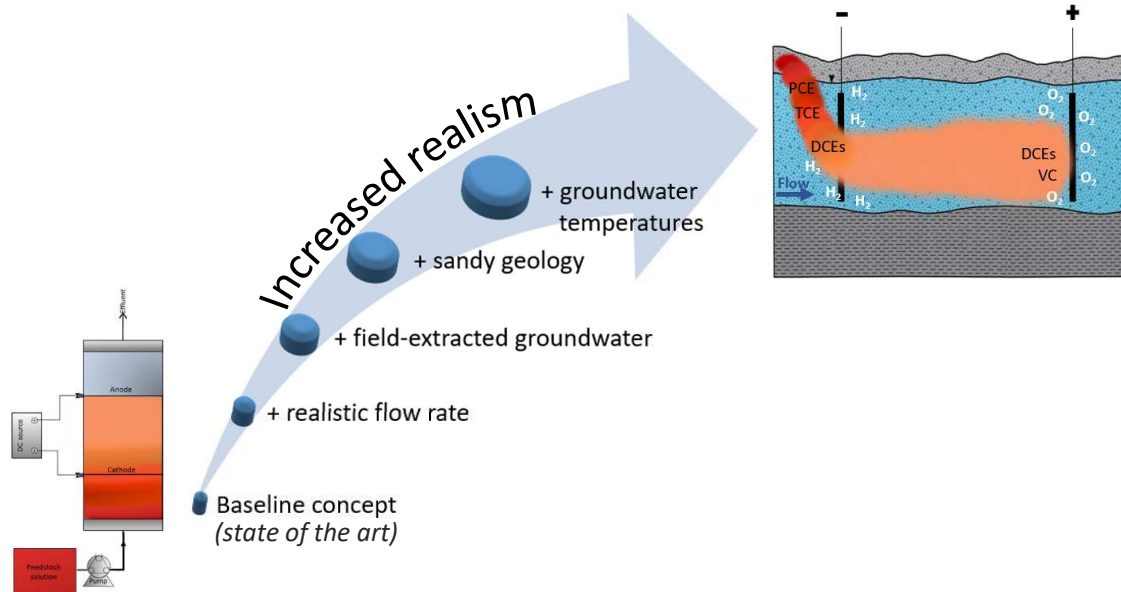


Figure 14. Illustration of the stepwise addition of field-parameters to the electrochemical reactor in the assessment of electrochemical removal of chlorinated ethenes in field-realistic systems.

A discussion on electrochemically induced chlorinated ethene degradation pathways in field-realistic systems is given in Section 5.5, induced hydrogeochemical changes are compiled in Section 5.6, and an overview of the electrochemical performance in field-realistic systems is presented in Section 5.7.

5.1 FIELD-REALISTIC FLOW RATE

The field-realistic seepage velocity studied was 150 m/yr for synthetic groundwater flowing through a porous matrix of glass beads in the horizontally oriented electrochemical reactor designed with a C – BPE – A (Pd/Fe foam – MMO mesh – MMO mesh) electrode configuration, 4 cm electrode spacing, a Pd load of 1.33 mg/cm² and operated at a constant current of 120 mA (Figure 7, Appendix V). A control test without application of current showed no mass loss of PCE. The electrochemically induced removal of PCE at a field-realistic flow rate was 50±8.6%. Final concentrations reached were 17.5±3.0 µg/l. I.e. the reactor was not optimized for complete removal, which based on the findings in literature (Table 1) and observed trends in influence of reactor design (Chapter 4) is considered possible. Trichloromethane/chloroform (TCM) was the only chlorinated contaminant species accumulating downgradient the electrochemical zone, reaching concentrations of 28.6±26.4 µg/l. TCM formed near the anode, with decreasing concentrations over time by 57.3±30.6%. The potential difference stabilized at 24±2V.

5.2 FIELD-EXTRACTED GROUNDWATER WITH AN AGED CONTAMINATION

The synthetic groundwater was replaced with field-extracted groundwater containing an aged contamination of PCE. The resulting removal of PCE was 70±9% with concentrations measured downgradient the electrochemical zone of 13±4 µg/l. TCE and cis-DCE were removed completely. I.e. testing in groundwater with complex chemistry improved the PCE removal with a concurrent treatment of the chlorinated intermediates in the aged contamination. Thus, individual groundwater species may compete with the chlorinated ethenes for reduction and/or oxidation or enhance the removal, as suggested in literature [54,56–58,60,82], but the net result of the species found in the groundwater in this study was an overall enhanced removal. The isolated effect of field-extracted groundwater and/or a mixed composition of chlorinated ethenes on the application of electrochemical degradation in undivided flow-through reactors without the influence of a geological material has not been reported elsewhere. TCM formation was observed near the anode, reaching concentrations downgradient the electrochemical zone of 52.3±12.7 µg/l with a tendency of decreasing concentrations over time by 17.1±17.1%. The conductivity of the field-extracted groundwater was lower than that of the synthetic groundwater. Consequently, the potential difference was elevated and stabilized at 113±23 V.

5.3 SANDY AQUIFER GEOLOGY

When proceeding with the field-extracted groundwater, but replacing the inert porous matrix with sandy sediment, the PCE removal observed was $81\pm 7\%$ reaching PCE concentrations of 7.8 ± 2.3 $\mu\text{g/l}$. TCE and cis-DCE were completely removed. Compared with the simple system of synthetic groundwater and glass beads, the enhanced PCE removal for application in sandy sediment is statistically significant, while the trend of enhancement when compared with the electrochemical application in field-extracted groundwater and glass beads is not statistically significant. The trend of enhancement could be due to a lower gas intrusion into the sandy sediment compared to glass beads, as previously discussed (Section 4.2.3). At least, the removal trend indicated, that the added complexity of geochemistry was not inhibiting the governing chlorinated ethene removal processes and that lower PCE concentrations could be reached. The PCE removal obtained in the sandy sediment was similar to the removal of 85% observed when using an electrode configuration of C – C – A in the sandy sediment at a flow rate of 61 m/yr (Figure 10, IIIb, Appendix I). Few studies have assessed electrochemical removal of chlorinated ethenes in undivided flow-through reactors containing a geological matrix, but those who have reported TCE removal of app. 77% in sandy sediment operated at 20 V constant voltage [95] and app. 83% in limestone gravel at 60-90 mA [54,57]. In the present study, elevated TCM formation was observed in the sandy sediment near the anode with decreasing concentrations over time by $38.7\pm 2.2\%$. The TCM concentrations were 385 ± 60 $\mu\text{g/l}$ at the conclusion of the test, i.e. app. seven times higher than when applying the electrochemistry in field-extracted groundwater flowing through glass beads. The electrical resistivity over the sandy sediment was lower than that of the glass beads, resulting in stabilization of the potential difference at a lower level of $62\pm 4\text{V}$, showing that the higher TCM concentration was not related to a higher resulting potential difference.

5.4 GROUNDWATER AQUIFER TEMPERATURES

The electrochemical application in field-extracted groundwater, containing an aged PCE contamination, and sandy sediment at field-realistic flow rates was combined with testing at natural groundwater aquifer temperatures of 8-10 °C. The resulting PCE removal was $74\pm 7.5\%$ with final concentrations of 19.3 ± 6.3 $\mu\text{g/l}$. TCE and cis-DCE were completely removed. The influence of reduced temperature on PCE removal was not statistically significant compared to testing in field-extracted groundwater flowing through both glass beads and sandy sediment, but

statistically enhanced the removal when compared to the simple system of synthetic groundwater and glass beads. The reduced temperatures were expected to reduce the removal performance, because the electrochemical method relies on chemical reactions, for which the reaction kinetics are temperature dependent [96,97]. The observed trend of a lower PCE removal obtained at temperatures of 8-10 °C compared to at 22 °C in sandy sediment indicate slowing reaction kinetics for the transformation of PCE at reduced temperatures. However, the PCE removals observed were not statistically significant. The influence on the removal from the lower temperature was less than anticipated.

Laboratory studies on electrochemical remediation in such field-realistic settings of a realistic flow rate, field-extracted and contaminated groundwater, sandy sediment and temperatures of 8-10 °C has not been reported elsewhere. One field-application has been carried out in which electrode meshes were installed as a physical barrier throughout a TCE plume and operated at constant voltage (Figure 2) [52]. Highest removal observed was 90% at 6.5V, reaching concentrations of 5 µg/l downgradient the electrochemical zone. Over time, TCM was detected immediately downgradient the electrochemical barrier in concentrations of app. 3250 µg/l, but the concentration decreased over time and distance to below detectable levels at 4 m downgradient the electrochemical barrier [52]. In the present study, TCM formed near the anode with final concentrations of 445±10 µg/l and decreased over time by 15±6%. The potential difference stabilized at 60±2V, i.e. was unaffected by the reduced temperature.

5.5 ELECTROCHEMICAL DEGRADATION PATHWAYS IN FIELD-REALISTIC SYSTEMS

Redox zones in the electrochemical reactor consisted of a reducing zone around the cathode, mixed redox zone around the BPE and an oxidizing zone around the anode, which may have stimulated several degradation pathways (Section 1.2.2). The chlorinated ethene removals were assessed throughout the reactors of stepwise more complex and field-realistic systems, revealing different dominant removal mechanisms depending on the nature of the porous matrix and the resulting distribution of electrochemically generated H₂O₂ (Figure 15). For the tests using glass beads, with synthetic groundwater or field-extracted groundwater at a typical groundwater flow rate, H₂O₂ was distributed throughout the electrochemical reactors (Figure 15, Δ-□). Thereby, the reducing zone of the cathodes were destroyed, facilitating indirect oxidation as the major PCE removal pathway in glass beads. In sandy sediment, the H₂O₂ distribution was limited to the vicinity of the anode (Figure 15, ○-◇), shifting the PCE removal mechanisms towards mainly

reduction. H_2O_2 was not detected in any of the tests prior to the electrochemical application. The maximum generated levels of H_2O_2 were similar for application in glass beads and sandy sediment and stoichiometrically capable of oxidizing 12 mg/l PCE, while theoretically, 0.5 mg/l H_2O_2 was sufficient for obtaining complete PCE removal in the concentration tested. In all the tests conducted, complete removal of TCE and cis-DCE was a result of reduction and/or oxidation. In sandy sediment, the TCE and cis-DCE concentrations were gradually decreasing as the groundwater passed through the reducing zone of the cathode followed by the oxidizing zone of the anode.

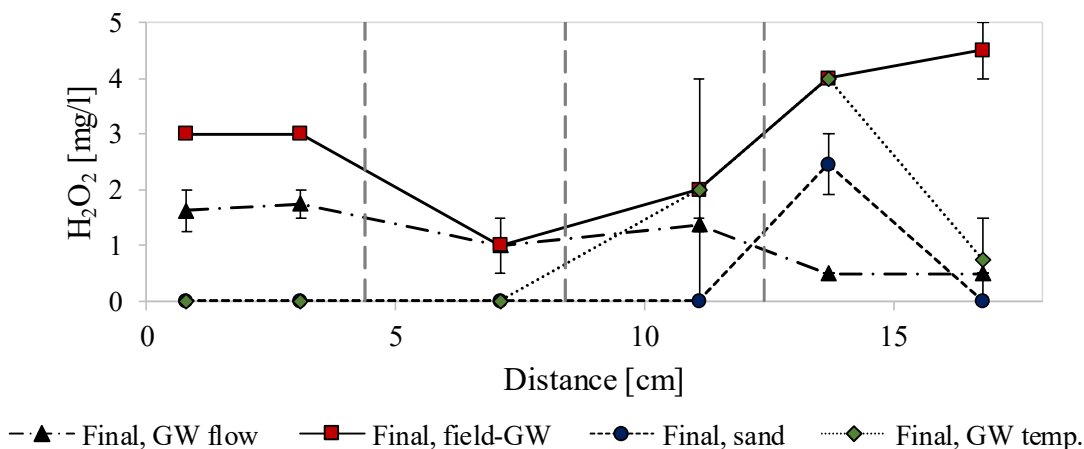


Figure 15. Concentrations of electrochemically generated H_2O_2 throughout the electrochemical reactor influenced by a field-realistic flow rate of synthetic groundwater through glass beads (Δ), field-extracted groundwater flowing through glass beads (\square), field-extracted ground-water in sandy sediment (\circ), and field-extracted groundwater flowing through sandy sediment at groundwater aquifer temperatures (\diamond).

Error bars are based on duplicate testing. Figure adapted from Appendix V.

With the reactor design applied, it was not possible to distinguish between direct or indirect reduction, while indirect abiotic oxidation via H_2O_2 was plausible. Reduction appeared more efficient for PCE removal based on the tendency of enhanced removal with increasingly complex field-realistic settings, and limited distribution of H_2O_2 (Figure 15). Comparing with the reduction and oxidation potentials listed in Table 5, abiotic PCE reduction is energetically preferred over abiotic oxidation. PCE removals observed when applying electrode rods (Appendix I-II, Supporting note I) and when using Pd coated cathodes (Figure 9) [69,77] suggest indirect reduction rather than direct reduction. With no formation of chlorinated ethene intermediates, reduction was either complete or followed the β -elimination pathway via (chlorinated) acetylenes (Figure 3). Finally, biotic activity due to a natural presence of degrading cultures, e.g. *Dehalococcoides*, in the field-extracted groundwater [98] could contribute to the removals

observed, based on previous indications of biotic activity (Supporting note I-II) and studies on bio-electrochemical reactors [50,70,71,73,99].

In closed experimental set-ups, as the ones designed in this project, mass should be conserved despite of volatilization, transformation, sorption, precipitation etc. Chloride is a good tracer in the balancing of mass. The mass conservation of chloride in the performed electrochemical experiments (summing aqueous and gaseous Cl in VOCs and free Cl⁻) was highest in the reactors of glass beads and synthetic groundwater (97 %), while lowest in the most complex system of field-extracted groundwater, sandy sediment and testing at groundwater temperatures (85±3.6%) (Appendix V). The lower mass conservation in complex systems may be explained by conversion of naturally present Cl⁻ into chlorinated species, which were not included in the analytical scheme, e.g. ClO⁻, ClO₃⁻, HClO, ClO₄⁻, Cl₂ [69,100–102]. Similar recoveries of Cl are reported for electrochemical removal of TCE [49,60]. In this study, the measured mass loss through volatilization of chlorinated contaminant species accounted for 0.10±0.05% of the removals (Appendix V), i.e. stripping was insignificant. Less than 1% stripping was also observed by Sale et al. [52].

The formation of TCM near the anode cannot be linked to a known direct transformation pathway from chlorinated ethenes to TCM. Since, the observed formation of TCM was significantly enhanced during electrochemical testing in the sandy sediment, and the concentrations exceeded what could be stoichiometrically accounted for by chlorinated ethene removal, the formation mechanism appears not to be related to the chlorinated ethene degradation. Sale et al. [52] suggested that the observed TCM formation in their electrochemical barrier was a result of oxidation of chloride to chlorine, subsequently reacting with organic compounds in the adhesives used in the construction process. However, only low levels of organic compounds are expected to be introduced in the assembly of the reactors used in the present study. Instead, naturally present organic matter in the sandy sediment is suggested to react with possibly formed chlorine, as indicated in the literature [101,103–106]. A significant stimulation of TCM formation by presence of organic matter in the sediment can also explain a) the decreasing TCM concentrations over time, since the content of organic matter within the electrochemical zone was presumably exhausted locally over time, b) the limited distribution of H₂O₂ observed during testing in the sandy sediment due to oxidation of organic matter in the sediment (Figure 15), and c) the lower TCM concentrations formed during the tests using glass beads. The low concentrations of TCM formed in tests using glass beads may be due to a residue of sandy sediment in the column reactor

after cleaning, and traces of organic matter in construction components used [52], e.g. O-rings, silicone grease and/or in tubing. The decreasing concentrations of TCM over time may also be due to electrochemical removal of TCM itself [107–111].

5.6 ELECTROCHEMICALLY INDUCED HYDROGEOCHEMICAL CHANGES

The evaluation of changes in the hydrogeochemistry due to electrochemical application is based on observations in the studies incorporating field-extracted groundwater and sandy sediment (Appendix I-II,V, Supporting note I). An immediate change when applying electrochemistry was local alterations in pH and conductivity and not only in the vicinity of the electrodes (Figure 16). When applying electrochemistry in glass beads and synthetic or field-extracted groundwater, pH was elevated upgradient the electrochemical zone (Figure 16, Δ -□, 0-3 cm) and decreased downgradient the electrochemical zone (Figure 16, Δ -□, 14-16 cm). For the applications in the sandy sediment, the pH remained neutral up- and downgradient the electrochemical zone (Figure 16, \circ -◇), indicating a poorer distribution within the sandy sediment of the OH^- and H^+ formed, and buffering of the H^+ formed from the content of calcium carbonate in the sandy sediment. The ionic conductivity increased downgradient the electrochemical zone when applied in glass beads, while recovered to pre-treatment levels when applied in sandy sediment (Figure 16, Δ -□ vs. \circ -◇, 14-16 cm). This deviation possibly is related to the different buffering capacities for the H^+ formed, which was highest in the sandy sediment. The significant increase in conductivity near the cathode for electrochemical application in sandy sediment (Figure 16, \circ -◇, 7 cm) could be due to dissolution of other minerals in the sandy sediment (presumably silicates [112]) at the high pH of 12 and re-precipitation in the lower pH region of the anode.

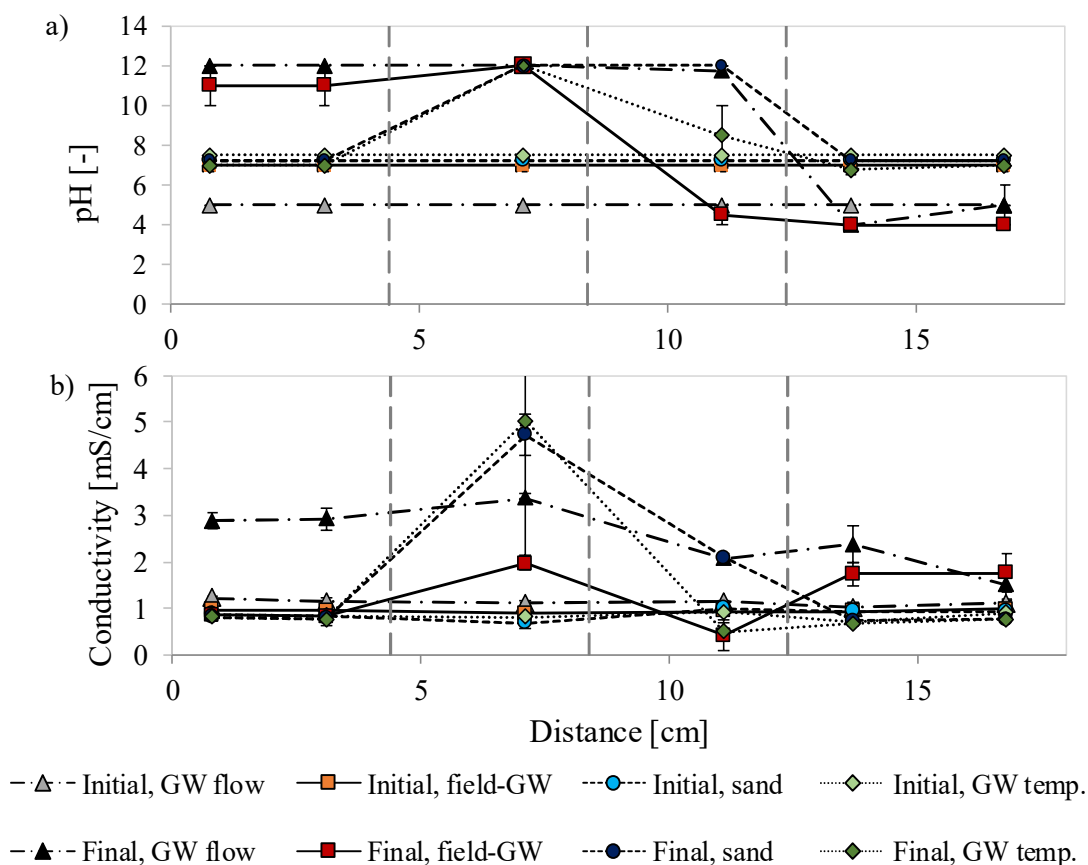


Figure 16. Changes in a) pH and b) conductivity throughout the electrochemical reactor under influence of a field-realistic flow rate of synthetic groundwater through glass beads (Δ), field-extracted groundwater flowing through glass beads (\square), field-extracted groundwater in sandy sediment (\circ), and field-extracted groundwater flowing through sandy sediment at groundwater aquifer temperatures (\diamond). Initial levels, prior to electrochemical application (light colors), and final levels, measured at conclusion of the electrochemical application (dark colors), are included. Error bars are based on duplicate testing. Figure adapted from Appendix V.

Changes in the porewater chemistry within the electrochemical zone was observed in the studies using field-extracted groundwater and sandy sediment. Major ionic species included Ca, Mg, K, Na, SO_4^{2-} , Cl^- and NO_3^- . The concentrations of Ca, Mg and K decreased near the cathode and increased near the anode. For Ca and Mg, it was suggested, that colloids formed near the cathode, which flowed with the groundwater towards the anode and dissolved (Appendix I). The changes in K concentration could be due to cation exchange (Appendix I). Electromigration towards the cathode of initially present and formed Ca^{2+} , Mg^{2+} and K^+ was likely. The Na concentration increased near the cathode and decreased near the anode, suggesting electromigration against the groundwater flow direction towards the cathode. A similar finding was observed by Pamukcu et

al. [113]. The concentrations of SO_4^{2-} , Cl^- and NO_3^- decreased near the cathode and increased near the anode, which could be explained by reduction and subsequent oxidation (Appendix I) and/or electromigration. Concentration build-up of Cl^- near the anode could promote formation of the reactive oxidative species ClO_3^- , ClO_4^- and $\text{Cl}_{2(g)}$ (Section 1.2.3) [69]. An illustration of the observed fate of hydrogeochemical species within the electrochemical reactor is shown in Figure 17.

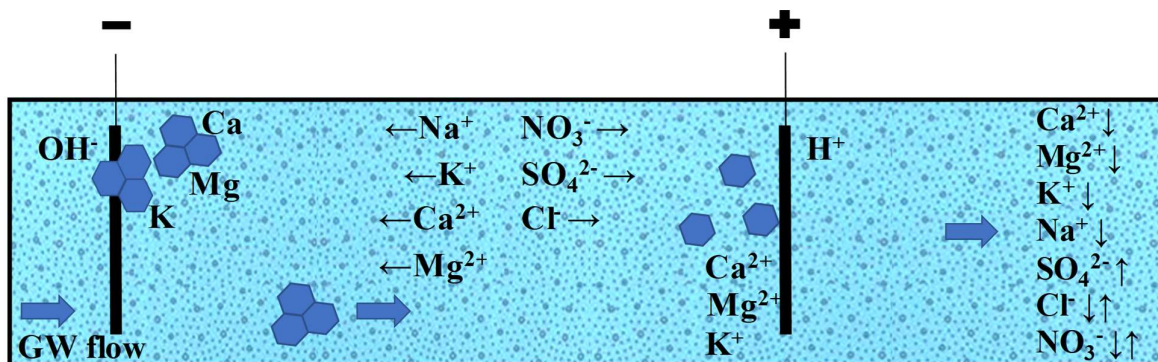


Figure 17. Schematic of possible formation of colloids and ion exchange (Ca, Mg, K) at the cathode (-), colloid dissolution at the anode (+), electromigration of Na^+ , K^+ , Ca^{2+} , Mg^{2+} , NO_3^- , SO_4^{2-} and Cl^- , and the overall change in concentration (\downarrow decrease, \uparrow increase) downgradient the electrochemical zone in field-extracted groundwater and sandy sediment. The electrochemical reactor is illustrated with an electrode configuration of C – A. The diagram is based on findings in the studies presented in Appendix I-II, V and Supporting note I.

Changes in porewater composition in one redox zone of the electrochemical reactor appeared to be counterbalanced in the following redox zone of opposite conditions. However, overall changes in the porewater chemistry was observed: Ca, Mg, K and Na decreased in concentration, SO_4^{2-} increased, while Cl^- and NO_3^- showed no clear trend (Figure 17). Decreasing concentrations suggest precipitation, while increases could be due to dissolution of minerals. Cation exchange is also expected within the sandy sediment (Appendix I). Specifically for Cl^- , decreasing concentrations close to the anode could also indicate formation of e.g. $\text{Cl}_{2(g)}$. Furthermore, the content of calcium carbonate in the sandy sediment may decrease due to buffering for the acid generated at the anode (Section 5.6). The content of organic matter in the sandy sediment may decrease due to oxidation forming TCM (Section 5.5). Decreasing concentrations of Ca due to calcite formation was also observed during field-application of the electrode barrier [52], where the decreasing Ca concentrations were limited to the vicinity of the electrode barrier, and the concentrations recovered to pre-treatment levels at 0.5 m downgradient to the electrode barrier.

5.7 OVERVIEW OF ELECTROCHEMICAL PERFORMANCE IN FIELD-REALISTIC SYSTEMS

With the research performed, it was found that complex settings approaching that of a contaminated site improved the electrochemical performance in term of chlorinated ethene removal when compared to tests using simple settings of synthetic groundwater and glass beads. An overview of the removals obtained with increasing system complexity is shown in Figure 18. If the reactor with synthetic groundwater and glass beads had been optimized, which based on the findings in literature and the observed trends of influence of reactor design is possible (Table 1, Chapter 4), complete removal of chlorinated ethenes in field-realistic aquifer settings seems obtainable. Testing with electrode rods in similar complex systems at a low current intensity and a larger electrode spacing also demonstrated high removals (Figure 10, IIIb vs. Ia, Appendix I).

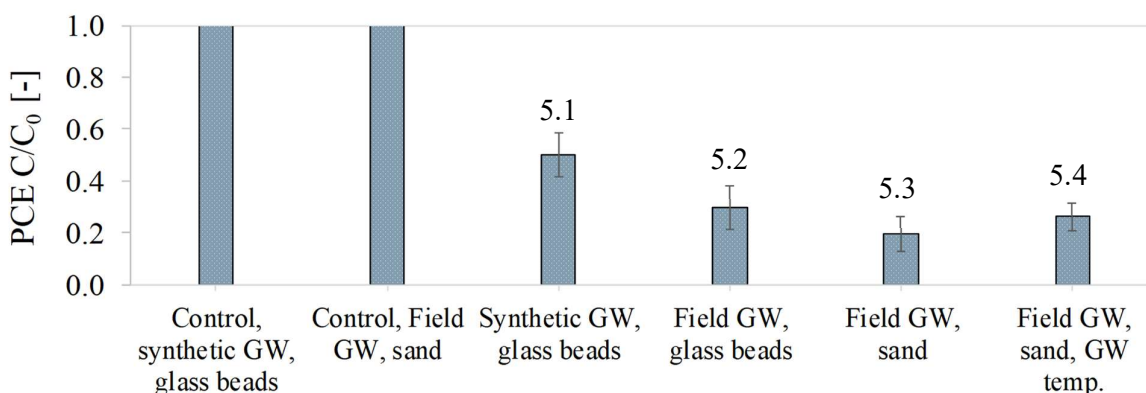


Figure 18. PCE removals, given as a fraction of final concentration (C) over initial concentration (C_0), obtained in electrochemical reactors of increasing complexity and thereby realism. Error bars are based on duplicate testing. Figures above bars refer to the specific sections describing the tests. Figure adapted from Appendix V.

Normalizing the current intensity against flow rate and final PCE concentrations reached in the studies performed, indicated that the lowest contaminant concentrations were the most time and power consuming to treat. The power consumed per volume of water treated during the electrochemical removal of chlorinated ethenes in the different experiments was estimated (Figure 19).

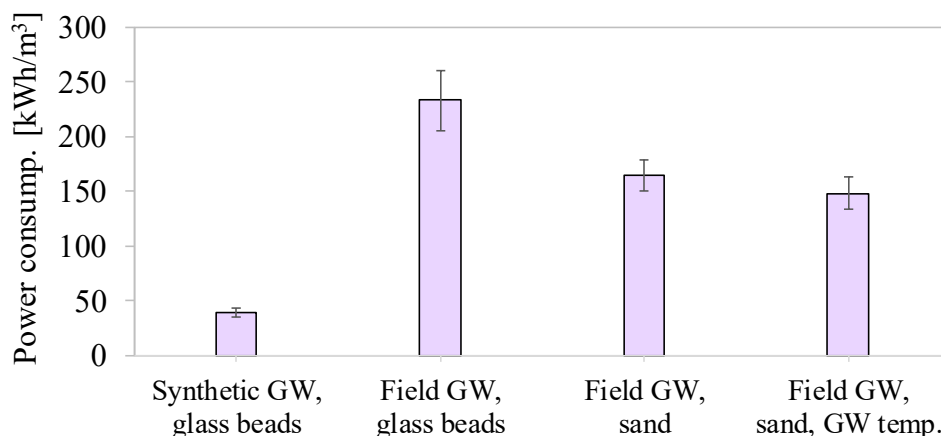


Figure 19. Power consumption of electrochemical removal of chlorinated ethenes in systems of increasing complexity and thereby realism at a constant current of 120 mA. GW; groundwater. Error bars are based on duplicate testing. Figure adapted from Appendix V.

According to Figure 19, the power consumption in the most complex system studied (realistic flow rate, field-extracted groundwater, sandy sediment, groundwater aquifer temperatures) at a constant current of 120 mA was 147 kWh/m³ water treated. The power consumed during electrochemical treatment in the completely water-filled box reactor at a constant current of 57 mA was 47 kWh/m³ of water treated. Since, the electrochemical remediation of chlorinated ethenes in groundwater plumes is in the development stage, the estimated power consumptions are expectedly high. Furthermore, scaling the power consumption from laboratory studies to field-scale is intricate. In comparison, the power consumption observed during field-application of the electrode barrier operated under constant voltage was 9.4 kWh/m³ treated [52]. The full-scale electrode barrier design is different from the concept studied in this project, but reported trends in chlorinated ethene removal, changes in hydrogeochemistry and power consumption are good indicators of what to expect during upscaling. With the trends in chlorinated ethene removal observed in complex systems in this study, and the reported power consumption of a field-implementation, the potential of electrochemical remediation is encouraging. A more detailed description of the perspectives of electrochemical remediation and suggestions to further actions are outlined in Chapter 6.

6 PERSPECTIVES OF ELECTROCHEMICAL TREATMENT OF CHLORINATED ETHENE PLUMES

The branch of electrochemical remediation studied in this project was sequential abiotic reduction and oxidation in undivided flow-through reactors aiming at controlling fluxes of chlorinated ethene contaminations in groundwater aquifers. To reduce cost and simplify the installation, the concept was to treat contaminated groundwater flowing in between the electrode wells via *in situ* formation and spreading of reactants, and establishment of suitable redox conditions. Depending on the extent of the groundwater plume, more sequences of electrodes can be installed. A drawing of this concept is shown in Figure 20.

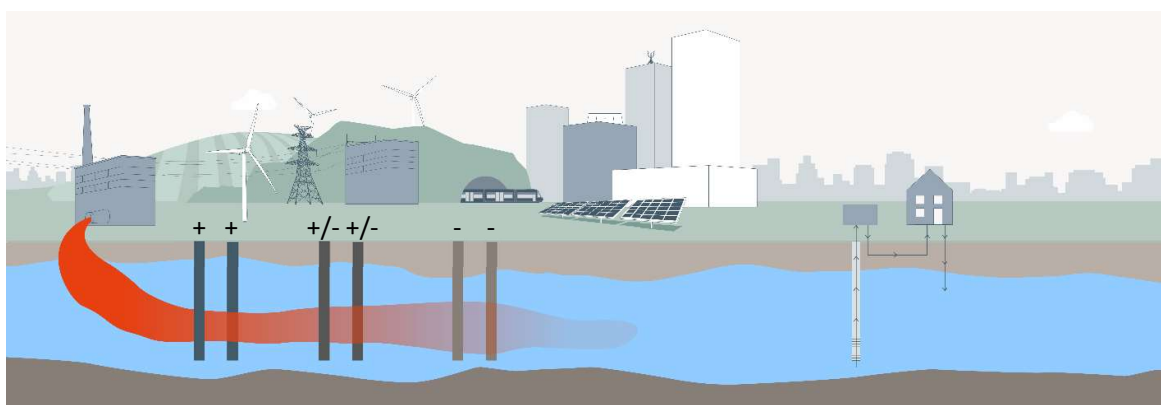


Figure 20. A conceptual illustration of *in situ* implementation of the electrochemical concept studied in this PhD project for management of chlorinated ethene plumes in high-permeable aquifers to e.g. protect drinking-water extraction areas. Copyright © COWI A/S.

Experiences gained with electrochemical application in realistic systems in this project point towards an encouraging potential of the method. As is the case for the current well-established remediation technologies, the electrochemical method also has its challenges. Some of the challenges are related to the early stage of development. Identified advantages and challenges are:

Advantages

- The method forms in a way a treatment train with a continuous supply and uptake of electrons: stimulating both abiotic and biotic reduction and oxidation. Therefore, concurrent treatment of mixtures of organic and inorganic contaminants, which challenge current remediation technologies, is possible if designed accordingly [39,40,42,51,52,69]. E.g., electrochemistry has also shown to have the ability to remove PFOS, PFOA, PFAAs [114–116], hydrocarbons [117,118], pesticides [119–121], metals [58,122] and other organics [123–125].

- The electrodes and thereby redox zones are installed where the treatment is needed, i.e. the method does not suffer from insufficient delivery of reactants, consumption of reactants before reaching the contamination or short longevity as sometimes can be the case for ISCO and PRB.
- It can be applied *in situ* in heterogeneous aquifers with minimal soil disruption [39–42], in contrast to thermal remediation [39,40,42]. Precipitation of groundwater species close to electrodes [39] can be dissolved by polarity reversals [40,42,51,52]. Changing the redox conditions locally during application is in common for e.g. the electrochemical method, ISCO and PRB. The technology infrastructure can be installed underground [42], allowing site-activities to continue as business as usual.
- Electrochemical remediation may be cost competitive if matured, where low operational costs and e.g. reuse of stable electrodes [40,69] compensate for installation costs [39,41,42,51,69]. Especially if used for treatment of complex mixtures of contaminants, which are expensive to treat with the current remediation options.
- Electrochemistry is a sustainable remediation alternative, which is not challenged by injection of chemicals [40,42,51,52], no/minimal secondary waste stream to be treated *ex situ* is generated [39,40], stimulation of biodegradation is possible, no residual product is left in the ground after treatment, which is the case for ISCO and PRB, and the power input required can be coupled with renewable energy sources [41,51,52,69].
- Additional redox sequences can be established to cover large plumes and enhance performance by installing more electrodes [51]. I.e., site-specific contaminant plume characteristics determine the amount of electrode sequences needed.
- Contaminant transformation rates and pathways can be remotely controlled by monitoring established potentials and adjusting the current input accordingly [40,51,52].

Current challenges

- Electrochemical transformation of contaminants is an immature technology and optimization requires collaboration between researchers and practitioners for the technology to become a viable and economical competitive alternative [42,51,52] and to overcome potential formation of undesirable compounds, e.g. TCM [51,69].
- Long-term performance of the electrochemical remediation requires further investigation. In addition, it needs to be assessed whether *in situ* electrochemical application is able to reach concentrations of chlorinated ethenes that comply with regulatory maximum

contaminant levels [42,52]. Pilot and full-scale implementations carried out by practitioners are rarely published [42], which hamper the development, exchange of experiences and identification of challenges.

- High concentrations of dissolved solids may impact the performance [52]. So may precipitation of species close to electrodes [39], if polarity reversal is not applied, which again influence the choice of electrode materials.
- Laboratory work is holding on to testing in simplified systems. Focus of testing should shift towards enhanced applicability and thereby use of e.g. field-extracted groundwater, aged contaminations and geological matrices. In addition, the impact on natural hydrogeochemistry and microbial communities should be assessed [42].

Most experiences with electrochemical remediation of chlorinated ethenes has been gained in laboratory studies. Some challenges from the lab will not be challenges in the field, e.g. venting for gases generated or leaking, but new challenges may arise in the field. Thus, there is a need for pilot-field testing to identify field-related challenges and for viable assessments of the real potential of *in situ* electrochemical degradation of chlorinated ethenes in groundwater plumes. Follow up on certain aspects and continued research in the lab should apply the undivided flow-through reactors and focus on:

- Measurements of the potentials established near the electrodes during testing in complex field-realistic systems to be able to tune in on the potentials suitable for chlorinated ethene reduction and oxidation. Based on obtained removals in the experiments conducted in field-realistic systems in this project at a low current of 12 mA and a low flow rate (Appendix I, Figure 10 IIIb), and seen in relation to other studies [55,60], the current intensity applied in the stepwise addition of field-realistic parameters of 120 mA (Appendix V) is possibly higher than needed. Potential measurements would clarify this. If the current intensity can be lowered, it is more cost efficient and may limit formation of TCM; Sale et al. [52] saw a limited TCM formation in the field when applying constant potentials < 6.5 V.
- Long-term performances in field-realistic systems (flow-through for minimum four pore volumes) to study the potential for complying with regulatory maximum contaminant levels and to identify potential challenges related to long-term performance, e.g. the need for short-term polarity reversal to dissolve precipitates on the cathode. If it turns out, that polarity

reversal is needed, use of stable cathodes, e.g. MMO should be studied, to avoid release of e.g. noble metals.

- The use of electrode rods or meshes cut to e.g. rectangles in field-realistic systems such that only a fraction of the contamination is flowing through the electrodes. This would mimic the design of a field-implementation better and could indicate whether the preferable indirect reduction and oxidation pathways are indeed dominating the contaminant removal. The test applying electrode rods in this project (Appendix I), demonstrated high chlorinated ethene removals in spite of a low current of 12 mA and significantly extended electrode spacings (Figure 10, IIIb). Removal performances at higher currents when using electrode rods look promising.

A different interesting aspect to assess, which is related to the holistic assessment of electrochemical remediation, is the use of fuel cells: If potentially escaping electrolytically generated O_2 and H_2 can be captured and converted into power via use of fuel cells, the method could to some extent be self-sustaining, reducing the costs and carbon footprint.

7 MAIN CONCLUSIONS

The potential of electrochemical zones for removal of chlorinated ethenes in systems simulating high-permeability aquifers was assessed in this PhD project. Reported experiences on e.g. material properties and degradation pathways were compiled and knowledge gaps focusing on applied electrochemistry identified. The main conclusions of the project are related to the performance of electrochemically stimulated PCE removal under influence of various reactor design parameters and complex field-realistic parameters towards field-application, and electrochemically induced changes in natural hydrogeochemistry.

Major conclusions related to the influence of electrochemical reactor design on PCE removal and induced changes in natural hydrogeochemical settings are:

- Application of electrode rods in complex field-realistic systems demonstrated high PCE removal performance at low current intensity and flow rate. This suggested, that the indirect reduction and oxidation pathways via electrochemically generated reactants within the reducing and oxidizing conditions established were responsible for the PCE removal.
- A redox sequence of reduction followed by oxidation in complex field-realistic systems was best suited for treatment of an aged contamination of PCE with degradation products. This sequence also disturbed the natural hydrogeochemistry less with local changes in conductivity and pH, but recovery of pre-treatment levels downgradient the treatment zone. Overall, naturally present Ca, Mg, K and Na decreased in concentration, SO_4^{2-} increased, while Cl^- and NO_3^- showed no clear trend.
- The electrochemical system's ability to release electrolytically generated gases influenced the performance: Gas coverage of the electrode surfaces, and thereby a reduction in the active electrode surface area, influenced the electrochemical performance at high current intensity, short electrode spacing, vertical reactor orientation and low flow rate. In addition, the electrochemical performance in a porous matrix with large pore spaces was to a larger extent impacted by gas intrusion into the pore spaces than porous matrices with smaller pores.

- Corrosion of Fe anodes during electrochemical application was significant and resulted in clogging of porous matrices, which outperformed the advantageous of using Fe anodes.
- The complex hydrogeochemistry of the field-realistic parameters studied stimulated significant formation of TCM through multistep reactions of oxidation of naturally present chloride and organic matter. Over time, TCM concentrations decreased.

The assessment of the influence of a field-realistic flow rate, field-extracted groundwater with an aged contamination of PCE, sandy sediment and groundwater aquifer temperatures on electrochemical removal of PCE overall showed:

- Highest PCE removals were obtained during electrochemical application in field-realistic systems in spite of competing redox reactions. PCE concentrations reached from at starting concentration of 50 µg/l were 7.8 ± 2.3 µg/l. Reduction transformation pathways were more efficient than the oxidation pathways for removal of PCE.
- Degradation products in the aged contamination of PCE were concurrently and completely removed and no chlorinated ethene intermediates accumulated. Volatilization of the chlorinated ethenes was insignificant.

This research project contributes with knowledge on mechanisms influencing the electrochemical removal of PCE, the performance in complex field-realistic aquifer settings, induced degradation pathways and changes in natural hydrogeochemistry. The outlined findings are promising for the prospective application of electrochemical redox zones for control of chlorinated ethene plumes in high-permeable aquifers.

REFERENCES

- [1] I. Mahmood, S.R. Imadi, K. Shazadi, A. Gul, K.R. Hakeem, Effects of pesticides on environment, in: K.R. Hakeem, M.S. Akhtar, S.N.A. Abdullah (Eds.), *Plant, Soil Microbes Vol. 1 Implic. Crop Sci.*, Springer International Publishing, Switzerland, 2016: pp. 253–269. doi:10.1007/978-3-319-27455-3.
- [2] N. Donley, The USA lags behind other agricultural nations in banning harmful pesticides, *Environ. Heal.* 18 (2019) 44–56. doi:10.1186/s12940-019-0488-0.
- [3] C. Rudén, Science and policy in risk assessments of chlorinated ethenes, *Ann. N. Y. Acad. Sci.* 1076 (2006) 191–206. doi:10.1196/annals.1371.046.
- [4] A.M. Ruder, Potential health effects of occupational chlorinated solvent exposure, *Ann. N. Y. Acad. Sci.* 1076 (2006) 207–227. doi:10.1196/annals.1371.050.
- [5] A. Cordner, V.Y. De La Rosa, L.A. Schaider, R.A. Rudel, L. Richter, P. Brown, Guideline levels for PFOA and PFOS in drinking water: the role of scientific uncertainty, risk assessment decisions, and social factors, *J. Expo. Sci. Environ. Epidemiol.* 29 (2019) 157–171. doi:10.1038/s41370-018-0099-9.
- [6] J.W.N. Smith, B. Beuthe, M. Dunk, S. Demeure, J.M.M. Carmona, A. Medve, M.J. Spence, T. Pancras, G. Schrauwen, T. Held, K. Baker, I. Ross, H. Slenders, Environmental fate and effects of polyand perfluoroalkyl substances (PFAS), *CONCAWE Reports*. (2016) 1–107.
- [7] WWAP (United Nations World Water Assement Programme), *The United Nations World Water Development Report 2015: Water for a Sustainable World*. Paris, UNESCO., (2015) 122. <http://unesdoc.unesco.org/images/0023/002318/231823E.pdf>.
- [8] M. Rolle, U. Maier, P. Grathwohl, Contaminant Fate and Reactive Transport in Groundwater, in: F.A. Swartjes (Ed.), *Deal. with Contam. Sites, From Theory Towar. Pract. Appl.*, Springer, Dordrecht, 2011: pp. 851–885. doi:10.1007/978-90-481-9757-6_19.
- [9] M.J. Moran, J.S. Zogorski, P.J. Squillace, Chlorinated solvents in groundwater of the United States, *Environ. Sci. Technol.* 41 (2007) 74–81. doi:10.1021/es061553y.
- [10] K. Wolf, T.W. Chesnutt, Chlorinated solvents: Market interactions and regulation, *J. Hazard. Mater.* 15 (1987) 137–161. doi:10.1016/0304-3894(87)87033-4.
- [11] J.F. Pankow, S. Feenstra, J.A. Cherry, C.M. Ryan, *DENSE CHLORINATED SOLVENTS and other DNAPLs in Groundwater: History, Behavior, and Remediation*, Waterloo Press, Portland, Oregon, 1996.
- [12] *Garner Insights, 2013-2028 Report on Global C2 Chlorinated Solvents Market by Player, Region, Type, Application and Sales Channel*, 2018. <https://garnerinsights.com/Global-C2-Chlorinated-Solvents-Market-Insights-Forecast-to-2025>.
- [13] X. Maymó-gatell, Y. Chien, J.M. Gossett, S.H. Zinder, Isolation of a Bacterium That Reductively Dechlorinates Tetrachloroethene to Ethene, *Science*. 276 (1997) 1568–1571. doi:10.1126/science.276.5318.1568.
- [14] B. Van Der Zaan, F. Hannes, N. Hoekstra, H. Rijnaarts, W.M. De Vos, H. Smidt, J. Gerritse, Correlation of Dehalococcoides 16S rRNA and chloroethene-reductive dehalogenase genes with geochemical conditions in chloroethene-contaminated groundwater, *Appl. Environ. Microbiol.* 76 (2010) 843–850. doi:10.1128/AEM.01482-09.

- [15] C. Scheutz, N.D. Durant, P. Dennis, M.H. Hansen, T. Jørgensen, R. Jakobsen, E.E. Cox, P.L. Bjerg, Concurrent ethene generation and growth of *Dehalococcoides* containing vinyl chloride reductive dehalogenase genes during an enhanced reductive dechlorination field demonstration, *Environ. Sci. Technol.* 42 (2008) 9302–9309. doi:10.1021/es800764t.
- [16] D.E. Fennell, J.M. Gossett, S.H. Zinder, Comparison of butyric acid, ethanol, lactic acid, and propionic acid as hydrogen donors for the reductive dechlorination of tetrachloroethene, *Environ. Sci. Technol.* 31 (1997) 918–926. doi:10.1021/es960756r.
- [17] P.K.H. Lee, D. Cheng, K.A. West, L. Alvarez-Cohen, J. He, Isolation of two new *Dehalococcoides mccartyi* strains with dissimilar dechlorination functions and their characterization by comparative genomics via microarray analysis, *Environ. Microbiol.* 15 (2013) 2293–2305. doi:10.1111/1462-2920.12099.
- [18] X. Maymó-Gatell, T. Anguish, S.H. Zinder, Reductive Dechlorination of Chlorinated Ethenes and 1,2-Dichloroethane by “*Dehalococcoides ethenogenes*” 195, *Appl. Environ. Microbiol.* 65 (1999) 3108–3113.
- [19] A.C. Heimann, A.K. Friis, C. Scheutz, R. Jakobsen, Dynamics of reductive TCE dechlorination in two distinct H₂ supply scenarios and at various temperatures, *Biodegradation.* 18 (2007) 167–179. doi:10.1007/s10532-006-9052-z.
- [20] WHO, World Health Organization (WHO), Int. Program. Chem. Saf. - Environ. Heal. Criteria. (2019). <https://www.who.int/ipcs/publications/ehc/en/> (accessed June 22, 2019).
- [21] US Environmental Protection Agency of Water, 2018 Edition of the Drinking Water Standards and Health Advisories; EPA 822-F-18-001, Washington, DC, USA, 2018.
- [22] Miljøstyrelsen (Danish EPA), Liste over kvalitetskriterier i relation til forurennet jord og kvalitetskriterier for drikkevand, June (2015) 1–13. doi:10.1002/0471743984.vse9126.
- [23] B.L. Parker, J.A. Cherry, S.W. Chapman, M.A. Guilbeault, Review and Analysis of Chlorinated Solvent Dense Nonaqueous Phase Liquid Distributions in Five Sandy Aquifers, *Vadose Zo. J.* 2 (2003) 116–137. doi:10.2136/vzj2003.1160.
- [24] B.H. Kueper, G.P. Wealhall, J.W.N. Smith, S.A. Leharne, D.N. Lerner, An illustrated handbook of DNAPL transport and fate in the subsurface - Environment Agency R&D Publication 133, Environment Agency, Bristol, UK, 2003. <http://www.environment-agency.gov.uk>.
- [25] D.M. Mackay, J.A. Cherry, Groundwater contamination: Pump-and-treat remediation, *Environ. Sci. Technol.* 23 (1989) 630–636. doi:10.1021/es00064a001.
- [26] Interstate Technology & Regulatory Council, Integrated DNAPL Site Strategy, Washington, DC, USA, 2011. <http://www.itrcweb.org>.
- [27] B.H. Kueper, H.F. Stroo, C.M. Vogel, C.H. Ward, Chlorinated Solvent Source Zone Remediation, Springer, New York, USA, 2014. doi:10.1007/978-1-4614-6922-3.
- [28] R.L. Siegrist, M. Crimi, M.M. Broholm, J.E. McCray, T.H. Illangasekare, P.L. Bjerg, Advances in Groundwater Remediation: Achieving Effective In Situ Delivery of Chemical Oxidants and Amendments, in: F.F. Quercia, D. Vidojevic (Eds.), *Clean Soil Safe Water*, Springer, Dordrecht, The Netherlands., 2012: pp. 197–212. doi:10.1007/978-94-007-2240-8_22.
- [29] Interstate Technology & Regulatory Council, Permeable Reactive Barriers: Lessons Learned/New Directions. PRB-4, Washington, DC, USA, 2005.

-
- [30] Y.T. He, J.T. Wilson, C. Su, R.T. Wilkin, Review of Abiotic Degradation of Chlorinated Solvents by Reactive Iron Minerals in Aquifers, *Groundw. Monit. Remediat.* 35 (2015) 57–75. doi:10.1111/gwmr.12111.
 - [31] M.H. Stenzel, U. Sen Gupta, Treatment of Contaminated Groundwaters with Granular Activated Carbon and Air Stripping, *J. Air Pollut. Control Assoc.* 35 (1985) 1304–1309. doi:10.1080/00022470.1985.10466035.
 - [32] D.H. Bass, N.A. Hastings, R.A. Brown, Performance of air sparging systems: a review of case studies, *J. Hazard. Mater.* 72 (2000) 101–119. doi:10.1016/S0304-3894(99)00136-3.
 - [33] H.F. Stroo, A. Leeson, J.A. Marqusee, P.C. Johnson, C.H. Ward, M.C. Kavanaugh, T.C. Sale, C.J. Newell, K.D. Pennell, C.A. Lebrón, M. Unger, Chlorinated Ethene Source Remediation: Lessons Learned, *Environ. Sci. Technol.* 46 (2012) 6438–6447. doi:10.1021/es204714w.
 - [34] C. Scheutz, M.M. Broholm, N.D. Durant, E.B. Weeth, T.H. Jørgensen, P. Dennis, C.S. Jacobsen, E.E. Cox, J.C. Chambon, P.L. Bjerg, Field evaluation of biological enhanced reductive dechlorination of chloroethenes in clayey till, *Environ. Sci. Technol.* 44 (2010) 5134–5141. doi:10.1021/es1003044.
 - [35] F. Aulenta, A. Pera, S. Rossetti, M. Petrangeli Papini, M. Majone, Relevance of side reactions in anaerobic reductive dechlorination microcosms amended with different electron donors, *Water Res.* 41 (2007) 27–38. doi:10.1016/j.watres.2006.09.019.
 - [36] D. O'Connor, D. Hou, Y.S. Ok, Y. Song, A.K. Sarmah, X. Li, F.M.G. Tack, Sustainable in situ remediation of recalcitrant organic pollutants in groundwater with controlled release materials: A review, *J. Control. Release.* 283 (2018) 200–213. doi:10.1016/j.jconrel.2018.06.007.
 - [37] K. Urano, E. Yamamoto, M. Tonegawa, K. Fujie, Adsorption of chlorinated organic compounds on activated carbon from water, *Water Res.* 25 (1991) 1459–1464. doi:10.1016/j.arabjc.2015.04.013.
 - [38] H.F. Stroo, C.H. Ward, *In Situ Remediation of Chlorinated Solvent Plumes*, Springer, New York, NY, 2010. doi:10.1007/978-1-4419-1401-9.
 - [39] A.B. Ribeiro, E.P. Mateus, *Electrokinetics Across Disciplines and Continents, New Strategies for Sustainable Development*, Springer, London, 2016. doi:10.1007/978-3-319-20179-5.
 - [40] A.N. Alshawabkeh, Electrokinetic soil remediation: Challenges and opportunities, *Sep. Sci. Technol.* 44 (2009) 2171–2187. doi:10.1080/01496390902976681.
 - [41] A.T. Lima, A. Hofmann, D. Reynolds, C.J. Ptacek, P. Van Cappellen, L.M. Ottosen, S. Pamukcu, A.N. Alshawabkeh, D.M. O'Carroll, C. Riis, E. Cox, D.B. Gent, R. Landis, J. Wang, A.I.A. Chowdhury, E.L. Secord, A. Sanchez-Hachair, Environmental Electrokinetics for a sustainable subsurface, *Chemosphere.* 181 (2017) 122–133. doi:10.1016/j.chemosphere.2017.03.143.
 - [42] K.R. Reddy, C. Cameselle, *Electrochemical remediation technologies for polluted soils, sediments and groundwater*, John Wiley & Sons, Inc., Hoboken, New Jersey, 2009.
 - [43] B.H. Hansen, L.W. Nedergaard, L.M. Ottosen, C. Riis, M.M. Broholm, Experimental design for assessment of electrokinetically enhanced delivery of lactate and bacteria in 1,2-cis-dichloroethylene contaminated limestone, *Environ. Technol. Innov.* 4 (2015) 73–81. doi:10.1016/j.eti.2015.04.006.
 - [44] Y.B. Acar, A.N. Alshawabkeh, Principles of Electrokinetic Remediation, *Environ. Sci. Technol.* 27 (1993) 2638–2647. doi:10.1021/es00049a002.
-

- [45] J.-W. Moon, H.-S. Moon, H. Kim, Y. Roh, Remediation of TCE-contaminated groundwater using zero valent iron and direct current: experimental results and electron competition model, *Environ. Geol.* 48 (2005) 805–817. doi:10.1007/s00254-005-0023-1.
- [46] C.C. Liu, S.F. Liao, D.H. Tseng, Effects of the electrode arrangements on reductive dechlorination of trichloroethylene in an electro-enhanced iron wall, *Environ. Technol.* 27 (2006) 683–693. doi:10.1080/09593332708618681.
- [47] M.Z. Wu, D.A. Reynolds, A. Fourie, H. Prommer, D.G. Thomas, Electrokinetic in situ oxidation remediation: Assessment of parameter sensitivities and the influence of aquifer heterogeneity on remediation efficiency, *J. Contam. Hydrol.* 136–137 (2012) 72–85. doi:10.1016/j.jconhyd.2012.04.005.
- [48] X. Mao, J. Wang, A. Ciblak, E.E. Cox, C. Riis, M. Terkelsen, D.B. Gent, A.N. Alshawabkeh, Electrokinetic-enhanced bioaugmentation for remediation of chlorinated solvents contaminated clay, *J. Hazard. Mater.* 213–214 (2012) 311–317. doi:10.1016/j.jhazmat.2012.02.001.
- [49] X. Mao, A. Ciblak, M. Amiri, A.N. Alshawabkeh, Redox Control for Electrochemical Dechlorination of Trichloroethylene in Bicarbonate Aqueous Media, *Environ. Sci. Technol.* 45 (2011) 6517–6523. doi:10.1021/es200943z.
- [50] F. Aulenta, L. Tocca, R. Verdini, P. Reale, M. Majone, Dechlorination of Trichloroethene in a Continuous-Flow Bioelectrochemical Reactor: Effect of Cathode Potential on Rate, Selectivity, and Electron Transfer Mechanisms, *Environ. Sci. Technol.* 45 (2011) 8444–8451. doi:10.1021/es202262y.
- [51] D. Gilbert, T. Sale, M.A. Petersen, Electrolytic reactive barriers for chlorinated solvent remediation, in: H.F. Stroo, C.H. Ward (Eds.), *Situ Remediation of Chlorinated Solvent Plumes*, Springer, New York, USA, 2010: pp. 573–590. doi:10.1007/978-1-4419-1401-9.
- [52] T. Sale, M. Petersen, D. Gilbert, Electrically Induced Redox Barriers for Treatment of Groundwater, Colorado, USA, 2005. https://clu-in.org/download/contaminantfocus/dnapl/Treatment_Technologies/CU-0112-fr-01.pdf.
- [53] B.H. Hyldegaard, R. Jakobsen, E.B. Weeth, N.D. Overheu, D.B. Gent, L.M. Ottosen, Challenges in electrochemical remediation of chlorinated solvents in natural groundwater aquifer settings, *J. Hazard. Mater.* 368 (2019) 680–688. doi:10.1016/j.jhazmat.2018.12.064.
- [54] X. Mao, S. Yuan, N. Fallahpour, A. Ciblak, J. Howard, I. Padilla, R. Loch-Caruso, A.N. Alshawabkeh, Electrochemically Induced Dual Reactive Barriers for Transformation of TCE and Mixture of Contaminants in Groundwater, *Environ. Sci. Technol.* 46 (2012) 12003–12011. doi:10.1021/es301711a.
- [55] L. Rajic, N. Fallahpour, A.N. Alshawabkeh, Impact of electrode sequence on electrochemical removal of trichloroethylene from aqueous solution, *Appl. Catal. B Environ.* 174–175 (2015) 427–434. doi:10.1016/j.apcatb.2015.03.018.
- [56] S. Yuan, M. Chen, X. Mao, A.N. Alshawabkeh, A three-electrode column for Pd-catalytic oxidation of TCE in groundwater with automatic pH-regulation and resistance to reduced sulfur compound fouling, *Water Res.* 47 (2013) 269–278. doi:10.1016/j.watres.2012.10.009.
- [57] L. Rajic, N. Fallahpour, R. Nazari, A.N. Alshawabkeh, Influence of humic substances on electrochemical degradation of trichloroethylene in limestone aquifers, *Electrochim. Acta.* 181 (2015) 123–129. doi:10.1016/j.electacta.2015.03.121.

- [58] N. Fallahpour, X. Mao, L. Rajic, S. Yuan, A.N. Alshawabkeh, Electrochemical dechlorination of trichloroethylene in the presence of natural organic matter, metal ions and nitrates in a simulated karst media, *J. Environ. Chem. Eng.* 5 (2017) 240–245. doi:10.1016/j.jece.2016.11.046.
- [59] L. Rajic, N. Fallahpour, S. Yuan, A.N. Alshawabkeh, Electrochemical transformation of trichloroethylene in aqueous solution by electrode polarity reversal, *Water Res.* 67 (2014) 267–275. doi:10.1016/j.watres.2014.09.017.
- [60] L. Rajic, N. Fallahpour, E. Podlaha, A.N. Alshawabkeh, The influence of cathode material on electrochemical degradation of trichloroethylene in aqueous solution, *Chemosphere.* 147 (2016) 98–104. doi:10.1016/j.chemosphere.2015.12.095.
- [61] L. Rajic, N. Fallahpour, E. Oguzie, A.N. Alshawabkeh, Electrochemical transformation of thichloroethylene in groundwater by Ni-containing cathodes, *Electrochim. Acta.* 181 (2015) 118–122. doi:10.1016/j.electacta.2015.03.112.
- [62] L. Rajic, R. Nazari, N. Fallahpour, A.N. Alshawabkeh, Electrochemical degradation of trichloroethylene in aqueous solution by bipolar graphite electrodes, *J. Environ. Chem. Eng.* 4 (2016) 197–202. doi:10.1016/j.jece.2015.10.030.
- [63] K.E. Carter, J. Farrell, Electrochemical Oxidation of Trichloroethylene Using Boron-Doped Diamond Film Electrodes, *Environ. Sci. Technol.* 43 (2009) 8350–8354. doi:https://doi.org/10.1021/es9017738.
- [64] N. Fallahpour, S. Yuan, L. Rajic, A.N. Alshawabkeh, Hydrodechlorination of TCE in a circulated electrolytic column at high flow rate, *Chemosphere.* 144 (2016) 59–64. doi:10.1016/j.chemosphere.2015.08.037.
- [65] B. Marselli, J. Garcia-gomez, P. Michaud, M.A. Rodrigo, M. Mo, Electrogenation of Hydroxyl Radicals on Boron-Doped Diamond Electrodes, *J. Electrochem. Soc.* 150 (2003) 79–83. doi:10.1149/1.1553790.
- [66] X. Mao, K. Baek, A.N. Alshawabkeh, Iron Electrocoagulation With Enhanced Cathodic Reduction for the Removal of Aqueous Contaminant Mixtures, *Environ. Eng. Manag. J.* 14 (2015) 2905–2911. <http://omicron.ch.tuiasi.ro/EEMJ>.
- [67] X. Mao, A. Ciblak, K. Baek, M. Amiri, R. Loch-Caruso, A.N. Alshawabkeh, Optimization of electrochemical dechlorination of trichloroethylene in reducing electrolytes, *Water Res.* 46 (2012) 1847–1857. doi:10.1016/j.watres.2012.01.002.
- [68] V. Sáez, M.D. Esclapez, I. Tudela, P. Bonete, J. González-García, Electrochemical degradation of perchloroethylene in aqueous media: Influence of the electrochemical operational variables in the viability of the process, *Ind. Eng. Chem. Res.* 49 (2010) 4123–4131. doi:10.1021/ie100134t.
- [69] C.A. Martínez-Huitle, M.A. Rodrigo, I. Sirés, O. Scialdone, Single and Coupled Electrochemical Processes and Reactors for the Abatement of Organic Water Pollutants: A Critical Review, *Chem. Rev.* 115 (2015) 13362–13407. doi:10.1021/acs.chemrev.5b00361.
- [70] R. Verdini, F. Aulenta, F. de Tora, A. Lai, M. Majone, Relative contribution of set cathode potential and external mass transport on TCE dechlorination in a continuous-flow bioelectrochemical reactor, *Chemosphere.* 136 (2015) 72–78. doi:10.1016/j.chemosphere.2015.03.092.
- [71] S.T. Lohner, D. Becker, K.M. Mangold, A. Tiehm, Sequential reductive and oxidative biodegradation of chloroethenes stimulated in a coupled bioelectro-process, *Environ. Sci. Technol.* 45 (2011) 6491–6497. doi:10.1021/es200801r.

- [72] F. Aulenta, R. Verdini, M. Zeppilli, G. Zanaroli, F. Fava, S. Rossetti, M. Majone, Electrochemical stimulation of microbial cis-dichloroethene (cis-DCE) oxidation by an ethene-assimilating culture, *N. Biotechnol.* 30 (2013) 749–755. doi:10.1016/j.nbt.2013.04.003.
- [73] A. Tiehm, S.T. Lohner, T. Augenstein, Effects of direct electric current and electrode reactions on vinyl chloride degrading microorganisms, *Electrochim. Acta.* 54 (2009) 3453–3459. doi:10.1016/j.electacta.2009.01.002.
- [74] J. Farrell, N. Melitas, M. Kason, T. Li, Electrochemical and Column Investigation of Iron-Mediated Reductive Dechlorination of Trichloroethylene and Perchloroethylene, *Environ. Sci. Technol.* 34 (2000) 2549–2556. doi:10.1021/es991135b.
- [75] J. Wang, J. Farrell, Investigating the role of atomic hydrogen on chloroethene reactions with iron using Tafel analysis and electrochemical impedance spectroscopy, *Environ. Sci. Technol.* 37 (2003) 3891–3896. doi:10.1021/es0264605.
- [76] B. Huang, J. Long, W. Chen, Y. Zhu, G. Zeng, C. Lei, Linear free energy relationships of electrochemical and thermodynamic parameters for the electrochemical reductive dechlorination of chlorinated volatile organic compounds (Cl-VOCs), *Electrochim. Acta.* 208 (2016) 195–201. doi:10.1016/j.electacta.2016.04.182.
- [77] J.H. Brewster, Mechanisms of Reductions at Metal Surfaces. I. A General Working Hypothesis, *J. Am. Chem. Soc.* 76 (1954) 6361–6363. doi:10.1021/ja01653a034.
- [78] W.A. Arnold, A.L. Roberts, Pathways and Kinetics of Chlorinated Ethylene and Chlorinated Acetylene Reaction with Fe(0) Particles, *Environ. Sci. Technol.* 34 (2000) 1794–1805. doi:10.1021/es980252o.
- [79] A.L. Roberts, L.A. Totten, W.A. Arnold, D.R. Burris, T.J. Campbell, Reductive elimination of chlorinated ethylenes by zero-valent metals, *Environ. Sci. Technol.* 30 (1996) 2654–2659. doi:10.1021/es9509644.
- [80] P. Lakshmipathiraj, G. Bhaskar Raju, Y. Sakai, Y. Takuma, A. Yamasaki, S. Kato, T. Kojima, Studies on electrochemical detoxification of trichloroethene (TCE) on Ti/IrO₂-Ta₂O₅ electrode from aqueous solution, *Chem. Eng. J.* 198–199 (2012) 211–218. doi:10.1016/j.cej.2012.05.092.
- [81] M. Cheng, G. Zeng, D. Huang, C. Lai, P. Xu, C. Zhang, Y. Liu, Hydroxyl radicals based advanced oxidation processes (AOPs) for remediation of soils contaminated with organic compounds: A review, *Chem. Eng. J.* 284 (2016) 582–598. doi:10.1016/j.cej.2015.09.001.
- [82] S. Yuan, X. Mao, A.N. Alshawabkeh, Efficient Degradation of TCE in Groundwater Using Pd and Electro-generated H₂ and O₂: A Shift in Pathway from Hydrodechlorination to Oxidation in the Presence of Ferrous Ions, *Environ. Sci. Technol.* 46 (2012) 3398–3405. doi:10.1021/es204546u.
- [83] L.M. Ottosen, T.H. Larsen, P.E. Jensen, G.M. Kirkelund, H. Kern-Jespersen, N. Tuxen, B.H. Hyldegaard, Electrokinetics applied in remediation of subsurface soil contaminated with chlorinated ethenes – A review, *Chemosphere.* 235 (2019) 113–125. doi:10.1016/j.chemosphere.2019.06.075.
- [84] S.S. Zumdahl, Electrochemistry, in: R.B. Schwartz, C.L. Brooks, A. Galvin (Eds.), *Chem. Princ.*, 6th ed., Houghton Mifflin Company, Boston, MA, 2009: pp. 472–520.
- [85] P.H. Fallgren, J.J. Eisenbeis, S. Jin, In situ electrochemical manipulation of oxidation-reduction potential in saturated subsurface matrices, *J. Environ. Sci. Heal. Part A.* 53 (2018) 517–523. doi:10.1080/10934529.2017.1422951.

- [86] T.H. Wiedemeier, H.S. Rifai, C.J. Newell, J.T. Wilson, Overview of intrinsic bioremediation, in: T.H. Wiedemeier, H.S. Rifai, C.J. Newell, J.T. Wilson (Eds.), *Nat. Attenuation Fuels Chlorinated Solvents Subsurf.*, John Wiley & Sons, Inc., 1999: pp. 162–188. doi:10.1016/S0169-7722(99)00099-6.
- [87] E. Strandgaard Andersen, P. Jespersgaard, O. Østergaard, *Datbog fysik kemi*, 8th ed., F & K Forlaget, Copenhagen, DK, 1993.
- [88] W.W. Nazaroff, L. Alvarez-Cohen, eds., *A Further Look at Transformation Processes*, in: *Environ. Eng. Sci.*, John Wiley & Sons, Inc., New York, USA, 2010: pp. 641–650.
- [89] C.A.J. Appelo, D. Postma, *Redox Processes*, in: C.A.J. Appelo, D. Postma (Eds.), *Geochemistry, Groundw. Pollut.*, 5th ed., CRC Press LLC, Leiden, The Netherlands, 2010: pp. 415–487.
- [90] Parsons, *Principles and practices of enhanced anaerobic bioremediation of chlorinated solvents*, 2004. https://frtr.gov/costperformance/pdf/remediation/principles_and_practices_bioremediation.pdf.
- [91] W. Xie, S. Yuan, X. Mao, W. Hu, P. Liao, M. Tong, A.N. Alshawabkeh, Electrocatalytic activity of Pd-loaded Ti/TiO₂ nanotubes cathode for TCE reduction in groundwater, *Water Res.* 47 (2013) 3573–3582. doi:10.1016/j.watres.2013.04.004.
- [92] Capital Region of Denmark, *Innovation Garage - Cross Sections*, Copenhagen, DK, 2011. https://www.danishsoil.org/media/test_sites/1/documents/Cross-sections_2011.pdf.
- [93] A. Taqieddin, R. Nazari, L. Rajic, A.N. Alshawabkeh, Review—Physicochemical Hydrodynamics of Gas Bubbles in Two Phase Electrochemical Systems, *J. Electrochem. Soc.* 164 (2017) E448–E459. doi:10.1149/2.1161713jes.
- [94] W. Zhou, L. Rajic, Y. Zhao, J. Gao, Y. Qin, A.N. Alshawabkeh, Rates of H₂O₂ electrogeneration by reduction of anodic O₂ at RVC foam cathodes in batch and flow-through cells, *Electrochim. Acta.* 277 (2018) 185–196. doi:10.1016/j.electacta.2018.04.174.
- [95] M.A. Petersen, T.C. Sale, K.F. Reardon, Electrolytic trichloroethene degradation using mixed metal oxide coated titanium mesh electrodes, *Chemosphere.* 67 (2007) 1573–1581. doi:10.1016/j.chemosphere.2006.11.056.
- [96] I.A. Leenson, Old Rule of Thumb and the Arrhenius Equation, *J. Chem. Educ.* 76 (2009) 1459–1460. doi:10.1021/ed076p1459.
- [97] D.W. Sundstrom, H.E. Klei, T.A. Nalette, D.J. Reidy, B.A. Weir, Destruction of Halogenated Aliphatics by Ultraviolet Catalyzed Oxidation with Hydrogen Peroxide, *Hazard. Waste Hazard. Mater.* 3 (1986) 101–110. doi:10.1089/hwm.1986.3.101.
- [98] A.A. Schiefler, D.J. Tobler, N.D. Overheu, N. Tuxen, Extent of natural attenuation of chlorinated ethenes at a contaminated site in Denmark, *Energy Procedia.* 146 (2018) 188–193. doi:10.1016/j.egypro.2018.07.024.
- [99] F. Aulenta, A. Canosa, P. Reale, S. Rossetti, S. Panero, M. Majone, Microbial reductive dechlorination of trichloroethene to ethene with electrodes serving as electron donors without the external addition of redox mediators, *Biotechnol. Bioeng.* 103 (2009) 85–91. doi:10.1002/bit.22234.
- [100] J. Radjenovic, D.L. Sedlak, Challenges and Opportunities for Electrochemical Processes as Next-Generation Technologies for the Treatment of Contaminated Water, *Environ. Sci. Technol.* 49 (2015) 11292–11302. doi:10.1021/acs.est.5b02414.

-
- [101] A.Y. Bagastyo, J. Radjenovic, Y. Mu, R.A. Rozendal, D.J. Batstone, K. Rabaey, Electrochemical oxidation of reverse osmosis concentrate on mixed metal oxide (MMO) titanium coated electrodes, *Water Res.* 45 (2011) 4951–4959. doi:10.1016/j.watres.2011.06.039.
- [102] G. Chen, E.A. Betterton, R.G. Arnold, Electrolytic oxidation of trichloroethylene using a ceramic anode, *J. Appl. Electrochem.* 29 (1999) 961–970. doi:10.1023/A:1003541706456.
- [103] K.F. Haselmann, F. Laturus, B. Svensmark, C. Gron, Formation of chloroform in spruce forest soil - Results from laboratory incubation studies, *Chemosphere.* 41 (2000) 1769–1774. doi:10.1016/S0045-6535(00)00044-8.
- [104] Y. Zhao, H. wei Yang, S. ting Liu, S. Tang, X. mao Wang, Y.F. Xie, Effects of metal ions on disinfection byproduct formation during chlorination of natural organic matter and surrogates, *Chemosphere.* 144 (2016) 1074–1082. doi:10.1016/j.chemosphere.2015.09.095.
- [105] A. Rebelo, I. Ferra, A. Marques, M.M. Silva, Wastewater reuse: modeling chloroform formation, *Environ. Sci. Pollut. Res.* 23 (2016) 24560–24566. doi:10.1007/s11356-016-7749-z.
- [106] C.I. Chaidou, V.I. Georgakilas, C. Stalikas, M. Saraçi, E.S. Lahaniatis, Formation of chloroform by aqueous chlorination of organic compounds, *Chemosphere.* 39 (1999) 587–594. doi:10.1016/S0045-6535(99)00124-1.
- [107] N. Sonoyama, T. Sakata, Electrochemical Continuous Decomposition of Chloroform and Other Volatile Chlorinated Hydrocarbons in Water Using a Column Type Metal Impregnated Carbon Fiber Electrode, *Environ. Sci. Technol.* 33 (1999) 3438–3442. doi:10.1021/es980903g.
- [108] G. Chen, E.A. Betterton, R.G. Arnold, W.P. Ela, Electrolytic reduction of trichloroethylene and chloroform at a Pt- or Pd-coated ceramic cathode, *J. Appl. Electrochem.* 33 (2003) 161–169. doi:10.1023/A:1024076419515.
- [109] J.C. Velázquez, S. Leekumjorn, G.D. Hopkins, K.N. Heck, J.S. McPherson, J.A. Wilkens, B.S. Nave, M. Reinhard, M.S. Wong, High activity and regenerability of a palladium–gold catalyst for chloroform degradation, *J. Chem. Technol. Biotechnol.* 91 (2016) 2590–2596. doi:10.1002/jctb.4851.
- [110] W.W. McNab, R. Ruiz, Palladium-catalyzed reductive dehalogenation of dissolved chlorinated aliphatics using electrolytically-generated hydrogen, 37 (1998) 925–936.
- [111] V.M. Molina, D. González-Arjona, E. Roldán, M. Dominguez, Electrochemical Reduction of Tetrachloromethane. Electrolytic Conversion to Chloroform, *Collect. Czechoslov. Chem. Commun.* 67 (2002) 279–292. doi:10.1135/cccc20020279.
- [112] G. Skibsted, L.M. Ottosen, M. Elektorowicz, P.E. Jensen, Effect of long-term electrochemical soil remediation on Pb removal and soil weathering, *J. Hazard. Mater.* 358 (2018) 459–466. doi:10.1016/j.jhazmat.2018.05.033.
- [113] S. Pamukcu, E. Ghazanfari, K. Wittle, Reduction of Contaminants in Soil and Water By Direct Electric Current, in: G.V. Chilingar, M. Haroun (Eds.), *Electrokinet. Pet. Environ. Eng.*, John Wiley & Sons, Inc., 2014: pp. 33–101.

-
- [114] C.E. Schaefer, C. Andaya, A. Urtiaga, E.R. McKenzie, C.P. Higgins, Electrochemical treatment of perfluorooctanoic acid (PFOA) and perfluorooctane sulfonic acid (PFOS) in groundwater impacted by aqueous film forming foams (AFFFs), *J. Hazard. Mater.* 295 (2015) 170–175. doi:10.1016/j.jhazmat.2015.04.024.
- [115] Y. Wang, H. Lin, F. Jin, J. Niu, J. Zhao, Y. Bi, Y. Li, Electrocoagulation mechanism of perfluorooctanoate (PFOA) on a zinc anode: Influence of cathodes and anions, *Sci. Total Environ.* 557–558 (2016) 542–550. doi:10.1016/j.scitotenv.2016.03.114.
- [116] S. Liang, R. “David” Pierce, H. Lin, S.Y.D. Chiang, Q. “Jack” Huang, Electrochemical oxidation of PFOA and PFOS in concentrated waste streams, *Remediation.* 28 (2018) 127–134. doi:10.1002/rem.21554.
- [117] Y. Lei, G. Zhao, Y. Zhang, M. Liu, L. Liu, B. Lv, J. Gao, Highly Efficient and Mild Electrochemical Incineration: Mechanism and Kinetic Process of Refractory Aromatic Hydrocarbon Pollutants on Superhydrophobic PbO₂ Anode, *Environ. Sci. Technol.* 44 (2010) 7921–7927. doi:10.1021/es101693h.
- [118] N. Oturan, E.D. van Hullebusch, H. Zhang, L. Mazeas, H. Budzinski, K. Le Menach, M.A. Oturan, Occurrence and Removal of Organic Micropollutants in Landfill Leachates Treated by Electrochemical Advanced Oxidation Processes, *Environ. Sci. Technol.* 49 (2015) 12187–12196. doi:10.1021/acs.est.5b02809.
- [119] E. Guivarch, N. Oturan, M.A. Oturan, Removal of organophosphorus pesticides from water by electrogenerated Fenton’s reagent, *Environ. Chem. Lett.* 1 (2003) 165–168. doi:10.1007/s10311-003-0029-4.
- [120] C.A. Martínez-Huitle, A. De Battisti, S. Ferro, S. Reyna, M. Cerro-López, M.A. Quiro, Removal of the Pesticide Methamidophos from Aqueous Solutions by Electrooxidation using Pb/PbO₂, Ti/SnO₂, and Si/BDD Electrodes, *Environ. Sci. Technol.* 42 (2008) 6929–6935. doi:10.1021/es8008419.
- [121] E.T. Martin, C.M. McGuire, M.S. Mubarak, D.G. Peters, Electroreductive Remediation of Halogenated Environmental Pollutants, *Chem. Rev.* 116 (2016) 15198–15234. doi:10.1021/acs.chemrev.6b00531.
- [122] K. Baek, N. Kasem, A. Ciblak, D. Vesper, I. Padilla, A.N. Alshawabkeh, Electrochemical removal of selenate from aqueous solutions, *Chem. Eng. J.* 215–216 (2013) 678–684. doi:10.1016/j.cej.2012.09.135.
- [123] M. Zheng, J. Bao, P. Liao, K. Wang, S. Yuan, M. Tong, H. Long, Electrogenation of H₂ for Pd-catalytic hydrodechlorination of 2,4-dichlorophenol in groundwater, *Chemosphere.* 87 (2012) 1097–1104. doi:10.1016/j.chemosphere.2012.01.058.
- [124] X. Xu, P. Liao, S. Yuan, M. Tong, M. Luo, W. Xie, Cu-catalytic generation of reactive oxidizing species from H₂ and O₂ produced by water electrolysis for electro-fenton degradation of organic contaminants, *Chem. Eng. J.* 233 (2013) 117–123. doi:10.1016/j.cej.2013.08.046.
- [125] L. Ma, M. Zhou, G. Ren, W. Yang, L. Liang, A highly energy-efficient flow-through electro-Fenton process for organic pollutants degradation, *Electrochim. Acta.* 200 (2016) 222–230. doi:10.1016/j.electacta.2016.03.181.
-

OWN PUBLICATIONS (APPENDIX I-V)

- Hyldegaard, B.H., Jakobsen, R., Weeth, E.B., Overheu, N.D., Gent, D.B. & Ottosen, L.M. (2019). Challenges in electrochemical remediation of chlorinated solvents in natural groundwater aquifer settings. *Journal of Hazardous Materials*, 368, pp. 680-688. doi: 10.1016/j.jhazmat.2018.12.064.
- Hyldegaard, B.H. & Ottosen, L.M. (n.d.). Selecting electrode materials and sequence for electrochemical removal of chlorinated ethenes in groundwater. *Submitted*.
- Ottosen, L.M., Larsen, T.H., Jensen, P.E., Kirkelund, G.M., Kern-Jespersen, H., Tuxen, N. & Hyldegaard, B.H. (2019). Electrokinetics applied in remediation of subsurface soil contaminated with chlorinated ethenes – A review. *Chemosphere*, 235, pp. 113-125. doi: 10.1016/j.chemosphere.2019.06.075.
- Hyldegaard, B.H., Ottosen, L.M. & Alshawabkeh, A.N. (2019). Transformation of tetrachloroethylene in a flow-through electrochemical reactor. *Science of The Total Environment*, 135566. doi: 10.1016/j.scitotenv.2019.135566.
- Hyldegaard, B.H., Jakobsen, R. & Ottosen, L.M. (2020). Electrochemical transformation of an aged tetrachloroethylene contamination in realistic aquifer settings. *Chemosphere*, 243. doi: 10.1016/j.chemosphere.2019.125340.

APPENDIX I

Challenges in electrochemical remediation of chlorinated solvents in natural groundwater
aquifer settings

Hyldegaard, B.H., Jakobsen, R., Weeth, E.B., Overheu, N.D. Gent, D.B. & Ottosen, L.M.

(Published in Journal of Hazardous Materials, 2019)



Contents lists available at ScienceDirect

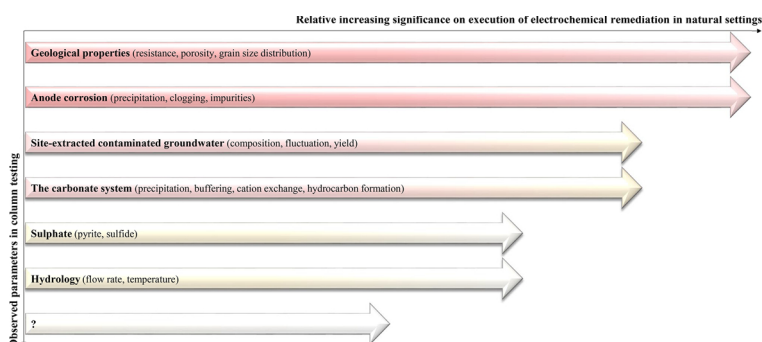
Journal of Hazardous Materials

journal homepage: www.elsevier.com/locate/jhazmat

Challenges in electrochemical remediation of chlorinated solvents in natural groundwater aquifer settings

Bente H. Hyldegaard^{a,b,*}, Rasmus Jakobsen^c, Eline B. Weeth^a, Niels D. Overheu^d, David B. Gent^e, Lisbeth M. Ottosen^b^a COWI A/S, Department of Waste and Contaminated Sites, 2800 Kongens Lyngby, Denmark^b DTU (Technical University of Denmark), Department of Civil Engineering, 2800 Kongens Lyngby, Denmark^c GEUS, Department of Geochemistry, 1350 København K, Denmark^d CRD (Capital Region of Denmark), Centre for Regional Development, 3400 Hillerød, Denmark^e USACE (US Army Corps of Engineers), Engineer Research and Development Center, 39180 MS, United States

GRAPHICAL ABSTRACT



ARTICLE INFO

Keywords:

Electrochemical
Geology
Groundwater
Modelling
Ranking

ABSTRACT

Establishment of electrochemical zones for remediation of dissolved chlorinated solvents in natural settings was studied. An undivided 1D-experimental column set-up was designed for the assessment of the influence of site-extracted contaminated groundwater flowing through a sandy aquifer material, on the execution of laboratory testing. A three-electrode system composed of palladium coated pure iron cathodes and a cast iron anode was operated at 12 mA under varying flow rates. The natural settings added complexity through a diverse groundwater chemistry and resistance in the sand. In addition, significant precipitation of iron released through anode corrosion was observed. Nevertheless, the complex system was successfully modelled with a simple geochemical model using PHREEQC. A ranking of the significances of system parameters on the laboratory execution of electrochemical remediation in natural settings was proposed: Geological properties > anode corrosion > site-extracted contaminated groundwater > the carbonate system > sulphate > hydrology > less significant unidentified parameters. This study provides insight in actual challenges that need to be overcome for *in situ* electrochemical remediation.

* Corresponding author at: COWI A/S, Department of Waste and Contaminated Sites, Parallelvej 2, 2800 Kongens Lyngby, Denmark.

E-mail address: behd@cowi.com (B.H. Hyldegaard).

<https://doi.org/10.1016/j.jhazmat.2018.12.064>

Received 1 September 2017; Received in revised form 9 December 2018; Accepted 17 December 2018

Available online 18 December 2018

0304-3894/ © 2018 Elsevier B.V. All rights reserved.

1. Introduction

Chlorinated solvents threaten groundwater resources. The widespread contamination by chlorinated solvents is a relic from the past with extensive use of tetrachloroethylene (PCE) and trichloroethylene (TCE) in e.g. dry-cleaning facilities and metal processing [1]. The chlorinated solvents and their chlorinated degradation products are acute toxic and carcinogenic [2]. Furthermore, the compound's high solubility, volatility and low sorption to sediments challenge the current treatment systems. Thus, optimised means of protecting the groundwater from these contaminants are important. Pump-and-treat (P&T) systems are commonly used to keep plumes from reaching water supply wells. However, these treatment facilities are long-term solutions with substantial operation and maintenance requirements. In addition, the P&T plants are challenged by weak sorption of the chlorinated degradation products to the activated carbon.

We propose, as an alternative to P&T, establishment of an electrochemical zone for *in situ* degradation of PCE and degradation products. Hence, the focus of this study is on application and combination of the different electrochemical processes to optimise the electrochemical zone for complete degradation of chlorinated solvents in natural groundwater settings. This is vital for proving the methods applicability. Following a successful adaption to field settings, electrochemical remediation is considered superior to P&T facilities even in high-permeability zones, because i) chlorinated parent components and chlorinated degradation products can be equally targeted, ii) no hazardous waste is generated, iii) the electrochemical remedy can be installed fully underground, i.e. site-activities can resume, and iv) the carbon footprint is lower.

It is known that i) fast electrochemical reduction of chlorinated solvents near the electrodes can be obtained [3] and ii) reactants can be generated, and subsequently reduce or oxidise the chlorinated solvents [4]. Thus, the treatment can be designed without addition of e.g. substrate or generation of waste products like spent activated carbon.

1.1. Knowledge gaps

Undivided flow-through cells operated with solid-state electrodes under constant current simulate realistic field scale designs for remediation in primary aquifers. Studies assessing degradation of chlorinated solvents in such systems have focused on the significance of electrode composition, configurations and system parameters such as current density and flow rate (Table 1).

Based on Table 1, knowledge gaps have been identified:

- Method efficiency in the degradation from the parent compound PCE to harmless ethenes
- Effects of the sandy aquifer geology on the electrochemical processes, degradation etc.
- Significance of field-extracted contaminated groundwater on method performance; influence of naturally occurring geochemistry and aged contamination at natural groundwater temperatures
- The role of iron purity of cathodes on degradation in view of commercial application cost
- The true feasibility of the method: *in situ* implementation and assessment of the method including up-scaling challenges, power consumption etc.

This study is part of an industrial PhD addressing these challenges and developing systems for optimisation of plume control by electrochemical zones in complex natural settings. A multi-disciplinary study involving industry experts from; COWI A/S, researchers from; DTU, GEUS and USACE, and a public authority and problem-owner; CRD.

The focus of the present paper is on the added complexity of operation under near natural settings compared to state-of-the-art simplified laboratory experiments. Thus, emphasis is on the influence of

site characteristics and not on contaminant degradation efficiency. For this purpose, an undivided 1D-experimental column set-up is studied for assessment of electrochemical zones established within a sandy material saturated with site-extracted contaminated groundwater.

2. Materials and methods

An acrylic column set-up was designed for 1D-tests on electrochemical zones in natural settings (Fig. 1). The dimensions were chosen such, that the total sample volume to be extracted during each sampling round would account for less than 2% of the total water volume contained within the saturated porous matrix. Darcy velocities of 61 m/year (0.28 ml/min), 122 m/year (0.56 ml/min) and 305 m/year (1.4 ml/min) were maintained by a Watson-Marlow qdos30 manual peristaltic pump. Contaminated groundwater was collected from primary aquifers at two PCE contaminated sites in Denmark. For low flow testing, the groundwater was collected in Skovlunde, while for medium and high flow testing, the groundwater was collected in Lyngby because of a decreasing yield in Skovlunde. The groundwater samples were stored in multi-layered 25 l Tedlar bags in a fridge at 5 °C. The contaminant composition of the groundwater from Skovlunde and Lyngby is shown in Table 2.

Volatile organic carbons were measured by Eurofins, Denmark using a Teledyne Texmar Atomx Purge & Trap system with Vocarb 3000 trap followed by an Agilent 7890 GC with Agilent 5977 MSD equipped with a DB-624 Ultra Inert 1 µm FT column (ID 0.18 mm x 20 m). Hydrocarbons were measured by Eurofins, Denmark using an Agilent 6890 GC-FID and CTC headspace sampler equipped with a HP-PLOT Q 40 µm FT column (ID 0.53 mm x 15 m). Analysis of anions was conducted on a Thermo Scientific Dionex ICS-1100 equipped with an AS14 A column using an eluent of Na₂CO₃/NaHCO₃ at a flow rate of 1.0 ml/min. Cation analysis was measured on a Varian ICP-EOS 720-ES. Alkalinity was determined by Gran titration using 0.02 M HNO₃.

The column was loaded with unrefined, excavated sandy aquifer material collected in Svogerslev sand quarry, Denmark (characterisation according to Table 3). To separate the sand from the electrodes, perforated PTFE cover plates were installed on each side of the electrodes to simulate well screens.

The electrode configuration comprised two pure iron cathodes and a downstream cast iron anode (Table 4), because two cathodes have shown to more than double the reaction kinetics [6]. The electrode rods (6.35 mm x 130 mm) were mounted at 22.3 cm, 39.9 cm and 73.5 cm. This electrode spacing was chosen to i) be able to separate and identify the mechanisms occurring at each electrode via analysis of extracted water samples having a limited impact of dragging towards the sampling points, ii) be able to assess the longitudinal extend of influence of each electrode's specific electrochemistry, and iii) accommodate the desire of increased electrode spacing during field-implementations to reduce costs, where the electrode spacing in the literature published is usually limited to a few centimeters. The cathodes were coated with Pd acquired from Thermo Fisher Scientific as 99.9% crystalline PdCl₂. Palladization followed the procedure outlined in [11] for a loading of 0.76 mg/cm² on Fe. A constant current intensity of 12 mA was applied over two cathodes and one anode using one Agilent E3612 A 0–120 V, 0–0.25 A power supply. The voltage was measured with a Hyelec MAS830B.

Prior to the electrochemical test, the sand-filled column was saturated with the contaminated groundwater for two pore volumes (PV) at 0.56 ml/min. In addition, the column was flushed for 2 PV at 1.4 ml/min in between concluded testing at one flow rate and continuation at the next higher flow rate. For each flow rate tested, sampling of pore water was conducted after 1 PV and 2 PV.

3. Results and discussion

Only the data from the first round of measurements is shown for

Table 1

Summary of electrochemical remediation of dissolved chlorinated solvents in undivided cells under constant current with solid-state electrodes.

Experimental design ^{a,b,c}	Power supply	Target contaminant	Findings	Reference
Fluid: Synthetic Geology: Limestone gravel Configuration: A→C→A Anode: Cast Fe, MMO Cathode: Cu Catalyst: -	15-120 mA	TCE	Cast iron anodes enhanced TCE removal. The three-electrode configuration further enhanced the removal. Lower flow rate enhanced removal, exceeding 82.2 %. Correlation between current density and influent concentration with upper threshold for current on removal.	[5]
Fluid: Synthetic Geology: "Glass beads" Configuration: C→C→A, A→C, C→A Anode: MMO, cast Fe Cathode: MMO, cast Fe Catalyst: Pd/C, Pd/Al pellets	30-90 mA	TCE	Increased electrode spacing and flow rate reduced the removal efficiency. Higher surface area (foam) improved conversion of TCE. Removal rates at 60 mA exceeded those at 30 and 90 mA. C-C-A and Pd coating significantly increased removal rates and efficiencies. > 99 % removal of TCE was achieved.	[6]
Fluid: Synthetic Geology: "Glass beads" Configuration: A→C→C Anode: MMO Cathode: MMO Catalyst: Pd/Al ₂ O ₃ pellets	60 mA	TCE	Presence of Fe(II) significantly enhanced TCE removal through Fenton reaction. Addition of sulfite improved TCE removal due to transformation into SO ₄ ²⁻ , reaching a removal efficiency of 71 %. Fouling of Pd by sulfide was assessed and found insignificant.	[7]
Fluid: Synthetic Geology: Limestone gravel, "glass beads" Configuration: C→A Anode: MMO Cathode: Fe Catalyst: Pd	60 mA	TCE	Presence of humic substance (HS) reduced TCE removal in a linear relationship. HS influenced the electrochemical processes of the cathode. TCE degradation in limestone without HS reached 82.9 %, which was superior to that in glass beads.	[8]
Fluid: Synthetic Geology: Limestone block Configuration: Anode: Cast Fe Cathode: Cu Catalyst: -	90 mA	TCE	Humic acids decreased TCE removal to 80 % compared to a 90 % removal in the control test, dichromate to 53-70 %, selenate to 76-89 %, while nitrate to 81-91 %. A mixture of the latter three contaminants reduced TCE removal to around 40 %. The limestone block enhanced removal of TCE when compared to an acrylic column.	[9]
Fluid: Synthetic Geology:- Configuration: A→C, C→A Anode: MMO Cathode: MMO Catalyst: Pd/Al ₂ O ₃ pellets	30-120 mA	TCE	Configuration of C-A was superior in performance to A-C with TCE removal of 54.5 % and 34.8 %, respectively. Polarity reversal enhanced the removal to 69.3 %. Optimal design of polarity reversal for TCE removal was 15 cycles h ⁻¹ at 60 mA resulting in a power consumption of 13 W cm ⁻² .	[10]
Fluid: Synthetic Geology: - Configuration: C→A Anode: MMO Cathode: Fe, Ni, Cu, C, Al Catalyst: Pd	30-90 mA	TCE	Highest removal was obtained with foam cathodes of Ni > C > Cu > Fe > Al. 60 mA DC was most efficient. Removal with Fe foam increased from 43.5 % to 99.8 % when coated with Pd. Upper threshold existed for removal vs. Pd loading. Coating changed cathode material performance Fe > Cu > C > Al > Ni. Nitrates negatively influenced the removal.	[11]
Fluid: Synthetic Geology: - Configuration: C→A Anode: C Cathode: C Catalyst: -	60-120 mA	TCE	Monopolar mode resulted in TCE removal of 29 %. Introducing two bipolar electrodes increased removal to 66 % due to enhanced peroxide formation. In bipolar mode, a current of 120 mA enhanced the removal, while highest current efficiency was obtained for 60 mA.	[12]

^a A-C : Anode and cathode.^b →: Flow direction.^c MMO: Mixed metal oxide coating on titanium.

each flow rate. The trends were similar in the two periods. Included in the evaluation are Cl, F, S(VI), N(V), Ca, Fe, Na, K, Mg, Al, Mn, Ni, Pb. The elements P, Cu, Ba, As, Cd, Cr and Zn are not shown because of concentrations below detection limits.

3.1. Geological properties

The sand gave a high resistance for the flow of both water and current. The latter was expressed as a high voltage even at the low current intensity (127.8 V at 12 mA, initially) (data not shown). The high resistance resulted in the three-electrode configuration operating as a two-electrode system, with the first cathode being passive. This is evident in Figs. 2 and 3: Most parameters remained steady when passing the first cathode, while changes appeared on passing the second cathode. To manage this, two power supplies or e.g. rheostats must be

incorporated to force the current through the geological media to each cathode. Such measures were taken for column studies in limestone gravel [5] and glass beads [6,7]. It has a further advantage of enabling control of the specific current supplied to each cathode. To maintain current control even with high electrical resistance in the system and to be able to increase the current density, a higher voltage DC supply must be applied.

In electrokinetics, an increase in pH at the cathode and a decrease at the anode is most often reported. In accordance, the pH reached levels exceeding 11 after the active cathode and decreased to around 6 at the anode (Fig. 2).

3.1.1. The carbonate system

Water samples extracted near the second cathode had a milky colour. The ion analysis revealed a significant decrease in Ca here

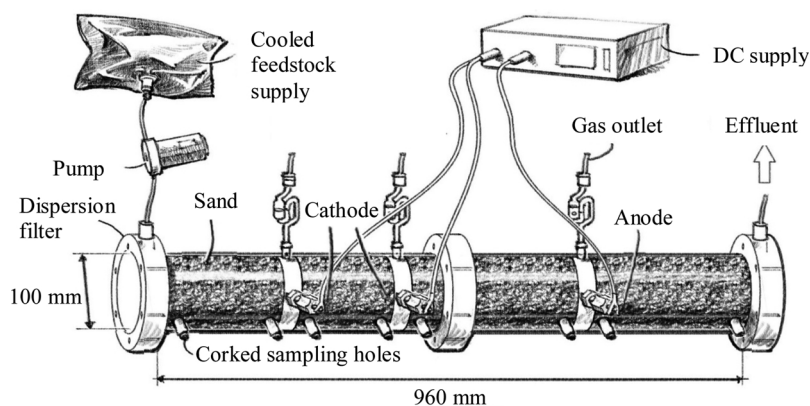


Fig. 1. Sketch of the undivided flow-through electrochemical reactor loaded with sand. The feedstock supply illustrates the field-extracted contaminated groundwater stored at 5 °C.

Table 2

Contaminant composition of the field-extracted groundwater from Skovlunde and Lyngby.

Component	Skovlunde, DK	Lyngby, DK
Tetrachloroethylene [µg/l]	27	12
Trichloroethylene [µg/l]	69	27
1,1-dichloroethylene [µg/l]	0.06	0.29
Cis-1,2-dichloroethylene [µg/l]	86	65
Trans-1,2-dichloroethylene [µg/l]	0.81	1.4
Vinyl chloride [µg/l]	< 0.05	1.3
1,1,1-trichloroethane [µg/l]	< 0.05	< 0.05
1,1-dichloroethane [µg/l]	< 0.05	< 0.05
1,2-dichloroethane [µg/l]	< 0.05	< 0.05
Chloroethane [µg/l]	< 0.05	< 0.05
Tetrachloromethane [µg/l]	< 0.05	< 0.05
Trichloromethane [µg/l]	< 0.05	< 0.05
1,4-dioxane [µg/l]	< 10	< 10

Table 3

Characterisation of the sandy aquifer material from Svogerslev, Denmark.

Parameter	Method/Apparatus
Porosity [%]	31
Grain density [g/cm ³]	2.57
Conductivity ^a [µS/cm]	82.5
pH ^a [-]	8.62
Carbon content [%]	0.952
Sulphur content [%]	0.007
Chalk content [%]	15
d(0.1) [mm]	0.198
d(0.5) [mm]	0.407
d(0.9) [mm]	0.895

^a Measured in the aqueous phase of 10 g dry sand mixed with 25 ml demineralised water for an hour at 215 rounds per minute.

(Fig. 3). According to Table 3, the sand was composed of 15% chalk, and the extracted groundwater showed significant Ca concentration (Fig. 3 at 0 cm). To obtain information on the carbonate system, alkalinity was measured in selected samples and from this total inorganic carbon (TIC) was calculated using the software PHREEQC [13] (Fig. 4). The alkalinity indicated an active carbonate system with buffering of the acidity developed at the anode. Hence, compared to the pH of the

inlet water, the insignificant decrease in pH near the anode can be attributed to the carbonate system. This impact of the groundwater chemistry is fortunate with respect to the commercial potential of the method, where highly acidic groundwater is undesirable. For longer durations, the buffering capacity of the system might become depleted, leading to acidic conditions near the anode. However, highly acidic conditions are not expected because of the reducing environment produced by iron anodes [5,6].

The triggered changes in the carbonate system significantly altered the conductivity of the groundwater when Ca precipitated (Figs. 2 and 3) and an effect from this deposition is clogging. However, in this study the dissolved Ca re-established near the anode, which indicated formation of colloids: Supersaturation of Ca-carbonate can result in the forming of Ca-carbonate colloids, which can move with the groundwater towards the anode, where the colloids then re-dissolve because of acid produced, thereby enhancing buffering. Concurrent dissolution of the chalk embedded in the sand is expected until depletion is reached. Clogging can affect the performance of the method, while formation of colloids is of little concern.

When Ca precipitates as calcite, Mg can be incorporated in the mineral structure [14]. This can explain the concurrent decrease in Ca, Mg and TIC (Figs. 3 and 4). Furthermore, exchange of cations on the mineral surface is likely [15]. Cation exchange appeared to influence the observed levels of Mg, K, Na and Al apparent for the flow rates tested (Fig. 3). For Al, the changes could also be due to dissolution of Al-hydroxide stimulated by formation of aluminium hydroxyl complexes at the cathode and re-precipitation at the anode. Despite the significant alterations in groundwater chemistry resulting from cation exchange when considering the individual species Mg, K, Na and Al, the overall impact of these cation exchanging species on the contaminant degradation is considered low, because the changes appear to be a side-effect of redox changes and not a direct competitive mechanism.

In the electrochemical system with iron electrodes, Pd catalyst and field-extracted groundwater, three overall chlorinated solvent removal mechanisms can occur: abiotic reduction utilizing hydrogen formed at the cathode (Eq. 1) [16] or Fe(0) (Eq. 2) [3,17], oxidation via reactive oxidative species like OH[•] and H₂O₂ (Eqs. 3 and 4) [4], or sequential biotic reduction if a dechlorinating microbial culture like *Dehalococcoides* (*Dhc*) is present in the groundwater, which can benefit from the electrochemical formation of reducing conditions and hydrogen

Table 4

Electrode specifications.

Electrode composition	C [%]	Mn [%]	P [%]	S [%]	Si [%]	Supplier
99.8 % soft ingot iron	< 0.02	< 0.08	< 0.02	< 0.015	–	GoodFellow, UK
Cast iron, EN-GJL-250 C	3.25	0.77	0.148	0.066	2.39	Tasso A/S, DK

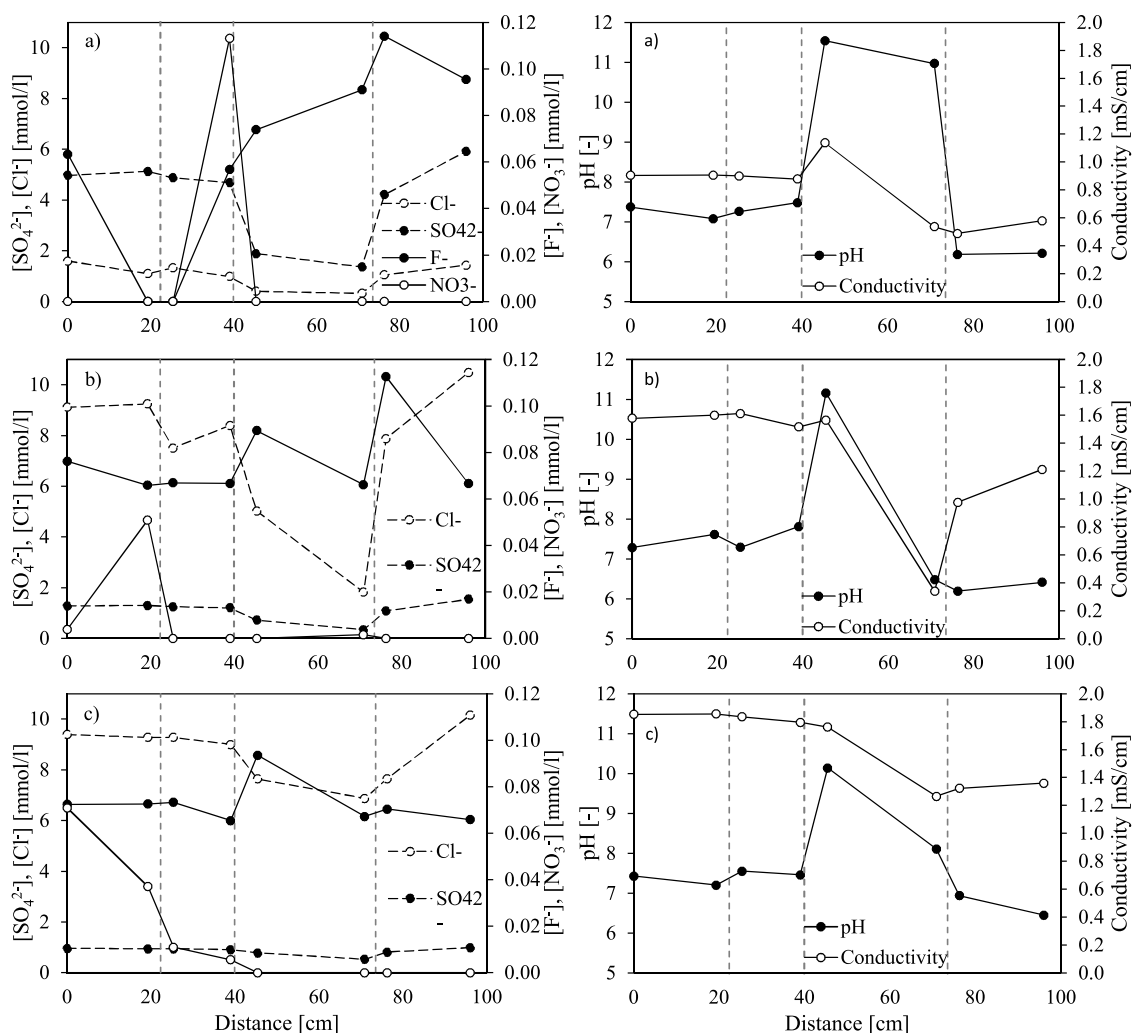
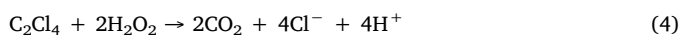
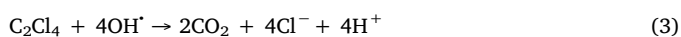
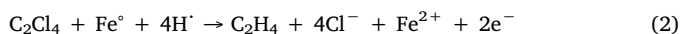
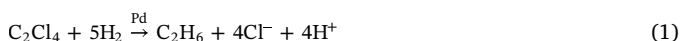


Fig. 2. Concentrations of anions, pH and conductivity measured in the pore water throughout the sand loaded column for flow rates of a) 61 m/year (0.28 ml/min), b) 122 m/year (0.56 ml/min) and c) 305 m/year (1.4 ml/min). The dashed vertical lines indicate the position of the electrodes; two cathodes and a downstream anode, which were operated at 12 mA DC. Sampling occurred after 1 PV. Note, the contaminated groundwater used for (a) is of another origin than the groundwater used for the remaining tests.

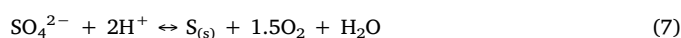
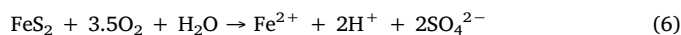
near the cathode (Eq. 5) [18]. Common for complete abiotic and biotic reduction is formation of ethene and/or ethane (Eqs. 1–5) [e.g. 4,5,19].



However, stoichiometry of the contaminant removal observed in this study is not sufficient in explaining the remarkably high levels of ethene and ethane measured in the pore water downstream the anode (Fig. 5). Instead, this could form via electrochemical reduction of CO_2 present as part of the carbonate system. The intermediate methane should then be formed near the cathode [20] and subsequently via polymerisation form ethane and ethene, possibly stimulated by anode processes [21]. Immediately downstream the second cathode, a low level of methane of 1.3 $\mu\text{mol/l}$ was measured (data not shown).

3.2. Sulphate

The sand contained 0.007% S (Table 3), possibly present as pyrite (FeS_2). Pyrite can be oxidised to SO_4 and Fe(II) (Eq. 6) [22], which may occur in the oxidising zone near the anode and explain the increase in SO_4 and Fe downstream the anode. However, possible presence of pyrite does not explain the decrease in SO_4 in the reducing zone of the second cathode. Instead, reduction of SO_4 to S(0) or S(-II) at the cathode followed by the reversed oxidation processes at the anode is expected (Eqs. 7 and 8). That pyrite oxidation is not supplying the majority of SO_4 is indicated by low levels or lack in detection of the common pyrite trace elements Ni, Pb, As and Zn (Fig. 3) [23].



The SO_4 concentration downstream the anode exceeded the inlet water concentration for the various flows by 3.1–17.2 % (Fig. 2). This increase could be a combination of low-level pyrite oxidation and release of S from corrosion of the anode (Section 3.3). Presence of S can inhibit contaminant degradation caused by poisoning of the Pd catalyst

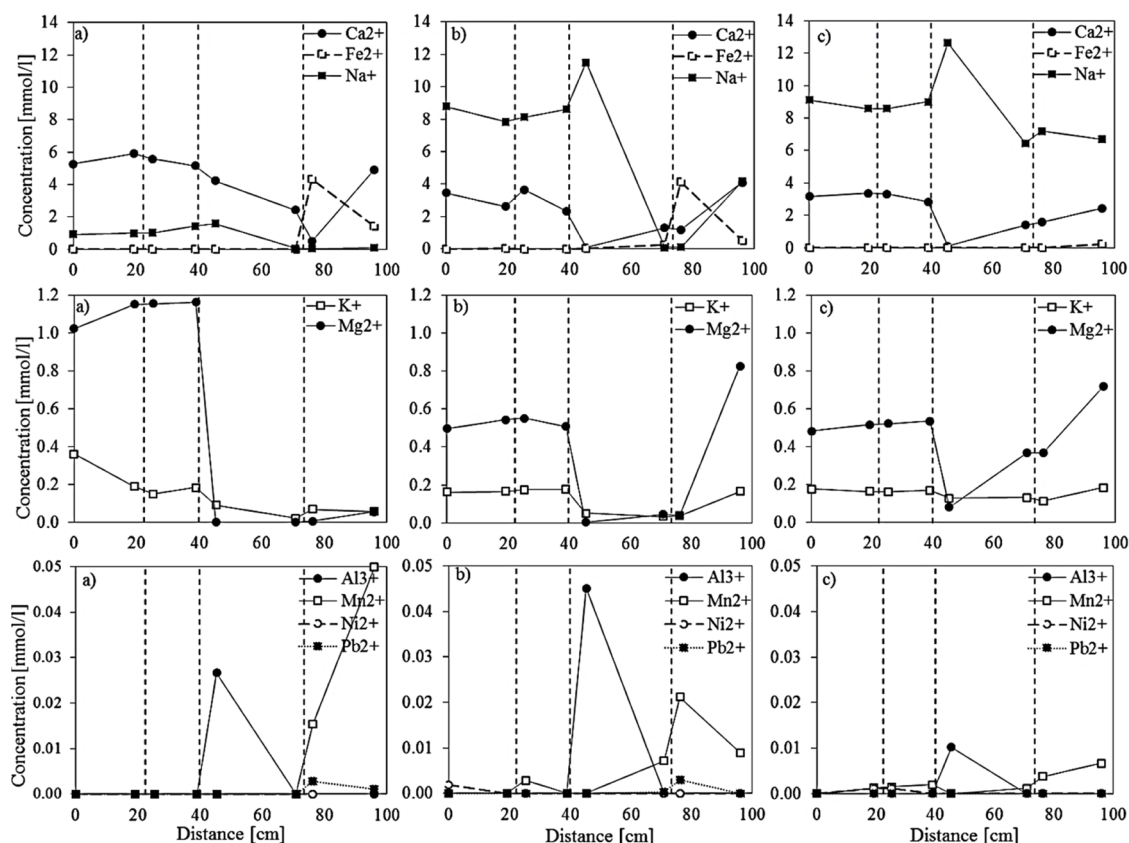


Fig. 3. Concentrations of cations measured in the pore water throughout the sand loaded column for flow rates of a) 61 m/year (0.28 ml/min), b) 122 m/year (0.56 ml/min) and c) 305 m/year (1.4 ml/min). The dashed vertical lines indicate the position of the electrodes; two cathodes and a downstream anode, which were operated at 12 mA DC. Sampling occurred after 1 PV. Note, the contaminated groundwater used for (a) is of another origin than the groundwater used for the remaining tests.

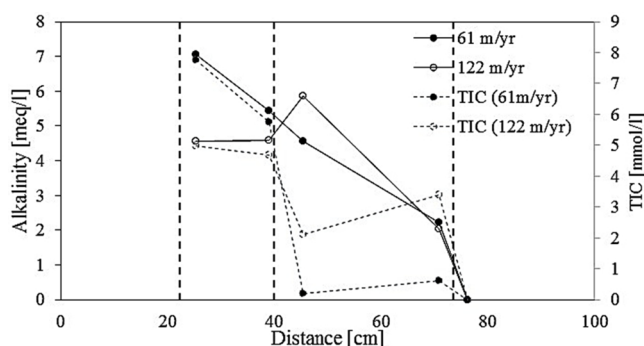


Fig. 4. Alkalinity estimated based on Gran titration and TIC calculated using PHREEQC [12] in the pore water of the sand loaded column for selected samples of two flow rates; 61 m/year (0.28 ml/min) and 122 m/year (0.56 ml/min). The dashed vertical lines indicate the position of the electrodes; two cathodes and a downstream anode, which were operated at 12 mA DC. Sampling occurred after 1 PV. Note, the contaminated groundwater used for the two flow rates originated from different sites.

[24]. However, the low-levels of S in this study possibly present from e.g. reduction of SO_4 are considered of low impact [7,24].

3.3. Corrosion of anode

The impact of corrosion on the groundwater chemistry is dependent on the anode material applied. Corrosion of the cast iron anode likely released impurities embedded in the iron (Table 4). The measured mass loss (by weight) of the anode was 23% lower than the calculated mass

loss from injected current. Based on the measured mass loss, the potential amount of Fe and Mn released during corrosion for the various flow rates exceeded the highest measured concentration of Fe and Mn downstream the anode with 56–1044 % and 98–197 %, respectively, indicating precipitation. Comparing corrosion levels with measured levels in the inlet water and detection of Fe and Mn in vicinity of the anode only, indicate that the main source of Fe and Mn was the corroding anode (Fig. 3).

The potential release of S based on the measured mass loss of the anode for the flow rates studied constituted between 0.14–0.27% of the highest measured concentrations of sulfate downstream the anode (Fig. 2). This contribution of S to the increase in sulfate concentration downstream the anode when comparing with the inlet concentration, was only 1.5–5.3 %. Thus, the data suggest that anode corrosion was not the main source of S.

Increasing the flow rate implied shortened duration between sampling rounds (for every 1 PV). Hence, less corrosion of the anode (as the current was unchanged) explain the lower concentrations of Fe and Mn detected with increasing flow rate (Fig. 3).

The effect of Fe release from corrosion is precipitation of iron oxides and/or iron hydroxides, and clogging. In early stages of the test, black deposits formed. With time, deposition expanded to cover the majority of sand located downstream the anode. Water samples extracted in this region had a grey transparent shade, which gradually changed to a red shade. Thus, these black deposits likely were wüstite (FeO) (Eqs. 9 and 10) or magnetite (Fe_3O_4) (Eq. 11) or green rust transformed from $\text{Fe}(\text{OH})_2$. Reactive iron minerals such as magnetite, pyrite and green rust may improve the abiotic dechlorination of chlorinated ethenes [25]. When the samples were transferred to vials with a headspace containing oxygen, the precipitates possibly oxidised to the red $\text{Fe}(\text{OH})_3$ (Eq. 12).

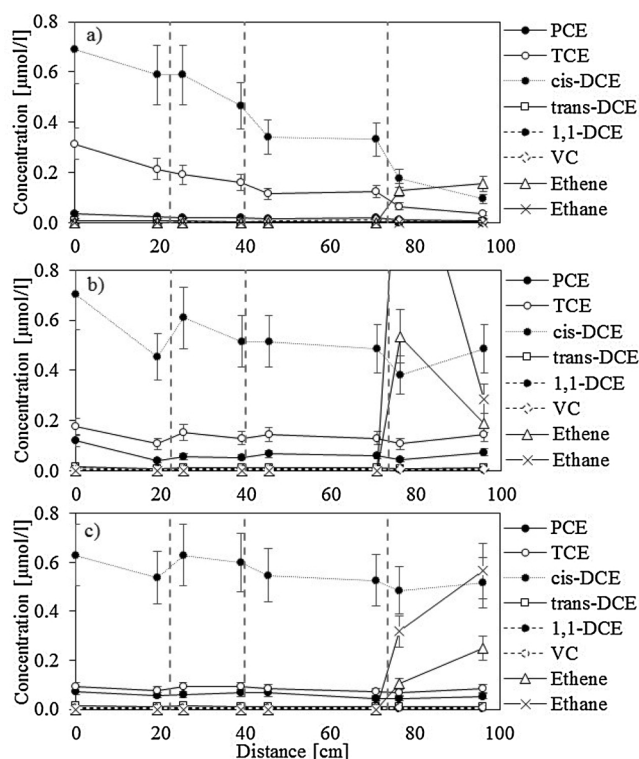
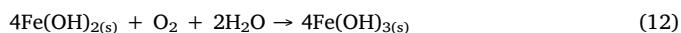


Fig. 5. Contaminant concentrations measured in the pore water throughout the sand loaded column for flow rates of a) 61 m/year (0.28 ml/min), b) 122 m/year (0.56 ml/min) and c) 305 m/year (1.4 ml/min). The dashed vertical lines indicate the position of the electrodes; two cathodes and a downstream anode, which were operated at 12 mA DC. Sampling occurred after 1 PV. In b) the outlying data point for ethane is at 1.5 µmol/l. Note, the contaminated groundwater used for (a) is of another origin than the groundwater used for the remaining tests.

Concurrent with the precipitation of iron oxides, the pressure within the column rose and venting above the electrodes was increasingly challenging because of leakage of pore water. Thus, clogging caused by the iron precipitates is assumed important to the overall process.



The contribution of reactive iron minerals to the chlorinated solvent removal can not compensate for the practical issues experienced in laboratory set-ups arising from clogging. In the field, the conclusion may be different in that the system studied is not closed, wherefore issues with leaking and altered pressure is of less concern. For lab-studies, it is suggested to apply dimensionally stable anodes like MMO (Table 1). However, the reducing zone favoring dechlorination will be shortened and more oxygen will be generated at the anode when replacing the anode of cast Fe with MMO [26]. Gas bubbles in the pore space may also lead to decreased permeability leading to elevated pressure and leaking if no adequate means of venting is installed.

3.4. Site-extracted contaminated groundwater

Performing tests with contaminated site groundwater adds complexity besides the solution chemistry, since it contains chlorinated degradation products (Table 2). Hence, the design of the test must cope with the diverse composition of contamination, each component having a unique half-cell reaction potential [27,28]. Furthermore, the net

reactions stimulated will complicate the interpretation of the parameters studied.

Working with field-extracted contaminated groundwater for testing of remediation also challenges the comparability of each study conducted because of fluctuations in contaminant composition, groundwater composition and concentrations of the ionic species and contaminant components on site. For the electrochemical remediation, this means a variation in redox reactions competing with the hydrodechlorination. Hence, ongoing adjustments of the applied specifications may be needed. In addition, the yield of the groundwater supply from one site can change over time and result in a need for a complete change of site (Section 2).

3.5. Hydrology

For the flow rates studied, insignificant alterations in trends of the recorded groundwater chemistry components were observed (Figs. 2 and 3). The main effect observed when varying flow rates was the changing release of corrosion products from the anode resulting from these being a function of the constant current input (Section 3.3). The contaminant removal decreased with increasing flow rate (Fig. 5) possibly due to the shorter residence time [5] or lower mass loss of the volatile contaminants at higher flow rates. Analysis of the gas phase extracted above the electrodes indicated a trend of less volatilisation with increasing flow (data not shown).

Performing electrochemical experiments at near natural groundwater temperatures possibly further challenges the removal of the contaminants attributable to the nature of the degradation mechanisms for this technology: Dechlorination rates are mainly limited by chemical dependent factors such as chemisorption and rates of bond-breaking, which decrease with decreasing temperature [29]. One way to overcome this challenge may be extension of the treatment zone with installation of more electrodes for a prolonged retention time.

3.6. PHREEQC model

A simple equilibrium 1D model was defined in the geochemical software PHREEQC – a computer program for speciation, batch-reaction, one-dimensional transport, and inverse geochemical calculations, version 3 [13]. The inlet concentrations of the elements Al, As, Ba, Ca, Cd, Cl, Cr, Cu, F, Fe, K, Mg, Mn, Na, N(V), Ni, P, Pb, S(VI) and Zn measured during the experimental work were used for the flushing solutions. To simulate the cathode, the pH was forced to increase by adding RbOH (12 mmol, Rb is not included in the ion-exchange) and the electron activity (pe) forced to decrease by adding H₂ (6 mmol). The anode was simulated by decreasing pH and increasing Fe²⁺ by adding FeBr₂ (16 mmol, Br is unreactive), while pe was increased by adding O₂ (8 mmol). The model uses the standard phreeqc.dat database, which includes all the measured ions in the model as well as relevant exchanger coefficients. Partial pressures are not considered as such; the H₂ and O₂ gasses added react immediately, leading to very low partial pressures of both. Though the model is an equilibrium model, kinetic effects have to some extent been included by fixing the saturation state of calcite, dolomite and magnetite at SI > 0 (SI = log (IAP/K)); 0.74, 0.89 and 10. In general, kinetic effects would lead to gradual rather than abrupt changes. The model output showed:

- Low levels of methane formed near the cathode from reduction of CO₂
- Reduction of SO₄ to S(-II) near the cathode followed by oxidation to SO₄ at the anode
- A decrease in Ca, Mg and TIC resulting from deposition of calcite
- Ion exchange of K leading to decreasing concentrations downstream of the cathode. The more complex pattern seen for Na was not reproduced
- Supersaturation and precipitation of magnetite near the anode

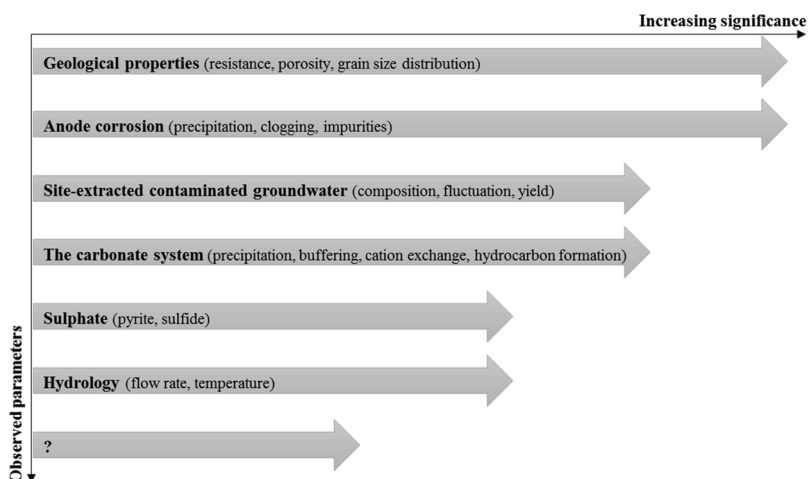


Fig. 6. Experienced significance of parameters on the execution of electrochemical remediation of groundwater in natural environmental settings. The overall parameter is in bold, while inherent parameters in focus are in brackets. The length of the arrows indicate the relative influence. Note, the influence might be positive, e.g. buffering of acidity by the carbonate system.

possibly explaining the black iron precipitates

Hence, the simple model supports the interpretation of the analytical results of the water samples extracted during the experimental work.

3.7. Rating of parameter influence

Based on the observations and data interpretations made on the performed test on electrochemical remediation of groundwater in natural settings, a rating of parameters affecting the execution of the methodology is proposed (Fig. 6).

Experiences gained during the experimental work point to a strong influence of the geological properties and the corrosion of the anode on the execution of electrochemical laboratory testing (Fig. 6). The challenges with a corroding iron anode can be overcome by use of dimensionally stable anodes, e.g. MMO, though more oxygen will be generated. The influence of the geology needs to be better understood to be able to engineer the system for application in various geologies and more complex geological matrices. For calcium rich geologies, i.e. limestone aquifers, elevated calcium precipitation on the cathode may be experienced, which can be overcome by exhausting the buffering capacity through addition of acid to the well containing the cathode. For geologies containing a fraction of charged soil particles, e.g. clay particles, the additional transport mechanism electroosmosis may establish, which introduces a flow directed towards the cathode. In addition, heterogeneous geologies likely have a non-uniform electrical conductivity distribution and thereby varying resistivities. In between a pair of electrodes, the electrical current is expected to travel through the least resistive fractions of the soil matrix. Thus, it will be important to get the conceptual model of a site right and to continue research on applied electrochemistry for improved knowledge on the influence of site-specific parameters. The influence of less significant parameters is easily blurred by the alterations from more significant parameters. Hence, Fig. 6 is not the complete picture.

4. Conclusions

The performed 1D-column study revealed a high complexity in electrochemical remediation of site-extracted contaminated groundwater in a sandy aquifer material. Further complication was attributed to corrosion of the cast iron anode because of e.g. precipitation. The complex system was modelled in a simple geochemical PHREEQC model, which was able to capture the main observed system responses to changes in pH and pe. Hence, the simple model could be used to assist in the understanding of the coupled geochemical processes. Based on the experiences gained, the significances of system parameters on

the execution of electrochemical remediation in natural settings were ranked, with geology and anode corrosion being most important. Further work will address the observed challenges to optimize the method performance for *in situ* plume control.

Acknowledgements

This work was funded by the Innovation Fund Denmark [grant number 5016-00165B], COWIfonden [grant number C-131.01], the Capital Region of Denmark [grant number 14002102], COWI A/S and Technical University of Denmark.

References

- [1] J.F. Pankow, S. Feenstra, J.A. Cherry, M.C. Ryan, Dense chlorinated solvents in groundwater: background and history of the problem, in: J.F. Pankow, S. Feenstra (Eds.), *Dense Chlorinated Solvents and Other DNAPLs in Groundwater*, Waterloo Press, Oregon, 1996, pp. 1–52 ISBN: 9780964801417.
- [2] A.M. Ruder, Potential health effects of occupational chlorinated solvent exposure, *Ann. N. Y. Acad. Sci.* 1076 (2006) 207–227, <https://doi.org/10.1196/annals.1371.050>.
- [3] J. Wang, J. Farrell, Investigating the role of atomic hydrogen on chloroethene reactions with iron using tafel analysis and electrochemical impedance spectroscopy, *Environ. Sci. Technol.* 37 (2003) 3891–3896, <https://doi.org/10.1021/es0264605>.
- [4] S. Yuan, X. Mao, A.N. Alshawabkeh, Efficient degradation of TCE in groundwater using Pd and electro-generated H₂ and O₂: a shift in pathway from hydrodechlorination to oxidation in the presence of ferrous ions, *Environ. Sci. Technol.* 46 (2012) 3398–3405, <https://doi.org/10.1021/es204546u>.
- [5] X. Mao, S. Yuan, N. Fallahpour, A. Ciblak, J. Howard, I. Padilla, R. Loch-Carusio, A.N. Alshawabkeh, Electrochemically induced dual reactive barriers for transformation of TCE and mixture of contaminants in groundwater, *Environ. Sci. Technol.* 46 (2012) 12003–12011, <https://doi.org/10.1021/es301711a>.
- [6] L. Rajic, N. Fallahpour, A.N. Alshawabkeh, Impact of electrode sequence on electrochemical removal of trichloroethylene from aqueous solution, *Appl. Catal. B: Environ.* 174–175 (2015) 427–434, <https://doi.org/10.1016/j.apcatb.2015.03.018>.
- [7] S. Yuan, M. Chen, X. Mao, A.N. Alshawabkeh, A three-electrode column for Pd-catalytic oxidation of TCE in groundwater with automatic pH-regulation and resistance to reduced sulfur compound fouling, *Wat. Res.* 47 (2013) 269–278, <https://doi.org/10.1016/j.watres.2012.10.009>.
- [8] L. Rajic, N. Fallahpour, R. Nazari, A.N. Alshawabkeh, Influence of humic substances on electrochemical degradation of trichloroethylene in limestone aquifers, *Electrochim. Acta* 181 (2015) 123–129, <https://doi.org/10.1016/j.electacta.2015.03.121>.
- [9] N. Fallahpour, X. Mao, L. Rajic, A.N. Alshawabkeh, Electrochemical dechlorination of trichloroethylene in the presence of natural organic matter, metal ions and nitrates in a simulated karst media, *J. Environ. Chem. Eng.* 5 (2017) 240–245, <https://doi.org/10.1016/j.jece.2016.11.046>.
- [10] L. Rajic, N. Fallahpour, S. Yuan, A.N. Alshawabkeh, Electrochemical transformation of trichloroethylene in aqueous solution by electrode polarity reversal, *Wat. Res.* 67 (2014) 267–275, <https://doi.org/10.1016/j.watres.2014.09.017>.
- [11] L. Rajic, N. Fallahpour, E. Podlaha, A. Alshawabkeh, The influence of cathode material on electrochemical degradation of trichloroethylene in aqueous solution, *Chemosphere* 147 (2016) 98–104, <https://doi.org/10.1016/j.chemosphere.2015.12.095>.
- [12] L. Rajic, R. Nazari, N. Fallahpour, A.N. Alshawabkeh, Electrochemical degradation of trichloroethylene in aqueous solution by bipolar graphite electrode, *J. Environ. Chem. Eng.* 4 (2016) 197–202, <https://doi.org/10.1016/j.jece.2015.10.030>.

- [13] D.L. Parkhurst, C.A.J. Appelo, Description of input and examples for PHREEQC version 3 – A computer program for speciation, batch-reaction, one-dimensional transport, and inverse geochemical calculations: U.S. Geological Survey Techniques and Methods, 2013, book 6, chap. A43, pp. 497. Available only at <http://pubs.usgs.gov/tm/06/a43>.
- [14] C.A.J. Appelo, D. Postma, Carbonates and carbon dioxide, in: C.A.J. Appelo, D. Postma (Eds.), *Geochemistry, Groundwater and Pollution*, second edition, CRC Press, Taylor & Francis Group, Leiden, 2005, pp. 176–240 ISBN10: 04 1536 428 0.
- [15] C.A.J. Appelo, D. Postma, Ion exchange, in: C.A.J. Appelo, D. Postma (Eds.), *Geochemistry, Groundwater and Pollution*, second edition, CRC Press, Taylor & Francis Group, Leiden, 2005, pp. 242–309 ISBN10: 04 1536 428 0.
- [16] W.W. McNab, R. Ruiz, Palladium-catalyzed reductive dehalogenation of dissolved chlorinated aliphatics using electrolytically-generated hydrogen, *Chemosphere* 37 (1998) 925–936, [https://doi.org/10.1016/S0045-6535\(98\)00095-2](https://doi.org/10.1016/S0045-6535(98)00095-2).
- [17] W.A. Arnold, A.L. Roberts, Pathways and kinetics of chlorinated ethylene and chlorinated acetylene reaction with Fe(0) particles, *Environ. Sci. Technol.* 34 (2000) 1794–1805, <https://doi.org/10.1021/es980252o>.
- [18] F. Aulenta, L. Tocca, R. Verdini, P. Reale, M. Majone, Dechlorination of trichloroethene in a continuous-flow bioelectrochemical reactor: effect of cathode potential on rate, selectivity, and electron transfer mechanisms, *Environ. Sci. Technol.* 45 (2011) 8444–8451, <https://doi.org/10.1021/es202262y>.
- [19] X. Mao, J. Wang, A. Ciblak, E.E. Cox, C. Riis, M. Terkelsen, D.B. Gent, A.N. Alshawabkeh, Electrokinetic-enhanced bioaugmentation for remediation of chlorinated solvents contaminated clay, *J. Hazard. Mater.* 213–214 (2012) 311–317, <https://doi.org/10.1016/j.jhazmat.2012.02.001>.
- [20] M. Azuma, K. Hashimoto, M. Hiramoto, Electrochemical reduction of carbon dioxide on various metal electrodes in low-temperature aqueous KHCO_3 media, *J. Electrochem. Soc.* 137 (1990) 1772–1778, <https://doi.org/10.1149/1.2086796>.
- [21] S. Petrovic, J.C. Donini, S.S. Thind, S. Tong, A.R. Sanger, *Electrochemical Conversion of Hydrocarbons*, US006294068B1 (2001).
- [22] C.A.J. Appelo, D. Postma, Redox processes, in: C.A.J. Appelo, D. Postma (Eds.), *Geochemistry, Groundwater and Pollution*, second edition, CRC Press, Taylor & Francis Group, Leiden, 2005, pp. 415–487 ISBN10: 04 1536 428 0.
- [23] M.K. Baruah, P. Kotoky, G.C. Borah, Geochemical association of Ni^{2+} , Zn^{2+} , Pb^{2+} , Ag^+ , Cu^{2+} , and CO_2 ions in natural pyrite, *J. Geochem.* (2014) 1–20, <https://doi.org/10.1155/2014/161850>.
- [24] S. Yuan, M. Chen, X. Mao, A.N. Alshawabkeh, Effects of reduced sulfur compounds on Pd-catalytic hydrodechlorination of trichloroethylene in groundwater by cathodic H_2 under electrochemically induced oxidizing conditions, *Environ. Sci. Technol.* 47 (2013) 10502–10509, <https://doi.org/10.1021/es402169d>.
- [25] Y.T. He, J.T. Wilson, C. Su, R.T. Wilkin, Review of abiotic degradation of chlorinated solvents by reactive iron minerals in aquifers, *Groundw. Monit. Remediat.* 35 (2015) 57–75, <https://doi.org/10.1111/gwrmr.12111>.
- [26] N. Fallahpour, S. Yuan, L. Rajic, A.N. Alshawabkeh, Hydrodechlorination of TCE in a circulated electrolytic column at high flow rate, *Chemosphere* 144 (2016) 56–64, <https://doi.org/10.1016/j.chemosphere.2015.08.037>.
- [27] T.H. Wiedemeier, H.S. Rifai, C.J. Newell, J.T. Wilson, Overview of intrinsic bioremediation, in: T.H. Wiedemeier, H.S. Rifai, C.J. Newell, J.T. Wilson (Eds.), *Natural Attenuation of Fuels and Chlorinated Solvents in the Subsurface*, John Wiley & Sons, Inc., New York, 1999, pp. 162–188 ISBN: 9780471197492.
- [28] A.L. Roberts, L.A. Totten, W.A. Arnold, D.R. Burris, T.J. Campbell, Reductive elimination of chlorinated ethylenes by zero-valent metals, *Environ. Sci. Technol.* 30 (1996) 2654–2659, <https://doi.org/10.1021/es9509644>.
- [29] T. Li, J. Farrell, Electrochemical investigation of the rate-limiting mechanisms for trichloroethylene and carbon tetrachloride reduction at iron surfaces, *Environ. Sci. Technol.* 35 (2001) 3560–3565, <https://doi.org/10.1021/es0019878>.

APPENDIX II

Selecting electrode materials and sequence for electrochemical removal of chlorinated ethenes
in groundwater

Hyldegaard, B.H. & Ottosen, L.M.

(Submitted)

Selecting electrode materials and sequence for electrochemical removal of chlorinated ethenes in groundwater

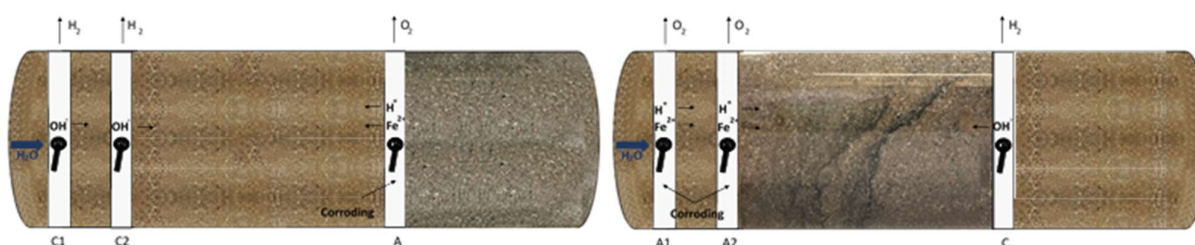
Bente Højlund Hyldegaard^{a,b,*} and Lisbeth M. Ottosen^b

^a COWI A/S, Department of Waste & Contaminated Sites, Parallelsvej 2, 2800 Kgs. Lyngby, Denmark

^b Technical University of Denmark, Department of Civil Engineering, Building 118, Brovej, 2800 Kgs. Lyngby, Denmark

* Corresponding author. E-mail address: behd@cowi.com / benho@byg.dtu.dk. Tel.: +45 56 40 87 70. ORCID: 0000-0002-3155-5012.

Graphical abstract



Abstract

Chlorinated ethene contaminations are a widespread environmental hazard and a threat to drinking water supplies. Electrochemical methods for *in situ* degradation of the chlorinated ethenes in the plume are under development. In laboratory, complete electrochemical removal of chlorinated ethenes in undivided flow-through reactors is reported when using palladized iron (Fe) cathodes and cast Fe anodes. The cost of the electrodes depends on the Fe purity. In this study, 99.95%, 99.8% and 98+% palladized Fe cathodes, and 99.8% Fe and cast Fe anodes were investigated. The surfaces of the palladized Fe electrodes were examined by scanning electron microscopy. Deposition of palladium by electroless plating onto the Fe surfaces was uneven and disconnected. The less pure the Fe material, the higher degree of oxide coverage of the cathode's surface during electroless plating. Electrochemical application via Fe electrodes installed in a flow-through reactor of field-extracted groundwater and sandy sediment was studied for three-electrode configurations of A – A – C and C – C – A. The anodes of 99.8% Fe and cast Fe demonstrated different corrosion patterns; uniform corrosion and graphitization, respectively. Corrosion products clogged the sandy matrix. The corrosion product compositions differed between the A – A – C and C – C – A electrode configurations. The groundwater pH of 7.3 changes downgradient to the electrochemical zone to 9.5 and 6.2 for the A – A – C and C – C – A reactors, respectively. The response of the hydrogeochemical settings to the established redox zones showed that the C – C – A electrode configuration was less intrusive to the surrounding environment.

Keywords

Electrochemistry; electrode material; electrode sequence; corrosion; precipitation; hydrogeochemistry

1. Introduction

Groundwater contaminated with chlorinated ethenes are hazardous to the environment, and pose a health risk to humans if used for drinking water [1]. Electrochemistry may be a solution for *in situ* groundwater remediation. The applied electrochemical concept is best studied in undivided flow-through reactors, i.e. in one-compartment reactors with aquifer material and water flowing through, which simulate the groundwater reservoir. In flow-through electrochemical reactors, the electrode configuration determines the order of the redox zones and thereby the processes for chlorinated ethene transformation and the overall removal [2, 3]. Thus, the electrode configuration is a major design parameter. Three-electrode configurations of C – C – A have demonstrated higher reaction rates for transformation of chlorinated ethenes than two-electrode configurations of C – A [2]. The studies on electrochemical removal of chlorinated ethenes in undivided flow-through reactors have demonstrated the importance in the selection of the electrode materials [3–6]. Advantages and disadvantages of different anode and cathode materials as well as catalysts on cathodes are listed in Table 1.

An important consideration for choosing the cathode material and e.g. use of catalyst is whether polarity reversal is to be applied. Noble catalysts applied on cathodes may be repelled during polarity reversal. In addition, some anode materials may release toxic metals during corrosion [14], e.g. cobber and nickel. Besides electrode material, the shape of the electrode influences the chlorinated ethene removal. E.g. foams demonstrate higher removals due to the large electrode surface area and thereby number of sites available for the electrochemical processes governing the contaminant transformation [2, 3, 7, 15].

According to Table 1, iron (Fe) electrodes show various advantages for electrochemical removal of chlorinated ethenes. Fe cathodes in combination with palladium (Pd) has demonstrated chlorinated ethene removals up to 99% [2, 4]. Fe anodes release ferrous ions rather than oxygen during electrolysis, which contribute to highly reducing conditions promoting efficient removal of chlorinated ethenes up to 99% [3, 6, 7]. Despite reported insignificant challenges posed by corrosion of Fe anodes in short-term simplified experimental conditions, coverage of the anodes and clogging of pore spaces in porous matrices are mentioned as possible adverse effects [2, 6, 7].

Table 1 Advantages and disadvantages of different anode and cathode materials incl. catalysts for removal of chlorinated ethenes in groundwater

Electrode material	Advantages	Disadvantages	Reference
Anodes			
Cast iron, Fe	<ul style="list-style-type: none"> • Ferrous iron is released rather than O₂ (corrosion); low VOC^a stripping • Maintains a reducing environment suitable for fast reductive dechlorination • Easily acquired and in various purities and costs 	<ul style="list-style-type: none"> • Formation of Fe complexes, i.e. possibly clogging and electrode coverage • Elevated pH downgradient the electrochemical zone due to low H⁺ formation • Potential release of impurities embedded in the Fe 	[2, 6, 7] [3, 6, 7] [5, 8]
Mixed metal oxide, MMO	<ul style="list-style-type: none"> • Dimensionally stable, i.e. retains its structure; can be reused • Maintains the pH and oxidation-reduction potential of the water 	<ul style="list-style-type: none"> • Low O₂ overpotential: generates oxidizing conditions, i.e. VOC stripping may increase • O₂ evolution competes with oxidation of the chlorinated ethenes 	[2, 6, 7] [2, 3]
Graphite	<ul style="list-style-type: none"> • Slow decomposition of H₂O₂ generates •OH 	<ul style="list-style-type: none"> • Oxidizes chloride to chlorine gas 	[9]
Boron-doped diamond, BDD	<ul style="list-style-type: none"> • Affinity to produce •OH 	<ul style="list-style-type: none"> • Removal of organics in competition with •OH transformation to O₂ 	[10, 11]
Cathodes			
Iron, Fe	<ul style="list-style-type: none"> • Performs better than MMO for removal of chlorinated ethenes • Pd coated Fe is superior to coated Ni, Al, C, Cu • Low cost 	<ul style="list-style-type: none"> • High H₂ overpotential; slower hydrodechlorination than noble metals 	[2] [4]
Mixed metal oxide, MMO	<ul style="list-style-type: none"> • Low cost 	<ul style="list-style-type: none"> • Interacts with H₂ on its surface, forming oxides: less H₂ for hydrodechlorination 	[2, 6, 7]
Carbon, C	<ul style="list-style-type: none"> • High surface area and porosity. Low reactivity • Superior to Fe, Cu, Al in terms of chlorinated ethene removal • Low cost 	<ul style="list-style-type: none"> • Fragile, i.e. not suitable in the field 	[2, 4] [4]
Graphite	<ul style="list-style-type: none"> • Produces H₂O₂ and •OH • Cheap, safe material 	<ul style="list-style-type: none"> • Slow H₂ formation due to limited reactivity 	[7] [9]
Copper, Cu	<ul style="list-style-type: none"> • Performs better than Fe and Al • Low cost 	<ul style="list-style-type: none"> • Induces precipitation and electrode coverage • Higher H₂ evolution overpotential than noble metals; slower hydrodechlorination 	[6, 7] [4, 6, 7]
Nickel, Ni	<ul style="list-style-type: none"> • Lower H₂ overpotential supports higher hydrodechlorination than C, Cu, Al, Fe 	<ul style="list-style-type: none"> • Accumulates H₂ bubbles on its surface 	[4]
Aluminum, Al	<ul style="list-style-type: none"> • Low cost 	<ul style="list-style-type: none"> • Corrodes with Al-complex formation • Weak bond strength with H₂ reduces hydrodechlorination 	[4] [4]
Catalysts			
Nobel metals, e.g. Ag, Pt	<ul style="list-style-type: none"> • Low H₂ overpotentials, i.e. fast reduction by hydrodechlorination • Affinity for absorption of H₂ favors hydrodechlorination 	<ul style="list-style-type: none"> • Costly 	[2, 10] [12, 13]
Palladium, Pd	<ul style="list-style-type: none"> • Catalyzes formation of H₂O₂, i.e. oxidation of chlorinated ethenes • Improves hydrodechlorination of Ni < Al < C < Cu < Fe and reaction rates • Higher surface area and sufficient bond strength with H₂ 	<ul style="list-style-type: none"> • Low Pd load incapable of binding reactive H₂ on its surface • High Pd load enhances proton reduction, i.e. competing with hydrodechlorination • Costly 	[2, 4] [4] [2, 6]

^a VOC: Volatile organic compounds

Fe is available in various compositions and costs. Awareness of toxic impurities embedded in the Fe material is especially important when used as anodes, since these may be released to the solution [8]. To our knowledge, possible differences in the distribution of Pd on Fe cathode materials of different purities during electroless plating has not previously been studied. Further, previous research has been conducted as testing in simplified environmental settings of synthetic groundwater at elevated flow through vertical oriented reactors [2–4, 8, 9, 16–19]. There is a need for assessments in near natural aquifer settings of field-extracted groundwater containing an aged contamination and flowing through an aquifer material in horizontal reactors at a realistic flow rate to study the Fe specific mechanisms in the complex hydrogeochemical settings, and the impact from electrochemical treatment on the hydrogeochemistry itself.

The objective of this study is to examine a) the surface characteristics of cast Fe and the significance of purity via examination of three compositions of high-purity Fe materials (99.95%, 99.8% and 98+% Fe), b) the distribution of Pd on the three high-purity Fe materials after electroless plating, c) the differences in corrosion patterns when applying palladized 99.8% Fe and cast Fe in A – A – C versus C – C – A electrode configurations in near natural hydrogeochemical settings, and d) the changes in the hydrogeochemical surroundings when introducing oxidizing and reducing zones of different arrangements. Despite the high purities of >98%, the cost varies significantly between these products. I.e., by using the 98+% Fe instead of the 99.95% Fe, the cost for the cathodes strongly decreases.

2. Materials and methods

2.1 Materials

Cast Fe and three high-purity Fe materials were selected (Table 2). Crystalline palladium dichloride (PdCl_2 , 99.9%, Thermo Fisher Scientific) was used for the electroless plating of the three high-purity Fe materials. Hydrochloric acid (HCl, 35%, VWR) was used for rinsing of Fe materials and dissolution of PdCl_2 .

Table 2 Compositions of the cast Fe and three high-purity Fe materials studied.
The concentrations are provided by the suppliers listed

Composition	Cast Fe ^a	99.95% Fe ^a	99.8% Fe ^a	98+% Fe ^a
Ag [%]	-	-	-	< 0.0001
Al [%]	-	0.0003	-	0.010
C [%]	3.25	-	< 0.02	0.200
Ca [%]	-	0.010	-	-
Cd [%]	-	-	-	< 0.0001
Co [%]	-	0.005	-	0.005
Cr [%]	-	-	-	0.030
Cu [%]	-	0.020	-	0.100
Ge [%]	-	-	-	0.001
Mg [%]	-	0.0001	-	< 0.0001
Mn [%]	0.770	-	< 0.08	0.94
Mo [%]	-	-	-	0.020
Ni [%]	-	0.020	-	0.020
P [%]	0.148	-	< 0.02	-
S [%]	0.066	-	< 0.015	-
Si [%]	2.39	0.0001	-	0.31
Sn [%]	-	-	-	0.005
Ti [%]	-	-	-	0.0003
V [%]	-	-	-	0.003
Supplier	Tasso A/S, DK EN-GJL-250 C	GoodFellow, UK	GoodFellow, UK	GoodFellow, UK

^a -: Not present in the Fe material

2.2 Preparation of Fe materials used for examination of surfaces

The Fe materials were rinsed using 1 M HCl, washed with deionized water and air-dried. The surfaces of the rinsed materials were visually examined by SEM. Next, the Fe materials were electroless plated with Pd: PdCl₂ was dissolved in 0.1 M HCl, the Fe was then submerged into the solution and together rotated until the solution turned colorless, confer the procedure outlined in Rajic et al. [4] for a loading of 0.76 mg/cm². Following, mapping of elements on the Fe material surfaces was carried out by SEM.

2.3 The column experiments

For the electrochemical application in natural hydrogeochemical settings, a three-electrode configuration (E1 – E2 – E3) and constant current of 12 mA was applied in a column reactor (Fig. 1, [8]). E1 and E2 were identical electrodes of Pd coated Fe (99.8% Fe) rods, while E3 was a cast Fe. Investigated electrode configurations were A – A – C and C – C – A.

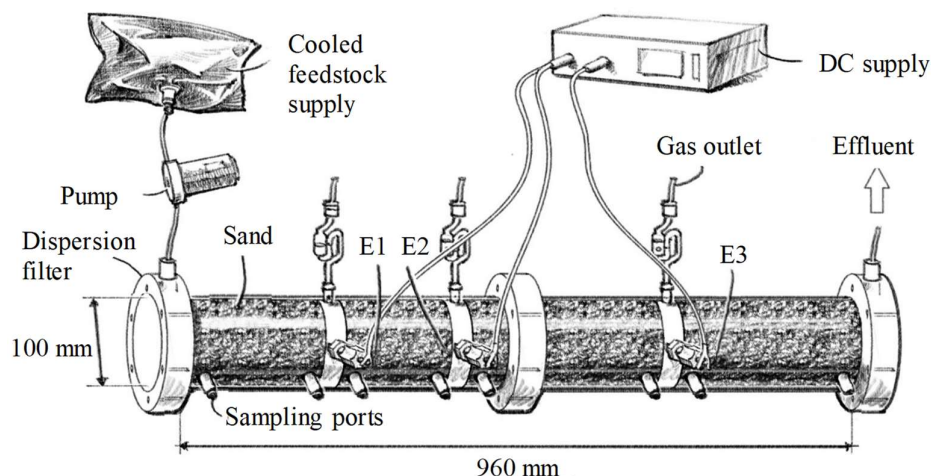


Fig. 1 Illustration of the undivided flow-through electrochemical reactor loaded with sandy sediment. The feedstock supply of field-extracted groundwater containing an aged PCE contamination was stored at 5°C. E1, E2 and E3 indicate positions of electrodes

Groundwater was collected from two different wells in Skovlunde, Denmark. For testing with an A – A – C electrode configuration, groundwater was tapped directly from an onsite pump-and-treat facility subsequent to the sand filters to eliminate the impact of precipitation due to oxidation of naturally present Fe^{2+} . For C – C – A testing, groundwater was extracted directly from a well installed in a contaminated groundwater aquifer at a site in Skovlunde, Denmark [8]. Specifications are given in Table 3.

Table 3 Specifications for the electrochemical column experiments performed

	A – A – C	C – C – A [8]
Conductivity [$\mu\text{S}/\text{cm}$]	766 \pm 7.0	830 \pm 77
pH [-]	7.3	7.4
Seepage velocity [m/yr]	48	61
Flow [ml/min]	0.23	0.28
Tetrachloroethylene [$\mu\text{g}/\text{l}$]	3.9	27
Trichloroethylene [$\mu\text{g}/\text{l}$]	3.7	69
1,1-dichloroethylene [$\mu\text{g}/\text{l}$]	< 0.05	0.06
Cis-1,2-dichloroethylene [$\mu\text{g}/\text{l}$]	6.2	86
Trans-1,2-dichloroethylene [$\mu\text{g}/\text{l}$]	< 0.05	0.81
Ca^{2+} [mg/l]	98	211
Mg^{2+} [mg/l]	13	25
Fe^{2+} [mg/l]	< 0.02	< 0.02
Na^{+} [mg/l]	14	21
SO_4^{2-} [mg/l]	128	478
Cl^{-} [mg/l]	37	57
NO_3^{-} [mg/l]	2.3	< 0.02

The groundwater feedstock solutions were stored at 5 °C as described in Hyldegaard et al. [8]. Sandy sediment from Nymølle Sand quarry in Svogerslev, Denmark, was collected to represent the geology of a primary aquifer, which was characterized in Hyldegaard et al. [8] (15% calcium carbonate, 0.952% carbon, 0.007% Sulphur, 0.36 mg iron per kg sand, grain size d(0.5) of 0.407 mm, d(0.9) of 0.895 mm). The sand-filled reactor was saturated with the groundwater by pumping the contaminated groundwater through the sandy sediment for two pore volumes (PV) prior to the electrochemical application. For assessment of changes in the hydrogeochemistry, porewater was sampled from the eight sampling ports after 1 PV and 2 PV of electrochemical application.

2.4 Analytical methods

For visual examination of the surfaces of the Fe materials investigated prior to electroless plating with Pd, scanning electron microscopy (SEM) using a FEI Quanta 200 ESEM with a LFD detector was used. Mapping of elements on the surfaces of the cast Fe and Pd coated Fe materials was performed using a FEI Inspect S microscope with an EDS Oxford Instruments 50 mm² X-Max silicon drift detector and an Everhart-Thornley solid state BSE, Large Field and CCF Camera imaging detector. For the assessment of electrochemical application in the column reactors, potential differences were measured, and samples were extracted for analysis of VOC, hydrocarbons, cationic and anionic species, pH and conductivity. Details are specified in Hyldegaard et al. [8]. NETZSCH STA 449 F3 Jupiter® was used for thermogravimetric analysis (TGA) of white precipitates formed during the electrochemical application.

3. Results and discussion

3.1 Electrode surfaces, macroscopic level

The appearance of the four rinsed Fe materials studied is shown in Fig. 2(a-d) and of the three Pd coated high-purity Fe materials in Fig. 2(e-g).

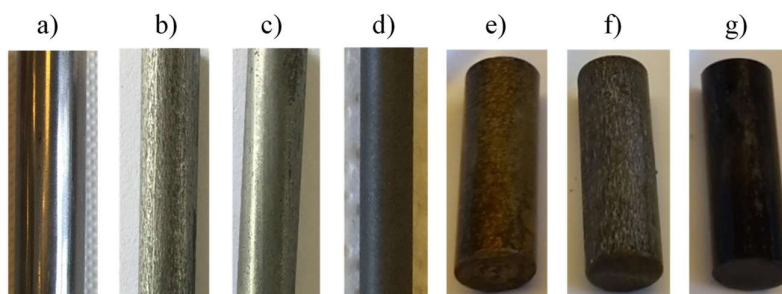


Fig. 2 Surfaces of a) 99.95% Fe, b) 99.8% Fe, c) 98+% Fe, d) cast Fe, e) Pd coated 99.95% Fe, f) Pd coated 99.8% Fe and g) Pd coated 98+% Fe

The 99.95% Fe material had a uniform, smooth, shiny grey surface, whereas the less pure Fe materials had a spotted, smooth and less shiny grey surface (Fig. 2a-c). The cast Fe was dark grey and had a less smooth surface (Fig. 2d). After electroless plating with Pd, the 99.95% Fe appeared golden with spots, the 99.8% Fe dark grey with spots, and the 98+% Fe grey (Fig. 2e-g). Differences in appearance between the high-purity Fe materials became more notable after palladization.

3.2 Electrode surfaces, microscopic level

The characteristics of the surfaces of the four Fe materials examined in microscopic level are exemplified in Fig. 3.

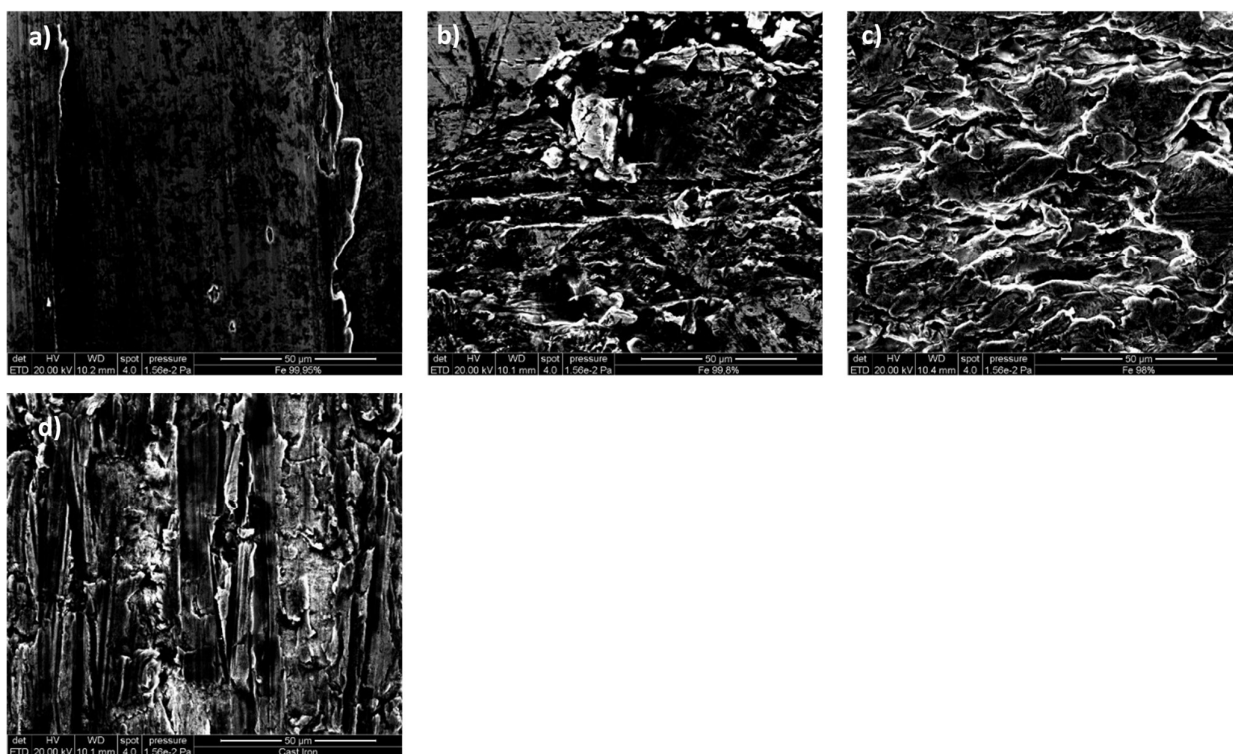


Fig. 3 SEM images of a) 99.95% Fe, b) 99.8% Fe, c) 98+% Fe, d) cast Fe. The surfaces are magnified x1000. The scale on the images indicates 50 µm

The SEM images in Fig. 3 verify the smoother surface of the 99.95% Fe material. The irregularities of the cast Fe appear as thin flakes arising from the material surface in a similar orientation (Fig. 3d), whereas for the 99.8% Fe and 98+% Fe, the irregularities appeared rounded in edges and with a more random, interconnected orientation (Fig. 3b-c).

3.3 Palladized iron, microscopic level

SEM images of the deposited layer of Pd after electroless plating of the high-purity Fe materials is shown in Fig. 4.

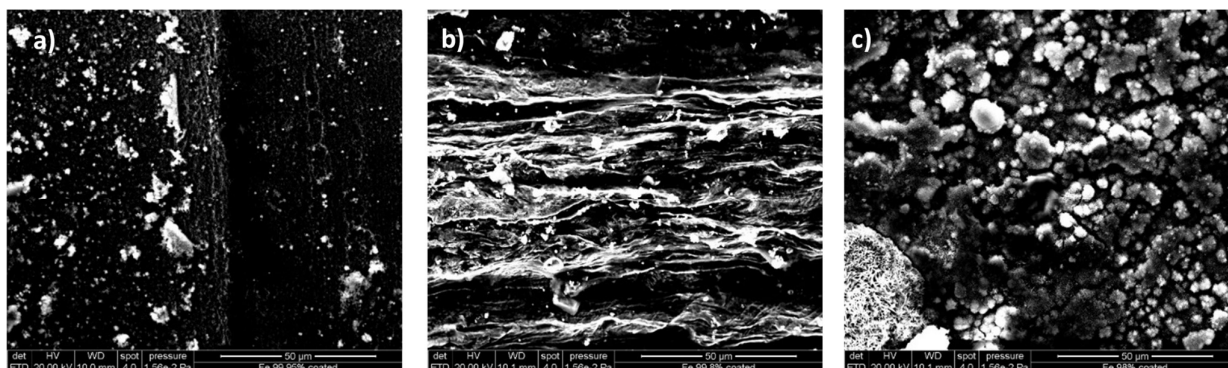


Fig. 4 SEM images of Pd electroless plated materials of a) 99.95% Fe, b) 99.8% Fe, c) 98+% Fe. The surfaces are magnified x1000. The scale on the images indicates 50 μm

The electroless plating of high-purity Fe with Pd resulted in a deposition of Pd in lumps, i.e. an uneven, disjoint distribution of Pd on the Fe metal surfaces (Fig. 4). Similar was found for deposition of Pd onto a 98% pure Fe foam [2]. The shape of the absorbed lumps onto 99.95% Fe and 99.8% Fe were irregular, but with defined edges, whereas on the 98+% Fe appeared, the Pd lumps appeared blurred. Therefore, mapping of the elements on the surfaces of the Fe materials was carried out, which is exemplified in Fig. 5. The mapping revealed, that

- 99.95% Fe: Pd was deposited in lumps with few oxides on the Fe surface
- 99.8% Fe: Pd was deposited in lumps and some oxides had formed on the Fe surface at locations different from the deposited Pd
- 98+% Fe: Pd was deposited in lumps, more oxides had formed on the Fe surface at locations different from the deposited Pd and Cl was deposited on the surface in areas of oxides formed, i.e. opposite to Pd

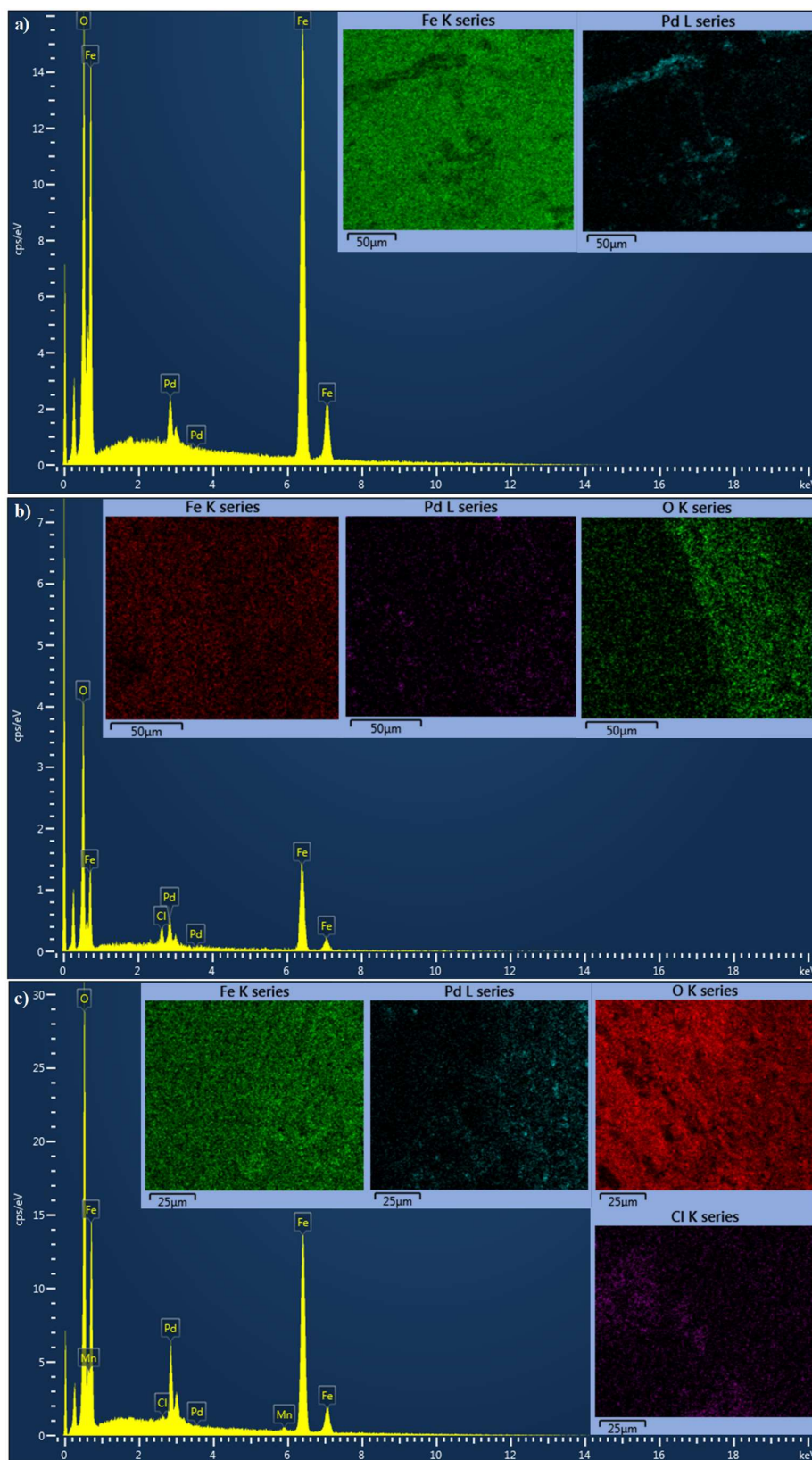


Fig. 5 Mapping of elements on the Pd electroless plated materials of a) 99.95% Fe, b) 99.8% Fe, c) 98+% Fe

The mapping of elements thus showed, that the higher the Fe purity, the less oxides had formed. Locally, the noble Pd increases the standard potential of the surface of the supporting Fe materials, which may induce corrosion of Fe at locations with lower standard potential, i.e. where no Pd is deposited. Opposite, impurities imbedded in the Fe material locally may decrease the standard potentials of the supporting Fe materials. Hence, the increasing formation of oxides with less Fe purity is suggested to be due to the introduced elevated difference between standard potentials of locations with Pd vs. adjacent locations of impure Fe, causing corrosion of Fe, which facilitates formation of oxides. Despite differences in the amount of oxide formation, this may not influence the electrochemical removal of chlorinated ethenes, if the palladized materials are used as cathodes, since the oxides will be reduced and free up surface sites for contaminant destruction. The SEM investigation indicated, that the Pd lumps deposited on 98+% Fe were smaller (the larger formations visible in Fig. 4c were mainly oxides), but this needs verification. Mapping of elements on the cast Fe was also carried out, which clearly showed spots of carbon embedded in the material cf. Table 2 (Fig. 6).

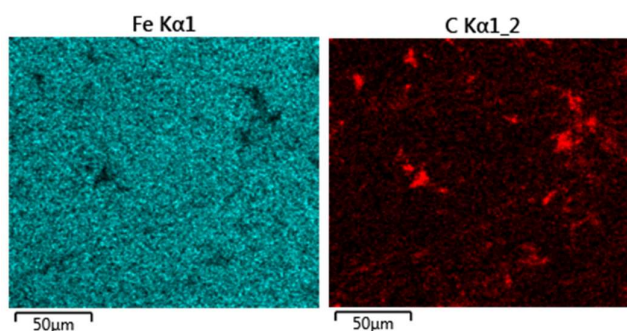


Fig. 6 Mapping of elements on the cast Fe

3.4 Corrosion of iron anodes

After the electrochemical application in configurations of A – A – C and C – C – A, it was observed, that the corrosion pattern differed for 99.8% Fe anodes and cast Fe anodes (Fig. 7).

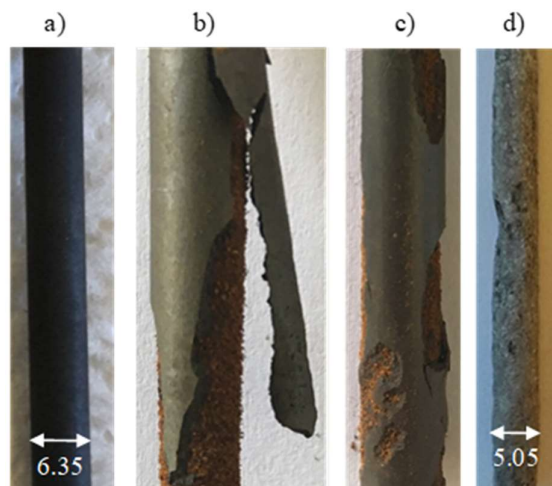


Fig. 7 Corrosion of a-c) a cast Fe anode and d) 99.8% Fe anode after electrochemical application for 14 days at 12 mA. Scales are in mm. The anodes had been washed in deionized water to remove a muddy layer of corrosion products

The cast Fe anode at first glance appeared to maintain its structure and dimensions (Fig. 7a). However, the surface had become fragile causing the outer layer to crack when drying up and revealing Fe oxides underneath (Fig. 7b-c). Cast Fe has a relatively high carbon content (>2%, Table 2) compared to other common Fe materials. As the cast Fe corrodes, graphite form on the surface, known as graphitization [20]. Graphitization can explain the immediate retained structure of the cast Fe anode and its increased fragility [20]. When the 99.8% Fe was used as anode, corrosion attacked the entire electrode, indicating uniform corrosion, resulting in decreasing thickness of the electrode (Fig. 7d).

3.5 Precipitation due to corroding anodes

Fe anodes release ferrous ions as they corrode [2, 6, 7]. The ferrous ions may precipitate as Fe oxides and/or Fe hydroxides on the anode surface or within pores of a geological matrix [6, 7]. With a continuous release of ferrous ions, precipitation may eventually result in complete clogging of the pores [6, 8]. In the flow-through reactor, the consequence can be leakage of porewater from the experimental set-up due to an elevated pressure [8]. The observed behavior of Fe precipitation was different for the A – A – C and C – C – A configurations (Fig. 8). For the A – A – C configuration, Fe precipitates shaped as angled lines in the mixed redox zone between the adjacent anode and cathode Fig. 8c. The precipitates were mainly black, but also white and least red. First, the black precipitates deposited, following the white appearance at the edge of the black precipitated front and finally red dots appeared. In the C – C – A configuration, the precipitates uniformly recolored the sandy sediment downstream the anode in the direction of flowing groundwater to a grey shaded appearance (Fig. 8b).

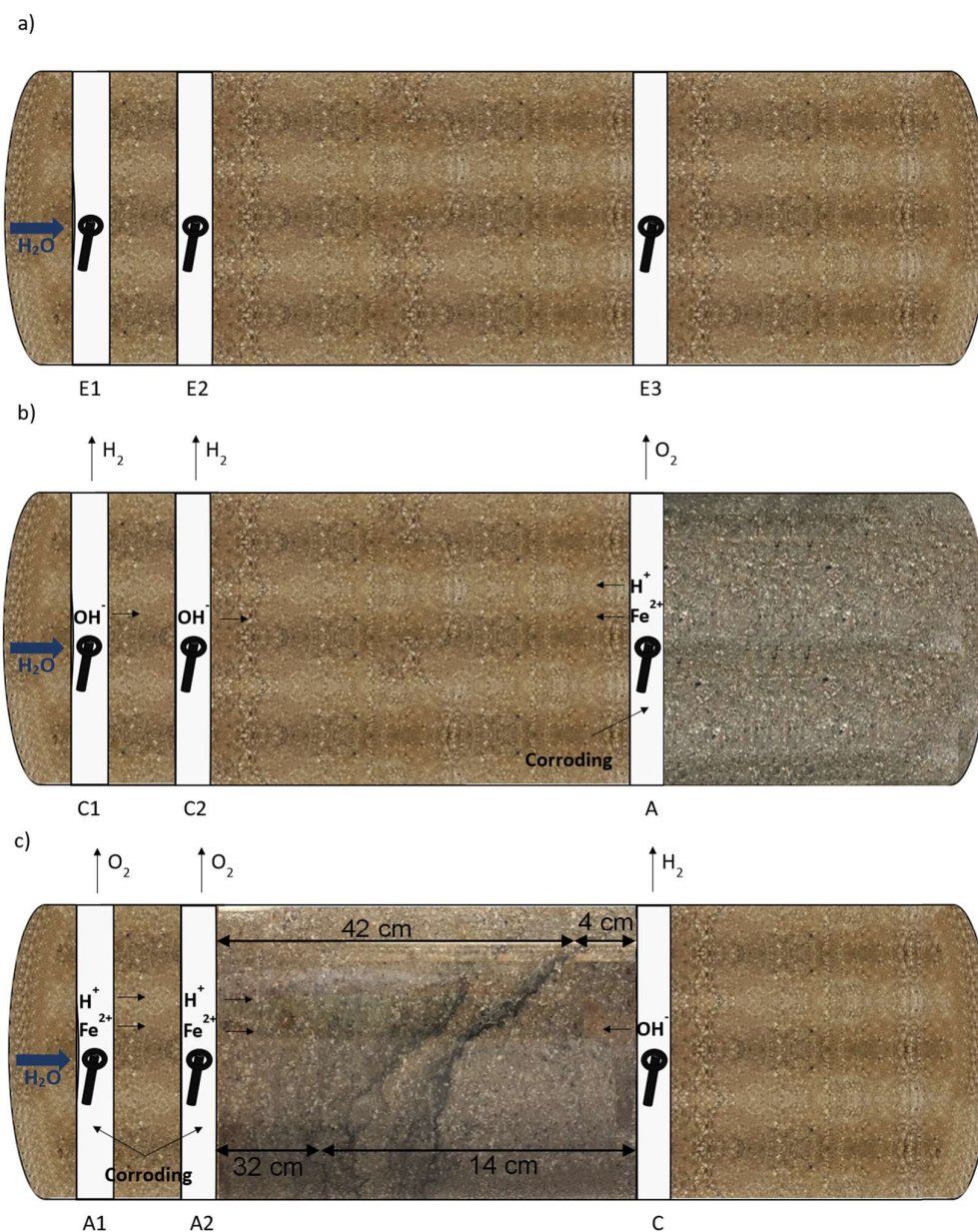


Fig. 8 Pictures of a) the saturated sandy sediment before application of the electric current, b) Fe precipitates formed due to electrolysis and corrosion of the anode in the C – C – A electrode configuration and c) Fe precipitates formed due to electrolysis and corrosion of the anodes in the A – A – C electrode configuration. Direction of electromigration of electrolytically formed species are indicated. Illustration is out of scale (Fig. 1)

For the Fe precipitates to form, ferrous ions from corrosion of the anodes reacted with the hydroxyl ions from electrolysis at the cathode. In the A – A – C reactor, ferrous ions electromigrate towards the cathode, which is also in the direction of the groundwater flow and thus advection may also contribute to the transport of Fe. The hydroxyl ions electromigrate towards the anodes, which may be hindered by the flowing water. Based on the position of the angled lines of precipitates observed in the system of A – A – C, the hydroxyl

ions migrated between 4-14 cm before depositing during the 14 days of applied electric current (2 PV), while ferrous ions migrated 32-42 cm before precipitating.

In the set-up assessing A – A – C, the white precipitates were likely ferrous hydroxide ($\text{Fe}(\text{OH})_2$), black precipitates wüstite (FeO) and/or magnetite (Fe_3O_4) [21], and red precipitates ferric hydroxide ($\text{Fe}(\text{OH})_3$) [8, 22]. When the reactor was disassembled, green porewater was observed downgradient the cathode, which rapidly disappeared, suggesting reduction of ferrous hydroxide into green rust. The grey shaded precipitates observed in the C – C – A configuration is suggested to be FeO and/or Fe_3O_4 [8, 21].

Despite the possible enhancement in abiotic degradation of the chlorinated ethenes due to formation of reactive Fe precipitates [23] and enhanced establishment of reducing conditions [2, 3, 6, 7, 14], the increasing challenge due to clogging, as experienced in this study, suggests use of dimensionable stable anodes, e.g. mixed metal oxides [2, 6].

3.6 Changes in hydrogeochemistry

In the sandy sediment, the electrical resistance was high and since no rheostat was used to split the current between the two identical electrodes (E1 and E2) in both set-ups studied, the set-ups operated as two-electrode systems (E2-E3). I.e. E1 was passive, wherefore changes in the hydrogeochemistry were observed mainly at E2 and E3. In the following, described changes in hydrogeochemistry is focused around E2 and E3.

The ionic species behaved differently within the oxidizing vs. reducing zones of the reactor. However, for both the A – A – C and C – C – A electrode configurations studied, the ionic species behaved similarly when comparing similar redox conditions, i.e. within the oxidizing, acidic zones of the anodes vs. within the reducing, alkaline environment of the cathodes. Due to the differences in electrode configurations and thereby the order of the redox zones, the conditions of the groundwater leaving the overall electrochemical zone differed between the two set-ups. The resulting major differences are explained in the following and concerns pH, conductivity, and concentrations of Ca, Mg, Na, Fe, Mn, Cl^- and SO_4^{2-} .

The pH decreased near the anodes and increased near the cathodes in the set-ups studied, as expected. Consequently, the pH downgradient the electrochemical zone composed of A – A – C and C – C – A was 9.5 and 6.2, respectively. For the A – A – C configuration, conductivity measured pre- and post-treatment was $766 \pm 7.0 \mu\text{S/cm}$ and $646 \pm 5.5 \mu\text{S/cm}$, respectively. The conductivity measured pre- and post-treatment the C – C – A application was $830 \pm 77 \mu\text{S/cm}$ and $560 \pm 16 \mu\text{S/cm}$, respectively. Thus, the conductivity decreased in both cases. It is relevant to look into the different ions in the groundwater, to explain this decrease.

Ca^{2+} precipitated in the reductive, alkaline zone of the cathodes with formation of white precipitates (Fig. 9, Fig. 10), i.e. possibly as calcite or reaction with hydroxyl ions forming $\text{Ca}(\text{OH})_2$. In the C – C – A configuration, Ca-complexes dissolved downgradient the anode and the Ca concentration reached a level similar to the initial (Fig. 10a) [8]. However, in the A – A – C reactor, Ca concentrations remain decreased (Fig. 10b), which may

contribute to the clogging of the pore spaces. The contribution of electromigration of Ca^{2+} and Mg^{2+} to the observed developments in concentrations of these ionic species appeared minor compared to oxidation and reduction. Mg^{2+} is suggested to co-precipitate with Ca^{2+} [8] or as $\text{Mg}(\text{OH})_2$, where Mg remained bound in complexes despite of electrode configuration applied (Fig. 10). TG analysis of the sand grains in Fig. 9, with white precipitates, showed best correlation with calcite (CaCO_3), though with some impurities as indicated by the measured mass loss and decomposition temperatures. The mass loss measured was 46%, which corresponds with that for dolomite ($\text{CaMg}(\text{CO}_3)_2$), and which is higher than for calcite of 44%. The decomposition temperature was app. 680 °C, while the decomposition temperature for calcite is app. 740 °C. The structures of the Ca deposits were assessed by SEM and showed heights of up to 0.5 mm. The mineral structures had a more complex rod-shaped structure than that of pure calcite, consistent with structures of dolomite. Formation of dolomite may explain the observed concurrent decrease in Ca and Mg concentrations near the cathode in Fig. 10a (note the differences in concentration scales: the decrease in Ca concentration is larger than the decrease in Mg concentration). The decrease in Ca and Mg concentration near the second anode in the A – A – C configuration (Fig. 10b) could be due to reaction with SO_4^{2-} , which increases in concentration near this anode (Fig. 11).

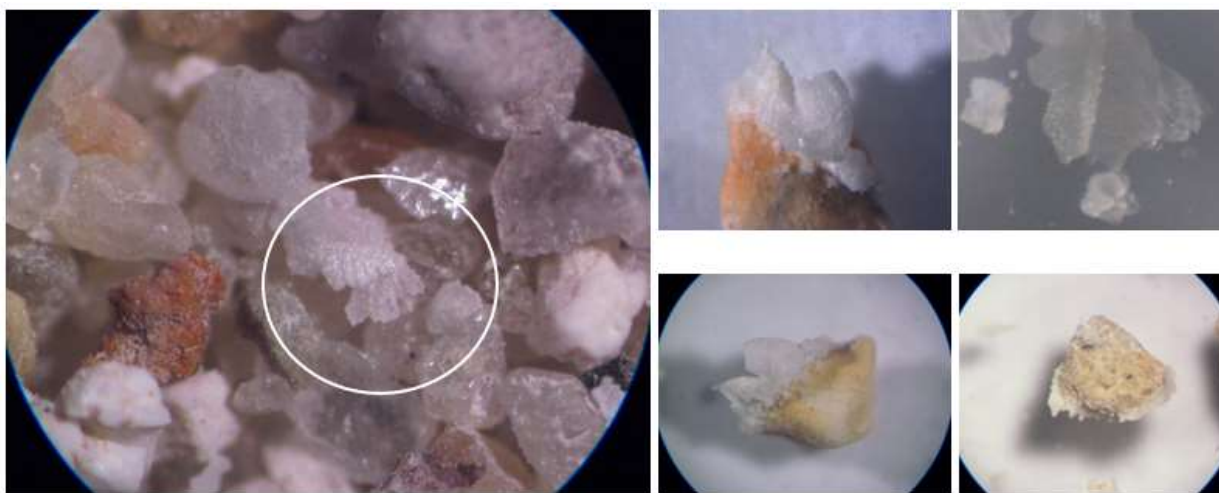


Fig. 9 White precipitates deposited on sand grains near cathodes after electrochemical application in a sandy sediment with flow-through of field-extracted groundwater

The Na concentration decreased near the anode of both C – C – A and A – A – C (Fig. 10), possibly due to reaction with HCO_3^- in the weak acidic environment. Subsequent flow through the alkaline environment of the downgradient cathode in the A – A – C reactor resulted in an increase in concentration to app. initial levels (Fig. 10b). The fate of Na appeared to be controlled by the pH conditions and the related ionic form of the carbonate system, i.e. HCO_3^- and CO_3^{2-} , but contribution of electromigration towards the cathode is also likely.

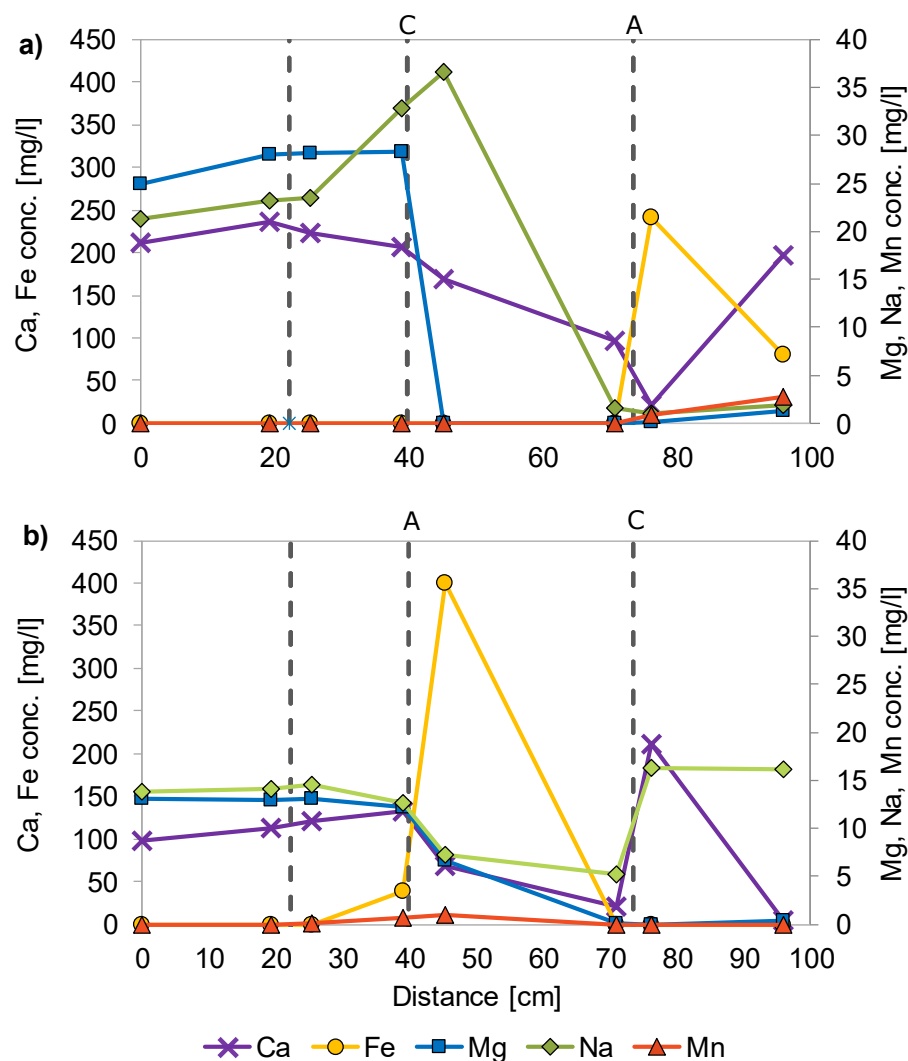


Fig. 10 Changes in concentrations of Ca (x), Fe (○), Mg (□), Na (◇) and Mn (Δ) throughout the electrochemical reactors of a) C – C – A electrode configuration (adapted from Hyldegaard et al. [8]) and b) A – A – C electrode configuration as measured after 7 days (1 PV). Dashed lines indicate positions of the electrodes

Fe^{2+} was released in both reactor set-ups studied due to corrosion of the Fe anodes (Fig. 10). In the C – C – A reactor, the concentrations remained elevated downgradient the electrochemical zone (Fig. 10a). However, in the A – A – C reactor, Fe^{2+} completely precipitated upgradient the cathode (Fig. 10b), which fit with observations (Fig. 8). Mn, an impurity in the electrode materials (Table 2), increased in concentration near anode (Fig. 10). In the A – A – C reactor, Mn^{2+} was removed from the porewater as it passed the cathode (Fig. 10b). Electromigration of Fe^{2+} and Mn^{2+} appear insignificant.

Cl^- and SO_4^{2-} decreased downgradient the cathodes, while increased downgradient the anodes in both set-ups (Fig. 11), which may partly be explained by electromigration towards the anode. Also, S is released during corrosion of the anode [8]. Due to the different redox sequence in the two electrode configurations studied, Cl^-

and SO_4^{2-} recover pre-treatment levels downgradient the overall electrochemical zone in the C – C – A configuration (Fig. 11a), while is removed downgradient the overall electrochemical zone in the A – A – C configuration (Fig. 11b).

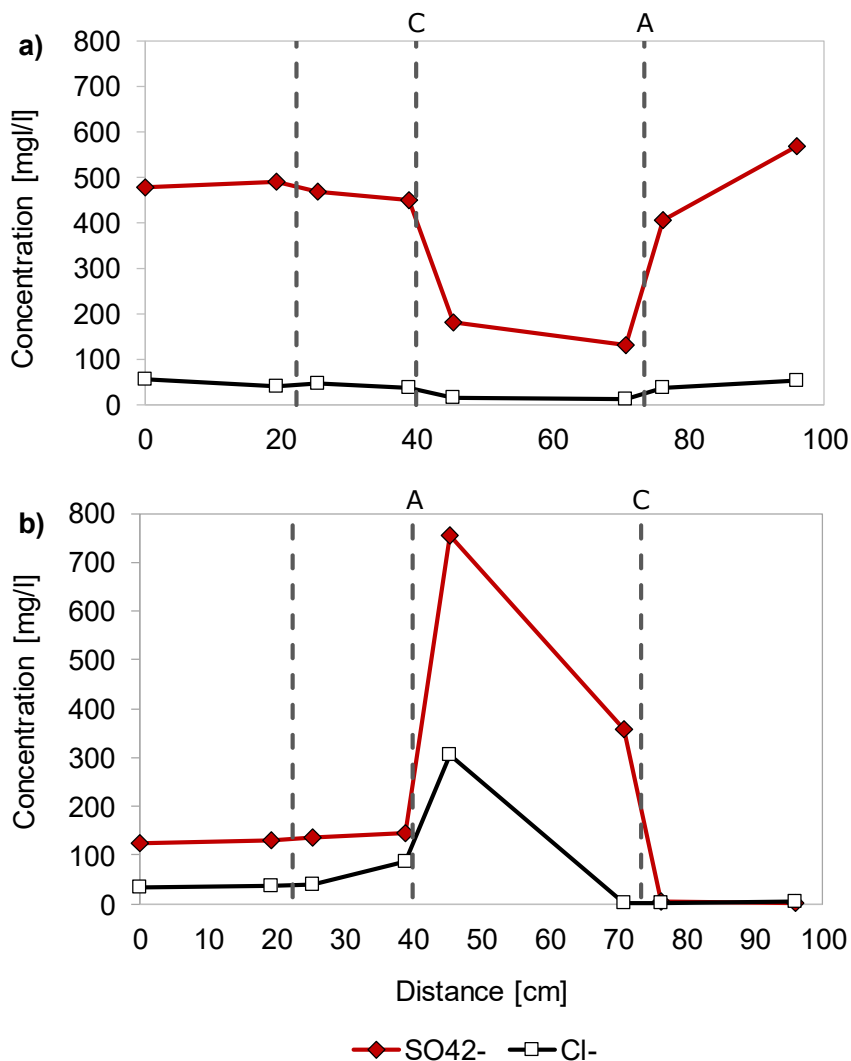


Fig. 11 Changes in concentrations of SO_4^{2-} (\blacklozenge) and Cl^- (\square) throughout the electrochemical reactors of a) C – C – A electrode configuration (adapted from Hyldegaard et al. [8]) and b) A – A – C electrode configuration as measured after 7 days (1 PV). Dashed lines indicate positions of the electrodes

4. Conclusion

Based on a literature review, Fe materials were identified as suitable electrodes for efficient electrochemical removal of chlorinated ethenes in undivided flow-through reactors. Further, that improved removal rates can be achieved with use of Pd coated high-purity Fe cathodes. The surface characteristics of three high-purity Fe

materials (99.95%, 99.8% and 98+%) before and after electroless plating with Pd, and of a cast Fe was examined. At macroscopic level, differences in homogeneity, shine and color was observed. At microscopic level, the smoothness of the Fe surfaces varied, with the 99.95% Fe being smooth and 99.8% Fe and 98+% Fe being irregular. Mapping of elements on the Fe surfaces via SEM revealed an uneven and disconnected distribution of Pd on the three high-purity Fe metals studied. In addition, oxides formed on the surfaces of 99.8% Fe and 98+% Fe after Pd electroless plating. The higher the Fe purity, the less oxide formation was observed. Using the 98+% Fe instead of 99.95% Fe, result in a significant cost reduction. Different corrosion patterns were observed when using 99.8% Fe and cast Fe as anodes for electrochemical application; graphitization of the cast Fe and uniform corrosion of the 99.8% Fe. Precipitation patterns of the Fe released from anode corrosion differed for electrochemical application in flow-through reactors of C – C – A and A – A – C configurations, including different shape and type of Fe complexes formed. The fate of hydrogeochemical ionic species in the reducing and oxidizing zones of the electrochemical reactor were generally similar within the similar redox zone of the two electrode configurations studied. However, the order of the redox zones influenced the chemical composition of the porewater leaving the treatment zone. The major difference was pH measured downgradient the electrochemical zone of C – C – A and A – A – C of 6.2 and 9.5, respectively. Generally, the concentrations of dominating ionic species (Ca^{2+} , SO_4^{2-} , Cl^-) leaving the C – C – A treatment zone better recovered pre-treatment levels, whereas in the A – A – C reactor, the chemical elements precipitated. Hence, the C – C – A electrode configuration appeared less intrusive to the natural hydrogeochemical settings.

Acknowledgements

Funding: This work was funded by the Innovation Fund Denmark (grant number 5016-00165B), COWIfonden (grant number C-131.01), the Capital Region of Denmark (grant number 14002102), COWI A/S and Technical University of Denmark. A special thanks to Dr David Gent, US Army Corps of Engineers, Engineer Research and Development Centers Environmental Laboratory, for access to the acrylic column for customization to comply with the lab work requirements of this study. The sandy sediment was kindly donated by Nymølle Stenindustri A/S, Denmark. The cast iron was kindly donated by Velamp A/S.

Conflict of Interest: The authors declare that they have no conflict of interest.

References

1. Ruder AM (2006) Potential health effects of occupational chlorinated solvent exposure. *Ann N Y Acad Sci* 1076:207–227. <https://doi.org/10.1196/annals.1371.050>
2. Rajic L, Fallahpour N, Alshawabkeh AN (2015) Impact of electrode sequence on electrochemical removal of trichloroethylene from aqueous solution. *Appl Catal B Environ* 174–175:427–434. <https://doi.org/10.1016/j.apcatb.2015.03.018>

3. Mao X, Yuan S, Fallahpour N, et al (2012) Electrochemically Induced Dual Reactive Barriers for Transformation of TCE and Mixture of Contaminants in Groundwater. *Environ Sci Technol* 46:12003–12011. <https://doi.org/10.1021/es301711a>
4. Rajic L, Fallahpour N, Podlaha E, Alshawabkeh AN (2016) The influence of cathode material on electrochemical degradation of trichloroethylene in aqueous solution. *Chemosphere* 147:98–104. <https://doi.org/10.1016/j.chemosphere.2015.12.095>
5. Rajic L, Fallahpour N, Oguzie E, Alshawabkeh AN (2015) Electrochemical transformation of trichloroethylene in groundwater by Ni-containing cathodes. *Electrochim Acta* 181:118–122. <https://doi.org/10.1016/j.electacta.2015.03.112>
6. Fallahpour N, Yuan S, Rajic L, Alshawabkeh AN (2016) Hydrodechlorination of TCE in a circulated electrolytic column at high flow rate. *Chemosphere* 144:59–64. <https://doi.org/10.1016/j.chemosphere.2015.08.037>
7. Mao X, Ciblak A, Amiri M, Alshawabkeh AN (2011) Redox Control for Electrochemical Dechlorination of Trichloroethylene in Bicarbonate Aqueous Media. *Environ Sci Technol* 45:6517–6523. <https://doi.org/10.1021/es200943z>
8. Hyldegaard BH, Jakobsen R, Weeth EB, et al (2019) Challenges in electrochemical remediation of chlorinated solvents in natural groundwater aquifer settings. *J Hazard Mater* 368:680–688. <https://doi.org/10.1016/j.jhazmat.2018.12.064>
9. Rajic L, Nazari R, Fallahpour N, Alshawabkeh AN (2016) Electrochemical degradation of trichloroethylene in aqueous solution by bipolar graphite electrodes. *J Environ Chem Eng* 4:197–202. <https://doi.org/10.1016/j.jece.2015.10.030>
10. Carter KE, Farrell J (2009) Electrochemical Oxidation of Trichloroethylene Using Boron-Doped Diamond Film Electrodes. *Environ Sci Technol* 43:8350–8354. <https://doi.org/10.1021/es9017738>
11. Marselli B, Garcia-gomez J, Michaud P, et al (2003) Electrogeneration of Hydroxyl Radicals on Boron-Doped Diamond Electrodes. *J Electrochem Soc* 150:79–83. <https://doi.org/10.1149/1.1553790>
12. Brewster JH (1954) Mechanisms of Reductions at Metal Surfaces. I. A General Working Hypothesis. *J Am Chem Soc* 76:6361–6363. <https://doi.org/10.1021/ja01653a034>
13. Cheng IF (1997) Electrochemical Dechlorination of 4-Chlorophenol to Phenol. *Environ Sci Technol* 31:1074–1078. <https://doi.org/10.1021/es960602b>
14. Mao X, Baek K, Alshawabkeh AN (2015) Iron Electrocoagulation With Enhanced Cathodic Reduction for the Removal of Aqueous Contaminant Mixtures. *Environ Eng Manag J* 14:2905–2911
15. Sáez V, Escalpez MD, Tudela I, et al (2010) Electrochemical degradation of perchloroethylene in aqueous media: Influence of the electrochemical operational variables in the viability of the process. *Ind Eng Chem Res* 49:4123–4131. <https://doi.org/10.1021/ie100134t>
16. Yuan S, Chen M, Mao X, Alshawabkeh AN (2013) A three-electrode column for Pd-catalytic oxidation of TCE in groundwater with automatic pH-regulation and resistance to reduced sulfur compound fouling. *Water Res* 47:269–278. <https://doi.org/10.1016/j.watres.2012.10.009>
17. Rajic L, Fallahpour N, Nazari R, Alshawabkeh AN (2015) Influence of humic substances on electrochemical degradation of trichloroethylene in limestone aquifers. *Electrochim Acta* 181:123–129. <https://doi.org/10.1016/j.electacta.2015.03.121>
18. Fallahpour N, Mao X, Rajic L, et al (2017) Electrochemical dechlorination of trichloroethylene in the presence of natural organic matter, metal ions and nitrates in a simulated karst media. *J Environ Chem Eng* 5:240–245. <https://doi.org/10.1016/j.jece.2016.11.046>
19. Rajic L, Fallahpour N, Yuan S, Alshawabkeh AN (2014) Electrochemical transformation of trichloroethylene in aqueous solution by electrode polarity reversal. *Water Res* 67:267–275. <https://doi.org/10.1016/j.watres.2014.09.017>
20. Mattsson E (2001) Types of corrosion. In: Mattsson E (ed) *Basic corrosion technology for scientists and engineers*, 2nd ed. The Chameleon Press, Ltd., Wandsworth, pp 37–63
21. Parkinson GS (2016) Iron oxide surfaces. *Surf Sci Rep* 71:272–365. <https://doi.org/10.1016/j.surfrep.2016.02.001>
22. Sarin P, Snoeyink VL, Bebee J, et al (2004) Iron release from corroded iron pipes in drinking water distribution systems: Effect of dissolved oxygen. *Water Res* 38:1259–1269. <https://doi.org/10.1016/j.watres.2003.11.022>
23. He YT, Wilson JT, Su C, Wilkin RT (2015) Review of Abiotic Degradation of Chlorinated Solvents by Reactive Iron Minerals in Aquifers. *Groundw Monit Remediat* 35:57–75. <https://doi.org/10.1111/gwmr.12111>

APPENDIX III

Electrokinetics applied in remediation of subsurface soil contaminated with chlorinated ethenes
– A review

Ottosen, L.M., Larsen, T.H., Jensen, P.E., Kirkelund, G.M., Kern-Jespersen, H., Tuxen, N. &
Hyldegaard, B.H.

(Published in Chemosphere, 2019)



Contents lists available at ScienceDirect

Chemosphere

journal homepage: www.elsevier.com/locate/chemosphere

Review

Electrokinetics applied in remediation of subsurface soil contaminated with chlorinated ethenes – A review



Lisbeth M. Ottosen^{a,*}, Thomas H. Larsen^b, Pernille E. Jensen^a, Gunvor M. Kirkelund^a, Henriette Kern-Jespersen^c, Nina Tuxen^c, Bente H. Hyldegaard^{d,a}

^a Department of Civil Engineering, Building 118, Technical University of Denmark, 2800, Lyngby, Denmark

^b Department of Contaminated Sites & Groundwater, Orbicon, Linnés Allé 2, 2630, Taastrup, Denmark

^c Centre for Regional Development, Capital Region of Denmark, Kongens Vænge 2, 3400, Hillerød, Denmark

^d Department of Waste & Contaminated Sites, COWI, Parallelvej 2, 2800, Lyngby, Denmark

HIGHLIGHTS

- EK-combined techniques overcome transport limitations experienced in low-permeable soils.
- EK velocity of PCE and TCE is of comparable size to supplied reactants.
- In EK-BIO, transport velocity of lactate and biodegrading bacteria are in the same order of magnitude.
- General knowledge on the dependency of EK transport velocity on soil type is lacking.
- Identified knowledge gaps must be filled in for robust and successful field-implementations.

ARTICLE INFO

Article history:

Received 12 March 2019

Received in revised form

9 June 2019

Accepted 10 June 2019

Available online 11 June 2019

Handling Editor: E. Brillas

Keywords:

Electrokinetics

Chlorinated ethenes

PCE

TCE

Low permeable soil

Transport velocities

ABSTRACT

Electrokinetics is being applied in combination with common insitured remediation technologies, e.g. permeable reactive barriers, bioremediation and in-situ chemical oxidation, to overcome experienced limitations in remediation of chlorinated ethenes in low-permeable subsurface soils. The purpose of this review is to evaluate state-of-the-art for identification of major knowledge gaps to obtain robust and successful field-implementations. Some of the major knowledge gaps include the behavior and influence of induced transient changes in soil systems, transport velocities of chlorinated ethenes, and significance of site-specific parameters on transport velocities, e.g. heterogeneous soils and hydrogeochemistry. Furthermore, the various ways of reporting voltage distribution and transport rates complicate the comparison of transport velocities across studies. It was found, that for the combined EK-techniques, it is important to control the pH and redox changes caused by electrolysis for steady transport, uniform distribution of the electric field etc. Specifically for electrokinetically enhanced bioremediation, delivery of lactate and biodegrading bacteria is of the same order of magnitude. This review shows that enhancement of remediation technologies can be achieved by electrokinetics, but major knowledge gaps must be examined to mature EK as robust methods for successful remediation of chlorinated ethene contaminated sites.

© 2019 Elsevier Ltd. All rights reserved.

Contents

1. Introduction	114
2. Electrode reactions, potential difference and current	114
3. Electrokinetic transport processes	115
3.1. Electromigration	115
3.2. Electrophoresis	115

* Corresponding author.

E-mail address: lo@byg.dtu.dk (L.M. Ottosen).

3.3.	Electroosmosis	115
3.4.	Influence from non-linear and transient changes on remediation	116
4.	Chlorinated ethene degradation pathways	116
4.1.	Abiotic reduction	116
4.2.	Biotic reduction	116
4.3.	Abiotic oxidation	116
5.	Electrokinetic remediation of chlorinated ethene contaminated soil – overview	117
6.	EK-reactive barriers. Abiotic reduction	117
6.1.	Transport of chlorinated ethenes by advection in an electroosmotic flow	117
6.2.	Types and placement of PRB	118
6.3.	In situ pilot and full scale actions	118
7.	EK-bioremediation. Biotic reduction	119
7.1.	EK-bioaugmentation	119
7.1.1.	EP transport of bacteria in soil	119
7.1.2.	Transport of bacteria by advection in an electroosmotic flow	119
7.1.3.	Electrophoresis vs electroosmosis	120
7.2.	EK-biostimulation	120
7.3.	Pilot scale action	120
8.	EK-ISCO. Abiotic oxidation	120
8.1.	EK-ISCO permanganate	120
8.2.	EK-persulfate	121
8.3.	Modelling EK-ISCO	122
9.	Discussion	122
9.1.	Summary of transport velocities reported	122
9.2.	Importance of side effects and transient changes	122
9.3.	EK in heterogeneous subsurface soils	122
10.	Conclusions	123
	Acknowledgements	124
	References	124

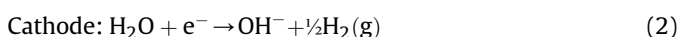
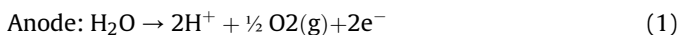
1. Introduction

Electrokinetic (EK) remediation is a group of remediation techniques utilizing the transport processes obtained when applying an electric DC field to soil. EK has the major advantage of being applicable to fine-grained soils in which other remediation techniques tend to fail. EK enables transport of ions by electromigration (EM), water by electroosmosis (EO) and charged particles by electrophoresis (EP). In recent years, research, development and implementations within EK have combined the unique EK transport processes with already practised remediation techniques to overcome the inefficiency of these latter in fine-grained soils (Lima et al., 2017).

This paper is a focused review on the results obtained with EK (from laboratory scale to full scale) in combination with other techniques for remediation of subsurface soil contaminated by chlorinated ethenes: bioremediation, in situ chemical oxidation (ISCO) and reactive barriers. The objective of the paper is to identify important knowledge and knowledge gaps in order to engineer EK in combination with other in-situ technologies for remediation of heterogeneous subsurface soils contaminated with chlorinated ethenes.

2. Electrode reactions, potential difference and current

When applying an electric DC field to soil, coupled electrode reactions occur; oxidation at the anode and reduction at the cathode. In EK remediation systems, electrolysis of water most often prevails:



Thus, around the cathode, a reducing and alkaline environment develops, whereas the environment around the anode becomes oxidized and acidic. A variety of other electrode processes may occur simultaneously depending on the applied potential, electrode material and solution chemistry. For example, when removed chloride ions reach the anode, there will be oxidation to



or when iron anodes are used the process, the anode corrods:



In EK remediation, the electric DC field is applied as constant voltage (Bruell et al., 1992), (Chang et al., 2006) or constant current (Chowdhury et al., 2017b). When applying a constant current, the average charge transfer (the current) is the same in every cross section between the electrodes. When the resistivity differs over the cross-section of soil, the current will be highest in the zone with the lowest resistivity. Applying a constant voltage, on the other hand, does not necessarily result in the same potential drops [V cm^{-1}] throughout the soil. Varying resistivities result in different potential differences. Zones with high resistivity will have a high potential drop compared to zones with a low resistivity. In experimental work with EK remediation, a constant voltage is often applied to the electrodes, which is then directly related to an average potential difference in the soil, e.g. 1 V cm^{-1} . It must be stressed, that there can be huge variations from the average potential gradient in heterogeneous soil systems, not at least because the soil conductivity will change due to geochemical changes caused by the treatment. These changes will not be equally distributed throughout the soil, and the potential differences change accordingly. A primary challenge for engineering field implementation of EK is the development of non-linear geo- and

physicochemical conditions between the electrodes (Gabrieli and Alshawabkeh, 2010).

In published research on EK-remediation of chlorinated ethenes, the average potential drop in the soil is calculated directly from the applied voltage. However, a fraction of the potential drop will be at the electrodes, which should be subtracted from the applied voltage before the average voltage gradient in the soil is calculated. As the potential drop at the electrodes is often low compared to the total voltage applied, it is neglected. Ho et al. (1997) studied the relationship between applied voltage and EO in natural clay. The flow rate varied almost linearly with the applied voltage in the range of 0.1–1 V cm⁻¹. Extrapolating the fitted line showed, that at 0.06 V cm⁻¹, the potential gradient would be too low to drive EO. This voltage probably reflects the voltage required to drive the electrode reactions and the over-voltages associated with the particular setup (Ho et al., 1997).

When comparing transport velocities by EM, EO or EP [cm d⁻¹], for different systems or components, it is necessary to relate the velocity to the driving force, i.e. the potential gradient [V cm⁻¹]. The transport velocity per voltage applied thus have the unit [cm²d⁻¹V⁻¹]. In this review, the potential gradient used in the calculation is the average, calculated based on the applied voltage reported. Hence, the potential differences caused by the electrode reactions are neglected.

3. Electrokinetic transport processes

EK-transport processes are described in this chapter together with the factors determining their velocities. The basis for EK-transport processes is charge and specifically for EP and EO that particles carry a net surface charge, which is counter-balanced by ions in the liquid phase in the very close vicinity of the particle (the electric double layer). The first layer comprises ions adsorbed onto the positively or negatively charged particle by chemical interactions. The second layer is composed of ions attracted electrostatically. This second layer is diffuse and more loosely associated with the particle. It consists of free ions that constantly move in the thin fluid layer under the influence of electric attraction to the particle and thermal motion. The charge of a particle is often expressed by the zeta potential. However, in principle, the zeta potential is the potential difference between the two layers in the electrical double layer. Hence, the zeta potential is not a characteristic of the actual particle. It is influenced by the chemistry of the soil solution. For example, the zeta potential of bacteria decreases with increasing ionic strength of the solution (Zhang et al., 2015). The sign of the zeta potential can be changed near the electrodes during the EK process due to the electrode reactions and the movement of the acid front near the anode. Hence, the direction of the EO/EP can be reversed if the movement of the acid front is not controlled.

Table 1 summarizes the major parameters determining the velocity for the different transport processes (based on chapter 3.1–3.3).

Table 1
Soil characteristics and reactions in soil systems influencing electromigration, electrophoresis and electroosmosis in the electric field.

Transport process	Transport of:	Transport velocity depends on:
Electromigration (EM)	Ions	Ionic mobility, adsorption/desorption, precipitation/dissolution, water content, pore volume and geometry
Electrophoresis (EP)	Particles, colloids, bacteria	Soil zeta potential, pore water chemistry and conductivity, pore sizes, water content
Electroosmosis (EO)	Water	Soil zeta potential, pore water chemistry and conductivity

3.1. Electromigration

While EP and EO are electrokinetic transport processes, EM is the electric current itself. In soil, ions in the soil solution carry the current. Anions move towards the anode and cations towards the cathode. At infinite dilution in water, the ionic mobilities of common ions are in the range of $1 \cdot 10^{-8}$ to $10 \cdot 10^{-8}$ m²V⁻¹s⁻¹ (Mitchell, 1993), which corresponds to 69–690 cm²V⁻¹d⁻¹. The ionic mobility of an ion relates closely to the aqueous diffusion coefficient in non-flowing systems and the dispersion tensor in flowing systems. In soils, however, the velocity is significantly lower as the ions cannot move by EM to the electrodes by the shortest route. Soil particles and air-filled voids block the direct path. The effective ionic mobility of a specific ion is a function of its molecular diffusion coefficient, soil porosity, tortuosity factor, and charge (Reddy and Cameselle, 2009). Also adsorption/desorption and precipitation/dissolution processes influence the amount and type of ions in solution under different conditions, and thereby EM of the specific ions.

The electric current is carried by ions in the electric double layer and by the ions dissolved in the pore water, which have different characteristics (Pengra and Wong, 1996). Charged porous media are filled at least by counter-ions. The dynamics of counter-ions, water molecules and co-ions depend strongly on the water content of the soil matrix. For compact matrices, the water content is low, and EM is slowed down. For less compact matrices, the dynamics of water molecules and counter-ions approach that in the bulk solution (Marry et al., 2003).

3.2. Electrophoresis

Charged particles will move by EP. The applied electric field, which sets the ions in the double layer in motion, acts with an electrostatic force on the particle itself due to the surface charge. The EP will be in the direction of the cathode if the particle has a net positive surface charge, and towards the anode, if the charge is negative. DeFlaun and Condee (1997) found reduced rates of transport for EP of bacteria in soils with silt and clay fractions compared to sand, indicating a major importance from the pore size on the EP mobility. The closer the particle is to a solid surface, the more profound is the boundary retarding effect, which is measured as a reduction in particle EP mobility (Tsai et al., 2011). Up to a 90% mobility reduction was observed when the thickness of the double layer surrounding the particle was comparable to the particle radius if the particle was sufficiently close to the solid plane. The lower the permeability of the medium, the more profound is this retarding effect (Tsai et al., 2011).

3.3. Electroosmosis

EO is a coupled flow (Heister et al., 2005). When the electric field is applied to soil, ions in the diffuse layer will move. Generally, the diffuse layer in soils mainly consists of cations. They are transported towards the cathode, and push and drag water molecules towards the cathode. This movement of water is EO, and the amount of water moved per ion in solution is large (Ballou, 1955).

EO is only significant in materials with fine pores due to their high relative surface charge. For example, Mikkola et al. (2008) reported insignificant EO in pure sand, whereas EO increased with increasing fraction of silt. Further, EO is most significant when the ion concentration in the pore water outside the electric double layer is low. West et al. (1999) experienced that EO in a clayey soil was significantly lower when the clay was contaminated with Pb above the cation exchange capacity than when below. The pH also influences the surface charge of the particle and hereby EO. At low pH, the flow direction can reverse. For example, Cherepy and Wildenschild (2003) experimentally illustrated the necessity for neutralizing the pH changes at the electrodes to obtain steady EO. They studied a natural clayey soil in which both the EO and hydraulic conductivity decreased over time. When neutralizing the pH changes at the electrodes, steady EO was obtained during 31 days of testing. In this soil, the EO velocity was three orders of magnitude larger than the hydraulic velocity (Cherepy and Wildenschild, 2003). EK-remediation techniques are often targeted towards removal of contaminants or supply of reagents by EP, EO or EM, thus soil chemistry changes over time, thus continuously influencing EO.

3.4. Influence from non-linear and transient changes on remediation

The soil system changes during EK treatment and strongly influences the transport velocities. This is important to consider when designing full-scale remediation. As Reynolds et al. (2008) states, many complicating phenomena occur due to the application of an electric field, including ion diffusion, ion exchange, development of osmotic and pH gradients, desiccation due to heat generation at the electrodes, mineral decomposition, precipitation of salts or secondary minerals, electrolysis, hydrolysis, oxidation, reduction, physical and chemical adsorption.

Knowledge of the site-specific electrical conductivity distribution and induced changes is important to design the remediation such that the current flow where the contaminants are. The conductivity in homogeneous, inert porous materials depends on the ion concentration, composition and water content. However, soils are heterogeneous, and degradation of contaminants along with the before mentioned changes stated by Reynolds et al. (2008) will influence the electrical conductivity. The overall pattern is highly complex, partly because the changes induced by the applied electric field are transient (time and space dependent). The often non-linear response in remediation time and energy consumption required to degrade a target level of contaminants indicates the need for a site-specific approach and optimization (Wu et al., 2013). In addition, the relatively low permeability of silt and clay soils coupled with the transient and heterogeneous geochemical conditions result in transient fluid flow and development of negative or positive pore pressure (Gabrieli and Alshawabkeh, 2010), which will influence transport patterns. In summary, for the most complicated cases, concentration, temperature and pressure gradients are in play in addition to the applied potential gradient, i.e. all direct and coupled flows as outlined in Heister et al. (2005) are possible.

Table 2 organizes the outlined phenomena into three categories: (I) effects from applying the DC field to an inert system, (II) changes in the soil in response to the effects in (I), and (III) effects caused by the nonlinear and transient nature of the effects and changes in (I–II).

4. Chlorinated ethene degradation pathways

Chlorinated ethenes are subject to abiotic and biotic

degradation (Vogel et al., 1987), following specific degradation pathways depending on the mechanisms involved (Fig. 1). Combination of EK with other techniques induce specific degradation pathways.

4.1. Abiotic reduction

The abiotic reduction requires a supply of electron donors, for which zero valent metals can be applied (Roberts et al., 1996). During chemical reduction, chlorinated ethenes can concurrently follow β -elimination with the formation of chlorinated acetylenes (Fig. 1, dotted arrows), and hydrogenolysis forming chlorinated intermediates or hydrocarbons (Fig. 1, solid arrows) (Arnold and Roberts, 2000). For β -elimination, the formation of toxic chlorinated intermediates is bypassed and the reaction products include chloride ions (Cl^-) and metal ions (Durante et al., 2013), e.g. Fe^{2+} when zero valent iron (ZVI) is used as a reductant. For ZVI it has been shown, that 87% of PCE, 97% of TCE, 94% of cis-DCE, 99% of trans-DCE follows β -elimination (Arnold and Roberts, 2000). Hence, limited formation of vinyl chloride (VC).

EK has been applied to transport chlorinated ethenes towards permeable reactive barriers (PRB) in low permeable soils for abiotic degradation of the contaminants. These PRBs often contain ZVI (details in chapter 6). Hence, in such barriers, the degradation follows these above outlined pathways β -elimination and secondary hydrogenolysis.

4.2. Biotic reduction

Generally, microbial degradation is facilitated only if the reaction can yield energy (Gibbs free-energy below 0), which is true for reduction of chlorinated ethenes and oxidation of the chlorinated intermediates. Microbial reductive dechlorination of chlorinated ethenes follows a sequence with the stepwise formation of the degradation intermediates (Fig. 1, solid arrows) (Maymó-Gatell et al., 1997). Specific redox conditions are required for this reductive biodegradation to occur. The *Dehalococcoides* (*Dhc*) group of bacteria enable reductive dechlorination of tetrachloroethylene (PCE) and trichloroethylene (TCE) beyond the dichloroethylene intermediates (cis-DCE, trans-DCE, 1,1-DCE). For complete reductive dechlorination of chlorinated ethenes to the nontoxic end-product ethene, *Dhc* must carry a specific gene for vinyl chloride reductase (*vcrA*) (Lee et al., 2013; van der Zaan et al., 2010). In addition, hydrogen (H_2) must be available as an electron donor for the reduction of chlorinated solvents by *Dhc* (Fennell et al., 1997), possibly supplied by fermentation of a carbon source, e.g. lactate (Scheutz et al., 2008). The *Dhc* are strict anaerobes. Consequently, the surrounding environment must be sulfate reducing and/or methane forming, preferably with an oxidation-reduction potential (ORP) below -100 mV (Kästner, 1991). Furthermore, the activity of *Dhc* is affected by the pH, with pH 6.8–7.8 being optimum (Middeldorp et al., 1999). *Dhc* appear to be inhibited for pH below 5 and above 10, with recovered activity when favorable pH conditions are reestablished (Rowlands, 2004), however, the duration of low pH exposure affects the ability of *Dhc* to recover activity at circumneutral pH (Yang et al., 2017).

Application of EK enhanced bioremediation is relying on an active phase with EK applied for delivery of an electron donor and/or bacteria (potentially *Dhc*) into the contaminated soil, followed by a passive phase of biodegradation (details in chapter 7).

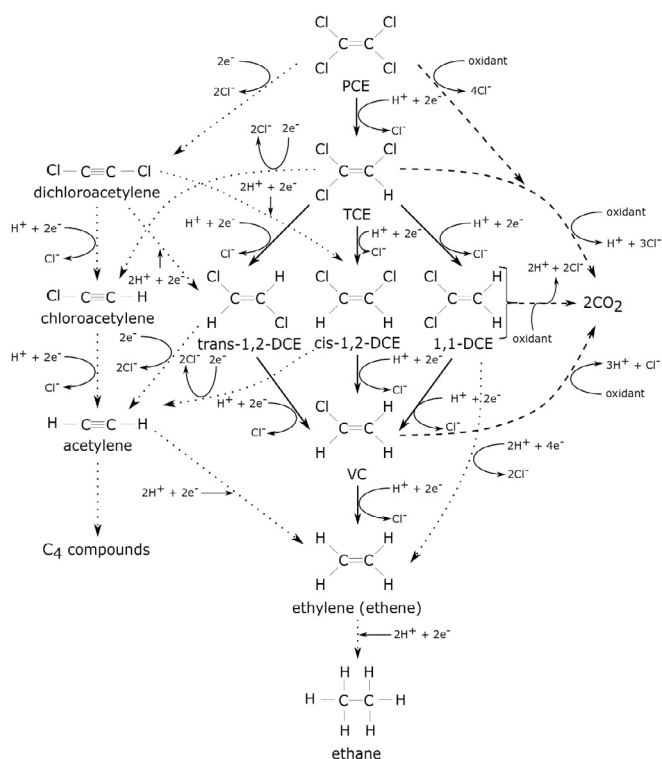
4.3. Abiotic oxidation

Abiotic oxidation of chlorinated ethenes requires an external supply of electron acceptors. Common oxidants used include

Table 2

Possible effects, changes in soil and transient changes when applying an electric DC field to a natural soil.

I. Effects from applying DC field to an inert system	II. Changes in soil	III. Transient changes
Transport processes Electromigration Electroosmosis Electrophoresis At electrodes Anode: Oxidation and pH decrease Cathode: Reduction and pH increase	Mineral decomposition Precipitation/dissolution of salts Precipitation/dissolution of secondary minerals Physical and chemical adsorption/desorption Ion exchange Joule heating pH and redox changes	Non-uniform current and voltage distribution Concentration gradients Pore pressure (negative or positive) Temperature gradient pH and redox gradients

**Fig. 1.** Degradation pathways for the chlorinated ethenes tetrachloroethylene (PCE), trichloroethylene (TCE), dichloroethenes (DCEs) and vinyl chloride (VC) subject to biotic reduction (solid arrows), abiotic reduction (dotted arrows) or abiotic oxidation (dashed arrows).

Fenton's reagent, permanganate and persulfate (Siegrist et al., 2014). The chemical oxidation of chlorinated ethenes breaks down the compounds entirely (Fig. 1, dashed arrows) and thereby avoids accumulation of the reductive dechlorination intermediates. The end-products of chemical oxidation are hydrogen (H^+), chloride ions (Cl^-), carbon dioxide (CO_2) and the reduced catalytic compound, e.g. $MnO_2(s)$ when permanganate is used as an oxidant (Schroth et al., 2001). Thus, chemical oxidation gradually generates acidic conditions. Successful delivery of the oxidant is crucial for efficient degradation of the chlorinated ethenes.

The desire of the methods of EK-delivery of chemical oxidants (EK-ISCO) is following this outlined degradation pathway (details in chapter 8).

5. Electrokinetic remediation of chlorinated ethene contaminated soil – overview

Table 3 summarizes the different techniques involving EK for remediation of soils contaminated by chlorinated ethenes.

Each method is described in the following chapters along with

the transport velocities related to the different techniques and a short description of the experimental data leading to the numbers. Results obtained in experiments using these methods, but targeting other contaminants are included in the discussion to extend the data volume for validation of e.g. EK transport velocities of bacteria. It is important to note that the transport velocities herein reported are calculated from varying fundamentals reported in the literature, since there is no coherency in the way to report experimental data on transport velocities. However, the information is important as it gives the order of magnitude of the transport velocity.

6. EK-reactive barriers. Abiotic reduction

The general PRB concept involves emplacement of a reactive media perpendicular to the flow direction of contaminated groundwater. The contaminant plume passively migrates through the reactive media under the influence of the natural hydraulic gradient. Obiri-Nyarko et al. (2014) reviewed the general PRB technology, while Weng (2009) reviewed the combined EK-PRB technology for contaminated soil in general. When dealing with chlorinated ethenes, the contaminants are mainly transported by electrokinetics to the PRB, and if successful, the contaminants are degraded to nonhazardous compounds by abiotic reduction (Fig. 1).

Another possibility for utilizing abiotic reduction in combination with EK is to transport nano-ZVI (nZVI) into the contaminated zone by EP (Pamukcu et al., 2008; Jones et al., 2011; Reddy et al., 2011; Gomes et al., 2012b). However, this possibility has not yet been applied for the remediation of soil contaminated by chlorinated ethenes, and thus the transport of these contaminants towards PRBs for abiotic reduction is the principle reviewed here. As early as in the 1990s a technology named Lasagna™ was developed based on this concept (Ho et al., 1997; Ho et al., 1999a,b).

6.1. Transport of chlorinated ethenes by advection in an electroosmotic flow

Bruell et al., 1992 first reported TCE removal from kaolin columns under the influence of EO. In a laboratory study on EK transport of bacteria in soils, DeFlaun and Condee (1997) observed, that TCE moved in the direction opposite to the bacteria, i.e. towards the cathode. The transport of TCE was suggested to be either due to advection in the EO flow, or that TCE is acting as a polar compound with some positive charge associated with it (DeFlaun and Condee, 1997). Chlorinated solvents can form positively charged ion pairs with protons in the dissolved phase (Chen et al., 2002). Thus, chlorinated solvents can be subject to EM (Chen et al., 2002; Mao et al., 2012). Other researchers explain the transport of TCE towards the cathode solely by advection in the EO flow (Bruell et al., 1992; Weng et al., 2003; Chang et al., 2006). Yang and Yeh (2011) reported TCE transport in an EO flow within a spiked sandy clay with accumulation in the cathode reservoir without significant TCE degradation. The EO transport rate of TCE was

Table 3

Methods involving EK for remediation of soils contaminated with chlorinated ethenes, including substances transported and transport processes utilized.

Method	Remediation strategy	Substance transported by EK	Transport process	References
EK-PRB	Transport to treatment zone with abiotic reduction	Chlorinated ethenes	Electroosmosis	Bruell et al. (1992), Ho et al. (1997), Ho et al. (1999b), Ho et al. (1999a), Weng et al. (2003), Athmer (2004), Chang et al. (2006), Athmer and Ho (2009), Athmer (2014)
EK-BIO	In situ biotic reduction	Bacteria	Electrophoresis and/or electroosmosis	DeFlaun and Condee (1997)
		Substrate and bacteria	Electromigration, Electromigration, electrophoresis and/or electroosmosis	Rabbi et al. (2000), Wu et al. (2007), Wu et al. (2012b) Mao et al. (2012), Hansen et al. (2015)
EK-ISCO	In situ abiotic oxidation	Permanganate Persulfate	Electromigration Electromigration	Chowdhury et al. (2017b) Yang and Yeh (2011), Chowdhury et al. (2017a)

superior to that of PCE in a soil sampled at a contaminated site, explained by the higher water solubility of TCE (Chang et al., 2006). By relating TCE and PCE removal to changes in pore volumes by EO, they found that 85% TCE was removed after three pore volumes and 90% PCE after five pore volumes. This difference was explained by the higher sorption of PCE to the soil.

The reported velocities to reach a minimum of 70% removal of chlorinated ethenes by advection in an EO flow are:

- Fine-grained soil: 85% TCE removal from 12 cm spiked fine-grained soil in 5 days under application of 1 V cm^{-1} (Weng et al., 2003), corresponding to $2.4 \text{ cm}^2 \text{ V}^{-1} \text{ d}^{-1}$
- Field-sampled clay: Removal of 83–87% TCE throughout 10 cm spiked clay at 2 V cm^{-1} during 8.3 days (Chung and Lee, 2007), corresponding to a velocity of $0.6 \text{ cm}^2 \text{ V}^{-1} \text{ d}^{-1}$
- Field-sampled clayey/silty soil: At 1.2 V cm^{-1} in 7 days, 85% removal was obtained in about 4.5 cm soil for PCE and 6.5 cm for TCE (Chang et al., 2006), corresponding to 0.5 and $0.8 \text{ cm}^2 \text{ V}^{-1} \text{ d}^{-1}$, respectively.
- Kaolin clay: An initial TCE concentration of 150 mg kg^{-1} was reduced with 85% 4 cm into kaolinite from the anode within 5 days at 0.4 V cm^{-1} (Bruell et al., 1992), corresponding to a velocity of $2 \text{ cm}^2 \text{ V}^{-1} \text{ d}^{-1}$
- Sandy Clay: 7 days with application of 1 V cm^{-1} decreased the TCE concentration in a spiked sandy clay (sampled from farmland) with about 70% in the 5 cm closest to the anode (Yang and Yeh, 2011). This corresponds to a velocity of $0.7 \text{ cm}^2 \text{ V}^{-1} \text{ d}^{-1}$.

Chang and Cheng (2006) reported an improvement of PRB when combined with EK in sandy soil for degradation of PCE. However, the improvement was obtained during the first 24 h whereafter the decrease in concentration had a similar slope as standalone EK or PRB. This reveals limited EO towards the PRB in this sandy soil and that EK only increased degradation of PCE initially in the vicinity of the PRB.

6.2. Types and placement of PRB

When combined with EK, different compositions and placements of the PRB have been suggested. Vertical barriers with iron filings in kaolin clay were found effective using the Lasagna™ process (Athmer and Ho, 2009). Chung and Lee (2007) used atomizing slag (PS Ball) and sand as the filter media in the PRB. Chang and Cheng (2006) found that PRB with zero valent Zn (ZVZ) performed better than ZVI for PCE degradation.

PRB is most efficient when placed close to the anode due to the proton production aiding the reduction at the ZVI, and the acidic environment prevented the formation of iron oxides at the ZVI surfaces and thereby passivation (Chang and Cheng, 2006; Chen

et al., 2010). The advantage of placing an anode near the PRB was also seen in relation to general PRB by Moon et al. (2005), where the contaminated groundwater moves through the PRB in a hydraulic flow; simultaneous application of ZVI and an external DC field enhanced dechlorination of TCE by 1.3–5.8 times compared to ZVI only. However, when utilizing the combined EK-PRB method in fine-grained clayey soils, the contaminants are transported by EM or advection in the EO flow towards the cathode, which suggests placing a cathode downstream the PRB.

6.3. In situ pilot and full scale actions

The Lasagna™ technology has been tested in-situ for treatment of clayey soil contaminated with chlorinated ethenes. The method uses DC current to heat the soil and to mobilize pore water and contaminants into the treatment zones. In the first full-scale field test, horizontal treatment zones were installed (Ho et al., 1999a). However, vertical emplacements were more practical (Athmer and Ho, 2009). With this method, no contamination is brought above-ground, since transport and destruction take place within the soil matrix (Athmer and Ho, 2004; Athmer and Ho, 2009).

Ho et al. (1999b) describe a small field test ($4.6 \text{ m} \times 3 \text{ m}$, and 4.6 m deep), which lasted 4 months. The purpose was to prove EO transport of TCE and to collect information for design, installation, and operation. The electrode spacing was 3 m . In between the electrodes, three treatment zones with granular activated carbon were installed to collect and confirm transport of TCE from soil into the treatment zones. A constant current (40 A) was applied. The voltage decreased from 138 V (0.45 V cm^{-1}) to 105 V (0.35 V cm^{-1}), where it stabilized. The decrease was ascribed Joule heating of the soil, as the temperature increased from 15 to 45°C . After plant adjustments, the EO flow rate was similar to the level obtained in the lab ($1.04 \text{ cm}^2 \text{ V}^{-1} \text{ d}^{-1}$). In total, about three pore volumes were transported with EO. The highest TCE concentration before treatment was 507 mg kg^{-1} with a TCE removal of 92–99.8%. About 4% of the removed TCE was volatilized. The remaining fraction of removed TCE was transported to the treatment zones where the concentration at the activated carbon reached $10,000 \text{ mg TCE kg}^{-1}$.

Ho et al. (1999a) describe a larger field scale test ($6.2 \text{ m} \times 9.2 \text{ m}$, and 13.7 m deep), which lasted a year. The purpose was to show effective in-situ treatment to a depth of 13.7 m (Athmer, 2004). The electrode spacing was 6.3 m and three treatment zones composed of iron filings in kaolinite were installed in between. Each electrode comprised of a 3.8 cm thick layer of 50/50 iron filings and coke to the depth of 13.7 m . The first two months, 150 V was applied (0.23 V cm^{-1}) corresponding to a current of 110 A . Hereafter, the voltage was increased to 200 V (0.31 V cm^{-1}) at 200 A . After about 5 months, the core soil temperature was increased to 80°C due to Joule heating, and the voltage was reduced to 120 V (0.19 V cm^{-1}).

The voltage distribution was reasonably uniform for the first 5 months, where after the anode filling started to dry out. About 2.8 pore volumes were transported by EO. Between the treatment zones, 96–99% TCE was removed. Between cathode and treatment zone the removal was 70% and between the anode and treatment zone, 43% was removed. The removal may be due to both evaporation and EK transport.

Athmer (2014) conducted full-scale remediation at an industrial complex, where two part-areas were remediated. The clayey soil contained aged contamination of TCE with significant levels of cis-DCE and VC. The treatment zone was installed under built infrastructure. The plant depth was 6 m. In part-area-1, two areas were treated (33 m × 21 m and 20 × 15 m). In part-area-2, 15 m × 15 m were treated. Treatment zones of iron filling mixed in kaolinite slurry were placed vertically at 1.5 m intervals between electrodes. Reductions of TCE in part-area-1 and part-area-2 were estimated to 76% and 83%, respectively.

These in-situ field experiences illustrate the ability of EK to mobilize chlorinated ethenes with EO in fine-grained clayey soils.

7. EK-bioremediation. Biotic reduction

Bioremediation techniques broadly fall into two categories: biostimulation and bioaugmentation (Lima et al., 2017). Biostimulation is a supply of nutrients, such as electron acceptors or donors, to promote biodegradation of contaminants by indigenous microbes. Bioaugmentation is the supply of microbes possessing specific capabilities to biodegrade the targeted contaminants. The biotic degradation pathways are shown in Fig. 1.

Successful bioremediation requires physical interaction between microorganisms, substrates and contaminants (Semple et al., 2004). EK transport processes can overcome the otherwise slow transport of bacteria and/or nutrients in low-permeable soils and thus improve the delivery of e.g. bacteria. Most research on EK-BIO has been on understanding and optimizing the transport processes. A review by Gill et al. (2014) examines the state of knowledge on EK-BIO and conclude that current research needs include analysis of EK-BIO in more representative environmental settings, such as those in physically heterogeneous systems in order to gain a greater understanding of the controlling mechanisms.

Crucial for EK-BIO is that the applied current does not inhibit the microorganisms. When hindering side effects, e.g. pH and redox changes, in developing inside the soil, no significant impact on the microbial activity is seen (Lear et al., 2005; Shi et al., 2008a). Jackman et al. (1999) have shown that the application of an electric DC field of 20 mA/cm² stimulates the activity of sulfur-oxidizing bacteria. No research has indicated bacterial growth inhibition by the applied electric field in the range used in EK remediation.

7.1. EK-bioaugmentation

7.1.1. EP transport of bacteria in soil

Bacteria have been transported by EP into sand (DeFlaun and Condee, 1997), Sandy/silty loam (DeFlaun and Condee, 1997) and field sampled clay (Wick et al., 2004; Mao et al., 2012) and bryozoan limestone (Hansen et al., 2015). EP of bacteria depends on the physico-chemical properties of both the porous media (DeFlaun and Condee, 1997) and the surface properties of individual bacteria (Wick et al., 2007; Shi et al., 2008b). Most bacterial strains carry a weak negatively charged cell surface at near neutral pH, and thus EP is in the direction towards the anode. EP transport of bacteria in solutions is widely used within the field of micro-electrophoresis for characterization of bacteria (van der Wal et al., 1997). The surface charge of individual bacteria, expressed by the zeta potential, is inconsistent since it is influenced by the surrounding solution. The

zeta potential of bacteria decreases with increasing ionic strength of the solution (Zhang et al., 2015). The zeta potential of three microorganisms capable of degrading chlorinated ethenes, *Dhc*, *Geobacter* and *Methanomethylovorans*, at low ionic strength was reported to −25 mV, −40 mV and −51 mV, respectively (Zhang et al., 2015). This reveals different EP transport velocities for those microorganisms since zeta potential and EP mobility are interconnected. Also, the pH of the soil solution influences the EP of bacteria. DeFlaun and Condee (1997) detected no EP transport at pH 5.5, whereas a high transport rate was seen at pH 8.5.

Soils can restrict EP of bacteria by direct adsorption and by the pore sizes, which need to be larger than the size of the bacteria. Wick et al. (2004) showed that EP transport of weakly negatively charged and moderately adhesive cells was faster than of strongly charged and highly adhesive cells. DeFlaun and Condee (1997) reported that the presence of silt and clay minerals retarded the EP transport of bacteria. Zhang et al. (2015) reported on the microbial cell diameters: *Dhc* 0.62 μm, *Geobacter* 0.70 μm and *Methanomethylovorans* 1–1.5 μm. The pore sizes vary largely in soils, but some examples give indications of the order of magnitudes: For a Brazilian soil, classified as sandy loam, 51.1% of the total porosity was in the 100–500 μm size and a third of total porosity had pores >500 μm (Pires et al., 2013). In clay, Ninjarav et al. (2007) reported pore sizes of 0.5–1 μm, and in kaolinite, the pore size was less <0.4 μm (Gingine and Cardoso, 2017). Thus, in clayey soils, the diameter of bacteria and pore sizes are in the same order, suggesting a limited possibility for EP transport unless the microbial structure is flexible. Blocking of the fine pores can be a result. Without applied current, high cell concentrations affect the overall retention of cells either positively by providing more surfaces for adhesion or negatively by leaving less favorable surfaces causing blocking (Camesano and Logan, 1998). These effects might also be important when combining with EK.

EP improved the transport of a TCE degrading, adhesion-deficient variant of *Burkholderiucepacia* G4 (1CB) in coarse-grained sand and sandy loam (DeFlaun and Condee, 1997). EP transport velocities of 7.2–14.4 cm² V^{−1} d^{−1} in sand and 2.4–3.6 cm² V^{−1} d^{−1} in sandy/silty loam were observed, while the bacteria did not move without applied current. Similarly, Wick et al. (2004) found no transport of the bacteria *Sphingomonas* sp L138 without applied current but reached EP transport velocities of 5.8 cm² V^{−1} d^{−1} in clayey soil. However, they found no EP transport of the bacteria *M. frederiksbergense* LB501TG. The two strains have approximately the same size, but the latter is strongly adhesive, which is likely the reason for the different mobilities by EP (Wick et al., 2004). Thus, the characteristics of the bacteria strain are of major importance to the transport by EP.

7.1.2. Transport of bacteria by advection in an electroosmotic flow

Bacteria can be transported by advection in the EO flow i.e. towards the cathode (Mao et al., 2012; Lee and Lee, 2001). Thus, transport of bacteria by EO is influenced by the same factors as EO (Table 1). In addition, Wick et al. (2004) reported EO transport of bacteria in soil to depend on bacteria retention by the solid phase. The transport by advection in the EO flow for *Sphingomonas* sp L138 and *M. frederiksbergense* LB501TG reached velocities of 0–3.8 cm² V^{−1} d^{−1} and 3.4–6.7 cm² V^{−1} d^{−1} in field-sampled clayey soil, respectively (Wick et al., 2004). In another field sampled clayey soil, the *vcrA* copies encoded for VC reductase) moved at least 16 cm into the soil in the direction of the cathode during 56 days of applied current at the average potential gradient of 0.8 V cm^{−1} (Mao et al., 2012). Thus, the transport rate of *Dhc* was 16 cm in 47 days, corresponding to 0.4 cm² V^{−1} d^{−1}.

7.1.3. Electrophoresis vs electroosmosis

The transport of bacteria in soil by EP and EO are of opposite directions. The dominating mechanism depends on the bacteria, soil characteristics and soil solution chemistry. *Sphingomonas sp* L138 was transported in 80–90% by EO (identified by transport towards the cathode) and 10–20% by EP (transported towards the anode) (Wick et al., 2004). Mao et al. (2012) supported EO to be the major transport mechanism. In contrast, Da Rocha et al. (2009) experimentally showed that EP was the main phenomenon responsible for the transport of bacteria in clayey soil. In summary, the specific soil system and bacteria culture determine the governing EK transport mechanism.

7.2. EK-biostimulation

Hydrogen can serve as an electron donor for biodegradation of chlorinated ethenes, and lactate is considered one of the best hydrogen donors (Wu et al., 2007). Lactate is tested in the literature on EK-biostimulation (alone or in combination with EK-bioaugmentation) for remediation of soil contaminated with chlorinated ethenes, and lactate is negatively charged and transported by EM towards the anode (Wu et al., 2007; Mao et al., 2012; Hansen et al., 2015). Wu et al. (2007) experienced significant EO flow in clay samples, but the opposite directed EM was still the governing transport mechanism for lactate. The EK transport of such organic additives is limited by adsorption, the natural oxygen demand and biological transformation (Wu et al., 2007). Only when the rate of injection is compatible with the rate of consumption, a homogeneous injection is possible throughout the soil (Rabbi et al., 2000). To evaluate the potential enhancement of bioremediation by injection of lactate, it is necessary to assess its reactive transport rates under the DC field (Wu et al., 2007):

- Natural clay: $4 \text{ cm}^2 \text{ V}^{-1} \text{ d}^{-1}$ calculated from the reported 3.2 cm d^{-1} and an average potential gradient of 0.8 V (Mao et al., 2012).
- Silty clay: $3.2 \text{ cm}^2 \text{ V}^{-1} \text{ d}^{-1}$ (Wu et al., 2012b).
- Clay: Lactate was detected 24 cm into clay towards the anode after 188 h at 0.8 V cm^{-1} , corresponding to $3.8 \text{ cm}^2 \text{ V}^{-1} \text{ d}^{-1}$ (Wu et al., 2007).
- Sand: Lactate was detected 24 cm into the sand towards the anode after 129 h at 0.5 V cm^{-1} (Wu et al., 2007), corresponding to $8.9 \text{ cm}^2 \text{ V}^{-1} \text{ d}^{-1}$.

Efficient supply of lactate by EM into a 40 cm long silty clay spiked with PCE and anaerobic degrading bacteria (culture KB1[®]) showed full degradation to ethene whereas a reference experiment without application of current resulted in limited degradation (Wu et al., 2012b). Hence, if a bacteria culture capable of degrading the contaminants is present, lactate can be supplied sufficiently by EM in fine grained soils.

7.3. Pilot scale action

Cox et al. (2018) conducted a pilot scale action with the overall goal to demonstrate and validate EK-enhanced amendment delivery for in-situ EK-BIO via enhanced reductive dechlorination of a PCE source area in clay. The EK plant consisted of 9 electrode wells and 8 supply wells located within an area of approximately $12 \times 12 \text{ m}$. The depth interval targeted by the treatment was 5–7 m. The remediation amendments distributed by EK included lactate, pH control reagents (potassium carbonate), and a dechlorinating microbial consortium (KB-1[®]) containing *Dhc*. The action included 2 separate stages, 5-month each, of active operation with a 6-month incubation period between the two active stages. A >60%

reduction in average PCE concentrations was achieved in soil and groundwater within the treated area. While groundwater data also showed coupled and comparable increases of dechlorination daughter (including VC) and end products, no such apparent increases of degradation products were observed in soil samples. Ethene was detected at 100% of groundwater monitoring wells and >10x increases of *Dhc* from baseline was observed at >60% of soil and groundwater samples collected from within the treated area.

8. EK-ISCO. Abiotic oxidation

In-situ chemical oxidation (ISCO) is a remediation technique where chemical oxidants are injected or mixed into the soil for rapid and complete contaminant mineralization. Most of the prevalent organic contaminants can be destroyed using catalyzed hydrogen peroxide (H_2O_2), potassium permanganate (KMnO_4), activated sodium persulfate ($\text{Na}_2\text{S}_2\text{O}_8$), ozone (O_3) or combinations of oxidants (Siegrist et al., 2014). ISCO is a promising technology, but successful delivery into low permeability zones or uniformly throughout heterogeneous zones is an unresolved challenge (Reynolds et al., 2008). To overcome this, EK-ISCO has been investigated for an optimized supply of permanganate and persulfate.

8.1. EK-ISCO permanganate

Use of KMnO_4 for ISCO is of significant interest due to its high oxidation-reduction potential, stability in aqueous solution, reactivity over a wide range of pH (3.5–12), ability to work without an activator, and production of non-toxic by-products after reaction with the chlorinated solvents (Chowdhury et al., 2017b). KMnO_4 can dechlorinate chlorinated ethenes completely (Huang et al., 2001).

EK permanganate transport into homogeneous, artificial, non-contaminated soil has been investigated (Roach and Reddy, 2006; Reynolds et al., 2008; Hodges et al., 2013). In experiments without pH neutralization at the electrodes, Roach and Reddy (2006) found that EM of permanganate (MnO_4^-) in kaolinite was limited to the proximity of the cathode due to a low pH in the remaining of the kaolinite. At low pH (<3.5), MnO_4^- is reduced to Mn^{2+} , i.e. a cation, which EM towards the cathode (Roach and Reddy, 2006). In addition, the oxidation potential of MnO_4^- is lost at acidic pH. Reynolds et al. (2008) obtained EM of MnO_4^- from the cathode reservoir into the anode reservoir through 7 cm mixed glass beads and kaolinite. In experiments with glass beads, the concentration in the anolyte relative to the catholyte was 10% with 10 V applied, while 15% with 20 V applied after 150 h. This exceeded the 5% obtained by diffusion but lacked full break-through. In experiments with kaolinite, the concentration of MnO_4^- in the anolyte increased with 13–15% when applying 10–20 V for 150 h. The results indicated a threshold in EM of permanganate due to competing processes or other phenomena (Reynolds et al., 2008). Hodges et al. (2013) defined those limitations as stalling. Hodges et al. (2011) developed an EK set-up in which pH changes were isolated from the soil. Using this set-up, Hodges et al. (2013) showed EM of MnO_4^- through a 10 cm long kaolinite core at neutral pH. After 5.2 days at 1.1 V cm^{-1} , MnO_4^- was measured in the anolyte, corresponding to a transport velocity of $2.3 \text{ cm}^2 \text{ V}^{-1} \text{ d}^{-1}$. The concentration in the kaolinite near the anode of 1 g L^{-1} was the lowest inside the core. Such differences in MnO_4^- distribution in the kaolinite is critical when considering implementation of EK-ISCO at full-scale because it can lead to inefficient contaminant degradation (Hodges et al., 2013). Thus, this needs to be overcome.

Reynolds et al. (2008) conducted experiments with fine-grained lenses of glass beads or kaolinite embedded in a non-contaminated artificial soil of coarser glass beads. The pink color of permanganate

was qualitatively used to assess EM into these lenses. As opposed to when not applying an electric field, the electric field intensified the pink appearance of the lenses. Thus, EM transport from a coarse medium into a fine-porous medium was shown. Chowdhury et al. (2017b) conducted experiments in a two-dimensional sandbox packed with layers of silt perpendicular to the electric field. The sand and silt were contaminated with aqueous TCE. EK successfully delivered MnO_4^- throughout the silt, while without EK, the MnO_4^- was delivered to the edges of the silt layer fringes only. TCE mass destruction in the silt could not be directly quantified, but image analysis of the silt showed a 240% increase in MnO_4^- delivery when EK was applied. Furthermore, EK-application significantly reduced the back-diffusion of TCE from the contaminated silt after active treatment for 25 days.

8.2. EK-persulfate

Persulfate offers some advantages over the other oxidants, such as high aqueous solubility, high stability in subsurfaces, lower affinity for organic matter, reduced cost, and nonhazardous end-products (Matzek and Carter, 2016). Persulfate refers to ions or compounds containing the anions SO_5^{2-} or $\text{S}_2\text{O}_8^{2-}$. Matzek and Carter (2016) reviewed in detail the use of activated persulfate for oxidation of organics. Persulfate oxidation requires activation by either heat, mineral-based activators, UV light or high pH (Matzek and Carter, 2016). Selecting the suitable activator depends on site conditions such as geology, hydrogeology and the application strategy (Yukselen-Aksoy and Reddy, 2012). EK assisted ISCO using persulfate is to transport the persulfate into the soil by EM or EO followed by in-situ activation.

The anionic persulfate is transported by EM towards the anode or by EO towards the cathode. Important findings on persulfate distribution in soil using EK can be extracted from papers on laboratory work with non-contaminated soil (Mikkola et al., 2008), soil contaminated with creosote (Isosaari et al., 2007) or PCB (Yukselen-Aksoy and Reddy, 2012; Fan et al., 2014). EM of persulfate in sand was found linearly related to the applied voltage in the range of $1\text{--}4\text{ V cm}^{-1}$ with transport rates of $12\text{ cm}^2\text{ V}^{-1}\text{ d}^{-1}$, (Mikkola et al., 2008). A tendency for higher EM velocities with increasing silt content was observed, reaching $19.8\text{ cm}^2\text{ V}^{-1}\text{ d}^{-1}$ in pure silt. This was ascribed to the higher electrical conductivity caused by higher water content and thus, higher current densities in the silt. Chowdhury et al. (2017a) successfully delivered persulfate with EM throughout a 36 cm silt sample at voltages of $12\text{--}18\text{ V}$ ($0.5\text{--}0.8\text{ V cm}^{-1}$) in a system where pH was controlled with phosphate buffers at the electrodes. An average transport rate of $2 \pm 0.7\text{ cm/day}$ was estimated based on the arrival times of 50% of the maximum persulfate concentration (Chowdhury et al., 2017a), corresponding to $3.1 \pm 1.1\text{ cm}^2\text{ V}^{-1}\text{ d}^{-1}$ based on an average voltage in the range given. The persulfate concentration in the soil solution reached 11 g L^{-1} near the cathode and 9 g L^{-1} near the anode.

In an EK system without pH control, EO was the most efficient process for transporting persulfate into a field-sampled soil (Fan et al., 2014). Persulfate was delivered 6 cm into the soil by EO within 3–6 days. Break-through of persulfate into the catholyte was not observed. On the contrary, break-through into the anolyte with EM was observed, but here the persulfate concentration in the soil was lower (Fan et al., 2014). Addition of persulfate from both electrodes simultaneously did not deliver persulfate uniformly (Fan et al., 2014). This work underlines the necessity to control pH.

Injection of persulfate at the anode has shown to increase the EO flow velocity (Yang and Yeh, 2011; Fan et al., 2014). Contrary, persulfate has also shown to reduce the EO flow rate significantly (Isosaari et al., 2007). Fan et al. (2016) showed that transport of persulfate by advection in an EO flow towards the cathode was

influenced by the persulfate activation method used: alkaline activation > zero valent iron activation > no activation > citric acid chelated Fe^{2+} activation > peroxide activation > iron electrode activation. Thus, the transport of persulfate by advection in EO flow depends on a variety of factors, which possibly are site-specific and thus calls for further assessment. In addition, the simultaneous addition of a suspended activator and persulfate decreased the persulfate distribution into the soil (Fan et al., 2016). Thus, adequate delivery of persulfate into the soil prior to activation is beneficial.

Efficient degradation (99% removal) of TCE in a 25 cm long, spiked, field-sampled soil under an applied electric field of 1 V cm^{-1} during 7 days with a high dose of 10 g L^{-1} of Na-persulfate at the anode is observed (Yang and Yeh, 2011), corresponding to $3.6\text{ cm}^2\text{ V}^{-1}\text{ d}^{-1}$. This high removal was ascribed EO transport of H_2SO_5 , which was suggested produced in the anolyte due to the strongly acidic environment.

In a study on PCB removal, Fan et al. (2016) reported the removal efficiency order of the activation methods to be: alkaline > peroxide > citric acid chelated Fe^{2+} > Zero-valent iron > no activation > Fe-electrode activation. The removal efficiencies varied between 41 and 31%. The activation methods tested and reported are: (I) *Electrochemical generation of Fe(II) using an iron anode*. This method was evaluated for the oxidation of phenol in a stirred solution with persulfate and phenol (Park et al., 2016). EK-transport was not included in this study, but it showed, that a continuous supply of Fe(II) from the anode was easier to control than direct addition of iron sulfate to the solution because excess Fe(II) impedes the activation of persulfate. Literature available on EK-persulfate for remediation of soil contaminated with chlorinated ethenes is yet scarce. (II) *Thermally Activated Persulfate*. Temperature is a strong activator of persulfate. EK-TAP is an abbreviation for “Electrokinetic Thermally Activated Persulfate”, i.e. a method in the EK-ISCO family. In brief, the persulfate is delivered into the soil by EK followed by a temperature increase by changing to an AC electric field for electrical resistivity heating (ERH). The application of heat is expected more uniformly distributed than other possible activation methods (Chowdhury et al., 2017a), and they also showed full degradation of PCE in soil solution samples after two periods with persulfate supply by EM and activation by ERH. Increase in sulfate concentration simultaneous to decrease in persulfate concentration during ERH indicated activation and decomposition of persulfate. Activation at 36°C was more efficient in eliminating PCE than at $>41^\circ\text{C}$. Yukselen-Aksoy and Reddy (2012) found that increasing the temperature to 45°C was efficient for PCB degradation after EK persulfate delivery. (III) *Persulfate activation with ZVI and nZVI*. Yang and Yeh (2011) reported that with nano-Fe the TCE concentration was reduced from 132 to 156 mg kg^{-1} to $<10\text{ mg kg}^{-1}$ all through the 25 cm long soil column, and without nano-Fe the final concentration was about $25\text{--}55\text{ mg kg}^{-1}$ TCE degradation in a spiked, field-extracted soil was app. $10\text{--}30\%$ more efficient when adding nZVI to the catholyte and persulfate to the anolyte than when adding persulfate alone.

Natural soil constituents influence EK-persulfate. Liang et al. (2003) showed that in aqueous systems, significant TCE degradation was obtained after 6 h at 40°C . However, longer treatment times and higher doses of persulfate were needed for effective treatment of soil slurries, because the organic matter competed for sulfate free radicals (Liang et al., 2003). Similar, Yukselen-Aksoy and Reddy (2012) observed enhanced degradation of PCB in kaolinite than in glacial till. The difference was attributed to the high buffering capacity, nonhomogeneous mineral content and high organic content of glacial till. In general, the natural oxidant demand in soil is the reaction of permanganate with immobile, sediment-bound reductants such as organic matter, or reduced minerals such as pyrite (FeS_2) (Mumford et al., 2005). Hence, the natural oxidant

demand of soil must be accounted for when dosing persulfate. Important findings on changing conditions in soil during persulfate treatment were reported by Isosaari et al. (2007). They periodically injected persulfate to a field-sampled clay and the DC field was applied from external electrodes. Phosphate buffers were added in order to control pH at the electrodes, but without success, i.e. pH changed in the injection wells throughout 8 weeks. Each injection of persulfate resulted in an increased current that leveled out over time. The authors explained the leveling out to be due to precipitation of sulfates, phosphates and hydroxides, which was verified by elemental analyses showing decreasing concentrations of Al and Ca in the soil near the anode and increasing concentrations near the cathode (Isosaari et al., 2007). P concentrations increased significantly throughout the soil originating from the buffer solutions in the electrolytes. The S concentration increased from 780 mg kg⁻¹ to 1040–2980 mg kg⁻¹, peaking in the soil midway between the electrodes, but whether this increase was due to the transport of persulfate or e.g. SO₄²⁻ was not identified. Similarly, Fan et al. (2014) reported an initial increase in current density followed by a decrease during the continuous supply of persulfate by EO, also ascribed to precipitation within the soil.

The influence of common anions and cations (CO₃²⁻, PO₄³⁻, HCO₃⁻, SO₄²⁻, NO₃⁻, Na⁺, K⁺, Mg²⁺ and Ca²⁺) on the Fe²⁺ activated persulfate process for treatment of aniline contaminated groundwater without EK was examined by Zhao et al. (2016). Under the optimum operating conditions, 86% aniline degradation was observed within 60 min. The effects of the cations on aniline degradation were negligible. Anions, on the other hand, decreased the removal of aniline because of radicals generated in the reaction of sulfate radical or hydroxyl radical with these anions. The order of inhibitory effects was PO₄³⁻ > CO₃²⁻ > SO₄²⁻ > HCO₃⁻ > NO₃⁻. The influence of anions on EK-ISCO of chlorinated ethenes using persulfate needs investigation in relation to EK. Especially of PO₄³⁻ since the phosphate buffering system is often used to buffer pH at the electrodes.

8.3. Modelling EK-ISCO

Wu et al. (2013) took the challenge to model different electrode configurations in EK-ISCO using permanganate. The focus was to achieve optimal coverage of the oxidant. As a supplement to the previous models focusing on electrode placement during EK-remediation, e.g. Alshawabkeh et al. (1999), this model takes into account the contaminant degradation. Greater contact between the injected permanganate and PCE in the model was achieved with horizontal electrodes (Wu et al., 2013). Furthermore, reduced time for remediation can best be achieved by an increased number of electrodes, adopting bidirectional and radial electrode configurations, incorporating oxidant injection wells and a pulsed injection of oxidant (Wu et al., 2013). This will come at the cost of increased capital expenditure and in some cases, increased oxidant or energy consumption. If low-cost remediation is the objective, the electrodes should be placed further apart or fewer electrodes used, which results in a longer treatment time. In both cases, periodic reversal of the electric field shortened the remediation time and energy consumption (Wu et al., 2013).

9. Discussion

9.1. Summary of transport velocities reported

The transport velocities calculated based on reported experimental results for chlorinated ethenes, lactate, bacteria, permanganate and persulfate are summarized in Table 4. It must be stressed, that the velocities are not directly comparable as available

data differed in origin. The velocities gives the orders of magnitude. In general, reported ranges on transport velocities of chlorinated ethenes in different soil types are limited. For designing and operating in-situ full-scale remediation actions with EK-enhanced technologies, velocities are necessary design parameters, and thus must be addressed in future research.

Transport velocities of TCE and PCE by advection in the EO flow are reported in the range of 0.2–2.4 cm² V⁻¹ d⁻¹ (Table 4). Thus, the velocity cannot be neglected in experimental work with all EK-enhanced methods. The main purpose with EK-BIO is to extend the bioremediation to also work in fine-grained soils, and it has been shown, that bacteria are transported by EP and EO in these. The EP-transport velocities for bacteria are 0–7.2 cm² V⁻¹ d⁻¹, and for advection in EO flow 0–6.7 cm² V⁻¹ d⁻¹. EM transports lactate towards the anode and the transport velocities reported are 2.6–8.9 cm² V⁻¹ d⁻¹. Thus, lactate and bacteria are transported with velocities in the same order of magnitude. The transport velocities reported for persulfate and permanganate in EK-ISCO are 1.7–20 cm² V⁻¹ d⁻¹. It has not been possible to conclude the dependency of transport velocities on soil type. Research is needed such that proper design parameters on transport velocities can be determined.

9.2. Importance of side effects and transient changes

The pH at the electrodes must be neutralized in all the EK enhanced techniques for remediation of soil contaminated with chlorinated ethenes, since changes in soil pH inhibit remediation, as experienced in many of the studies reported. In EK-PRB, the changes in pH strongly influence EO and hereby the transport of chlorinated ethenes towards the PRB. In EK-BIO, the changes in pH are negatively affecting the health of the bacterial community. In EK-ISCO, pH influences the reactivity and transport of the oxidants. When pH gradients in the soil are prevented, the changes in soil (Table 2) are less sensitive to mineral decomposition and precipitation, which thereby will contribute to a more uniform distribution of the applied electric field.

More focus needs to be given to the possible changes in soil redox conditions induced by the electrode reactions since these are important for successful remediation. The O₂ containing anolyte can be transported into the soil by EO and diffusion, thus increasing the redox potential. In EK-BIO of chlorinated ethenes, the bacteria *Dhc* require strict anaerobic conditions (Section 4.2), and thus, the oxidizing conditions from the anode must be managed. For EK-ISCO, the oxidant demand must be expected to increase or the remediation efficiency to decrease if the reducing conditions from the cathode are not controlled.

Joule heating has been investigated in a few studies only (Lageman and Godschalk, 2007; Ho et al., 1997, 1999a), which underline the importance of coming field-scale tests with EK-BIO and EK-ISCO to include an investigation of the effect from Joule heating to take advantage of the possibly increased solubility, reaction rates and transport velocities in the field compared to lab scale. Evaporation and unwanted transport into buildings etc. need to be considered as well. Also, the energy consumption required for Joule heating needs to be considered in cost calculations.

9.3. EK in heterogeneous subsurface soils

A general need for an understanding of EK in in-situ settings is stressed in recently published reviews. Research needs to include assessment of EK-technologies in more representative environmental settings, such as heterogeneous geologies, in order to I) understand the controlling mechanisms in natural settings (Gill et al., 2014), and II) be able to optimize the EK-technologies for

Table 4

Summary of transport velocities for chlorinated ethenes (>85% removal), lactate, bacteria, permanganate and persulfate in different soils calculated from literature. The velocities are not directly comparable since data available varies between references. The velocities are rather orders of magnitude than exact velocities. (OM = organic matter).

Method	Transported specie	Transport process	Soil	Voltage applied [V cm ⁻¹]	Transport rate [cm d ⁻¹]	Velocity [cm ² V ⁻¹ d ⁻¹]	References
EK-PRB	TCE	EO/EM	Field-sampled clay (d ₅₀ = 28 µm, OM 1.8%), spiked	1.0	2.4	2.4	Weng et al. (2003)
	TCE	EO/EM	Field-sampled clay (Particles < 75 µm 90%, OM 6.7%), spiked	2.0	1.2	0.6	Chung and Lee (2007)
	PCE	EO/EM	Field-sampled (48% clay, OM 1.7%), spiked	2.7	0.6	0.2	Chang et al. (2006)
	TCE	EO/EM	Field-sampled (48% clay, OM 1.7%), spiked	1.8	0.9	0.5	Chang et al. (2006)
	TCE	EO/EM	Kaolinite, spiked	0.4	0.8	2	Bruell et al., 1992
EK-BIO	Lactate	EM	Field-sampled low-plasticity silty clay, non-contaminated	0.8	3.1	3.8	Wu et al. (2007)
	Lactate	EM	Fine grained sand, non-contaminated	0.5	4.5	8.9	Wu et al. (2007)
	Lactate	EM	Field-sampled clay (<10% sand), aged contamination	0.8	3.2	2.6	Mao et al. (2012)
	<i>Burkholderiu cepacia</i> G4 (1CB)	EP	Coarse-grained sand, (~750 µm), non-contaminated	10	72	7.2	DeFlaun and Condee (1997)
	<i>Burkholderiu cepacia</i> G4 (1CB)	EP	Fine-grained sand, (70–350 µm), non-contaminated	10	72	14.4	DeFlaun and Condee (1997)
	<i>Burkholderiu cepacia</i> G4 (1CB)	EP	Sandy loam (14% clay, 1.4% OM), non-contaminated	10	36	3.6	DeFlaun and Condee (1997)
	<i>Burkholderiu cepacia</i> G4 (1CB)	EP	Silt loam (20% clay, 3.9% OM, non-contaminated	10	24	2.4	DeFlaun and Condee (1997)
	<i>Sphingomonas</i> sp L138	EP	Field-sampled clay (59% clay), non-contaminated	2	11.5	5.8	Wick et al. (2004)
	<i>M. frederiksbergense</i> LB501TG	EP	Field-sampled clay (59% clay), non-contaminated	2	0	0	Wick et al. (2004)
	<i>Sphingomonas</i> sp L138	EO	Field-sampled clay (59% clay), non-contaminated	2	0–7.7	0–3.8	Wick et al. (2004)
	<i>M. frederiksbergense</i> LB501TG	EO	Field-sampled clay (59% clay), non-contaminated	2	6.7–13.4	3.4–6.7	Wick et al. (2004)
	Dhc	EO	Field-sampled clay, aged contamination	0.8	0.3	0.4	Mao et al. (2012)
	Permanganate	EM	Kaolinitic pottery clay (28% clay), non-contaminated	1.1	1.9	1.7	Hodges et al. (2013)
	Persulfate	EM	Sand (100% sand) non-contaminated	4.0	48	12	Mikkola et al. (2008)
	Persulfate	EM	Silt (100% silt), non-contaminated	4.0	79	20	Mikkola et al. (2008)
	Persulfate	EM	Fine silt (d ₅₀ = 45 µm), Spiked with TCE	0.3–0.5	2	4–6	Chowdhury et al. (2017a)

full-scale implementation (Gomes et al., 2012a). The field parameters, which influence the modelling and design of full-scale EK-remediation include heterogeneous soils in which the electrical conductivity differs in the different layers. The present review supports this. In the subsurface, the water content may change significantly, from few percentages to saturated, influencing the resistivity, pressure gradients can distribute electrolyte solutions from electrode wells into coarse, unsaturated layers and groundwater flow may counteract or enhance transport velocities, and introduce e.g. vertical flow gradients. The influence from such factors determined by the site geology has not been assessed. The robustness of the EK-methods depends on knowledge on this for sufficient engineering. Following full-scale tests, it may be necessary to step back to redesigned laboratory tests to assess knowledge gaps identified during field-tests to avoid unforeseen situations in large scale, which increase the costs significantly. Acquisition of data in the field is expensive; it is, therefore, critical to identify which processes and system parameters that ultimately determine the success of a remediation strategy (Wu et al., 2012a). For example, transport mechanisms must be fully understood to ensure unintended spreading of the contaminants is avoided. Currently, however, scarcity of data particularly on the EK-parameters and at field-scale, and the related uncertainties, will affect the robustness of both model-based predictions and designs of EK-implementations (Wu et al., 2012a). A comprehensive study, which quantifies the effects of a wide range of natural and model-parameters on the efficiency of EK-combined technologies is requested.

10. Conclusions

The concept of EK-enhancement of PRB, BIO and ISCO has shown encouraging results at lab-scale and for PRB and BIO also at full-scale. A major finding is that the already established methods applied in high-permeability soils can be transferred to low-permeability soils when combined with EK. This is unique and calls for a systematic approach to fill in current knowledge gaps towards safe and successful remediation. This review has identified major knowledge gaps, including transport velocities for chlorinated ethenes, changes in redox conditions in different soils due to electrode reactions, significance of the advantageous Joule heating for reaction rates, transport velocities and bacteria activity, and significance of site-specific parameters on transport velocities, e.g. heterogeneous geology and thereby electrical conductivities, water content, pressure gradients, hydrology, hydrogeochemistry, and oxygen demand and buffering capacity of the soil. In addition, there is a lack of coherence on how to report data on voltage distribution and transport rates, which complicate the comparison of studies.

In this review, it was found, that for the combined EK-techniques, it is necessary to manage the induced changes in pH to obtain steady EO transport of chlorinated ethenes, EP of bacteria, a healthy bacteria community, uniform delivery and reactivity of oxidants, and to control mineral decomposition and precipitation for a uniformly distributed electric field. Calculated transport velocities based on reported data show, that for EK-BIO, EM of lactate and EP of the biodegrading bacteria are in the same order of magnitude. When applying EK-techniques, back-diffusion of contaminants from low-permeable soils is lowered, and periodic

reversal of the electric field appears to shorten the remediation time and energy consumption.

This review underlines the promising use of EK for enhancement of remediation technologies, but it also highlights some major knowledge gaps that must be understood for the EK-techniques to be optimized and become robust enough for successful field-implementation at different sites with heterogeneous subsurface.

Acknowledgements

The work was funded by the Capital Region of Denmark.

References

- Alshawabkeh, A., Yeung, A.T., Bricka, M.R., 1999. Practical aspects of in-situ electrokinetic extraction. *J. Environ. Eng.* 125, 27–35.
- Arnold, W.A., Roberts, Lynn, 2000. Pathways and kinetics of chlorinated ethylene and chlorinated acetylene reaction with Fe(0) particles. *Environ. Sci. Technol.* 34, 1794–1805.
- Athmer, C.J., 2004. In-situ remediation of TCE in clayey soils. *Soil and sediment contamination* 13, 381–390.
- Athmer, C.J., 2014. Use of large-scale electrokinetic and ZVI treatment for chlorinated solvent remediation at an active industrial facility. *Remediation* 24, 41–51.
- Athmer, C., Ho, S.V., 2009. Field studies: organic - contaminated soil remediation with lasagna technology. In: Reddy, K.R., Cameselle, C. (Eds.), *Electrochemical Remediation Technologies for Polluted Soils, Sediments and Groundwater*. John Wiley & Sons, Inc., Hoboken, New Jersey, pp. 625–646.
- Ballou, E.V., 1955. Electroosmotic flow in homogenic kaolinite. *J. Colloid Sci.* 10 (5), 450–460.
- Bruell, C.J., Segall, B.A., Walsh, M.T., 1992. Electroosmotic removal of gasoline hydrocarbons and TCE from clay. *J. Environ. Eng.* 118, 68–83.
- Camesano, T.A., Logan, B.E., 1998. Influence of fluid velocity and cell concentration on the transport of motile and nonmotile bacteria in porous media. *Environ. Sci. Technol.* 32, 1699–1708.
- Chang, J.H., Cheng, S.-F., 2006. The remediation performance of a specific electrokinetics integrated with zero-valent metals for perchloroethylene contaminated soils. *J. Hazard Mater.* B131, 153–162.
- Chung, H.I., Lee, M.H., 2007. A New Method for Remedial Treatment of Contaminated Clayey Soils by Electrokinetics Coupled with Permeable Reactive Barriers.
- Chang, J.-H., Qiang, Z., Huang, C.-P., 2006. Remediation and stimulation of selected chlorinated organic solvents in unsaturated soil by a specific enhanced electrokinetics. *Colloids Surf. A Physicochem. Eng. Asp.* 287, 86–93.
- Chen, S.S., Huang, Y.-C., Kuo, T.-Y., 2010. The remediation of perchloroethylene contaminated groundwater by nanoscale iron reactive barrier integrated with surfactant and electrokinetics. *Gr. Water Monit. Remediat.* 30, 90–98.
- Cherepy, N.J., Wildenschild, D., 2003. Electrolyte management for effective long-term electro-osmotic transport in low-permeability soils. *Environ. Sci. Technol.* 37, 3024–3030.
- Chowdhury, A.I.A., Gerhard, J.L., Reynolds, D., O'Carroll, D.M., 2017a. Low permeability zone remediation via oxidant delivered by electrokinetics and activated by electrical resistance heating: proof of concept. *Environ. Sci. Technol.* 51, 13295–13303.
- Chowdhury, A.I.A., Gerhard, J.L., Reynolds, D., Sleep, B.E., O'Carroll, D.M., 2017b. Electrokinetic-enhanced permanganate delivery and remediation of contaminated low permeability porous media. *Water Res.* 113, 215–222.
- Cox, E., Gent, D., Singletary, M., Wilson, A., 2018. Electrokinetic-enhanced (EK-Enhanced) Amendment Delivery for Remediation of Low Permeability and Heterogeneous Materials. Department of Defense Environmental Security Technology Certification Program (ESTCP) Project. ER-201325.
- Durante, C., Isse, A.A., Gennaro, A., 2013. Electrocatalytic dechlorination of polychloroethylenes at silver cathode. *J. Appl. Electrochem.* 43, 227–235.
- Da Rocha, U.N., Tótolá, M.R., Pessoa, D.M.M., Júnior, J.T.A., Neves, J.C.L., Borges, A.C., 2009. Mobilisation of bacteria in a fine-grained residual soil by electrophoresis. *J. Hazard Mater.* 161, 485–491.
- DeFlaun, M.F., Condee, C.W., 1997. Electrokinetic transport of bacteria. *J. Hazard Mater.* 55, 263–277.
- Fan, G., Cang, L., Fang, G., Qin, W., Ge, L., Zhou, D., 2014. Electrokinetic delivery of persulfate to remediate PCBs polluted soils: effect of injection spot. *Chemosphere* 117, 410–418.
- Fan, G., Cang, L., Gomes, H., Zhou, D., 2016. Electrokinetic delivery of persulfate to remediate PCBs polluted soils: effect of different activation methods. *Chemosphere* 144, 138–147.
- Fennell, D.E., Gossett, J.M., Zinder, S.H., 1997. Comparison of butyric acid, ethanol, lactic acid, and propionic acid as hydrogen donors for the reductive dechlorination of tetrachloroethene. *Environ. Sci. Technol.* 31, 918–926.
- Gabrieli, L., Alshawabkeh, A.N., 2010. Influence of boundary conditions on transient excess pore pressure during electrokinetic applications in soils. *J. Appl. Electrochem.* 40, 1113–1121.
- Gill, R.T., Harbottle, M.J., Smith, J.W.N., Thornton, S.F., 2014. Electrokinetic-enhanced bioremediation of organic contaminants: a review of processes and environmental applications. *Chemosphere* 107, 31–42.
- Gingine, V., Cardoso, R., 2017. Secondary consolidation of a consolidated kaolin slurry during electrokinetic treatment. *Eng. Geol.* 220, 31–42.
- Gomes, H.I., Dias-Ferreira, C., Ribeiro, A.B., 2012a. Review. Electrokinetic remediation of organochlorides in soil: enhancement techniques and integration with other remediation technologies. *Chemosphere* 87, 1077–1090. Chapter 9.3.
- Gomes, H.I., Dias-Ferreira, C., Ribeiro, A.B., Pamukcu, S., 2012b. Electrokinetic Enhanced Transport of zero valent iron nanoparticles for chromium(VI) reduction in Soils. *Chem. Eng. Trans.* 28, 139–144. Chapter 6.
- Hansen, B.H., Nedergaard, L.W., Ottosen, L.M., Riis, C., Broholm, M.M., 2015. Experimental design for assessment of electrokinetically enhanced delivery of lactate and bacteria in 1,2-cis-dichloroethylene contaminated limestone. *Environ. Technol. Innov.* 4, 73–81.
- Heister, K., Kleingeld, P.J., Keijzer, T.J.S., Loch, J.P.G., 2005. A new laboratory set-up for measurements of electrical, hydraulic, and osmotic fluxes in clays. *Eng. Geol.* 77, 295–303.
- Ho, S.V., Athmer, C., Sheridan, P.W., Shapiro, A., 1997. Scale-up aspects of the Lasagna™ process for in situ soil decontamination. *J. Hazard Mater.* 55, 39–60.
- Ho, S.V., Athmer, C., Sheridan, P.W., Hughes, B.M., Orth, R., McKensie, D., Brodsky, P.H., Shapiro, A., Sivavec, T.M., Salvo, J., Schultz, D., Landis, R., Griffith, R., Shoemaker, S., 1999a. The Lasagna Technology for in situ soil remediation 1. Large field test. *Environ. Sci. Technol.* 33, 1092–1099.
- Ho, S.V., Athmer, C., Sheridan, P.W., Hughes, B.M., Orth, R., McKensie, D., Brodsky, P.H., Shapiro, A., Thornton, R., Salvo, J., Schultz, D., Landis, R., Griffith, R., Shoemaker, S., 1999b. The Lasagna Technology for in situ soil remediation 1. Small field test. *Environ. Sci. Technol.* 33, 1086–1091.
- Hodges, D., Fouire, A., Reynolds, D., Thomas, D., 2011. Development of an apparatus for pH-isolated electrokinetic in situ chemical oxidation. *J. Environ. Eng.* 137, 809–816.
- Hodges, D., Fouire, A., Thomas, D., Reynolds, D., 2013. Overcoming permanganate stalling during electromigration. *J. Environ. Eng.* 139, 677–684.
- Huang, K.-C., Hoag, G.E., Chheda, P., Woody, B.A., Dobbs, G.M., 2001. Oxidation of chlorinated ethenes by potassium permanganate: a kinetics study. *J. Hazard Mater.* B87, 155–169.
- Isosaari, P., Piskonen, R., Ojala, P., Voipio, S., Eilola, K., Lehmus, E., Itävaara, M., 2007. Integration of electrokinetics and chemical oxidation for the remediation of creosote-contaminated clay. *J. Hazard Mater.* 144, 538–548.
- Jackman, S.A., Maini, G., Sharman, A.K., Knowles, C.J., 1999. The effects of direct electric current on the viability and metabolism of acidophilic bacteria. *Enzym. Microb. Technol.* 24, 316–324.
- Jones, E.H., Reynolds, D.A., Wood, A.L., Thomas, D.G., 2011. Use of electrophoresis for transporting nano-iron in porous media. *Gr. Water* 49, 172–183.
- Kästner, M., July 1991. Reductive dechlorination of Tri- and tetrachloroethylenes depends on transition from aerobic to anaerobic conditions. *Appl. Environ. Microbiol.* 2039–2046.
- Lageman, R., Godschalk, M.S., 2007. Electro-bioreclamation. A combination of in situ remediation techniques proves successful at a site in Zeist, The Netherlands. *Electrochim. Acta* 52, 3449–3453.
- Lear, G., Harbottle, M.J., van der Gast, C.J., Jackman, S.A., Knowles, C.J., Sills, G., Thompson, I.P., 2005. The effect of electrokinetics on soil microbial communities. *Soil Biol. Biochem.* 36, 1751–1760.
- Lee, H.-S., Lee, K., 2001. Bioremediation of diesel-contaminated soil by bacterial cells transported by electrokinetics. *J. Microbiol. Biotechnol.* 11, 1038–1045.
- Lee, P.K.H., Cheng, D., West, K.A., Alvarez-Cohen, L., He, J., 2013. Isolation of two new Dehalococcoides mccartyi strains with dissimilar dechlorination functions and their characterization by comparative genomics via microarray analysis. *Environ. Microbiol.* 15, 2293–2305.
- Liang, C.J., Bruell, C.J., Marley, M.C., Sperry, K.L., 2003. Thermally activated persulfate oxidation of trichloroethylene (TCE) and 1,1,1-trichloroethane (TCA) in aqueous systems and soil slurries. *Soil Sediment Contam.* 12, 207–228.
- Lima, A.T., Hofmann, A., Reynolds, D.R., Ptacek, C.J., Van Cappellen, P., Ottosen, L.M., Pamukcu, S., Alshawabkeh, A., O'Carroll, D.M., Riis, C., Cox, E., Gent, D.B., Landis, R., Wang, J., Chowdhury, A.I.A., Secord, E.L., Sanchez-Hachair, A., 2017. Environmental Electrokinetics for a sustainable subsurface. *Chemosphere* 181, 122–133.
- Mao, X., Wang, J., Cibla, A., Cox, E.E., Riis, C., Terkelsen, M., Gent, D.B., Alshawabkeh, A.N., 2012. Electrokinetic-enhanced bioaugmentation for remediation of chlorinated solvents contaminated clay. *J. Hazard Mater.* 213–214, 311–317.
- Marry, V., Duffreche, J.F., Jardat, M., Meriguet, G., Turq, P., Grun, F., 2003. Dynamics and transport in charged porous media. *Colloid. Surf. Physicochem. Eng. Asp.* 222, 147–153.
- Matzek, L.W., Carter, K.E., 2016. Activated persulfate for organic chemical degradation: a review. *Chemosphere* 151, 178–188.
- Middeldorp, P.J.M., Luijten, M.L.G.C., van de Pas, B.A., van Eekert, M.H.A., Kengen, S.W.M., Schraa, G., Stams, A.J.M., 1999. Anaerobic microbial reductive dehalogenation of chlorinated ethenes. *Bioremed. J.* 3, 151–169.
- Maymó-Gatell, X., Chien, Y.T., Gossett, J.M., Zinder, S.H., 1997. Isolation of a bacterium that reductively dechlorinates tetrachloroethene to ethene. *Science* 276, 1568–1571.
- Mikkola, H., Schmale, J.Y., Wesner, W., Petkovska, S., 2008. Laboratory pre-assays for soil remediation by electro synthesis of oxidants and their electrokinetic distribution. *J. Environ. Sci. Health A* 43, 907–912.
- Mitchell, J.K., 1993. *Fundamentals of Soil Behavior*, second ed. John Wiley & Sons,

- New York, USA.
- Moon, J.-W., Moon, H.-S., Kim, H., Roh, Y., 2005. Remediation of TCE-contaminated groundwater using zero valent iron and direct current: experimental results and electron competition model. *J. Environ. Geol.* 48, 805–817.
- Mumford, K.G., Thomson, N.R., Allen-King, R.M., 2005. Bench-scale investigation of permanganate natural oxidant demand kinetics. *Environ. Sci. Technol.* 39, 2835–2840.
- Ninjarav, E., Chung, S.-G., Jang, W.-Y., Ryu, C.-K., 2007. Pore size distribution of Pusan clay measured by mercury intrusion porosimetry. *Ksce J. Civil Eng.* 11, 133–139.
- Obiri-Nyarko, F., Grajales-Mesa, S.J., Malina, G., 2014. An overview of permeable reactive barriers for in situ sustainable groundwater remediation. *Chemosphere* 111, 243–259.
- Pamukcu, S., Hannum, L., Wittle, J.K., 2008. Delivery and activation of nano-iron by DC electric field. *J. Environ. Sci. Health A* 43, 934–944.
- Pires, L.F., Borges, F.S., Passoni, S., Pereira, A.B., 2013. Soil pore characterization using free software and a portable optical microscope. *Pedosphere* 23 (4), 503–510.
- Park, S.-M., Lee, S.-W., Jeon, P.-Y., Baek, K., 2016. Iron anode-mediated activation of persulfate. *Water Air Soil Pollut.* 227, 462.
- Pengra, D.B., Wong, P.Z., 1996. Electrokinetic phenomena in porous media. *Mater. Res. Soc. Symp. Proc.* 407, 3–14.
- Rabbi, M., Clark, B., Gale, R.J., Ozsu-Acar, E., Pardue, J., Jackson, A., 2000. In situ TCE bioremediation study using electrokinetic cometabolite injection. *Waste Manag.* 20, 279–286.
- Roberts, A.L., Totten, L.A., Arnold, W.A., Burris, D.R., Campell, T.J., 1996. Reductive elimination of chlorinated ethylenes by zero-valent metals. *Environ. Sci. Technol.* 31, 2654–2659.
- Reddy, K.R., Cameselle, C., 2009. Overview of electrochemical remediation technologies. In: Reddy, K.R., Cameselle, C. (Eds.), *Electrochemical Remediation Technologies for Polluted Soils, Sediments and Groundwater*. John Wiley & Sons, Inc., pp. 3–28.
- Rowlands, D., 2004. Development of Optimal pH for Degradation of Chlorinated Solvents by the KB-1TM Anaerobic Bacterial Culture. PhD Thesis. University of Guelph, Guelph, Ontario, Canada.
- Reddy, K.R., Darko-Kagy, K., Cameselle, C., 2011. Electrokinetic-enhanced transport of lactate-modified nanoscale iron particles for degradation of dinitrotoluene in clayey soils. *Separ. Purif. Technol.* 79, 230–237.
- Reynolds, D.A., Jones, E.H., Gillen, M., Yusoff, I., Thomas, D.G., 2008. Electrokinetic migration of permanganate through low-permeability media. *Gr. Water* 46, 629–637.
- Roach, N., Reddy, K.R., 2006. Electrokinetic delivery of permanganate into low-permeable soils. *Int. J. Environ. Waste Manag.* 1, 4–19.
- Semple, K.T., Doick, K.J., Jones, K.C., Buraue, P., Craven, A., Harms, H., 2004. Defining bioavailability and bioaccessibility of contaminated soil and sediment is complicated. *Environ. Sci. Technol.* 38, 228A–231A.
- Shi, L., Mueller, S., Harms, H., Wick, L.Y., 2008a. Effect of electrokinetic transport on the vulnerability of PAH-degrading bacteria in a model aquifer. *Environ. Geochem. Hlth.* 30, 177–182.
- Scheutz, C., Durant, N.D., Dennis, P., Hansen, M.H., Jørgensen, T., Jakobsen, R., Cox, E., Bjerg, P.L., 2008. Concurrent ethene generation and growth of dehalococcoides containing vinyl chloride reductive dehalogenase genes during an enhanced reductive dechlorination field demonstration. *Environ. Sci. Technol.* 42, 9302–9309.
- Shi, L., Mueller, S., Harms, H., Wick, L.Y., 2008b. Factors influencing the electrokinetic dispersion of PAH-degrading bacteria in a laboratory model aquifer. *Appl. Microbiol. Biotechnol.* 80, 507–515.
- Schroth, M.H., Oostrom, M., Wietsma, T.W., Istok, J.D., 2001. In-situ oxidation of trichloroethene by permanganate: effects on porous medium hydraulic properties. *J. Contam. Hydrol.* 50, 79–98.
- Siegrist, R.L., Crimi, M., Thomson, N.R., Clayton, W.S., Marley, M.C., 2014. In situ chemical oxidation. In: Kueper, B.H., Stroo, H.F., Vogel, C.M., Ward, C.H. (Eds.), *Chlorinated Solvent Source Zone Remediation*, pp. 253–305. Serdp/estcp Environmental Remediation Technology book series 7.
- Tsai, P., Huang, C.-H., Lee, E., 2011. Electrophoresis of a charged colloidal particle in porous media: boundary effect of a solid plane. *Langmuir* 27, 13481–13488.
- van der Wal, A., Minor, M., Norde, W., Zehnder, A.J.B., Lyklema, J., 1997. Electrokinetic potential of bacterial cells. *Langmuir* 13, 165–171.
- van der Zaan, B., Hannes, F., Hoekstra, N., Rijnaarts, H., de Vos, V.M., Smidt, H., Gerritse, J., 2010. Correlation of dehalococcoides 16S rRNA and chloroethene-reductive dehalogenase genes with geochemical conditions in chloroethene-contaminated groundwater. *Appl. Environ. Microbiol.* 76, 843–850.
- Vogel, T.M., Criddle, C.S., McCarty, P.L., 1987. ES Critical Reviews: transformations of halogenated aliphatic compounds. *Environ. Sci. Technol.* 21, 722–736.
- Weng, C.H., 2009. Coupled electrokinetic-permeable reactive barriers. In: Reddy, K.R., Cameselle, C. (Eds.), *Electrochemical Remediation Technologies for Polluted Soils, Sediments and Groundwater*. John Wiley & Sons, Inc., Hoboken, New Jersey, pp. 483–504.
- Weng, C.-H., Yuan, C., Tu, H.-H., 2003. Removal of trichloroethylene from clay soil by series-electrokinetic process. *Pract. Period. Hazard. Toxic. Radioact. Waste Manag.* 7, 25–30.
- West, L.J., Stewart, D.I., Binley, A.M., Shaw, B., 1999. Resistivity imaging of soil during electrokinetic transport. *Eng. Geol.* 53, 205–215.
- Wick, L.Y., Mattle, P.A., Wattiau, P., Harms, H., 2004. Electrokinetic transport of PAH-degrading bacteria in model aquifers and soil. *Environ. Sci. Technol.* 38, 4596–4602.
- Wick, L.Y., Shi, L., Harms, H., 2007. Electro-bioremediation of hydrophobic organic soil-contaminants: a review of fundamental interactions. *Electrochim. Acta* 52, 3441–3448.
- Wu, X., Alshawabkeh, A.N., Gent, D.B., Larson, S.L., Davis, J.L., 2007. Lactate transport in soil by DC fields. *J. Geotech. Geoenviron.* 133, 1587–1596.
- Wu, M.Z., Reynolds, D., Fourie, A., Prommer, H., Thomas, D.G., 2012a. Electrokinetic in situ oxidation remediation: assessment of parameter sensitivities and the influence of aquifer heterogeneity on remediation efficiency. *J. Contam. Hydrol.* 136, 72–85.
- Wu, X., Gent, D.B., Davis, J.L., Alshawabkeh, A.N., 2012b. Lactate injection by electric currents for bioremediation of tetrachloroethylene in clay. *Electrochim. Acta* 86, 157–163.
- Wu, M.Z., Reynolds, D.A., Fourie, A., Thomas, D.G., 2013. Optimal field approaches for electrokinetic in situ oxidation remediation. *Gr. Water Monit. Remediat.* 33, 62–74.
- Yang, G.C.C., Yeh, C.-F., 2011. Enhanced nano-Fe₃O₄/S₂O₈²⁻ oxidation of trichloroethylene in a clayey soil by electrokinetics. *Separ. Purif. Technol.* 79, 264–271.
- Yang, Y., Capiro, N.L., Yan, J., Marcet, T.F., Pennell, K.D., Löffler, F.E., 2017. Resilience and recovery of Dehalococcoides mccartyi following low pH exposure. *FEMS Microbiol. Ecol.* 93 (1–9), fix130.
- Yukselen-Aksoy, Y., Reddy, K.R., 2012. Effect of soil composition on electrokinetically enhanced persulfate oxidation of polychlorobiphenyls. *Electrochim. Acta* 86, 164–169.
- Zhang, H., Ulrich, A.C., Liu, Y., 2015. Retention and transport of an anaerobic trichloroethene dechlorinating microbial culture in anaerobic porous media. *Colloids Surf., B* 130, 110–118.
- Zhao, Y., Zhao, Y., Li, Q., Zhou, R., Chen, X., 2016. Effect of common inorganic ions on aniline degradation in groundwater by activated persulfate with ferrous iron. *Water Sci. Technol.* 16, 667–674.

APPENDIX IV

Transformation of tetrachloroethylene in a flow-through electrochemical reactor

Hyldegaard, B.H., Ottosen, L.M. & Alshawabkeh, A.N.

(Published in Science of the Total Environment, 2019)



Contents lists available at ScienceDirect

Science of the Total Environment

journal homepage: www.elsevier.com/locate/scitotenv

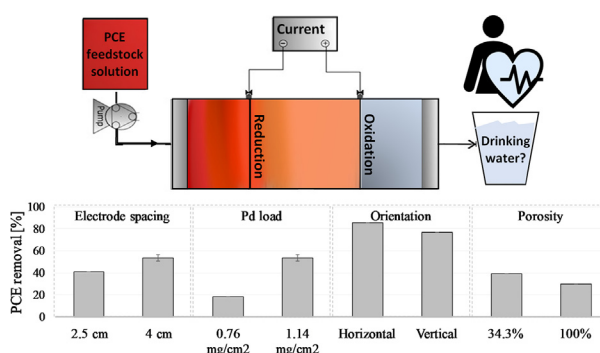
Transformation of tetrachloroethylene in a flow-through electrochemical reactor

Bente H. Hyldegaard^{a,b,c,*}, Lisbeth M. Ottosen^b, Akram N. Alshawabkeh^c^a Department of Waste & Contaminated Sites, COWI, Parallelsvej 2, 2800 Kgs. Lyngby, Denmark^b Department of Civil Engineering, Brovej, Building 118, Technical University of Denmark, 2800 Kgs. Lyngby, Denmark^c Department of Civil & Environmental Engineering, 501 Stearns, 360 Huntington Avenue, Boston, MA 02115, United States of America

HIGHLIGHTS

- Harmful chlorinated ethenes threaten the drinking water resource and its consumers.
- Transformation of PCE in electrochemical flow-through reactors was studied.
- Influence of various reactor design parameters was investigated, reaching 86% removal.
- Normalization of data improved understanding of mechanisms across tests and studies.
- Electrochemical reduction and oxidation can reduce mass flux of simulated PCE plumes.

GRAPHICAL ABSTRACT



ARTICLE INFO

Article history:

Received 18 July 2019

Received in revised form 4 November 2019

Accepted 15 November 2019

Available online xxxx

Editor: Renato Baciocchi

Keywords:

Chlorinated ethenes
Removal
Groundwater
Electrochemistry
Design screening

ABSTRACT

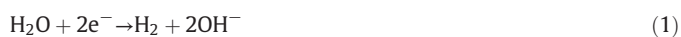
Electrochemical transformation of harmful tetrachloroethylene (PCE) is evaluated as a method for management of groundwater plumes to protect the drinking water resource, its consumers and the environment. In contrast to previous work that reported transformation of trichloroethylene, a byproduct of PCE, this work focuses on transformation of PCE in a saturated porous matrix and the influence of design parameters on the removal performance. Design parameters investigated were electrode configuration, catalyst load, electrode spacing, current intensity, orientation of reactor and flow through a porous matrix. A removal of 86% was reached in the fully liquid-filled, horizontally oriented reactor at a current of 120 mA across a cathode → bipolar electrode → anode arrangement with a Darcy velocity of 0.03 cm/min (150 m/yr). The palladium load on the cathode significantly influenced the removal. Enhanced removal was observed with increased electrode spacing. Presence of an inert porous matrix improved PCE removal by 9%-point compared to a completely liquid-filled reactor. Normalization of the data indicated, that a higher charge transfer per contaminant mass is required for removal of low PCE concentrations. No chlorinated intermediates were formed. The results suggest, that PCE can be electrochemically transformed in reactor designs replicating that of a potential field-implementation. Further work is required to better understand the reduction and oxidation processes established and the parameters influencing such. This knowledge is essential for optimization towards testing in complex conditions and variations of contaminated sites.

© 2019 Elsevier B.V. All rights reserved.

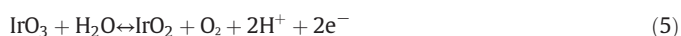
* Corresponding author at: Department of Waste & Contaminated Sites, COWI, Parallelsvej 2, 2800 Kgs. Lyngby, Denmark.
E-mail address: behd@cowi.com (B.H. Hyldegaard).

2. Introduction

Chlorinated ethenes have been unintentionally introduced to the environment causing extensive and harmful contamination of the sub-surface, potentially impacting the groundwater and indoor air quality (Pankow et al., 1996; Ruder, 2006). Effort has been put into remediation of low-permeable zones, where use of electrokinetics has shown to overcome some of the challenges faced (Alshawabkeh, 2009; Lima et al., 2017; Reddy and Cameselle, 2009; Ribeiro et al., 2016; Stroo and Ward, 2010). However, the dense chlorinated ethenes slowly leak into aquifers, causing an increase in detection above regulatory maximum contaminant levels (Moran et al., 2007). Current remedies used for chlorinated ethene plumes include pump-and-treat (Mackay and Cherry, 1989; Interstate Technology and Regulatory Council, 2011), enhanced reductive dechlorination (Pankow et al., 1996; Interstate Technology and Regulatory Council, 2011), in-situ chemical oxidation (Kueper et al., 2014; Siegrist et al., 2012), permeable reactive barriers (Interstate Technology and Regulatory Council, 2005; He et al., 2015) and air-sparging (Bass et al., 2000; Stenzel and Gupta, 1985). These technologies can be challenged by inadequate delivery of reactants (Siegrist et al., 2012; Stroo et al., 2012; Scheutz et al., 2010), short longevity of reactants (Siegrist et al., 2012; Aulenta et al., 2007; O'Connor et al., 2018) or varying contaminant phase transfer affinities with generation of contaminated waste (Stenzel and Gupta, 1985; Urano et al., 1991). Challenges, which may be overcome by adaptation of the mechanisms of electrokinetics towards mass flux reduction in these high-permeable zones by establishment of electrochemical zones. This is gaining increasing focus, since reducing and oxidizing zones sufficient for degradation of the chlorinated ethenes can be established (Mao et al., 2011; Mao et al., 2012a; Mao et al., 2012b; Fallgren et al., 2018). The reducing zone is generated from electrolysis at the cathode (Eq. (1)) (Acar and Alshawabkeh, 1993; Zheng et al., 2012), which can directly and indirectly reduce the parent components tetrachloroethylene (PCE) and trichloroethylene (TCE) and stimulate microbial degradation (Aulenta et al., 2011; Verdini et al., 2015; Lohner et al., 2011; Aulenta et al., 2013). In addition, hydrogen peroxide (H_2O_2), which is a strong oxidant that can break down the chlorinated ethenes (Yuan et al., 2013a; Zhou et al., 2018), can be effectively formed (Eq. (2)) at a sufficiently high dissolved oxygen concentration, or if a catalyst like palladium (Pd) is applied to the cathode. Furthermore, Pd can catalyze formation of $\bullet\text{OH}$ radicals (Eq. (3)), which also oxidize the chlorinated ethenes (Rajic et al., 2016a).



The anode generates oxidizing conditions (Eq. (4)) (Acar and Alshawabkeh, 1993), specifically by Ti/IrO₂-Ta₂O₅ mixed metal oxide (MMO) anodes (Eq. (5)) (Lakshmipathiraj et al., 2012), which can oxidize e.g. TCE and the chlorinated intermediates dichloroethylene (DCE) and vinyl chloride (VC). However, the oxygen evolution competes with oxidation of the chlorinated ethenes.



Research on electrochemical removal of chlorinated ethenes has focused on TCE (Mao et al., 2011; Mao et al., 2012a; Mao et al., 2012b; Aulenta et al., 2011; Yuan et al., 2013a; Rajic et al., 2016a; Lakshmipathiraj et al., 2012; Liu et al., 2018; Yuan et al., 2012; Xie et al., 2013; Petersen et al., 2007; Fallahpour et al., 2016; Rajic et al., 2015a; Rajic et al., 2016b; Rajic et al., 2015b; Rajic et al., 2014). Since TCE is more volatile than PCE, mass balances of TCE can be particularly

poor. Also, the reported optimal design parameters are dependent on the specific system studied, and little knowledge is available on the specific mechanisms responsible for degradation of PCE and TCE in flow-through electrochemical reactors. This makes it complex to adapt the current level of knowledge on electrochemical removal of TCE towards complete removal of PCE. The reduction mechanisms have been investigated on iron metal (Fe(0)) surfaces, showing higher dechlorination rates with increased halogenation (Gillham and O'Hannesin, 1994; Johnson et al., 1996; Scherer et al., 1998), but also the opposite trend (Butler and Hayes, 1999; Arnold and Roberts, 2000; Kim and Carraway, 2003). Arnold and Roberts (Arnold and Roberts, 2000) found, that 87% of PCE and 97% of TCE follow direct reduction on Fe(0), i.e. contact between the surface of Fe(0) and the chlorinated ethene is essential. During direct reduction on Fe(0) surfaces, the reaction rate constant for PCE is higher than that for TCE (Farrell et al., 2000). While during indirect reduction via atomic hydrogen formed from electrolysis (Eq. (1)) (Farrell et al., 2000), the reaction rate constant for PCE is lower than that for TCE. Thus, a smaller fraction of PCE than TCE follows the direct reduction pathway, but reaction kinetics is faster during direct reduction of PCE than TCE. The rate limiting steps for direct and indirect reduction are chemisorption onto the electrode, electron transfer, bond-breaking or molecular rearrangement (Li and Farrell, 2001).

Competing reactions, due to presence of ionic species in the electrolyte, can interfere with the chemical mechanisms responsible for removal of the chlorinated ethenes, which may be non-linearly distributed, and time and space dependent. This may explain observed variations over time, the course of reactors and between batch and column set-ups (Farrell et al., 2000; Wüst et al., 1999). In addition, electrode compositions and impurities influence the reduction processes (Arnold and Roberts, 2000; Su and Puls, 1999; Rajic et al., 2015c). For development of flexible full-scale remediation designs that can overcome the complexity and variations of contaminated sites, improved understanding of the transformation mechanisms and parameters controlling those is essential.

The objective of this study is to examine the influence of reactor design on the electrochemical removal of PCE in a flow-through reactor using palladized Fe foam cathodes and MMO anodes. The study is a screening of the significance of parameters relevant to a field design on the electrochemical PCE removal performance, e.g. a porous matrix and horizontal orientation. Such knowledge is required for development of a more robust test design for enhanced applicability and feasibility testing at conditions simulating that of potential in-situ applications. Previous work has studied electrochemical removal of mainly TCE in static reactors (Yuan et al., 2012; Yuan et al., 2013b), stirred reactors (Mao et al., 2011; Sáez et al., 2009), recirculated reactors (Mao et al., 2012a; Lakshmipathiraj et al., 2012; Fallahpour et al., 2016), vertical flow-through reactors (Mao et al., 2012b; Rajic et al., 2016a; Rajic et al., 2015a; Rajic et al., 2016b; Rajic et al., 2015b; Rajic et al., 2014; Yuan et al., 2013b; Fallahpour et al., 2017), applied constant voltage (Petersen et al., 2007; Scialdone et al., 2010; Li and Farrell, 2000) or studied electrochemistry in combination with other remediation strategies, e.g. bioremediation (Verdini et al., 2015; Tiehm et al., 2009; Aulenta et al., 2009; Aulenta et al., 2010; Lai et al., 2015). Assessment of the potential of flow-through electrochemical transformation of PCE is important to cover the full range of chlorinated ethene species detected at contaminated sites. This study differs from previous work by studying the electrochemical removal of PCE in horizontally oriented undivided reactors with flow through a porous matrix and operated at constant current. Studying such a reactor design is a necessary step towards upscaling of electrochemical remediation for treatment of contaminated groundwater. In the field, the primary groundwater flow direction is horizontal, flow is through a porous matrix, and the charge transfer is best controlled with application of constant current.

2. Materials and methods

2.1. Chemicals and materials

Chemicals used were of analytical grade: PCE (99%, Sigma-Aldrich), TCE (99.5%, Sigma-Aldrich), cis-DCE (97%, Sigma-Aldrich), calcium sulfate (JT Baker), hydrochloric acid (HCl) (37%, Carolina) and palladium (II) chloride (PdCl_2 , 99.9%, Alfa Aesar). MMO meshes (1.8 mm in width, 3 N International), composed of IrO_2 and Ta_2O_5 coating on titanium were used as bipolar electrodes (BPE) and anodes. Cathodes of Fe foam (3 mm in width, 45 pores per inch, 98% Fe, 2% Ni, Aibixi Ltd.) and/or 316 stainless steel discs (SS, 0.7 mm in width, 0.4 mm wire diameter, 20 × 20 mesh size, 0.86 mm opening size, 12% Ni, McMaster-Carr) were used. The diameter of electrodes used was 77 mm. The 316 SS cathode was assembled using four discs to increase the width. Fe foam cathodes were perforated with 4 mm holes for every 10 mm and coated with Pd. Prior to electroless plating with Pd, the Fe foam was rinsed in 1 M HCl for 10 min, thoroughly washed in deionized water, submerged in a solution of 0.1 M HCl and PdCl_2 , rotated until the orange solution turned colorless and washed with deionized water (Rajic et al., 2015a; Rajic et al., 2016b). Solid glass beads (5 mm, 2.23 g/cm³) were purchased from Propper Manufacturing Co. Inc. Nylon meshes (0.1 mm in width, 0.12 mm wire diameter, 61 × 61 mesh size, 0.3 mm opening size, McMaster-Carr) were mounted on each side of the electrodes to prevent glass beads in blocking openings of the electrode meshes. Feedstock solutions were stored in Tedlar® bags (Sigma-Aldrich) and prepared using 18.2 MΩcm high-purity water from a Millipore Milli-Q system. Tygon® tubing (2.06 mm ID, 3.79 mm OD, Cole-Parmer) and a peristaltic pump (0.4–85 ml/min, Cole-Parmer), were used to control the flow of liquid. Constant current was applied using one Agilent E3612A 0–120V, 0–0.25 A power supply.

2.2. Analytical methods

Concentrations of PCE, TCE and cis-DCE were measured in 2 ml samples by an Agilent 1200 Infinity Series HPLC with a 1260 DAD detector and a Thermo ODS Hypersil C18 column (4.6 × 50 mm) as described in Rajic et al. (Rajic et al., 2015a). Release of Pd ions was analyzed using a Varian ICP-EOS 720-ES. Samples were filtrated prior to analysis using 0.2 μm PVDF syringe filters from Jin Teng. Conductivity of the feedstock solutions was measured using a Thermo Orion 5 Star meter with corresponding probe. pH of the feedstock solutions was measured using a Mettler Toledo Seven Compact meter with corresponding probe. pH of samples collected from sampling ports was assessed using EMD Millipore™ MColorpHast™ pH test strips.

2.3. Electrochemical flow-through reactor

Synthetic groundwater simulating the conductivity of a sandy aquifer was prepared by dissolving 1600 mg/l calcium sulfate in deionized water. Calcium sulfate was used instead of calcium carbonate to limit the influence of the carbonate system on the electrochemical mechanisms and pH gradients established (Hyldegaard et al., 2019). The resulting conductivity was 700–890 μS/cm with a pH of 5.7 ± 0.4 and a constant temperature of 20 °C. The synthetic groundwater was spiked with PCE to a concentration of 2.7 mg/l. A saturated stock solution of free-phase PCE in deionized water was used. The feedstock solution was stored in Tedlar® bags with minimal headspace to limit mass loss by volatilization. Flow through the reactor was kept constant at velocities reported in Table 1.

An acrylic column was used as the flow-through electrochemical reactor (L 16.8 cm and D 7.8 cm in inner dimensions). The influence of reactor design on electrochemical removal of PCE was investigated in a sequence of a) electrode configurations and spacings. For three-electrode configurations, the constant current was split equally between the two cathodes by a rheostat, b) current intensities and Pd catalyst loadings, c) porous matrices and reactor orientations. The inert porous matrix was incorporated to replicate field-conditions and to reduce amount of contaminated waste generated, and d) groundwater flow and test duration (Table 1).

The position of electrodes and sampling ports (P0–P5) in the electrochemical reactor is shown in Fig. 1. In horizontally orientated reactors, electrolytically generated gases were extracted manually from sampling ports above the electrodes using syringes with needles. To limit mass loss by volatilization, the gas extraction occurred whenever a gas phase was observed. The frequency of this manual venting depended on current intensity, electrode configuration and electrode material with a range of once every 30–90 s. In vertically oriented reactors, released gases moved up through the reactor and out with the effluent.

Prior to the electrochemical application, the reactor was saturated with the feedstock solution at elevated flow to limit volatilization, followed by flow-through for one pore volume (PV) at the flow velocities given in Table 1 to ensure a uniform contaminant distribution. Direct current was applied for 3.5 PV and 1.2 PV for flow through the porous matrix (Table 1, test 1–5, 8–10) and completely liquid-filled reactor (Table 1, test 6–7, 11–12), respectively.

3. Results and discussion

Different designs of the electrochemical reactor were tested. To evaluate the influence of a design parameters on the PCE removal, each

Table 1
Experimental conditions for the electrochemical treatment of initially 2.7 mg/l PCE.

	Electrode configuration ^a	Electrode material	Electrode spacing [cm]	Column orientation	Current [mA]	Pd catalyst loading ^b [mg/cm ²]	Darcy velocity [cm/min]	Porosity, water-filled ^c [%]
0 ^d	C→BPE→A	Fe foam→MMO→MMO	4	Horizontal	0	0.76	0.09	31.1 ± 0.3
1	C→BPE→A	Fe foam→MMO→MMO	4	Horizontal	60	0.76	0.09	30.8
2	C→BPE→A	Fe foam→MMO→MMO	4	Horizontal	120	0.76	0.09	30.8
3 ^d	C→BPE→A	Fe foam→MMO→MMO	4	Horizontal	120	1.14	0.08	34.8 ± 0.5
4	C→BPE→A	Fe foam→MMO→MMO	4	Horizontal	180	1.14	0.08	35.3
5	C→BPE→A	Fe foam→MMO→MMO	2.5	Horizontal	120	1.14	0.08	34.1
6	C→BPE→A	Fe foam→MMO→MMO	4	Horizontal	120	1.14	0.03	100
7	C→BPE→A	Fe foam→MMO→MMO	4	Vertical	120	1.14	0.03	100
8	C→C→A	SS→Fe foam→MMO	4	Horizontal	120	1.14	0.08	34.2
9	C→C→A	Fe foam→Fe foam→MMO	4	Horizontal	120	1.14	0.08	35.0
10	C→A	Fe foam→MMO	8	Horizontal	120	1.14	0.08	34.3
11	C→A	Fe foam→MMO	2.5	Horizontal	120	1.14	0.25	100
12	C→A	Fe foam→MMO	2.5	Vertical	120	1.14	0.25	100

^a A: anode, C: cathode, BPE: bipolar electrode.

^b Catalyst applied on Fe foam only. Load is given as mass per geometric electrode surface area.

^c Porosities of 100% indicate a fully liquid-filled reactor, while tests with porosities <100% incorporate the porous matrix.

^d Duplicate testing.

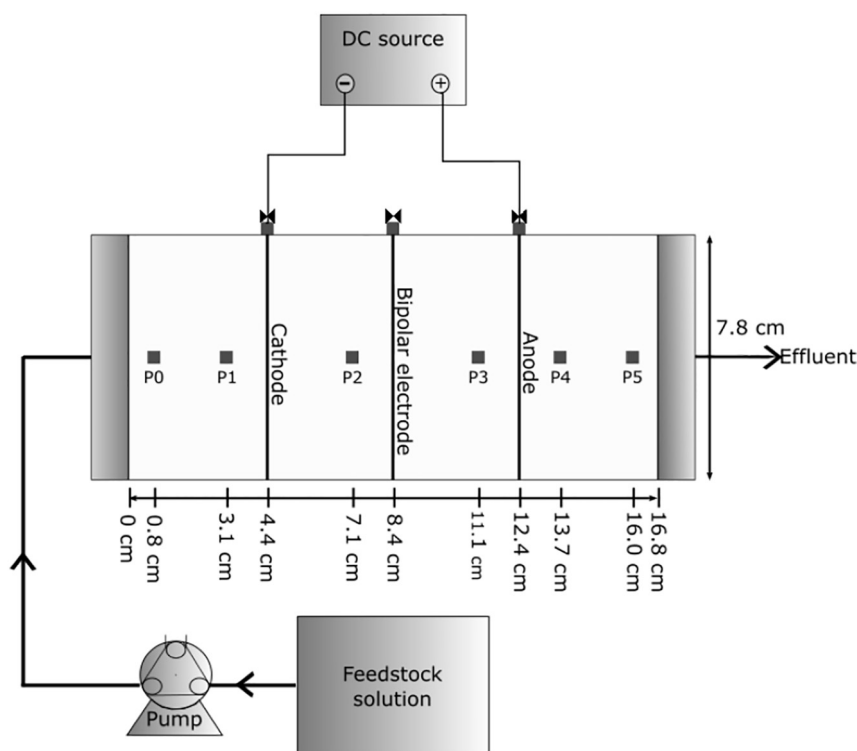


Fig. 1. The baseline flow-through electrochemical set-up composed of a feedstock solution, peristaltic pump, a cathode, bipolar electrode and an anode connected to a power supply. P0-P5 are sampling ports. Sampling ports above the electrodes served for manual extraction of gases generated. Measures are of inner dimensions.

experiment conducted is compared to similar ones of which one parameter varied only. Accordingly, the significance of electrode spacing, electrode configuration, current intensity, Pd loading on the cathode, duration of electrochemical treatment, orientation of reactor and porosity on PCE removal, potential difference over the electrodes and pH downstream of the electrochemical zone is assessable (Fig. 2). The design parameter category, e.g. electrode spacing, is indicated above comparable experiments, whereas the specific dimension of that design parameter, e.g. 2.5 cm and 4 cm, is given on the horizontal axis. Figures written on the bars refer to the experimental numbers given in Table 1.

3.1. Impact of electrode configuration and spacing on PCE removal

Influence of electrode configuration and spacing on electrochemical removal of PCE was investigated in the flow-through reactor with Fe and MMO electrodes at 120 mA and a Darcy velocity of 0.08 cm/min (experiments 3, 5, 8–10, Fig. 2a, Table 1).

A three-electrode configuration of two Pd coated Fe foam cathodes and an MMO anode performed similar to the corresponding two-electrode configuration, reaching removals of 42% and 39%, respectively (exp. 9–10, Fig. 2a). Rajic et al. (Rajic et al., 2015a) also observed comparable removals of TCE in two- and three-electrode configured reactors using Fe and MMO electrodes, while the reaction rate nearly doubled in the three-electrode arrangement. By replacing the first Pd/Fe foam cathode with 316 SS, the removal increased to 51% (exp. 8, Fig. 2a). The high content of Ni in this type of stainless steel can catalyze reduction, since Ni like Pd lowers the cathodic hydrogen overpotential (Rajic et al., 2015c; Brewster, 1954), enhancing the hydrodechlorination. Use of Ni-containing stainless steels for electrochemical removal of chlorinated ethenes has shown to be cost-efficient (Rajic et al., 2015c). The best performing electrode configuration was C → BPE → A with a removal of $54 \pm 3\%$ (exp. 3, Fig. 2a). By introducing a BPE, a supplementary oxidizing-reducing zone is established, enhancing the hydrodechlorination and oxidation by increased formation of H_2O_2

(Eq. (2)) (Rajic et al., 2016a). Of the electrode configurations and materials tested, the lowest potential difference of 17 V was obtained in the 316 SS → Pd/Fe → MMO arrangement, and the highest potential difference of 36 V in the Pd/Fe → MMO reactor (exp. 8 and 10, Fig. 2b). The BPE lowered the potential difference from 36 V to 32 V (exp. 3 and 10, Fig. 2b); a simple measure to potentially reduce the costs of power consumption in upscaling activities.

Increasing the electrode spacing from 2.5 cm to 4 cm in the C → BPE → A arrangement improved the PCE removal from 41% to $54 \pm 3\%$ (exp. 3 and 5, Fig. 2a). This is opposite to previous findings in completely liquid-filled reactors, where the observed decrease in removal with an increase in electrode spacing was explained by a resulting increase in potential difference over the reactor (Rajic et al., 2015a). In this study, the potential difference also increased, from 22 V to 31.6 ± 0.4 V (exp. 3 and 5, Fig. 2b), and thereby the resistivity of the system (Chen, 2004), but the increase did not inhibit the removal as previously shown for TCE (Rajic et al., 2015a; Ghosh et al., 2008). By increasing the electrode spacing, the redox zone is prolonged, which possibly accounts for the increased PCE removal. Considering upscaling, this can reduce the direct costs for the plant due to a cutback in the network of electrodes.

pH measured in the porewater downgradient the electrochemical zone (sampling port P5) was 4.5–5 in the C → C → A and C → A configurations tested (exp. 8–10, Fig. 2c). For C → BPE → A, pH was 8.5 ± 1.5 (exp. 3, Fig. 2c). The elevated pH in the latter configuration could be due to enhanced H_2O_2 formation when introducing a BPE: free oxygen and hydrogen ions generated at anodic sites (Eq. (4)) are consumed at adjacent cathodic sites (Eq. (2)), i.e. the acidic gradient is weakened and incapable of neutralizing the alkaline gradient established at cathodic sites. BPEs have shown to significantly assist in H_2O_2 formation in electrochemical flow-through reactors (Rajic et al., 2016a). For comparison, pH in the control experiment without applied current was 7 (exp. 0, Fig. 2c).

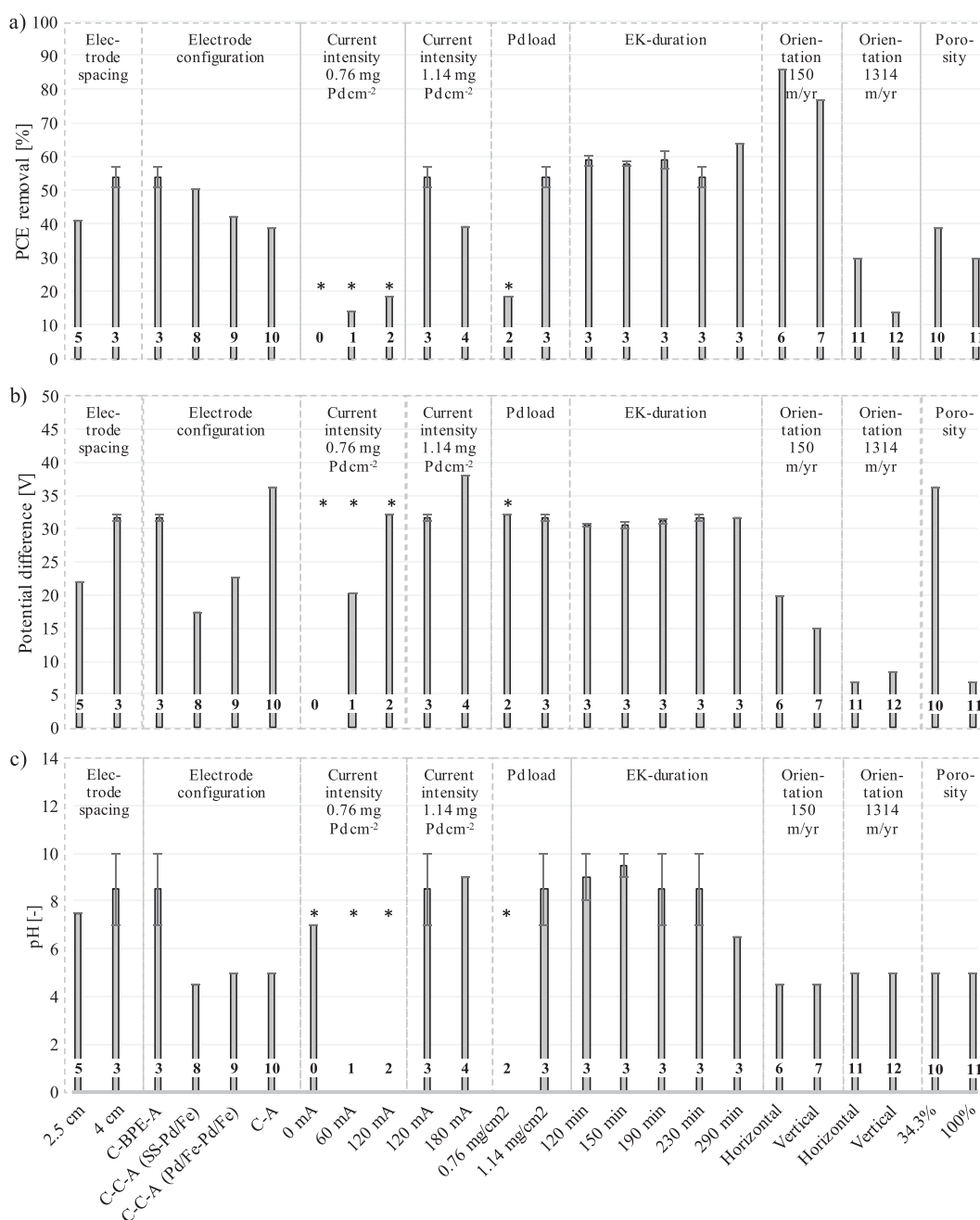


Fig. 2. Comparison of the experimental conditions tested on a) PCE removal obtained in sampling port P5, b) potential difference over the reactor measured after app. 1 PV (was rather constant), and c) pH measured in sampling port P5. Error bars are included for duplicate testing. * denotes direct reuse of the experimental set-up. Figures on the bars refer to experiment no. in Table 1.

3.2. Significance of current intensity and catalyst loading on PCE removal

Currents of 0 mA, 60 mA, 120 mA and 180 mA were tested in the C → BPE → A arrangement for electrochemical removal of PCE with Pd catalyst loadings on the Fe foam cathode of 0.76 mg/cm² and/or 1.14 mg/cm² (exp. 0–4, Fig. 2a).

For catalyst loadings of 0.76 mg/cm², PCE removals were 0%, 14% and 18% at currents of 0 mA, 60 mA and 120 mA, respectively (exp. 0–2, Fig. 2a). For catalyst loadings of 1.14 mg/cm², PCE removals were 54 ± 3% and 39% at 120 mA and 180 mA, respectively (exp. 3–4, Fig. 2a). Thus, the current intensity and PCE removal are parabolic correlated. The decline in removal at 180 mA is explained by increased competition of oxygen evolution at the anode. In addition, the oxygen

generated physically covered the anode and thereby occupied active sites for oxidation (Rajic et al., 2015a; Rajic et al., 2016b).

Catalysts are important for the transformation of PCE, since a 50% increase in Pd load enhanced PCE removal by 36%-point at 120 mA (exp. 2–3, Fig. 2a). The significance of Pd on chlorinated ethene removal has been studied previously, where an optimal concentration of 0.76 mg/cm² was found (Rajic et al., 2016b). The inconsistency in findings of optimal load of Pd on Fe foam cathodes possibly is associated with the geometry of the Fe foam cathodes used; the electrode surface areas tend to be estimated based on geometrical shape, since the actual surface area of the foams is unknown. Thus, the electrode surface area ratio between experimental set-ups cannot be applied directly in the dimensioning of Pd load.

In the set-up studied, a further increase in Pd load could optimize the removal performance, since the $C \rightarrow C \rightarrow A$ arrangement with 316 SS and Pd/Fe foam cathodes was superior to two Pd/Fe foam cathodes (Section 3.1., exp. 8–9, Fig. 2a), with higher catalytic content in the 316 SS than the resulting palladization. However, replacing the Pd/Fe foam cathode with 316 SS in a $C \rightarrow A$ set-up is insufficient (Rajic et al., 2015c). In the remainder of tests, a Pd load of 1.14 mg/cm^2 was applied. The voltage stabilized at 32 V at 120 mA independent of Pd load (exp. 2–3, Fig. 2b). Whereas the potential difference increased from 20 V to 32 V to 38 V at 60 mA, 120 mA and 180 mA, respectively (exp. 1–4, Fig. 2b), a linear correlation with R^2 of 0.93. According to Ohms Law, the electrical resistivity should remain constant when the experimental conditions, besides current intensity, are unaltered. In this study, the resistivity increased with increasing current, which possibly can be ascribed to increased oxygen and hydrogen generation at the anode (Eqs. (4)–(5)) and cathode (Eq. (1)) with increased current. The additional gases formed extended the gas coverage of the electrode surfaces. Evolving gas layers on the electrode surfaces reduce connectivity between electrodes and the conductive liquid phase, wherefore the electrical resistivity increases.

MMO anodes are known to maintain pH of the water treated (Rajic et al., 2015a). However, in the studied $C \rightarrow BPE \rightarrow A$ arrangement, pH of the porewater downgradient of the electrochemical zone (sampling port P5) was elevated to 8.5 ± 1.5 at 120 mA and 180 mA (exp. 0 and 3–4, Fig. 2c). The elevated pH post electrochemical treatment indicates formation of H_2O_2 (Eq. (2)) instead of neutralization of the alkaline front established at cathodic sites.

A concern of using catalysts like Pd and Ni for treatment of water, whether it is for drinking purposes or discharge into the nature, is the release of ions, which may inhibit living organisms (Umemura et al., 2015; Okamoto et al., 2015). If the catalyst is applied on the cathode and polarity is not reversed, release is of little concern. Whether Pd is released when no current is applied, is not reported. Therefore, effluent samples extracted throughout the 360 min of control testing (exp. 0) were analyzed for Pd. Concentration of Pd was below 0.002 mg/l . Tests on *Daphnia magna* indicate long-term effects of concentrations $>1 \text{ mg/l}$ (Lüderwald et al., 2016).

3.3. Influence of a porous matrix and orientation of reactor on PCE removal

Electrochemical performance in porous matrices was assessed for flow through a porous matrix of glass beads with a porosity of 34.3% at a Darcy velocity of 0.08 cm/min in the $C \rightarrow A$ electrochemical reactor at 120 mA. Presence of the porous matrix enhanced PCE removal to 39% compared to 30% in the completely liquid-filled reactor (exp. 10 and 11, Fig. 2a). The experimental parameters electrode spacing and flow are varied in this comparison (Table 1, test 10–11). Sorption of PCE onto glass beads is neglectable (Yuan et al., 2013a; Rajic et al., 2015b), verified by the insignificant mass loss in control experiments (exp. 0, Fig. 2a). The more complex flow pattern through a porous matrix than a completely liquid-filled reactor may improve the contact between generated reactants and the PCE and explain the enhanced removal in porous matrices. In the porewater downgradient of the electrochemical zone (sampling port P5), pH 5 was measured with and without presence of the porous matrix (exp. 10 and 11, Fig. 2c). The potential difference increased from 7 V to 36 V when including the porous matrix (exp. 10 and 11, Fig. 2b). Hence, resistivity was 5 times higher in the porous matrix. An increase in potential difference as the alkaline front progresses towards the anode in a porous matrix has been observed (Gabrieli and Alshawabkeh, 2010).

Vertical oriented reactors are applied in most studies on flow-through electrochemical removal of chlorinated ethenes (Mao et al., 2012b; Yuan et al., 2013a; Zhou et al., 2018; Rajic et al., 2016a; Fallahpour et al., 2016; Rajic et al., 2015a; Rajic et al., 2016b; Rajic et al., 2015b; Rajic et al., 2014; Rajic et al., 2015c; Fallahpour et al., 2017). One major advantage is automatic venting of gases generated,

since gases released from the electrodes will bubble up through the reactor and leave the reactor with the effluent. For horizontally oriented reactors, the gases will accumulate in a vapor phase above the electrodes, pressurize the system and eventually drain out the fluid, if no means of venting are installed. However, a horizontally oriented reactor may be desirable for feasibility studies of field-implementations of electrochemical contaminant transformation in saturated porous matrices. Whether orientation of the reactor influenced the treatment performance was assessed in the $C \rightarrow BPE \rightarrow A$ and $C \rightarrow A$ arrangement at 120 mA. At the two flow velocities tested, the horizontally oriented reactor was superior to the vertically oriented with 9–16%-point (exp. 6 vs. 7 and 11 vs. 12, Fig. 2a). pH in the porewater downgradient the electrochemical zone (sampling port P5) was similar in the horizontal and vertical orientations of 4.5 and 5 for the low and high flow velocity studied, respectively (exp. 6–7, 11–12, Fig. 2c). For the potential difference over the electrodes, no clear trend is observed (exp. 6–7, 11–12, Fig. 2b).

Based on observations, the differences in performance of horizontal and vertical oriented reactors probably were related to the system's ability to release gases generated at the electrodes. In the vertically oriented reactors, the gases accumulated on the upgradient side (lower) of the electrodes until a certain gas volume was reached. The bubbles then pushed through the perforated mesh electrodes and escaped the reactor with the effluent. During the buildup of gases, the potential difference increased followed by a sudden drop once the bubbles had migrated through the mesh electrodes. Accumulation of gases was most prevalent during the high flow tested. Significance of stripping of the volatile contaminant into those gas phases is unknown. In the horizontally oriented reactors, gas phases were immediately extracted above the electrodes using syringes. The gases appeared to be more readily and steadily released and extracted in the horizontal reactors, thus disturbing the system less: the potential difference remained steadier, less pressure build up and the vapor phases were less extensive. Mass loss through volatilization is considered less in the horizontally oriented reactors. Several means of automatic venting in the horizontally oriented reactors were tested; automatic vents, gas-liquid separation membranes, gravity and water-locks. Transient changes in the electrochemical system challenged these venting mechanisms, i.e. the manual extraction of gases was most suitable. Venting mechanisms are lab challenges only, because the test set-ups must be closed systems to hinder mass loss through volatilization. In the field, the test area is an open system from which gases can escape through the electrode wells, in which they are generated, or migrate through the soil matrix. If stripping of chlorinated ethenes is an issue, granular activated carbon above the electrodes can capture the volatilized fraction of the contamination.

3.4. Effect of flow and test duration on PCE removal

Flow rate is inverse proportional to residence time of PCE within the electrochemical reactor, i.e. lowering the flow rate prolongs the residence time. Effect of flow was studied in the completely liquid-filled reactor with a high flow in the $C \rightarrow A$ arrangement (exp. 11–12) and compared to a low flow in the $C \rightarrow BPE \rightarrow A$ configuration (exp. 6–7). The experimental parameters electrode spacing, electrode configuration and flow are varied in this comparison (Table 1, test 6–7 vs. 11–12), wherefore changes cannot solely be ascribed to altered flow. However, the effect of flow rate on the PCE removal is significant in comparison to the effect from electrode spacing and configuration alone (exp. 6–7, 11–12 vs. 3, 5, 8–10, Fig. 2a).

Reducing the Darcy velocity from 0.25 cm/min (1314 m/yr) to 0.03 cm/min (150 m/yr) increased PCE removal with 56–63%-point reaching a removal of 86%. For electrochemical treatment of TCE at 60 mA, a reduction in Darcy velocity from 2628 m/yr to 1314 m/yr resulted in a 31%-point improvement in TCE removal to 87% (Rajic et al., 2015a). The low flow in the present investigation is representative of common aquifer flows at contaminated sites.

pH of the porewater downgradient the electrochemical zone (sampling port P5) was similar of 4.5–5 (exp. 6–7 vs. 11–12, Fig. 2c). The potential difference decreased by 6.5–13 V at elevated flow (exp. 6–7 vs. 11–12, Fig. 2b), i.e. the resistivity of the high-flow system was lower, indicating a higher mass-transfer of ionic species.

Electrochemical treatment during 120 min and 290 min insignificantly influenced the PCE removal, pH in porewater downgradient the electrochemical zone (sampling port P5) and the potential difference over the electric field in the C → BPE → A configuration at 120 mA and a Darcy velocity of 0.08 cm/min (exp. 3, Fig. 2). The electrochemical processes appeared to rapidly establish and stabilize in this system having a simple hydrogeochemistry.

3.5. Charge transfer in the electrochemical set-up

Experimental specifications vary between studies, e.g. cross-sectional areas, flow velocities, current intensities etc. For comparison of data across studies, normalization of the experimental data is necessary. Many procedures exist for normalization. In the present study, normalization for current intensity (I), flow rate (Q) and contaminant concentration (C) was chosen. Flow rate was chosen instead of flow velocity to account for differences in cross-sectional areas of reactors. The output is charge transfer per contaminant mass and the lower the number, the better in terms of power consumption and thereby cost. The normalized data are plotted against PCE removal percentage (Fig. 3) and compared to data reported on electrochemical removal of TCE in a similar set-up (Rajic et al., 2015a) (Fig. 3, squares). The ratio of electrode surface area to liquid volume was different in the two experimental set-ups applied (lower in the present work) and was not optimized for in the experimental series carried out. Therefore, a deviation in levels of normalized data for a specific removal percentage obtained was expected. Fig. 3 allows to compare the overall level of the normalized data obtained for electrochemical removal of PCE and TCE and the shape of the resulting curves. Note, if sequential degradation via e.g. hydrogenolysis was in progress, a fraction of the current supplied would be directed towards concurrent transformation of the degradation products formed. In this case, however, TCE nor DCE was detected (VC analysis was not possible), neither in Rajic et al. (Rajic et al., 2015a).

For PCE removals beyond 30%, the charge input required increased, while for TCE a similar increase appeared for removals beyond 77% (Fig. 3). Thus, a higher charge transfer was required to remove PCE than TCE. The difference in electrode surface area to liquid volume ratio between the two experimental set-ups possibly contributed to the observed deviation, where the contact between contaminant, Pd catalyst on the cathode and the energy source itself is improved at a higher such ratio, enhancing the conditions for contaminant transformation at a specific charge input. A low ratio of electrode surface area

to liquid volume can be compensated for by increasing the current and/or Pd load. The similar levels of normalized data for PCE and TCE at a removal of 30% support this: MMO anodes and an electrode spacing of 2.5 cm were used in both set-ups. However, in the study on TCE, a Pd load of 0.76 mg/cm² and a current of 60 mA was applied (Rajic et al., 2015a). In the study on PCE, having a lower electrode surface area to liquid volume, a Pd load of 1.14 mg/cm² and a current of 120 mA was applied (exp. 11). I.e. the lower electrode surface area to liquid volume was counterbalanced by a 50% increase in Pd load and a 100% increase in current. A further increase in current would possibly not be beneficial (exp. 4 vs. 11, Fig. 2a). Instead, a reduction in flow (exp. 6 vs. 11, Fig. 2a) and an increase in Pd load is suggested for optimization of electrochemical removal of PCE in the experimental set-up studied.

If comparing the normalized data obtained from all sampling ports, sampling rounds and test designs (data not shown), and neglecting the associated removal levels, a generally best fit with those of Rajic et al. (Rajic et al., 2015a) is seen when set-ups are most alike. I.e., for vertically oriented reactors excluding a porous matrix (exp. 7 and 12), which illustrates the sensitivity towards the experimental design. The concept of electrochemical treatment of chlorinated ethenes must be strengthened to overcome the complex conditions of contaminated sites (Hyldegaard et al., 2019; Ottosen et al., 2019). Finally, removals beyond app. 60% and 90% for PCE and TCE, respectively, required a significant additional charge transfer, as indicated by the steep slope of curves in Fig. 3. Thus, treating the low levels of contaminant concentrations, which is required to comply with the regulatory contaminant level for PCE and TCE in drinking water, are the most expensive.

3.6. PCE transformation pathways in the electrochemical reactor

Mass loss is a concern when working with volatile contaminants like PCE, because it can give false positive test results and thereby incorrect foundations for decision making. Two control experiments were carried out in a set-up similar to that of experiment 1–4, except that no current was applied (exp. 0, Table 1). No mass loss was observed throughout the 360 min of testing, measured downgradient the electrochemical zone (sampling port P5, exp. 0, Fig. 2a). An observed drop in PCE concentration during experiments with applied current therefore is stimulated by the electrochemistry. Stripping of the contaminants due to the gas generating electrode processes (Eqs. (1) and (4)) rather than transformation is another concern when applying electrochemistry for removal of chlorinated ethenes. A risk especially at stable anodes like MMO, since these produce more oxygen (Eqs. (5) vs. (4)) (Rajic et al., 2015a) and PCE may be more prone to volatilization than oxidation at the anode, as opposite to the higher affinity of reduction near the cathode. The specific electrode's contribution to removal of PCE was found in the order of cathode > BPE > anode, indicating that electrochemically induced transformation was occurring rather than stripping. Furthermore, increasing the Pd load on the cathode from 0.76 mg/cm² to 1.14 mg/cm² improved the removal at 120 mA from 19% to 54 ± 3% (exp. 2 vs. 3, Fig. 2a), suggesting that the cathode induced processes removed PCE.

Transformation mechanisms at the cathode possibly were related to the catalytic properties of Pd through enhanced adsorption of atomic hydrogen, and thereby reductive hydrodechlorination of PCE, and/or formation of the strong oxidative species H₂O₂ and •OH (Eqs. (2)–(3)). Formation of H₂O₂ and •OH appeared to contribute to the transformation of PCE, since 12% more PCE was removed in the C → BPE → A arrangement than C → C → A (exp. 3 vs. 9, Fig. 2a). Rajic et al. (Rajic et al., 2016a) showed that using a BPE in between the cathode and anode strengthened the H₂O₂ formation. This could be due to i) oxygen and dihydrogen being formed concurrently on each side of the BPE, improving the contact necessary for conversion into H₂O₂, and ii) the anodic side of the BPE facing the cathode, i.e. in closer contact and thus, if the oxygen diffused towards the cathode, it could combine with the dihydrogen generated, forming H₂O₂ at the Pd surface (Yuan

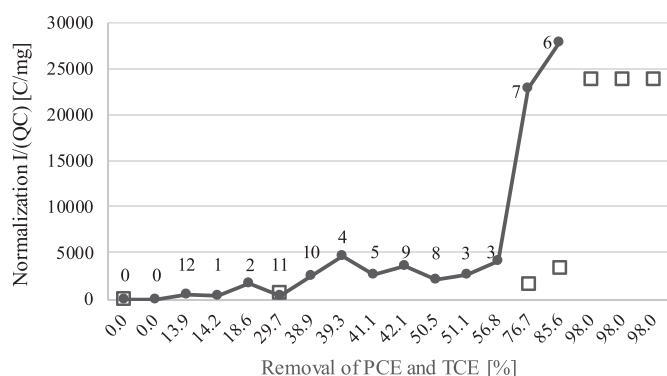


Fig. 3. Normalization of experimental data for PCE based on samples extracted in the final sampling port (solid dots) and data for TCE in Rajic et al. (Rajic et al., 2015a) (squares) for current intensity (I), flow (Q) and contaminant concentration (C) plotted against the removal of PCE and TCE. Numbers next to markers refer to experiment number (Table 1).

et al., 2013a). Elevated pH measured downstream the $C \rightarrow BPE \rightarrow A$ electrochemical zone (sampling port P5) indicated formation of H_2O_2 (Section 3.1).

The sequential hydrogenolysis products TCE and DCEs were not detected in any sampling point of the experiments conducted. This suggests fast concurrent hydrogenolysis of TCE and DCEs or another transformation pathway for PCE in the electrochemical reactor, e.g. oxidation by H_2O_2 and $\cdot OH$, and/or β -elimination (Ottosen et al., 2019). In parallel to the Fe cathodes applied in this study, degradation of PCE on $Fe(0)$ has shown to follow β -elimination for 87% of the contaminant mass (Arnold and Roberts, 2000). The electrochemical mechanisms responsible for PCE transformation along with the parameters controlling those should be studied in detail for design of a robust electrochemical methodology for removal of chlorinated ethenes.

4. Conclusion

Protection of the groundwater resource from harmful chlorinated ethenes is crucial and challenging. Electrochemically induced reduction and oxidation may overcome some of the difficulties experienced. In the development of the method, PCE must be included in the assessment of electrochemical transformation of chlorinated ethenes, but is mostly overlooked. This study screened the significance of parameters influencing electrochemical removal of PCE in a flow-through reactor using a palladized Fe foam cathode and an MMO mesh anode. The major findings are:

- Of the electrode configurations tested, presence of a BPE between the cathode and anode improved removal of PCE to $54 \pm 3\%$. The BPE added an oxidizing-reducing zone and lowered the electrical resistivity.
- Pd played a major role in the transformation of PCE with a 50% increase in Pd load on the cathode improving the removal by 36%-point.
- Increasing the electrode spacing from 2.5 cm to 4 cm enhanced the removal from 41% to $54 \pm 3\%$, due to extension of redox zones, which is a promising trend when considering the installation and cost of field-implementation.

PCE removal in liquid flowing through an inert porous matrix was investigated to simulate in-situ conditions. Presence of the porous matrix enhanced PCE removal by 9%-point compared to a completely liquid-filled reactor due to a more complex flow pattern within the porous matrix. A horizontally orientated reactor improved PCE removal by 9–16%-point compared to vertically oriented reactors. Release of oxygen and hydrogen gas from the electrode surfaces in the horizontal reactor was enhanced, wherefore a higher number of active electrode surface sites were available for PCE transformation. The highest removal of 86% was obtained using a horizontally oriented reactor at a current of 120 mA applied to an electrode configuration of $C \rightarrow BPE \rightarrow A$ with a Pd load on the cathode of 1.14 mg/cm^2 and a Darcy velocity of 0.03 cm/min (150 m/yr) through a fully liquid-filled reactor. No chlorinated ethene degradation products were detected in any of the test designs studied.

Normalization of the data revealed, that the low contaminant concentrations were the most difficult to treat in that a significant charge transfer was required for removal beyond 60%. The removal performance was found sensitive to dimensional changes in experimental reactors. The transformation mechanisms and the parameters controlling those need to be better understood to control and adjust the relevant parameters for a flexible remediation design, that can overcome the variations occurring between lab set-ups and not least at contaminated sites. Thus, this study identified some weaknesses in the current stage of development of electrochemical removal of chlorinated ethenes, but also some promising trends in conceptual designs that better simulate that of a potential field-implementation.

Acknowledgements

Funding: This work was supported by the Innovation Fund Denmark, Denmark [grant number 5016-00165B]; COWIfonden, Denmark [grant number C-131.01]; the Capital Region of Denmark, Denmark [grant number 14002101]; the Danish Ministry of Higher Education and Science, Denmark [grant number 7079-00012B] and the PROTECT Center under the National Institute Of Environmental Health Sciences [grant number P42ES017198]. The funding sources were not involved in the actual research conducted, nor in the preparation of this paper.

References

- Acar, Y.B., Alshawabkeh, A.N., 1993. Principles of electrokinetic remediation. *Environ. Sci. Technol.* 27, 2638–2647. <https://doi.org/10.1021/es00049a002>.
- Alshawabkeh, A.N., 2009. Electrokinetic soil remediation: challenges and opportunities. *Sep. Sci. Technol.* 44, 2171–2187. <https://doi.org/10.1080/01496390902976681>.
- Arnold, W.A., Roberts, A.L., 2000. Pathways and kinetics of chlorinated ethylene and chlorinated acetylene reaction with $Fe(0)$ particles. *Environ. Sci. Technol.* 34, 1794–1805. <https://doi.org/10.1021/es980252o>.
- Aulenta, F., Pera, A., Rossetti, S., Petrangeli Papini, M., Majone, M., 2007. Relevance of side reactions in anaerobic reductive dechlorination microcosms amended with different electron donors. *Water Res.* 41, 27–38. <https://doi.org/10.1016/j.watres.2006.09.019>.
- Aulenta, F., Canosa, A., Reale, P., Rossetti, S., Panero, S., Majone, M., 2009. Microbial reductive dechlorination of trichloroethene to ethene with electrodes serving as electron donors without the external addition of redox mediators. *Biotechnol. Bioeng.* 103, 85–91. <https://doi.org/10.1002/bit.22234>.
- Aulenta, F., Reale, P., Canosa, A., Rossetti, S., Panero, S., Majone, M., 2010. Characterization of an electro-active biocathode capable of dechlorinating trichloroethene and cis-dichloroethene to ethene. *Biosens. Bioelectron.* 25, 1796–1802. <https://doi.org/10.1016/j.bios.2009.12.033>.
- Aulenta, F., Tocca, L., Verdini, R., Reale, P., Majone, M., 2011. Dechlorination of trichloroethene in a continuous-flow bioelectrochemical reactor: effect of cathode potential on rate, selectivity, and electron transfer mechanisms. *Environ. Sci. Technol.* 45, 8444–8451. <https://doi.org/10.1021/es202262y>.
- Aulenta, F., Verdini, R., Zeppilli, M., Zanolari, G., Fava, F., Rossetti, S., Majone, M., 2013. Electrochemical stimulation of microbial cis-dichloroethene (cis-DCE) oxidation by an ethene-assimilating culture. *New Biotechnol.* 30, 749–755. <https://doi.org/10.1016/j.nbt.2013.04.003>.
- Bass, D.H., Hastings, N.A., Brown, R.A., 2000. Performance of air sparging systems: a review of case studies. *J. Hazard. Mater.* 72, 101–119. [https://doi.org/10.1016/S0304-3894\(99\)00136-3](https://doi.org/10.1016/S0304-3894(99)00136-3).
- Brewster, J.H., 1954. Mechanisms of reductions at metal surfaces. I. A general working hypothesis. *J. Am. Chem. Soc.* 76, 6361–6363. <https://doi.org/10.1021/ja01653a034>.
- Butler, E.C., Hayes, K.F., 1999. Kinetics of the transformation of trichloroethylene and tetrachloroethylene by iron sulfide. *Environ. Sci. Technol.* 33, 2021–2027. <https://doi.org/10.1021/es9809455>.
- Chen, G., 2004. Electrochemical technologies in wastewater treatment. *Sep. Purif. Technol.* 38, 11–41. <https://doi.org/10.1016/j.seppur.2003.10.006>.
- Fallahpour, N., Yuan, S., Rajic, L., Alshawabkeh, A.N., 2016. Hydrodechlorination of TCE in a circulated electrolytic column at high flow rate. *Chemosphere* 144, 59–64. <https://doi.org/10.1016/j.chemosphere.2015.08.037>.
- Fallahpour, N., Mao, X., Rajic, L., Yuan, S., Alshawabkeh, A.N., 2017. Electrochemical dechlorination of trichloroethylene in the presence of natural organic matter, metal ions and nitrates in a simulated karst media. *J. Environ. Chem. Eng.* 5, 240–245. <https://doi.org/10.1016/j.jece.2016.11.046>.
- Fallgren, P.H., Eisenbeis, J.J., Jin, S., 2018. In situ electrochemical manipulation of oxidation-reduction potential in saturated subsurface matrices. *J. Environ. Sci. Heal. Part A* 53, 517–523. <https://doi.org/10.1080/10934529.2017.1422951>.
- Farrell, J., Melitas, N., Kason, M., Li, T., 2000. Electrochemical and column investigation of iron-mediated reductive dechlorination of trichloroethylene and perchloroethylene. *Environ. Sci. Technol.* 34, 2549–2556. <https://doi.org/10.1021/es991135b>.
- Gabrieli, L., Alshawabkeh, A.N., 2010. Influence of boundary conditions on transient excess pore pressure during electrokinetic applications in soils. *J. Appl. Electrochem.* 40, 1113–1121. <https://doi.org/10.1007/s10800-010-0075-0>.
- Ghosh, D., Medhi, C.R., Solanki, H., Purkait, M.K., 2008. Decolorization of crystal violet solution by electrocoagulation. *J. Environ. Prot. Sci.* 2, 25–35.
- Gillham, R.W., O'Hannesin, S.F., 1994. Enhanced degradation of halogenated aliphatics by zero-valent iron. *Ground Water* 32, 958–967. <https://doi.org/10.1111/j.1745-6584.1994.tb00935.x>.
- He, Y.T., Wilson, J.T., Su, C., Wilkin, R.T., 2015. Review of abiotic degradation of chlorinated solvents by reactive iron minerals in aquifers. *Groundw. Monit. Remediat.* 35, 57–75. <https://doi.org/10.1111/gwmr.12111>.
- Hyldegaard, B.H., Jakobsen, R., Weeth, E.B., Overheu, N.D., Gent, D.B., Ottosen, L.M., 2019. Challenges in electrochemical remediation of chlorinated solvents in natural groundwater aquifer settings. *J. Hazard. Mater.* 368, 680–688. <https://doi.org/10.1016/j.jhazmat.2018.12.064>.
- Interstate Technology & Regulatory Council, 2005. *Permeable Reactive Barriers: Lessons Learned/New Directions*. PRB-4, Washington, DC, USA, pp. 1–202.
- Interstate Technology & Regulatory Council, 2011. *Integrated DNAPL Site Strategy*, Washington, DC, USA, pp. 1–209. <http://www.itrcweb.org>.

- Johnson, T.L., Scherer, M.M., Tratnyek, P.G., 1996. Kinetics of halogenated organic compound degradation by iron metal. *Environ. Sci. Technol.* 30, 2634–2640. <https://doi.org/10.1021/es9600901>.
- Kim, Y.H., Carraway, E.R., 2003. Dechlorination of chlorinated ethenes and acetylenes by palladized iron. *Environ. Technol.* 24, 809–819. <https://doi.org/10.1080/09593330309385618>.
- Kueper, B.H., Stroo, H.F., Vogel, C.M., Ward, C.H. (Eds.), 2014. *Chlorinated Solvent Source Zone Remediation*. Springer, New York, USA, pp. 1–759. <https://doi.org/10.1007/978-1-4614-6922-3>.
- Lai, A., Verdini, R., Aulenta, F., Majone, M., 2015. Influence of nitrate and sulfate reduction in the bioelectrochemically assisted dechlorination of cis-DCE. *Chemosphere* 125, 147–154. <https://doi.org/10.1016/j.chemosphere.2014.12.023>.
- Lakshminathiraj, P., Bhaskar Raju, G., Sakai, Y., Takuma, Y., Yamasaki, A., Kato, S., Kojima, T., 2012. Studies on electrochemical detoxification of trichloroethene (TCE) on Ti/IrO₂-Ta₂O₅ electrode from aqueous solution. *Chem. Eng. J.* 198–199, 211–218. <https://doi.org/10.1016/j.cej.2012.05.092>.
- Li, T., Farrell, J., 2000. Reductive dechlorination of trichloroethene and carbon tetrachloride using iron and palladized-iron cathodes. *Environ. Sci. Technol.* 34, 173–179. <https://doi.org/10.1021/es907358>.
- Li, T., Farrell, J., 2001. Electrochemical investigation of the rate-limiting mechanisms for trichloroethylene and carbon tetrachloride reduction at iron surfaces. *Environ. Sci. Technol.* 35, 3560–3565. <https://doi.org/10.1021/es0019878>.
- Lima, A.T., Hofmann, A., Reynolds, D., Ptacek, C.J., Van Cappellen, P., Ottosen, L.M., Pamukcu, S., Alshawabkeh, A.N., O'Carroll, D.M., Riis, C., Cox, E., Gent, D.B., Landis, R., Wang, J., Chowdhury, A.I.A., Secord, E.L., Sanchez-Hachair, A., 2017. Environmental electrokinetics for a sustainable subsurface. *Chemosphere* 181, 122–133. <https://doi.org/10.1016/j.chemosphere.2017.03.143>.
- Liu, B., Zhang, H., Lu, Q., Li, G., Zhang, F., 2018. A Cu Ni bimetallic cathode with nanostructured copper array for enhanced hydrodechlorination of trichloroethylene (TCE). *Sci. Total Environ.* 635, 1417–1425. <https://doi.org/10.1016/j.scitotenv.2018.04.238>.
- Lohner, S.T., Becker, D., Mangold, K.M., Tiehm, A., 2011. Sequential reductive and oxidative biodegradation of chloroethenes stimulated in a coupled bioelectro-process. *Environ. Sci. Technol.* 45, 6491–6497. <https://doi.org/10.1021/es200801r>.
- Lüderwald, S., Seitz, F., Seisenbaeva, G., Kessler, V., Schulz, R., Bundschuh, M., 2016. Palladium nanoparticles: is there a risk for aquatic ecosystems? *Bull. Environ. Contam. Toxicol.* 97, 153–158. <https://doi.org/10.1007/s00128-016-1803-x>.
- Mackay, D.M., Cherry, J.A., 1989. Groundwater contamination: pump-and-treat remediation. *Environ. Sci. Technol.* 23, 630–636. <https://doi.org/10.1021/es00064a001>.
- Mao, X., Ciblak, A., Amiri, M., Alshawabkeh, A.N., 2011. Redox control for electrochemical dechlorination of trichloroethylene in bicarbonate aqueous media. *Environ. Sci. Technol.* 45, 6517–6523. <https://doi.org/10.1021/es200943z>.
- Mao, X., Ciblak, A., Baek, K., Amiri, M., Loch-Carus, R., Alshawabkeh, A.N., 2012a. Optimization of electrochemical dechlorination of trichloroethylene in reducing electrolytes. *Water Res.* 46, 1847–1857. <https://doi.org/10.1016/j.watres.2012.01.002>.
- Mao, X., Yuan, S., Fallahpour, N., Ciblak, A., Howard, J., Padilla, I., Loch-Carus, R., Alshawabkeh, A.N., 2012b. Electrochemically induced dual reactive barriers for transformation of TCE and mixture of contaminants in groundwater. *Environ. Sci. Technol.* 46, 12003–12011. <https://doi.org/10.1021/es301711a>.
- Moran, M.J., Zogorski, J.S., Squillace, P.J., 2007. Chlorinated solvents in groundwater of the United States. *Environ. Sci. Technol.* 41, 74–81. <https://doi.org/10.1021/es061553y>.
- O'Connor, D., Hou, D., Ok, Y.S., Song, Y., Sarmah, A.K., Li, X., Tack, F.M.G., 2018. Sustainable in situ remediation of recalcitrant organic pollutants in groundwater with controlled release materials: a review. *J. Control. Release* 283, 200–213. <https://doi.org/10.1016/j.jconrel.2018.06.007>.
- Okamoto, A., Yamamoto, M., Tatarazako, N., 2015. Acute toxicity of 50 metals to *Daphnia magna*. *J. Appl. Toxicol.* 35, 824–830. <https://doi.org/10.1002/jat.3078>.
- Ottosen, L.M., Larsen, T.H., Jensen, P.E., Kirkelund, G.M., Kern-Jespersen, H., Tuxen, N., Hyldegaard, B.H., 2019. Electrokinetics applied in remediation of subsurface soil contaminated with chlorinated ethenes – a review. *Chemosphere* 235, 113–125. <https://doi.org/10.1016/j.chemosphere.2019.06.075>.
- Pankow, J.F., Feenstra, S., Cherry, J.A., Ryan, C.M. (Eds.), 1996. *Dense Chlorinated Solvents and Other DNAPLs in Groundwater: History, Behavior, and Remediation*. Waterloo Press, Portland, Oregon, pp. 1–522.
- Petersen, M.A., Sale, T.C., Reardon, K.F., 2007. Electrolytic trichloroethene degradation using mixed metal oxide coated titanium mesh electrodes. *Chemosphere* 67, 1573–1581. <https://doi.org/10.1016/j.chemosphere.2006.11.056>.
- Rajic, L., Fallahpour, N., Yuan, S., Alshawabkeh, A.N., 2014. Electrochemical transformation of trichloroethylene in aqueous solution by electrode polarity reversal. *Water Res.* 67, 267–275. <https://doi.org/10.1016/j.watres.2014.09.017>.
- Rajic, L., Fallahpour, N., Alshawabkeh, A.N., 2015a. Impact of electrode sequence on electrochemical removal of trichloroethylene from aqueous solution. *Appl. Catal. B Environ.* 174–175, 427–434. <https://doi.org/10.1016/j.apcatb.2015.03.018>.
- Rajic, L., Fallahpour, N., Nazari, R., Alshawabkeh, A.N., 2015b. Influence of humic substances on electrochemical degradation of trichloroethylene in limestone aquifers. *Electrochim. Acta* 181, 123–129. <https://doi.org/10.1016/j.electacta.2015.03.121>.
- Rajic, L., Fallahpour, N., Oguzie, E., Alshawabkeh, A.N., 2015c. Electrochemical transformation of trichloroethylene in groundwater by Ni-containing cathodes. *Electrochim. Acta* 181, 118–122. <https://doi.org/10.1016/j.electacta.2015.03.112>.
- Rajic, L., Nazari, R., Fallahpour, N., Alshawabkeh, A.N., 2016a. Electrochemical degradation of trichloroethylene in aqueous solution by bipolar graphite electrodes. *J. Environ. Chem. Eng.* 4, 197–202. <https://doi.org/10.1016/j.jece.2015.10.030>.
- Rajic, L., Fallahpour, N., Podlaha, E., Alshawabkeh, A.N., 2016b. The influence of cathode material on electrochemical degradation of trichloroethylene in aqueous solution. *Chemosphere* 147, 98–104. <https://doi.org/10.1016/j.chemosphere.2015.12.095>.
- Reddy, K.R., Cameselle, C. (Eds.), 2009. *Electrochemical Remediation Technologies for Polluted Soils, Sediments and Groundwater*. John Wiley & Sons, Inc, Hoboken, New Jersey, pp. 1–732.
- Ribeiro, A.B., Mateus, E.P., Couto, N. (Eds.), 2016. *Electrokinetics Across Disciplines and Continents, New Strategies for Sustainable Development*. Springer International Publishing, London, pp. 1–469. <https://doi.org/10.1007/978-3-319-20179-5>.
- Ruder, A.M., 2006. Potential health effects of occupational chlorinated solvent exposure. *Ann. N. Y. Acad. Sci.* 1076, 207–227. <https://doi.org/10.1196/annals.1371.050>.
- Sáez, V., Escalapez Vicente, M.D., Frias-Ferrer, A., Bonete, P., González-García, J., 2009. Electrochemical degradation of perchloroethylene in aqueous media: an approach to different strategies. *Water Res.* 43, 2169–2178. <https://doi.org/10.1016/j.watres.2009.02.019>.
- Scherer, M.M., Balko, B.A., Gallagher, D.A., Tratnyek, P.G., 1998. Correlation analysis of rate constants for dechlorination by zero-valent iron. *Environ. Sci. Technol.* 32, 3026–3033. <https://doi.org/10.1021/es9802551>.
- Scheut, C., Broholm, M.M., Durant, N.D., Weeth, E.B., Jørgensen, T.H., Dennis, P., Jacobsen, C.S., Cox, E.E., Chambon, J.C., Bjerg, P.L., 2010. Field evaluation of biological enhanced reductive dechlorination of chloroethenes in clayey till. *Environ. Sci. Technol.* 44, 5134–5141. <https://doi.org/10.1021/es1003044>.
- Scialdone, O., Guarisco, C., Galia, A., Herbois, R., 2010. Electroreduction of aliphatic chlorides at silver cathodes in water. *J. Electroanal. Chem.* 641, 14–22. <https://doi.org/10.1016/j.jelechem.2010.01.018>.
- Siegrist, R.L., Crimi, M., Broholm, M.M., McCray, J.E., Illangasekare, T.H., Bjerg, P.L., 2012. Advances in groundwater remediation: Achieving effective in situ delivery of chemical oxidants and amendments. In: Quercia, F.F., Vidoejic, D. (Eds.), *Clean Soil Safe Water*. Springer, Dordrecht, The Netherlands, pp. 197–212. https://doi.org/10.1007/978-94-007-2240-8_22.
- Stenzel, M.H., Gupta, U. Sen, 1985. Treatment of contaminated groundwaters with granular activated carbon and air stripping. *J. Air Pollut. Control Assoc.* 35, 1304–1309. <https://doi.org/10.1080/00022470.1985.10466035>.
- Stroo, H.F., Ward, C.H. (Eds.), 2010. *In Situ Remediation of Chlorinated Solvent Plumes*. Springer, New York, NY, pp. 1–786. <https://doi.org/10.1007/978-1-4419-1401-9>.
- Stroo, H.F., Leeson, A., Marqusee, J.A., Johnson, P.C., Ward, C.H., Kavanaugh, M.C., Sale, T.C., Newell, C.J., Pennell, K.D., Lebrón, C.A., Unger, M., 2012. Chlorinated ethene source remediation: lessons learned. *Environ. Sci. Technol.* 46, 6438–6447. <https://doi.org/10.1021/es204714w>.
- Su, C., Puls, R.W., 1999. Kinetics of trichloroethene reduction by zerovalent iron and tin: pretreatment effect, apparent activation energy, and intermediate products. *Environ. Sci. Technol.* 33, 163–168. <https://doi.org/10.1021/es980481a>.
- Tiehm, A., Lohner, S.T., Augenstein, T., 2009. Effects of direct electric current and electrode reactions on vinyl chloride degrading microorganisms. *Electrochim. Acta* 54, 3453–3459. <https://doi.org/10.1016/j.electacta.2009.01.002>.
- Umemura, T., Sato, K., Kusaka, Y., Satoh, H., 2015. Palladium. In: Nordberg, G., Fowler, B., Nordberg, M. (Eds.), *Handbook on the Toxicology of Metals 4E*. Academic Press, pp. 1113–1123. <https://doi.org/10.1016/B978-0-444-59453-2.00049-4>.
- Uran, K., Yamamoto, E., Tonegawa, M., Fujie, K., 1991. Adsorption of chlorinated organic compounds on activated carbon from water. *Water Res.* 25, 1459–1464. <https://doi.org/10.1016/j.arabjc.2015.04.013>.
- Verdini, R., Aulenta, F., de Tora, F., Lai, A., Majone, M., 2015. Relative contribution of set cathode potential and external mass transport on TCE dechlorination in a continuous-flow bioelectrochemical reactor. *Chemosphere* 136, 72–78. <https://doi.org/10.1016/j.chemosphere.2015.03.092>.
- Wüst, W.F., Köber, R., Schlicker, O., Dahmke, A., 1999. Combined zero- and first-order kinetic model of the degradation of tce and cis-DCE with commercial iron. *Environ. Sci. Technol.* 33, 4304–4309. <https://doi.org/10.1021/es980439f>.
- Xie, W., Yuan, S., Mao, X., Hu, W., Liao, P., Tong, M., Alshawabkeh, A.N., 2013. Electrocatalytic activity of Pd-loaded TiO₂ nanotubes cathode for TCE reduction in groundwater. *Water Res.* 47, 3573–3582. <https://doi.org/10.1016/j.watres.2013.04.004>.
- Yuan, S., Mao, X., Alshawabkeh, A.N., 2012. Efficient degradation of TCE in groundwater using Pd and electro-generated H₂ and O₂: a shift in pathway from hydrodechlorination to oxidation in the presence of ferrous ions. *Environ. Sci. Technol.* 46, 3398–3405. <https://doi.org/10.1021/es204546u>.
- Yuan, S., Chen, M., Mao, X., Alshawabkeh, A.N., 2013a. A three-electrode column for Pd-catalytic oxidation of TCE in groundwater with automatic pH-regulation and resistance to reduced sulfur compound fouling. *Water Res.* 47, 269–278. <https://doi.org/10.1016/j.watres.2012.10.009>.
- Yuan, S., Chen, M., Mao, X., Alshawabkeh, A.N., 2013b. Effects of reduced sulfur compounds on Pd-catalytic hydrodechlorination of trichloroethylene in groundwater by cathodic H₂ under electrochemically induced oxidizing conditions. *Environ. Sci. Technol.* 47, 10502–10509. <https://doi.org/10.1021/es402169d>.
- Zheng, M., Bao, J., Liao, P., Wang, K., Yuan, S., Tong, M., Long, H., 2012. Electrogeneration of H₂ for Pd-catalytic hydrodechlorination of 2,4-dichlorophenol in groundwater. *Chemosphere* 87, 1097–1104. <https://doi.org/10.1016/j.chemosphere.2012.01.058>.
- Zhou, W., Rajic, L., Zhao, Y., Gao, J., Qin, Y., Alshawabkeh, A.N., 2018. Rates of H₂O₂ electrogeneration by reduction of anodic O₂ at RVC foam cathodes in batch and flow-through cells. *Electrochim. Acta* 277, 185–196. <https://doi.org/10.1016/j.electacta.2018.04.174>.

APPENDIX V

Electrochemical transformation of an aged tetrachloroethylene contamination in realistic aquifer settings

Hyldegaard, B.H., Jakobsen, R. & Ottosen, L.M.

(Published in Chemosphere, 2020)



Contents lists available at ScienceDirect

Chemosphere

journal homepage: www.elsevier.com/locate/chemosphere

Electrochemical transformation of an aged tetrachloroethylene contamination in realistic aquifer settings



Bente H. Hyldegaard ^{a, b, *}, Rasmus Jakobsen ^c, Lisbeth M. Ottosen ^b

^a Department of Waste & Contaminated Sites, COWI A/S, Parallelvej 2, 2800, Kgs. Lyngby, Denmark

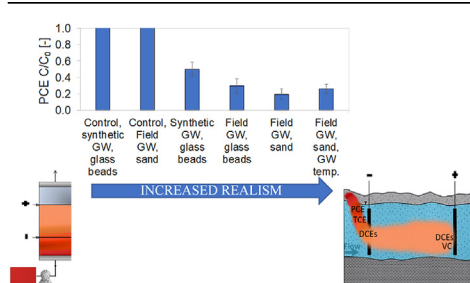
^b Department of Civil Engineering, Brovej, Building 118, Technical University of Denmark, 2800, Kgs. Lyngby, Denmark

^c Department of Geochemistry, Geological Survey of Denmark and Greenland, Øster Voldgade 10, 1350, København K, Denmark

HIGHLIGHTS

- There is a potential for electrochemical removal of chlorinated ethenes from aquifers.
- Chlorinated ethenes in a degraded tetrachloroethylene contamination were transformed.
- Highest removals were achieved in field-extracted groundwater and sandy sediment.
- Reduction pathways rather than oxidation pathways dominated the contaminant removal.
- Initial pH and conductivity were maintained downgradient the electrochemical zone.

GRAPHICAL ABSTRACT



ARTICLE INFO

Article history:

Received 24 September 2019

Received in revised form

6 November 2019

Accepted 7 November 2019

Available online 12 November 2019

Handling Editor: E. Brillas

Keywords:

Electrochemistry
Chlorinated ethenes
Groundwater
Sandy sediment
Remediation
Applied potential

ABSTRACT

Electrochemical removal of chlorinated ethenes in groundwater plumes may potentially overcome some of the challenges faced by current remediation technologies. So far, studies have been conducted in simplified settings of synthetic groundwater and inert porous matrices. This study is a stepwise investigation of the influence of field-extracted groundwater, sandy sediment and groundwater aquifer temperatures on the removal of an aged partially degraded contamination of tetrachloroethylene (PCE) at a typical groundwater flow rate. The aim is to assess the potential for applying electrochemistry at contaminated sites. At a constant current of 120 mA, pH and conductivity were unaffected downgradient the electrochemical zone. Major groundwater species were reduced and oxidized. Some minerals deposited, others dissolved. Hydrogen peroxide, a strong oxidant, was formed in levels up to 5 mg L^{-1} with a limited distribution into the sandy sediment. Trichloromethane was formed, supposedly by oxidation of organic matter in the sandy sediment in the presence of chloride. The more realistic the settings, the higher the PCE removal, bringing concentrations down to $7.8 \pm 2.3 \mu\text{g L}^{-1}$. A complete removal of trichloroethylene and *cis*-1,2-dichloroethylene was obtained. The results suggest that competing reactions related to the natural complex hydrogeochemistry are insignificant in terms of affecting the electrochemical degradation of PCE and chlorinated intermediates.

© 2019 Elsevier Ltd. All rights reserved.

* Corresponding author. Department of Waste & Contaminated Sites, COWI A/S, Parallelvej 2, 2800, Kgs. Lyngby, Denmark.

E-mail addresses: behd@cowi.com, benho@byg.dtu.dk (B.H. Hyldegaard).

1. Introduction

Electrochemistry is being assessed at laboratory scale as a technology for *in situ* transformation of the harmful and widespread chlorinated ethenes in groundwater. It is the ability to establish reducing and oxidizing zones, and to form reactive species, which makes electrochemistry interesting for remediation of this group of contaminants.

Under controlled and simplified conditions, undivided flow-through electrochemical reactors have previously demonstrated the capability of removing >99% trichloroethylene (TCE) (Rajic et al., 2015a, 2016a) and 86% tetrachloroethylene (PCE) (Hyldegaard et al., 2019b) without accumulation of hazardous degradation intermediates. Within the reducing and oxidizing zones established, it is the reducing conditions (Rajic et al., 2014, 2015a; 2015c, 2016a; 2016b), and formation of hydrogen peroxide (H_2O_2) and hydroxyl radicals ($\bullet\text{OH}$) (Yuan et al., 2013a; Rajic et al., 2016b; Hyldegaard et al., 2019b) that are proposed as the dominating factors promoting degradation. However, natural complex hydrogeochemistry may introduce competing reactions for electrons and oxidizing species, e.g. nitrate that has been shown to directly compete with TCE for reduction at the cathode (Rajic et al., 2016a; Fallahpour et al., 2017). Another possible adverse side-effect is covering of electrode surfaces, reducing the area of active sites available for chlorinated ethene transformation. Humic substances are shown to reduce TCE removal due to sorption of the humic substances onto the cathode as well as via competition for electrons and H_2 (Rajic et al., 2015b; Fallahpour et al., 2017). Further, chromate and selenate inhibit TCE removal due to precipitation at electrode surfaces (Fallahpour et al., 2017). The inhibitory effect of chromate, selenate, nitrate and/or arsenite is enhanced when present as a mixture (Mao et al., 2012b; Fallahpour et al., 2017). Contrary to this, enhancement of the chlorinated ethene removal is also observed (Yuan et al., 2013b; Rajic et al., 2015b). Addition of Fe(II) can enhance TCE removal via Fenton's reaction (Yuan et al., 2013b). Further, sulfite has shown to improve TCE removal due to transformation into the reactive radical $\text{SO}_4^{\bullet-}$, which oxidizes the chlorinated ethene (Yuan et al., 2013b). An indirect positive side-effect of the application of electrochemistry in more realistic settings is the enhanced release of electrolytically generated gases from the electrode surfaces and thereby maintenance of the active electrode surface area in presence of a geological matrix, as demonstrated for TCE in limestone (Rajic et al., 2015b). To better understand the challenges of upscaling to complex settings, it is essential to include more hydrogeochemical species and mixtures in the assessment of electrochemical remediation of chlorinated ethenes.

Electrochemical treatment is entirely based on chemical reactions and interactions, and the reaction kinetics are influenced by the temperature of the surroundings. If the temperature is decreased by 10°C , the reaction kinetics are typically reduced by a factor of two (Sundstrom et al., 1986; Leenson, 2009). Such a reduction in temperature is expected when advancing from laboratory testing to field-implementation in groundwater aquifers in Northern Europe and America. It is crucial for the feasibility of electrochemical remediation, that an adequate reaction rate compared to the natural flow rate can be maintained.

This will be the first study to evaluate the capabilities of electrochemical treatment operated at constant current for removal of PCE in flowing field-extracted groundwater containing an aged (partially degraded) contamination with degradation intermediates. The electrochemical application in this study is further challenged by low groundwater temperatures and a variety of competing reactions introduced with the complex hydrogeochemistry of natural groundwater and sandy sediment. Contaminated sites are complex and to assess the potential of

electrochemistry for *in situ* remediation, field-parameters like real groundwater and sediment must be incorporated into the testing. The objective of this study is to stepwise assess the influence of field-extracted groundwater, sandy sediment and groundwater aquifer temperatures on the removal of an aged contamination of PCE in a flow-through electrochemical reactor at a common aquifer flow rate. In addition, the electrochemically induced changes in hydrogeochemistry, e.g. precipitation and dissolution, are assessed.

2. Materials and methods

2.1. Column reactor

An undivided horizontal flow-through acrylic column reactor was used with an electrode configuration of cathode \rightarrow bipolar electrode \rightarrow anode ($\text{C} \rightarrow \text{BPE} \rightarrow \text{A}$) at a constant current of 120 mA. The level of the constant current was chosen based on a previous study with this reactor on the influence of current intensity on the contaminant removal (Hyldegaard et al., 2019b). The BPE polarizes between the cathode and anode, with a positive polarization of the side facing the cathode, while negative polarization of the side facing the anode (Rajic et al., 2016b). The set-up incl. dimensions, positions of electrodes and sampling ports is illustrated in Fig. 1. The electrode spacing was 4 cm, with the cathode positioned at 4.4 cm into the column. Sampling ports P0–P5 were glass tubes with fittings for mounting of syringes to facilitate sampling of porewater from within the middle of the porous matrix. Sampling ports for extraction of electrolytically generated gases were placed above the electrodes and contained septa for extraction using a syringe with needle. Gas extraction from the sampling ports above the electrodes occurred whenever a gas phase was visible in order to limit mass loss through volatilization of chlorinated ethenes. The need for gas extraction varied with the nature of the electrode, with an overall frequency of every 15–90 s.

The porous matrices were upstream, between and downstream the electrodes. Saturation of the electrochemical reactor with the groundwater feedstock solutions occurred at an elevated flow to limit volatilization of the chlorinated ethenes. A constant seepage velocity of 150 m yr^{-1} , corresponding to Darcy velocities of 0.01 cm min^{-1} , was maintained during the electrochemical application. An overview of the experiments carried out with the conditions of the stepwise more complex settings is given in Table 1. The temperatures given refer to the temperature of the test surroundings. Specifically for the reactor, heating near the electrodes was initially observed, but cooled over time to levels approximating those of the test surroundings. Heating locally near electrodes is also expected during a field-application.

The direct current was applied for a duration corresponding to one pore volume prior to the actual testing. The electrochemical treatment then continued for another two pore volumes, i.e. 20 h. Six sampling rounds were executed during this period. The samples extracted for analysis from each experiment were i) samples of the groundwater feedstock solution, ii) porewater extracted throughout the electrochemical reactor (sampling port P0–P5, Fig. 1), iii) effluent and iv) gas, continuously collected from above the electrodes in separate Tedlar® bags. The two control tests (Table 1 exp. 0) with no current applied were carried out with no electrodes mounted.

2.2. Chemicals and materials

Chemicals used were of analytical grade: PCE ($\geq 99\%$, Sigma-Aldrich), calcium sulfate dihydrate (Merck), hydrochloric acid (35%, VWR) and palladium(II) chloride (PdCl_2 , 99.9%, Alfa Aesar). Electrodes of mixed metal oxide meshes composed of IrO_2 and

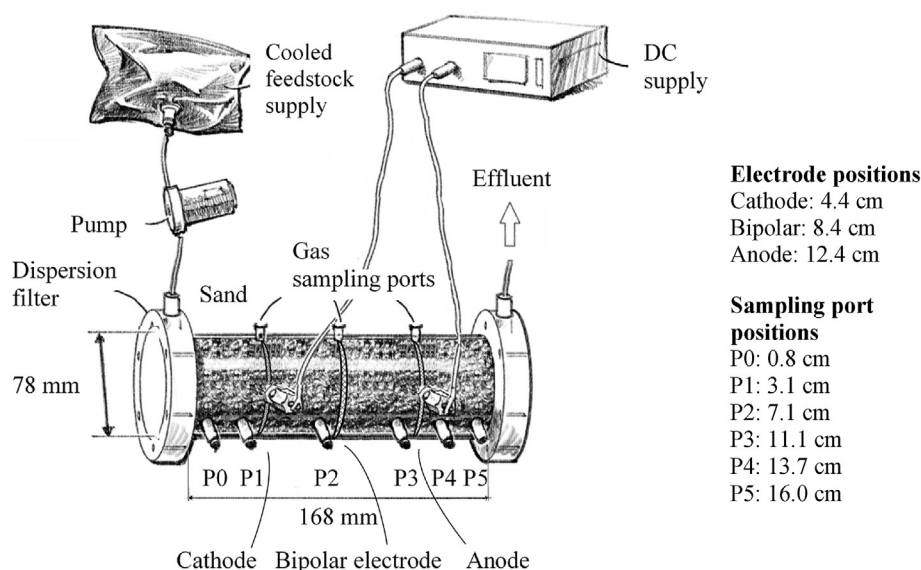


Fig. 1. Illustration of the electrochemical flow-through reactor with an electrode configuration of Pd/Fe foam cathode – MMO bipolar electrode – MMO anode. Sampling ports enable extraction of porewater (P0–P5) and gases generated. Measures refer to the inner dimensions.

Table 1

Experimental conditions for the assessment of electrochemical treatment in stepwise more complex and realistic aquifer conditions.

Exp.	Title ^b	Current [mA]	Groundwater solution	Porous matrix	Porosity, water-filled [%]	Temp. [°C]
0a	Control	0	Synthetic	Glass beads	30.1	22
0 b	Control	0	Field-extracted	Sandy sediment	34.6	22
1 ^a	Simple	120	Synthetic	Glass beads	38.9 ± 0.1	22
2 ^a	+ Field-GW	120	Field-extracted	Glass beads	39.0 ± 0.0	22
3 ^a	+ Sandy sediment	120	Field-extracted	Sandy sediment	40.7 ± 1.1	22
4 ^a	+ GW temp.	120	Field-extracted	Sandy sediment	41.7 ± 0.4	8–10

^a Duplicated testing.

^b GW: Groundwater.

Ta₂O₅ coating on titanium (MMO, 1.8 mm in width, diameter of 77 mm, 3 N International) were used as anodes and bipolar electrodes (BPE). Cathodes were iron foam (Fe, 3 mm in width, diameter of 77 mm, 45 pores per inch, 98% Fe, 2% Ni, Aibixi Ltd.) perforated with 4 mm holes with a spacing of 10 mm and coated with 1.33 mg Pd cm⁻² following the procedure previously described (Hyldegaard et al., 2019b). Porous matrices included inert solid glass beads (5 mm, 2.23 g cm⁻³, Propper Manufacturing Co. Inc.) and unrefined sandy aquifer material (15% calcium carbonate, 0.4% organic matter, grain size d(0.5) of 0.41 mm, and d(0.9) of 0.90 mm, Svogerslev Sand Quarry, DK) as previously characterized (Hyldegaard et al., 2019a). To prevent clogging of electrode openings, porous matrices were separated from electrodes by nylon meshes (0.1 mm in width, 0.12 mm wire diameter, 61 × 61 mesh size, 0.3 mm opening size, McMaster-Carr). Feedstock solutions of i) synthetic groundwater, prepared using 18.2 MΩcm high-purity Milli-Q water (Merck Synergy® UV Water Purification System) with 1.6 g L⁻¹ calcium sulfate, or ii) field-extracted groundwater (Skovlunde, DK) were stored in Tedlar® bags (Sigma-Aldrich) with minimal headspace to limit mass loss by volatilization. Major groundwater species are presented in Table 2.

The synthetic and field-extracted groundwater was spiked with PCE to a concentration of 2.7 mg L⁻¹. A saturated stock solution of free-phase PCE in deionized water was used. The field-extracted groundwater contained low levels of lower chlorinated ethenes (0.96 ± 0.29 μg TCE L⁻¹, 2.3 ± 0.53 μg *cis*-DCE L⁻¹). Constant groundwater flow was maintained by a peristaltic pump (Watson-

Marlow qdos30). Tygon® tubing (2.06 mm ID, 3.79 mm OD, Cole-Parmer) and Nalgene® PVC tubing (4 mm ID, 6 mm OD, VWR) was used to carry the effluent and inlet solution, respectively. Constant current was applied using one Magna-Power SL800–3.2/380 + LXI 0–800 V, 0–3.2 A, 0–2.6 kW power supply.

2.3. Analytical methods

Twelve volatile organic carbons (VOCs) were included in the analysis of liquid and gas samples: PCE, TCE, *cis*-1,2-dichloroethylene (*cis*-DCE), *trans*-1,2-dichloroethylene (*trans*-DCE), 1,1-dichloroethylene (1,1-DCE), vinyl chloride (VC), 1,1,1-trichloroethane (1,1,1-TCA), 1,2-dichloroethane (1,2-DCA), 1,1-dichloroethane (1,1-DCA), chloroethane, tetrachloromethane (PCM), trichloromethane (TCM) and for liquid samples also 1,4-dioxan. VOCs in liquid samples were measured as described in Hyldegaard et al. (2019a) after diluting 0.4 mL sample in 1.6 mL Milli-Q water to reduce the total sampling volume. VOCs in collected gas from above each electrode were trapped by pumping each sample from the Tedlar® bags through a tube containing activated carbon (Dräger Orsa 5 sampling tubes, Eurofins, Denmark) at a flow of 30 mL min⁻¹. Subsequently, before analysis, VOCs were desorbed at Eurofins using carbon disulfide for analysis on an Agilent 7890 GC with Agilent 5977 HES MSD equipped with an Agilent DB-624 1.8 μm FT column (ID 0.32 mm × 30 m). The hydrocarbons acetylene, ethene, ethane and methane were measured in 4 mL of porewater extracted from sampling port

Table 2
Characterization of the synthetic and field-extracted groundwater tested.

	Synthetic groundwater	Field-extracted groundwater
Cl ⁻ [mM]	< D.L. ^a	1.17 ± 0.072
NO ₃ ⁻ [mM]	0.019	0.016 ± 0.003
SO ₄ ²⁻ [mM]	6.73	1.12 ± 0.054
Ca [mM]	6.26 ± 0.648	3.59 ± 0.612
K [mM]	0.0005 ± 0.0001	0.057 ± 0.009
Mg [mM]	0.001 ± 0.0005	0.567 ± 0.083
Na [mM]	0.008 ± 0.0002	0.698 ± 0.124
Si [mM]	0.0002 ± 0.0001	0.326 ± 0.046
pH [-]	5	7
Conductivity [μS cm ⁻¹]	1175 ± 71.4	804 ± 62.6

^a D.L.: Detection limit.

P0–P5 of the final sampling round of each experiment according to the procedure previously described (Hyldegaard et al., 2019a). Concentrations of anionic species (Cl⁻, NO₃⁻, SO₄²⁻) were measured using 0.5 mL of every liquid sample extracted (i-iii) following the previously outlined method (Hyldegaard et al., 2019a). Chemical elements (As, Ba, Ca, Cd, Co, Cr, Cu, K, Mg, Mo, Na, Ni, P, Pb, Sb, Se, Si, Sr, Ti, V, Zn, Zr) in the groundwater feedstock solution and effluent were measured using 5 mL sample and the equipment specified earlier (Hyldegaard et al., 2019a). Prior to analysis of the chemical elements in groundwater feedstock solutions, samples were filtered using 0.2 μm PVDF syringe filters from Jin Teng. Conductivity, pH and hydrogen peroxide (H₂O₂) content of each liquid sample extracted was measured using a Horiba Scientific LAQUAtwin-EC-11 m, EMD Millipore™ MColorpHast™ pH test strips and EMD Millipore™ MQuant™ Peroxide Test strips in intervals of 0.5–25 and 1–100 mg L⁻¹, respectively, requiring 0.2 mL of sample for each analytical parameter. The content of organic matter in the sandy sediment was determined as loss of ignition at 550 °C. Standard deviations of the analytical data set were derived using the Microsoft Excel function “stdev.p”.

3. Results and discussion

A significant mass loss of PCE between the groundwater feedstock solution and column reactor, i.e. over the tubing and/or pump, was seen. The mass loss was up to 91% PCE. Thus, in the following, all initial concentrations of PCE have been adjusted for the 91% mass loss such that the data present the true changes induced by the electrochemical treatment. The adjustment level is conservatively defined and covers the mass loss upstream the column reactor (from the groundwater feedstock solution to sampling port P0) and the possible low contribution of sorption to the sandy sediment.

3.1. The hydrogeochemistry

For electrochemical testing in reactors loaded with glass beads using synthetic groundwater (exp. 1) and field-extracted groundwater (exp. 2), the development in pH throughout the reactors were similar, with increase to pH 10–12 in sampling ports P0–P2 and decrease to pH 4–5 in sampling ports P4–P5 (Fig. 2a, Δ-□). Thus, with glass beads, the alkaline front distributed upgradient the electrochemical zone to sampling ports P0–P1, and the acidic front distributed downgradient the electrochemical zone to sampling ports P4–P5. The conductivity was elevated throughout the reactor at the final sampling round compared to the initial levels for testing with synthetic groundwater (Fig. 2b, Δ, exp. 1), and elevated in sampling ports P4–P5 for testing with field-extracted groundwater (Fig. 2b, □, 14–16 cm, exp. 2). Thus, in glass beads, the conductivity downgradient the electrochemical zone in sampling ports P4–P5

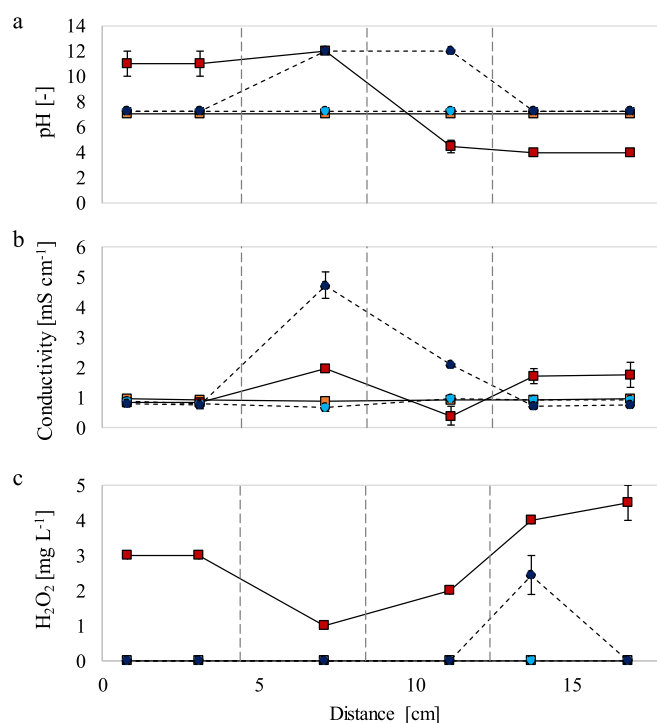


Fig. 2. Development in a) pH, b) conductivity and c) H₂O₂ throughout the electrochemical reactors measured pre- and post-treatment for testing in simplified settings (exp. 1, Δ, light grey vs. black), field-extracted groundwater (exp. 2, □, orange vs. red), sandy sediment (exp. 3, ○, light blue vs. dark blue) and groundwater temperatures of 8–10 °C (exp. 4, ◇, light green vs. dark green). Following the flow direction, the position of cathode – bipolar electrode – anode is marked with grey dashed vertical lines. Experiment numbers refer to specifications in Table 1. (For interpretation of the references to colour in this figure legend, the reader is referred to the Web version of this article.)

increased beyond the initial levels. Hydrogen peroxide (H₂O₂) formed during the electrochemical application in glass beads and distributed throughout the reactors (Fig. 2c, Δ-□). When replacing the glass beads with the sandy sediment using field-extracted groundwater (exp. 3), the patterns for changes in pH, conductivity and concentration of H₂O₂ changed (Fig. 2, ○): pH was maintained neutral upgradient (P0–P1) and downgradient (P4–P5) the electrochemical zone (Fig. 2a, 0–3 cm, 14–16 cm), indicating that OH⁻ formed at the cathode was less distributed and H⁺ formed at the anode was buffered by the carbonate system within the sandy sediment and thereby less distributed. The conductivity in the solution downgradient the electrochemical zone in sampling ports P4–P5 stabilized at levels corresponding to initially (Fig. 2b, ○). Another significant effect from the sandy sediment (exp. 3)

compared to glass beads (exp. 2) is the distribution of H_2O_2 , which in the sandy sediment was limited to the oxidizing zone of the anode (P4), while it was distributed throughout the entire reactor with glass beads (Fig. 2c, \circ vs. \square). For testing at groundwater temperatures of 8–10 °C (exp. 4), levels of H_2O_2 formed were similar to those in glass beads (exp. 2), while the distribution remained limited to the vicinity of the anode (P3–P5) (Fig. 2c, \diamond vs. \square). The elevated levels of H_2O_2 measured at temperatures of 8–10 °C compared to at 22 °C may be an indication of temperature dependent reaction kinetics expressed as a slowed H_2O_2 consumption for decomposition of e.g. organic matter.

Changes in concentrations of SO_4^{2-} , NO_3^- and Cl^- were observed as a result of the applied current (Fig. S1). With field-GW (exp. 2), the concentrations of SO_4^{2-} , NO_3^- and Cl^- overall increased within the electrochemical zone from 0.07, 0.01 and 0.04 mM in sampling port P0 to 1.6, 0.03 and 1 mM, respectively in sampling ports P4–P5 (Fig. S1b). This could be due to electromigration in the groundwater between the electrodes towards the anode. The electromigration of these anions was in the direction of groundwater flow, and since a concentration was seen, the electromigration occurred at a higher flow than advection. With the sandy sediment (exp. 3), the concentrations of SO_4^{2-} and Cl^- decreased to 0.2 and 0.03 mM, respectively, in sampling port P2 (in the reducing zone), whereas the concentrations increased in sampling port P4 (in the oxidizing zone), to app. initial levels of 1 mM (Fig. S1c). Concentrations of NO_3^- continuously increased throughout the reactor from initially below detection limit to app. 0.02 mM. The increase in NO_3^- could be due to oxidation of NH_4^+ possibly present in the water, or release of organic N in the sandy sediment, which is then oxidized. At GW temperatures of 8–10 °C (exp. 4), the behavior of SO_4^{2-} and Cl^- was similar, while NO_3^- maintained a more steady level throughout the reactor (Fig. S1d). Based on these trends in the sandy sediment, electromigration, and electrochemical oxidation and reduction processes seemed to control the changes observed in porewater composition. Over time, the concentrations of SO_4^{2-} , Cl^- and NO_3^- downgradient the electrochemical zone (sampling port P5) showed a decreasing trend in each of the experiments conducted (exp. 1–4). Reduction and oxidation of SO_4^{2-} and Cl^- within the electrochemical reactor was observed in a previous study (Hyldegaard et al., 2019a). The decrease in SO_4^{2-} could also be due to deposition of CaSO_4 , with Ca being released during buffering of the H^+ formed at the anode. The decrease in Cl^- could be an indication of $\text{Cl}_{2(g)}$ formation at the anode (Bagastyo et al., 2011; Martínez-Huitle et al., 2015).

Changes in concentrations of Ca, Si, Mg, Na, K in the porewater were observed (Fig. S1). During exp. 2 with field-GW, a decrease of 97% Ca (4.5–0.13 mM), 99% Mg (0.80–0.01 mM), 89% Na (1.1–0.12 mM) and 89% K (0.09–0.01 mM) was found in samples of the effluent (Fig. S1b), which indicates precipitation within the column and/or surface reactions on the glass beads (Gin et al., 2016). The precipitation and/or surface reactions on the glass beads were probably in the reducing zone (sampling ports P1–P2) due to the high pH here (Backhouse et al., 2018). The Si concentration increased by 34% (0.46–0.62 mM), confirming the surface reactions on the glass beads (Abraitis et al., 2000; Backhouse et al., 2018). In exp. 3 with sandy sediment, the decrease in concentration was less for Ca (19%, 4.9 to 4.0 mM) and Mg (81%, 0.25 to 0.05 mM) in samples of the effluent, and a similar decrease was seen for Na (93%, 1.3 to 0.09 mM) and K (84%, 0.18 to 0.03 mM), whereas the concentration of Si increased by 72% (0.34–0.58 mM) (Fig. S1c). At GW temperatures of 8–10 °C (exp. 4), decreases of 22% Ca (4.3–3.3 mM), 89% Mg (0.35–0.04 mM), 64% Na (0.97–0.35 mM) and 74% K (0.16–0.04 mM) were observed, while Si increased by 36% (0.28–0.37 mM) (Fig. S1d). White precipitates formed over time on the uppermost part of the cathode and BPE in exp. 1–4,

where the gas phase shortly accumulated prior to extraction, which suggests precipitation of Ca (Hyldegaard et al., 2019a). An overall lower removal of Ca within the sandy sediment (exp. 3–4), combined with the maintained neutral pH (Fig. 2a, \circ – \diamond , 14–16 cm), indicate dissolution of calcite in the sandy sediment in the acidic zone of the anode (sampling ports P3–P4), possibly related to a higher buffering capacity of the sandy sediment. In addition, supersaturation of Ca-carbonate may lead to formation of colloids in the reducing zone of the cathode, which are carried by flotation and subsequently dissolved in the oxidizing zone of the anode (Hyldegaard et al., 2019a). Mg possibly co-precipitate with Ca, and is subject to cation exchange like Na and K (Hyldegaard et al., 2019a). Dissolution of silicate minerals in the sandy sediment may explain the higher increase in Si concentrations in comparison to the glass bead experiments. Electric fields are shown to induce weathering of soil particles with release of Si (Skibsted et al., 2018).

The simplest experiment using glass beads and synthetic groundwater (exp. 1) is most comparable with the experimental conditions in the literature (synthetic groundwater with few salts added, inert porous materials and testing at room temperature) (Carter and Farrell, 2009; Mao et al., 2012a, 2012b; Yuan et al., 2013a, 2013b; Rajic et al., 2014, 2015a; 2015b, 2015c; 2016a, 2016b; Fallahpour et al., 2016, 2017; Zhou et al., 2018). However, studies have focused on optimization for TCE removal with little information being available on developments in pH, conductivity and porewater composition throughout the reactors. Reported is:

- Distribution of H_2O_2 throughout the electrochemical zone (Rajic et al., 2016b)
- Formation of H_2O_2 in concentrations of $\geq 0.5 \text{ mg L}^{-1}$ (Mao et al., 2012a; Yuan et al., 2013a; Zhou et al., 2018)
- Depending on the reactor design, pH in the effluent was often alkaline (Mao et al., 2012a, 2012b; Fallahpour et al., 2016; Zhou et al., 2018) or acidic (Yuan et al., 2013a)

With offset in the literature on electrochemical treatment of chlorinated ethenes obtained in simplified systems, the main differences obtained in more realistic settings (field-realistic flow rate, field-extracted groundwater, sandy sediment and groundwater temperatures) are:

- Maintenance of neutral pH up- and downgradient the electrochemical treatment zone
- Higher ionic conductivity in the reducing zone, but overall unaffected when comparing final levels downgradient the electrochemical zone with the initial levels
- Less extensive distribution of H_2O_2 formed within the electrochemical zone
- Introduction of competing redox reactions mainly for SO_4^{2-} and Cl^-
- Removal of Ca, Mg, Na and K, and release of Si, presumably related to dissolution with net precipitation of minerals

Considering a field-application, a low impact on the environment around the treatment zone is preferable, wherefore the findings of unaltered pH and conductivity downgradient the electrochemical zone in sandy sediment are encouraging. Precipitation could lead to coverage of electrodes and clogging of pores in the sandy sediment for long-term applications, which may be solved by short-term polarity reversals (Gilbert et al., 2010). Less spreading of electrochemically generated H_2O_2 in sandy sediment than in glass beads may influence the needed electrode spacing in a field-application if this indirect oxidation pathway is a major factor for the chlorinated ethene removal, as discussed later in this paper.

3.2. Chlorinated ethene removal

The influence of natural field-parameters (typical flow rate, field-extracted groundwater, sandy sediment, groundwater temperatures) on the electrochemically induced PCE removal is summarized in Fig. 3. The control experiments (exp. 0a-0b) are included as references to the general mass loss and sorption to the sandy sediment, which accounted for <3%. A low sorption of the chlorinated ethenes to the sandy sediment was expected (Pankow et al., 1996; Zhao et al., 2005).

In the most simple system (exp. 1), the electrochemical method removed $50 \pm 9\%$ of PCE (Fig. 3), reaching concentrations of $17.5 \pm 3.0 \mu\text{g L}^{-1}$ in sampling port P5. In similar experiments, >99% removal of TCE has been reported (Rajic et al., 2015a, 2016a), suggesting that the reactor could be further optimized and/or TCE is more easily removed. Testing with field-extracted groundwater (exp. 2) increased the PCE removal to $70 \pm 9\%$ with final concentrations of $13 \pm 4 \mu\text{g L}^{-1}$. Thus, the observed competing redox reactions for SO_4^{2-} and Cl^- , and stimulated precipitation, dissolution and/or cation exchange for Ca, Mg, Na, K and Si did not influence the PCE removal negatively. The reported impact on TCE removal due to concurrent reduction of NO_3^- (Rajic et al., 2016a; Fallahpour et al., 2017), was not observed in this study where NO_3^- was not reduced. The different behaviors of NO_3^- may be related to a combination of differences in operation conditions and complexity of the systems studied. This study is operated at a higher current intensity, wherefore the reduction potentials near the cathode may be lower and thereby favoring reduction of other hydro-geochemical species present in the system before reduction of NO_3^- . Heavy metals have also been shown to negatively influence the electrochemical transformation of chlorinated ethenes (Mao et al., 2012b; Fallahpour et al., 2017), however, heavy metals (As, Ba, Cd, Co, Cr, Cu, Mo, Ni, Pb, Sb, Se, Sr, Ti, V, Zn, Zr) were not detected in the groundwater solutions studied. The additional influence on the PCE removal from the sandy sediment (exp. 3) and GW-temperatures of $8-10^\circ\text{C}$ (exp. 4) was not statistically significant. However, a tendency of enhanced removal in the sandy sediment, reaching $80 \pm 7\%$ with final concentrations of $7.8 \pm 2.3 \mu\text{g L}^{-1}$ at 22°C , was observed (Fig. 3, exp. 3). At temperatures of $8-10^\circ\text{C}$, the PCE removal of $74 \pm 5\%$ was also statistically insignificant (Fig. 3, exp. 4), reaching concentrations of $19.3 \pm 6.3 \mu\text{g L}^{-1}$. The reaction rates were expected to be lower at the low temperatures, but the data indicate, that the effect on PCE removal at temperatures of 8 and 22°C is little. Improved removal within the sandy sediment could be due to enhanced release of gases generated at the electrodes as

observed in a limestone setting (Rajic et al., 2015b). The pore spaces of the glass bead matrix were larger than those of the sandy sediment, which resulted in some gas accumulation in the glass bead matrix, leading to a partial gas coverage of the electrodes. Thus, less electrode surface sites were available for direct transformation of PCE. On the other hand, presence of organic matter in the sediment could inhibit the chlorinated ethene removal by consuming electrons available at the electrodes (Rajic et al., 2015b; Fallahpour et al., 2017). In the present study, the influence of organic matter on PCE removal appeared insignificant and/or counteracted by other mechanisms introduced with the complex hydro-geochemistry. The present results suggest that i) adequate reaction rates for electrochemical removal of PCE may be obtained in natural field-settings, and ii) overall trends on electrochemically induced PCE removal observed in room temperature lab studies may be transferred to the field, assuming only minor influence of additional site-related dynamics.

In the electrochemical systems assessed, the mass conservation of Cl (summing aqueous and gaseous Cl in VOCs and free Cl^-) was >81% and <97%, being lowest for the most complex system (exp. 4) and highest in the simple settings (exp. 1). Similar Cl recoveries have been reported for electrochemical treatment of TCE (Mao et al., 2011; Rajic et al., 2016a). With no mass loss observed during the control testing (exp. 0a-0b), the reduced mass conservation in electrochemical systems was possibly due to lack of analysis of commonly formed chlorinated compounds, e.g. ClO^- , ClO_3^- , HOCl , ClO_4^- , Cl_2 (Chen et al., 1999; Bagastyo et al., 2011; Radjenovic and Sedlak, 2015). VOCs in the gas collected accounted for $0.10 \pm 0.05\%$ of the chlorinated ethene removals observed in the porewater.

3.3. Transformation mechanisms

Reducing and oxidizing zones were formed in the electrochemical reactor. Consequently, several chlorinated ethene transformation mechanisms could occur concurrently; a) direct reduction at cathodic sites (Wang and Farrell, 2003; Mao et al., 2012b; Yuan et al., 2012), b) direct oxidation at anodic sites (Sáez et al., 2009; Lakshmipathiraj et al., 2012), c) indirect reduction via hydrogen formed within the electrochemical reactor (Farrell et al., 2000; Martínez-Huitle et al., 2015), d) indirect oxidation via reactive oxygen species formed within the electrochemical zone, e.g. H_2O_2 and $\bullet\text{OH}$ (Ndjou'ou et al., 2006; Yuan et al., 2012; Rajic et al., 2016b; Zhou et al., 2019a), e) biotic sequential reductive dechlorination by *Dehalococcoides* possibly present in the field-extracted

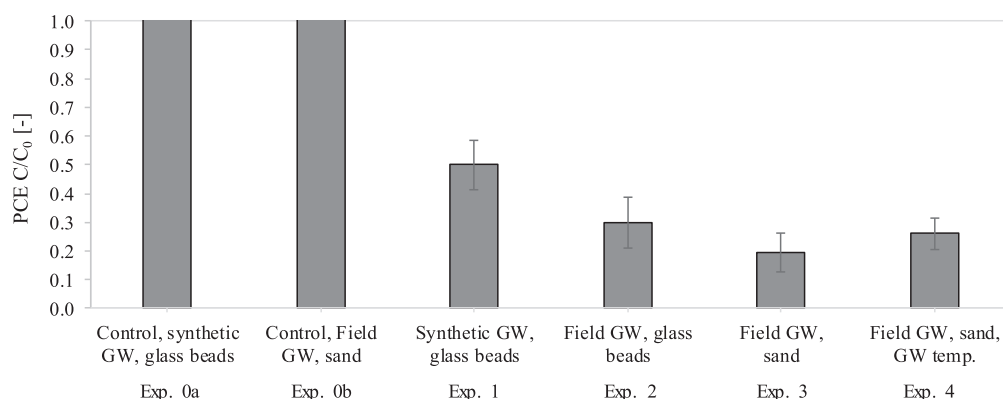


Fig. 3. PCE removal in the electrochemical reactor for a stepwise addition of the contaminated site parameters field-extracted groundwater (GW), sandy sediment and groundwater temperatures of $8-10^\circ\text{C}$. Experiment numbers refer to specifications in Table 1.

groundwater, being stimulated by reducing conditions and the generated H_2 electron donor (Aulenta et al., 2009, 2010, 2011, 2013; Lai et al., 2015; Li and Yu, 2015; Wang et al., 2015), and f) biotic stimulated oxidation (Tiehm et al., 2009; Aulenta et al., 2013). Chlorinated ethene degrading microbial cultures, e.g. *Dehalococcoides*, have been detected in low levels in the groundwater at the contaminated site from which the field-extracted groundwater was sampled (Schiefler et al., 2018).

Removal of PCE was observed throughout the electrochemical zone in glass beads (exp. 1–2), ascribed to the widespread distribution of H_2O_2 formed and thereby indirect oxidation (transformation mechanism d). In exp. 3 and 4, with sandy sediment, removal of PCE was mainly observed in the reducing zone of the cathode. The limited distribution of H_2O_2 in the sandy sediment (Fig. 2c, $\circ-\diamond$) could explain the observed behavior, since a reducing zone is maintained. In the glass beads, the widespread distribution of H_2O_2 destroyed the reducing zone here. Since, the highest removals were obtained in the complex settings (Fig. 3, exp. 3–4), where PCE removal was confined to the reducing zone (sampling ports P1–P2), PCE removal via reduction (transformation mechanism a and c) appeared more efficient than by indirect oxidation. From this investigation, it is not possible to determine the influence from each of the transformation mechanisms listed (a–f), however, data indicate, that reduction is more important than oxidation when the sand separates the two zones effectively.

The initial composition of the synthetic and field-extracted groundwater (sampling port P0) and after electrochemical treatment (sampling port P5) is shown in Fig. S2. The field-extracted groundwater contained an aged contamination of PCE with TCE and *cis*-DCE (Fig. S2a exp. 0 b, 2–4), with the majority of the PCE added by spiking. Within the electrochemical zone, intermediate chlorinated ethenes were formed in low amounts, but no chlorinated intermediates left the electrochemical zone. Thus, TCE and *cis*-DCE in the aged contamination were removed completely within the reducing and oxidizing zones of the reactor (Fig. S2b exp. 2–4). The only chlorinated compound that accumulated and thereby escaped the electrochemical zone was trichloromethane (TCM), also known as chloroform (Fig. S2b, exp. 1–4). Formation of TCM is problematic because TCM is e.g. hazardous to health (Ruder, 2006).

The amount of Cl^- available from transformation of PCE was low compared to the concentrations of TCM formed, making it improbable that PCE was the source of TCM. However, the natural content of Cl^- in the field-extracted groundwater was abundant, though not the only factor for TCM production. The electrochemical treatment within the sandy sediment increased the formation of

TCM by 750% compared to treatment in field-extracted groundwater and glass beads (Fig. 4, exp. 4 vs. 2). Obviously, the sandy sediment played an important, but unclear role in the formation of TCM (Fig. 4). Others have reported formation of TCM through i) a multistep process with oxidation of organic matter in presence of chloride (Chaidou et al., 1999; Haselmann et al., 2000; Bagastyo et al., 2011; Rebelo et al., 2016; Zhao et al., 2016), ii) a combination of photolysis and oxidation by H_2O_2 of chlorinated ethenes (Alibegic et al., 2001; Dobaradaran et al., 2014), and iii) reduction of carbon tetrachloride (Lowry and Reinhard, 1999; Doong et al., 2003; Molina et al., 2003). The fraction of organic matter in the sandy sediment was 0.4%, influence of UV may not have been entirely avoided despite attempts to do so, and it is possible that carbon tetrachloride formed by cleavage of PCE (Sáez et al., 2009) subsequently reduced to TCM. Thus, formation of TCM in the sandy sediment could be a contribution of multiple processes. The low concentrations of TCM formed in glass beads (exp. 1–2) could be due to a residue of sandy sediment in the column reactor and/or traces of organic matter in construction components used (Sale et al., 2005), e.g. O-rings, silicone grease and/or in tubing.

The reduced distribution of H_2O_2 observed within the sandy sediment (Fig. 2c, $\circ-\diamond$) could be partly due to oxidation of organic matter in the sediment. If the reactant, e.g. organic matter, involved in the production of TCM is locally exhausted within the electrochemical zone over time, the rate of electrochemically induced TCM transformation (McNab and Ruiz, 1998; Sonoyama and Sakata, 1999; Molina et al., 2002; Chen et al., 2003; Velázquez et al., 2016) eventually could exceed the rate of formation. In this study, the concentrations of TCM leaving the electrochemical zone decreased over time: In the simple system (exp. 1) by $57.3 \pm 30.6\%$, with field-GW (exp. 2) by $17.1 \pm 17.1\%$, with sandy sediment (exp. 3) by $38.7 \pm 2.2\%$, and at groundwater temperatures (exp. 4) by $15.0 \pm 6.0\%$. I.e., prolonged treatment time may overcome the challenge of TCM accumulation.

It is reported, that H_2O_2 formation can be effectively catalyzed by Pd on cathodes at $pH < 4$ (Yuan et al., 2013b; Rajic et al., 2014; Zhou et al., 2018). In this study, only tests conducted with glass beads reached a pH of 4, while testing in sandy sediment maintained a $pH \geq 7$ (Fig. 2a, $\Delta-\square$ vs. $\circ-\diamond$). Nevertheless, H_2O_2 was formed in every experiment conducted and in high quantities (Fig. 2c). At the anode or in the close proximity of the anode, pH could be lower than what was measured in sampling ports P3–P4. Also, Pd may be capable of catalyzing formation of H_2O_2 at neutral pH (Zhou et al., 2019b), or the formation of H_2O_2 was due to a sufficiently high concentration of dissolved oxygen. Based on stoichiometry calculations on oxidation of PCE by H_2O_2 , under

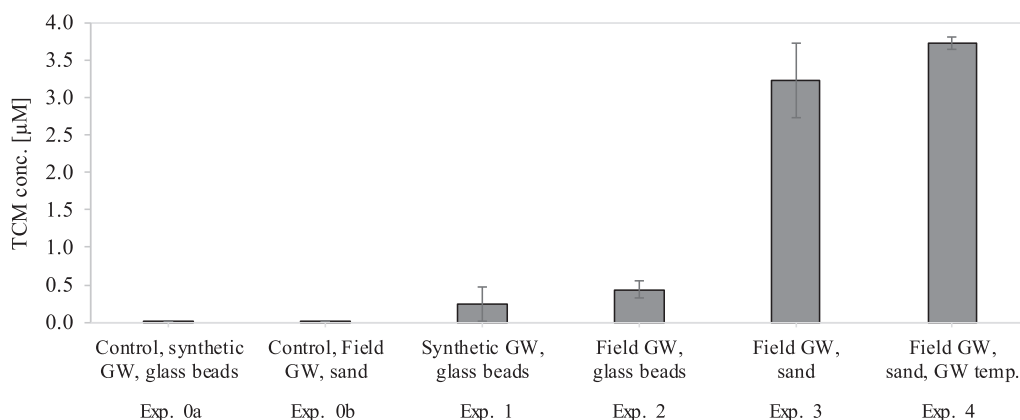


Fig. 4. TCM formation measured in sampling port P5 at conclusion of testing. Experiment numbers refer to specifications in Table 1.

assumption of no competing reactions, $0.5 \text{ mg H}_2\text{O}_2 \text{ L}^{-1}$ was sufficient for removal of the maximum $0.9 \text{ mg PCE L}^{-1}$ reaching the reactor. That is whether H_2O_2 oxidized PCE directly or was converted to $\bullet\text{OH}$, which then oxidized the PCE. The maximum concentration of H_2O_2 measured was 5 mg L^{-1} , which in theory could oxidize 12 mg PCE L^{-1} . I.e., despite possibly competing and concurrent consumption of H_2O_2 , the measured concentrations were in excess and exceeded the minimum required level for complete PCE removal by 4–10 times (Fig. 2c, $\circ-\diamond$). The concentration of H_2O_2 is considered being a net excess amount in that oxidation of H_2O_2 oxidizable compounds are assumed continuously ongoing.

Combining the outlined findings, reduction is suggested to be the dominant transformation mechanism for PCE in near-natural aquifer settings. Formation of reactive oxygen species followed by oxidation of organic matter may explain the formation of TCM. However, the reaction mechanisms need to be better understood and especially the role of the sandy sediment on formation of TCM. Reaction rates calculated based on PCE concentrations measured throughout the experiments in sampling port P5, in which the contribution of each transformation pathway is expected to be largest, did not follow a simple 0th, 1st, 2nd or 3rd order reaction. Overall, best fits were obtained with 3rd order reaction models. Over time, as the contaminant concentrations dropped, the reaction rates decreased despite a constant current and generally stable potential differences. Thus, the resulting low contaminant concentrations are probably the most challenging to treat, wherefore they require an extended treatment time, as indicated by lower reaction rates. As the concentration is lowered, the system approaches equilibrium, wherefore a higher electrochemical driving force is required to maintain the same rate.

3.4. Implications for in situ application

Power consumption during the electrochemical treatment was estimated via the constant current and measured potential differences. The power consumption was proportional to the ionic strength of the system tested, i.e. lowest for the synthetic groundwater (exp. 1) and highest for the field-extracted groundwater flowing through glass beads (exp. 2) (Fig. 5). For the most

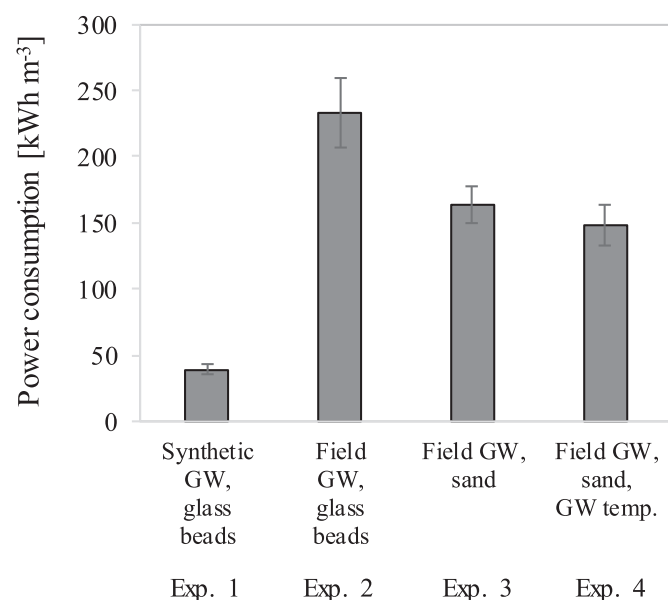


Fig. 5. Power consumption per volume of water treated, estimated based on constant current and measured voltages. Experiment numbers refer to specifications in Table 1.

complex system (exp. 4), the power consumption was around 0.25 kWh or 147 kWh m^{-3} of water treated (Fig. 5). For the electrochemical application in sandy sediment (exp. 3–4), the potential differences initially increased to levels of 320 V followed by a decrease and stabilization at around 60 V . Thus, prolonged treatment would lower the overall power consumed per volume of contaminated water treated. In comparison, for exp. 2, the potential difference stabilized at app. 110 V . In the field, the power supply can optionally be supported by sustainable power sources like solar panels (Sale et al., 2005; Martínez-Huitle et al., 2015; Lima et al., 2017).

Application of the electrochemical treatment in sandy sediment restricted the distribution of the reactive oxidant H_2O_2 to around the anode, shifting the PCE removal pathway from indirect oxidation towards reduction. The highest PCE removal reached was obtained within the most realistic aquifer settings studied, which is promising for the future of this technology. In addition, this study showed, that less chlorinated ethenes in an aged contamination can be targeted concurrently. Testing and optimization in the field is needed, but with the demonstrated removals reaching PCE concentrations of $7.8 \pm 2.3 \mu\text{g L}^{-1}$ in a simulated PCE plume in near-natural settings, combined with prolonged treatment and natural attenuation, regulatory levels of the chlorinated ethenes may be within reach (USA: $5 \mu\text{g L}^{-1}$ (US Environmental Protection Agency of Water, 2018), Denmark: $1 \mu\text{g L}^{-1}$ (Miljøstyrelsen Danish EPA, 2018).

4. Conclusions

Electrochemical removal of an aged, partially degraded PCE contamination was studied at a typical groundwater flow rate in a flow-through reactor. Field-extracted groundwater, sandy sediment and groundwater aquifer temperatures were stepwise added for assessment on the impact of complex hydrogeochemistry and temperatures of $8\text{--}10^\circ\text{C}$ on the contaminant removal. Major findings include:

- The aged, partially degraded, PCE contamination was concurrently degraded in the electrochemical treatment zone without formation of chlorinated degradation products
- Highest contaminant removal was observed in the most complex, field-realistic settings. PCE concentrations of $7.8 \pm 2.3 \mu\text{g L}^{-1}$ were reached with TCE and *cis*-DCE being completely removed
- High levels of the oxidant H_2O_2 of 5 mg L^{-1} were measured within the electrochemical zone. Yet, reduction processes appeared more efficient in removal of the chlorinated ethenes. The distribution of H_2O_2 was limited to the oxidizing zone in sandy sediment in contrast to throughout the reactor in glass beads
- Trichloromethane was formed mainly in sandy sediment explained by oxidation of organic matter in the sandy sediment in presence of Cl^- in the groundwater
- pH and conductivity maintained initial levels up- and down-gradient the electrochemical zone in sandy sediment, while they were altered for application in glass beads
- Competing redox reactions introduced with the complex chemistry of the field-extracted groundwater were limited to mainly SO_4^{2-} and Cl^-
- Dissolution and precipitation of minerals was observed, which affected the concentration of Ca, Mg, Na, K and Si

Despite presence of complex hydrogeochemistry and the implied competing reactions, the net influence on the chlorinated ethene removal was an overall enhancement. This study

demonstrates promising results for the further development of electrochemical treatment of chlorinated ethenes towards field-application for management of groundwater plumes.

Declaration of competing interest

None.

Acknowledgements

This work was supported by the Innovation Fund Denmark [grant number 5016-00165B]; COWIfonden [grant number C-131.01], the Capital Region of Denmark [grant number 14002102], the Danish Ministry of Higher Education and Science [grant number 7079-00012B], COWI A/S and Technical University of Denmark. A special thanks to Professor Akram Alshawabkeh, Northeastern University, for access to the acrylic column and associated fitted electrodes for customization to comply with the lab work requirements of this study. The sandy sediment was kindly donated by Nymølle Sand Quarry, Denmark.

Appendix A. Supplementary data

Supplementary data to this article can be found online at <https://doi.org/10.1016/j.chemosphere.2019.125340>.

References

- Abraitis, P.K., Livens, F.R., Monteith, J.E., Small, J.S., Trivedi, D.P., Vaughan, D.J., Wogelius, R.A., 2000. The kinetics and mechanisms of simulated British Magnox waste glass dissolution as a function of pH, silicic acid activity and time in low temperature aqueous systems. *Appl. Geochem.* 15, 1399–1416.
- Alibegic, D., Tsuneda, S., Hirata, A., 2001. Kinetics of tetrachloroethylene (PCE) gas degradation and byproducts formation during UV/H₂O₂ treatment in UV-bubble column reactor. *Chem. Eng. Sci.* 56, 6195–6203.
- Aulenta, F., Canosa, A., Reale, P., Rossetti, S., Panero, S., Majone, M., 2009. Microbial reductive dechlorination of trichloroethene to ethene with electrodes serving as electron donors without the external addition of redox mediators. *Biotechnol. Bioeng.* 103, 85–91.
- Aulenta, F., Reale, P., Canosa, A., Rossetti, S., Panero, S., Majone, M., 2010. Characterization of an electro-active biocathode capable of dechlorinating trichloroethene and cis-dichloroethene to ethene. *Biosens. Bioelectron.* 25, 1796–1802.
- Aulenta, F., Tocca, L., Verdini, R., Reale, P., Majone, M., 2011. Dechlorination of trichloroethene in a continuous-flow bioelectrochemical reactor: effect of cathode potential on rate, selectivity, and electron transfer mechanisms. *Environ. Sci. Technol.* 45, 8444–8451.
- Aulenta, F., Verdini, R., Zeppilli, M., Zanolli, G., Fava, F., Rossetti, S., Majone, M., 2013. Electrochemical stimulation of microbial cis-dichloroethene (cis-DCE) oxidation by an ethene-assimilating culture. *Nat. Biotechnol.* 30, 749–755.
- Backhouse, D.J., Fisher, A.J., Neeway, J.J., Corkhill, C.L., Hyatt, N.C., Hand, R.J., 2018. Corrosion of the international simple glass under acidic to hyperalkaline conditions. *npj Mater. Degrad.* 2, 1–10.
- Bagastyo, A.Y., Radjenovic, J., Mu, Y., Rozendal, R.A., Batstone, D.J., Rabae, K., 2011. Electrochemical oxidation of reverse osmosis concentrate on mixed metal oxide (MMO) titanium coated electrodes. *Water Res.* 45, 4951–4959.
- Carter, K.E., Farrell, J., 2009. Electrochemical oxidation of trichloroethylene using boron-doped diamond film electrodes. *Environ. Sci. Technol.* 43, 8350–8354.
- Chaidou, C.I., Georgakilas, V.I., Stalikas, C., Saraçi, M., Lahaniatis, E.S., 1999. Formation of chloroform by aqueous chlorination of organic compounds. *Chemosphere* 39, 587–594.
- Chen, G., Betterton, E.A., Arnold, R.G., 1999. Electrolytic oxidation of trichloroethylene using a ceramic anode. *J. Appl. Electrochem.* 29, 961–970.
- Chen, G., Betterton, E.A., Arnold, R.G., Ela, W.P., 2003. Electrolytic reduction of trichloroethylene and chloroform at a Pt- or Pd-coated ceramic cathode. *J. Appl. Electrochem.* 33, 161–169.
- Dobaradaran, S., Lutze, H., Mahvi, A.H., Schmidt, T.C., 2014. Transformation efficiency and formation of transformation products during photochemical degradation of TCE and PCE at micromolar concentrations. *J. Environ. Heal. Sci. Eng.* 12, 1–10.
- Doong, R.A., Chen, K.T., Tsai, H.C., 2003. Reductive dechlorination of carbon tetrachloride and tetrachloroethylene by zerovalent silicon - iron reductants. *Environ. Sci. Technol.* 37, 2575–2581.
- Fallahpour, N., Mao, X., Rajic, L., Yuan, S., Alshawabkeh, A.N., 2017. Electrochemical dechlorination of trichloroethylene in the presence of natural organic matter, metal ions and nitrates in a simulated karst media. *J. Environ. Chem. Eng.* 5, 240–245.
- Fallahpour, N., Yuan, S., Rajic, L., Alshawabkeh, A.N., 2016. Hydrodechlorination of TCE in a circulated electrolytic column at high flow rate. *Chemosphere* 144, 59–64.
- Farrell, J., Melitas, N., Kason, M., Li, T., 2000. Electrochemical and column investigation of iron-mediated reductive dechlorination of trichloroethylene and perchloroethylene. *Environ. Sci. Technol.* 34, 2549–2556.
- Gilbert, D., Sale, T., Petersen, M.A., 2010. Electrolytic reactive barriers for chlorinated solvent remediation. In: Stroo, H.F., Ward, C.H. (Eds.), *In situ remediation of chlorinated solvent plumes*. Springer, New York, USA, pp. 573–590.
- Gin, S., Neill, L., Fournier, M., Frugier, P., Ducasse, T., Tribet, M., Abdelouas, A., Parruzot, B., Neeway, J., Wall, N., 2016. The controversial role of inter-diffusion in glass alteration. *Chem. Geol.* 440, 115–123.
- Haselmann, K.F., Laturmus, F., Svensmark, B., Gron, C., 2000. Formation of chloroform in spruce forest soil - results from laboratory incubation studies. *Chemosphere* 41, 1769–1774.
- Hydegaard, B.H., Jakobsen, R., Weeth, E.B., Overheu, N.D., Gent, D.B., Ottosen, L.M., 2019a. Challenges in electrochemical remediation of chlorinated solvents in natural groundwater aquifer settings. *J. Hazard Mater.* 368, 680–688.
- Hydegaard, B.H., Ottosen, L.M., Alshawabkeh, A.N., 2019b. Transformation of tetrachloroethylene in a flow-through electrochemical reactor. *Sci. Total Environ.* *In Press*, <https://doi.org/10.1016/j.scitotenv.2019.135566>.
- Lai, A., Verdini, R., Aulenta, F., Majone, M., 2015. Influence of nitrate and sulfate reduction in the bioelectrochemically assisted dechlorination of cis-DCE. *Chemosphere* 125, 147–154.
- Lakshminathiraj, P., Bhaskar Raju, G., Sakai, Y., Takuma, Y., Yamasaki, A., Kato, S., Kojima, T., 2012. Studies on electrochemical detoxification of trichloroethene (TCE) on Ti/IrO₂-Ta₂O₅ electrode from aqueous solution. *Chem. Eng. J.* 198–199, 211–218.
- Leenson, I.A., 2009. Old rule of thumb and the Arrhenius equation. *J. Chem. Educ.* 76, 1459–1460.
- Li, W.-W., Yu, H.-Q., 2015. Electro-assisted groundwater bioremediation: fundamentals, challenges and future perspectives. *Bioresour. Technol.* 196, 677–684.
- Lima, A.T., Hofmann, A., Reynolds, D., Ptacek, C.J., Van Cappellen, P., Ottosen, L.M., Pamukcu, S., Alshawabkeh, A.N., O'Carroll, D.M., Riis, C., Cox, E., Gent, D.B., Landis, R., Wang, J., Chowdhury, A.I.A., Secord, E.L., Sanchez-Hachair, A., 2017. Environmental electrokinetics for a sustainable subsurface. *Chemosphere* 181, 122–133.
- Lowry, G.V., Reinhard, M., 1999. Hydrodehalogenation of 1- to 3-carbon halogenated organic compounds in water using a palladium catalyst and hydrogen gas. *Environ. Sci. Technol.* 33, 1905–1910.
- Mao, X., Ciblak, A., Amiri, M., Alshawabkeh, A.N., 2011. Redox control for electrochemical dechlorination of trichloroethylene in bicarbonate aqueous media. *Environ. Sci. Technol.* 45, 6517–6523.
- Mao, X., Ciblak, A., Baek, K., Amiri, M., Loch-Carusio, R., Alshawabkeh, A.N., 2012a. Optimization of electrochemical dechlorination of trichloroethylene in reducing electrolytes. *Water Res.* 46, 1847–1857.
- Mao, X., Yuan, S., Fallahpour, N., Ciblak, A., Howard, J., Padilla, I., Loch-Carusio, R., Alshawabkeh, A.N., 2012b. Electrochemically induced dual reactive barriers for transformation of TCE and mixture of contaminants in groundwater. *Environ. Sci. Technol.* 46, 12003–12011.
- Martínez-Huitle, C.A., Rodrigo, M.A., Sirés, I., Scialdone, O., 2015. Single and coupled electrochemical processes and reactors for the abatement of organic water pollutants: a critical review. *Chem. Rev.* 115, 13362–13407.
- McNab, W.W., Ruiz, R., 1998. Palladium-catalyzed reductive dehalogenation of dissolved chlorinated aliphatics using electrolytically-generated hydrogen. *Chemosphere* 37, 925–936.
- Miljøstyrelsen (Danish EPA), 2018. Liste over kvalitetskriterier i relation til forurenede jord og kvalitetskriterier for drikkevand. Miljøstyrelsen, Denmark.
- Molina, V.M., González-Arjona, D., Roldán, E., Domínguez, M., 2002. Electrochemical reduction of tetrachloromethane. Electrolytic conversion to chloroform. *Collect. Czechoslov. Chem. Commun.* 67, 279–292.
- Molina, V.M., Montiel, V., Domínguez, M., Aldaz, A., 2003. Electrolytic synthesis of chloroform from carbon tetrachloride in mild conditions. *Lab. Approach. Electrochem. Commun.* 5, 246–252.
- Ndjou'Ou, A.C., Bou-Nasr, J., Cassidy, D., 2006. Effect of fenton reagent dose on coexisting chemical and microbial oxidation in soil. *Environ. Sci. Technol.* 40, 2778–2783.
- Pankow, J.F., Feenstra, S., Cherry, J.A., Ryan, C.M., 1996. Dense chlorinated solvents and other DNAPLs in groundwater: history, behavior, and remediation. Waterloo Press, Portland, Oregon.
- Radjenovic, J., Sedlak, D.L., 2015. Challenges and opportunities for electrochemical processes as next-generation technologies for the treatment of contaminated water. *Environ. Sci. Technol.* 49, 11292–11302.
- Rajic, L., Fallahpour, N., Alshawabkeh, A.N., 2015a. Impact of electrode sequence on electrochemical removal of trichloroethylene from aqueous solution. *Appl. Catal. B Environ.* 174–175, 427–434.
- Rajic, L., Fallahpour, N., Nazari, R., Alshawabkeh, A.N., 2015b. Influence of humic substances on electrochemical degradation of trichloroethylene in limestone aquifers. *Electrochim. Acta* 181, 123–129.
- Rajic, L., Fallahpour, N., Oguzie, E., Alshawabkeh, A.N., 2015c. Electrochemical transformation of trichloroethylene in groundwater by Ni-containing cathodes. *Electrochim. Acta* 181, 118–122.
- Rajic, L., Fallahpour, N., Podlaha, E., Alshawabkeh, A.N., 2016a. The influence of cathode material on electrochemical degradation of trichloroethylene in

- aqueous solution. *Chemosphere* 147, 98–104.
- Rajic, L., Fallahpour, N., Yuan, S., Alshawabkeh, A.N., 2014. Electrochemical transformation of trichloroethylene in aqueous solution by electrode polarity reversal. *Water Res.* 67, 267–275.
- Rajic, L., Nazari, R., Fallahpour, N., Alshawabkeh, A.N., 2016b. Electrochemical degradation of trichloroethylene in aqueous solution by bipolar graphite electrodes. *J. Environ. Chem. Eng.* 4, 197–202.
- Rebelo, A., Ferra, I., Marques, A., Silva, M.M., 2016. Wastewater reuse: modeling chloroform formation. *Environ. Sci. Pollut. Res.* 23, 24560–24566.
- Ruder, A.M., 2006. Potential health effects of occupational chlorinated solvent exposure. *Ann. N. Y. Acad. Sci.* 1076, 207–227.
- Sáez, V., Esclapez Vicente, M.D., Frías-Ferrer, A.J., Bonete, P., González-García, J., 2009. Electrochemical degradation of perchloroethylene in aqueous media: an approach to different strategies. *Water Res.* 43, 2169–2178.
- Sale, T., Petersen, M., Gilbert, D., 2005. Electrically induced redox barriers for treatment of groundwater. Springer, Colorado, USA.
- Schiefler, A.A., Tobler, D.J., Overheu, N.D., Tuxen, N., 2018. Extent of natural attenuation of chlorinated ethenes at a contaminated site in Denmark. *Energy Procedia* 146, 188–193.
- Skibsted, G., Ottosen, L.M., Elektorowicz, M., Jensen, P.E., 2018. Effect of long-term electrochemical soil remediation on Pb removal and soil weathering. *J. Hazard Mater.* 358, 459–466.
- Sonoyama, N., Sakata, T., 1999. Electrochemical continuous decomposition of chloroform and other volatile chlorinated hydrocarbons in water using a column type metal impregnated carbon fiber electrode. *Environ. Sci. Technol.* 33, 3438–3442.
- Sundstrom, D.W., Klei, H.E., Nalette, T.A., Reidy, D.J., Weir, B.A., 1986. Destruction of halogenated aliphatics by ultraviolet catalyzed oxidation with hydrogen peroxide. *Hazard. Waste Hazard. Mater.* 3, 101–110.
- Tiehm, A., Lohner, S.T., Augenstein, T., 2009. Effects of direct electric current and electrode reactions on vinyl chloride degrading microorganisms. *Electrochim. Acta* 54, 3453–3459.
- US Environmental Protection Agency of Water, 2018. 2018 Edition of the Drinking Water Standards and Health Advisories. EPA 822-F-18-001. Washington, DC, USA.
- Velázquez, J.C., Leekumjorn, S., Hopkins, G.D., Heck, K.N., McPherson, J.S., Wilkens, J.A., Nave, B.S., Reinhard, M., Wong, M.S., 2016. High activity and regenerability of a palladium–gold catalyst for chloroform degradation. *J. Chem. Technol. Biotechnol.* 91, 2590–2596.
- Wang, H., Luo, H., Fallgren, P.H., Jin, S., Ren, Z.J., 2015. Bioelectrochemical system platform for sustainable environmental remediation and energy generation. *Biotechnol. Adv.* 33, 317–334.
- Wang, J., Farrell, J., 2003. Investigating the role of atomic hydrogen on chloroethene reactions with iron using Tafel analysis and electrochemical impedance spectroscopy. *Environ. Sci. Technol.* 37, 3891–3896.
- Yuan, S., Chen, M., Mao, X., Alshawabkeh, A.N., 2013a. Effects of reduced sulfur compounds on Pd-catalytic hydrodechlorination of trichloroethylene in groundwater by cathodic H₂ under electrochemically induced oxidizing conditions. *Environ. Sci. Technol.* 47, 10502–10509.
- Yuan, S., Chen, M., Mao, X., Alshawabkeh, A.N., 2013b. A three-electrode column for Pd-catalytic oxidation of TCE in groundwater with automatic pH-regulation and resistance to reduced sulfur compound foiling. *Water Res.* 47, 269–278.
- Yuan, S., Mao, X., Alshawabkeh, A.N., 2012. Efficient degradation of TCE in groundwater using Pd and electro-generated H₂ and O₂: a shift in pathway from hydrodechlorination to oxidation in the presence of ferrous ions. *Environ. Sci. Technol.* 46, 3398–3405.
- Zhao, X., Wallace, R.B., Hyndman, D.W., Dybas, M.J., Voice, T.C., 2005. Heterogeneity of chlorinated hydrocarbon sorption properties in a sandy aquifer. *J. Contam. Hydrol.* 78, 327–342.
- Zhao, Y., Yang, H.W., Liu, S.T., Tang, S., Wang, X.M., Xie, Y.F., 2016. Effects of metal ions on disinfection byproduct formation during chlorination of natural organic matter and surrogates. *Chemosphere* 144, 1074–1082.
- Zhou, W., Meng, X., Gao, J., Alshawabkeh, A.N., 2019a. Hydrogen peroxide generation from O₂ electroreduction for environmental remediation: a state-of-the-art review. *Chemosphere* 225, 588–607.
- Zhou, W., Rajic, L., Meng, X., Nazari, R., Zhao, Y., Wang, Y., Gao, J., Qin, Y., Alshawabkeh, A.N., 2019b. Efficient H₂O₂ electrogeneration at graphite felt modified via electrode polarity reversal: utilization for organic pollutants degradation. *Chem. Eng. J.* 364, 428–439.
- Zhou, W., Rajic, L., Zhao, Y., Gao, J., Qin, Y., Alshawabkeh, A.N., 2018. Rates of H₂O₂ electrogeneration by reduction of anodic O₂ at RVC foam cathodes in batch and flow-through cells. *Electrochim. Acta* 277, 185–196.

Supporting information

Electrochemical transformation of an aged tetrachloroethylene contamination in realistic aquifer settings

Bente H. Hyldegaard ^{a,b,*}, Rasmus Jakobsen ^c, Lisbeth M. Ottosen ^b

^a *Department of Waste & Contaminated Sites, COWI A/S, Parallelsvej 2, 2800 Kgs. Lyngby, Denmark*

^b *Department of Civil Engineering, Brovej, Building 118, Technical University of Denmark, 2800 Kgs. Lyngby, Denmark.*

^c *Department of Geochemistry, Geological Survey of Denmark and Greenland, Øster Voldgade 10, 1350 København K, Denmark*

^{*} *Corresponding author. E-mail: behd@cowi.com / benho@byg.dtu.dk (B.H. Hyldegaard).*

This supporting information (pp. S1-S3) includes two figures: **(i)** Changes in the inorganic chemistry due to electrochemical application (Fig. S1) ; **(ii)** Composition of the synthetic and field-extracted groundwater solutions before and after the electrochemical treatment (Fig. S2).

(i)

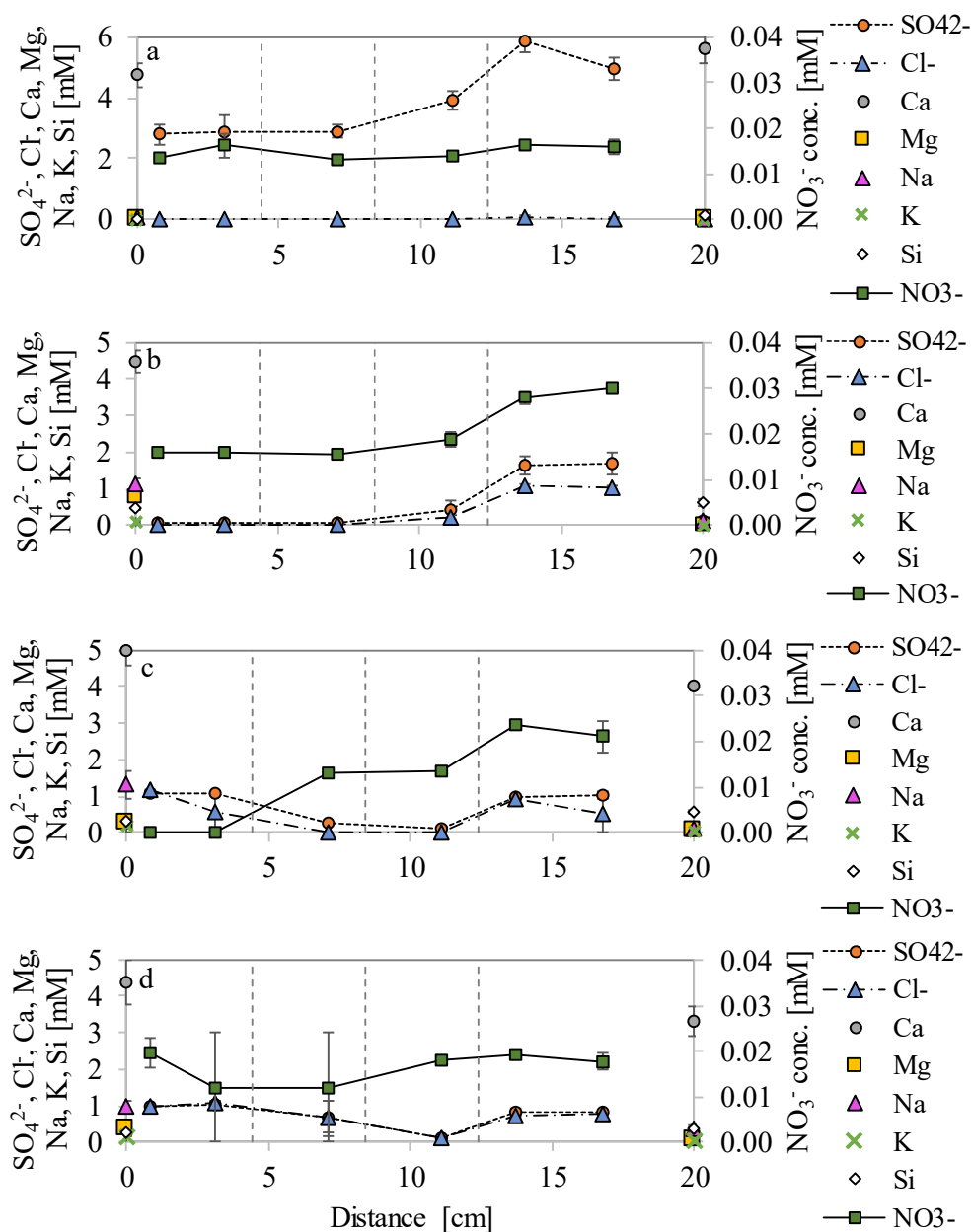


Fig. S1. Changes in inorganic chemistry for electrochemical application in a) simplified testing (exp. 1), b) field-extracted groundwater (exp. 2), c) sandy sediment (exp. 3) and d) groundwater temperatures of 8-10 °C (exp. 4). Development in concentrations throughout the electrochemical reactor at the final sampling round is shown for SO₄²⁻ (---○---, orange), Cl⁻ (---△---, blue) and NO₃⁻ (—□—, green). Concentrations in the feedstock solution prior to the electrochemical application and in the effluent at the final sampling round is shown for Ca (○, grey), Mg (□, orange), Na (△, pink), K (x, green) and Si (◇, white). Following the flow direction, the position of cathode – bipolar electrode – anode is marked with grey dashed vertical lines. Experiment numbers refer to specifications in Table 1.

ii)

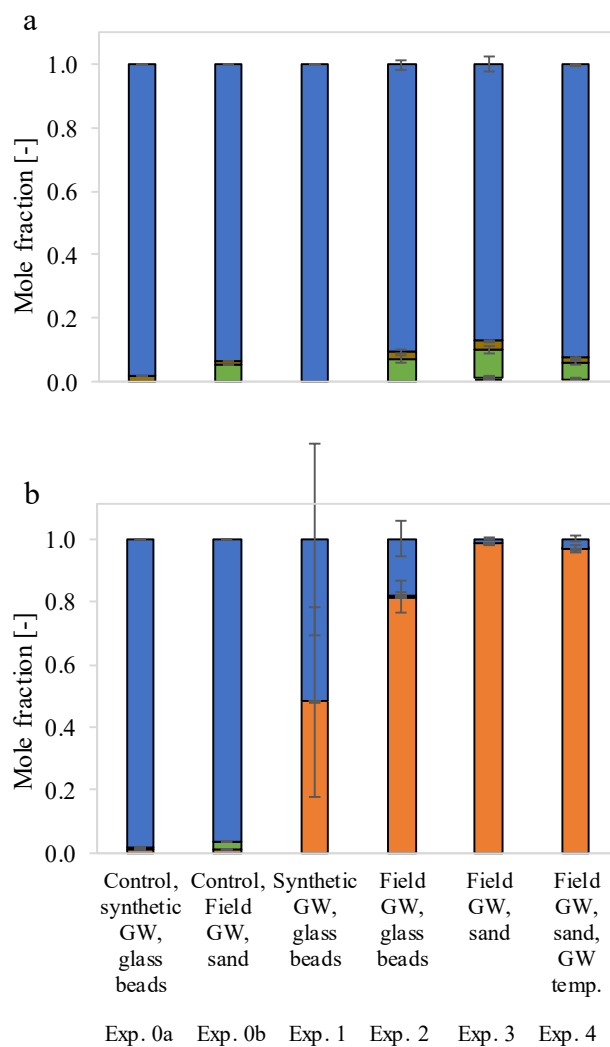


Fig. S2. Contaminant compositions of the groundwater (GW) solutions tested, a) initially in sampling port P0 and b) finally in sampling port P5. Detected contaminants include PCE (blue), TCE (brown), cis-DCE (green) and TCM (orange). Mole fraction is calculated as the measured moles of a specific component relative to the sum of moles of all contaminant components. Experiment numbers refer to specifications in Table 1.

SUPPORTING NOTE I

Electrochemically induced precipitation of groundwater species and anode composites in a flow-through box reactor

Electrochemically induced precipitation of groundwater species and anode composites in a flow-through box reactor

Abstract

A visual study of electrochemically induced precipitation in a flowing field-extracted, contaminated groundwater subject to a constant current over a three-electrode configuration of iron electrodes was performed. In the reducing zone, white clouds were observed, and a decreased concentration of e.g. Ca was measured. Corrosion of the anode resulted in an increase in Fe concentration downgradient the anode, leading to a red coloration of the solution. Net structured formations of unknown origin were observed between monitoring wells, suggested as microbial growth. Concurrent removal of tetrachloroethylene (26%), trichloroethylene (40%), cis-dichloroethylene (41%) and trans-dichloroethylene (39%) was measured, with volatilization accounting for 11%, 7%, 2% and 5%, respectively. I.e., the electrochemically induced degradation was 15% (PCE), 33% (TCE), 39% (cis-DCE) and 34% (trans-DCE). Challenges arising from formation of iron complexes due to anode corrosion, e.g. coverage of electrode surfaces and clogging of porous matrices, suggest use of stable anodes when applying electrochemical zones in complex chemical settings.

1. Introduction

Groundwater has a complex chemistry and precipitation of naturally present compounds during electrochemical treatment of contaminations is possible. Besides competing with the contaminant transformation for electrons, the precipitates may cover the electrodes and/or clog the system, increasing the overall electrical resistivity within the treatment zone. Also, the hydraulic resistivity increases by precipitation and this can result in a groundwater flow around the treatment zone instead of through it. Hence, it is relevant to assess the precipitation mechanisms.

Formation of precipitates containing Ca, Mg and Fe was observed during electrochemical treatment of chlorinated ethenes in groundwater flowing through a sandy sediment, in a set-up where Fe electrodes were used [1]. Fe anodes corrodes, but are considered used in the electrochemical treatment due to their abilities to establish reducing conditions of <600 mV, enhancing the removal of chlorinated ethenes [2,3]. At reducing conditions <450 mV, microbial cultures capable of degrading chlorinated ethenes have shown the ability to utilize electrons from cathodes directly in the biodegradation [4]. I.e., the dechlorinating microbial culture can be stimulated within electrochemical zones resulting in growth [5].

The objective of this study is to visually observe the precipitate formation of groundwater species occurring within a box electrochemical reactor with a three-electrode configuration of palladized Fe cathodes and a cast Fe anode with flow-through of field-extracted groundwater containing an aged contamination of tetrachloroethylene (PCE).

2. Materials and methods

2.1 Materials

Chemicals used were of analytical grade: Crystalline palladium (Pd) dichloride (99.9%, Thermo Fisher Scientific) and hydrochloric acid (35%, VWR). Groundwater containing a partially degraded aged contamination of PCE was sampled at a site in Skovlunde, Denmark (Appendix I, II, V). The groundwater composition is given in Table 1.

Table 1. Major ionic species of the field-extracted groundwater.

Groundwater specie	Field-extracted groundwater
Cl [mM]	1.20±0.02
NO ₃ [mM]	0.06±0.02
SO ₄ [mM]	3.86±0.08
F [mM]	0.06±0.00
Ca [mM]	8.67±0.23
K [mM]	0.13±0.00
Mg [mM]	1.16±0.02
Na [mM]	0.95±0.04
pH [-]	7
Conductivity [μS/cm]	1647±38

The groundwater was stored in a DuPont Tedlar® PVF film bag (100 L, CEL Scientific Corporation) with minimum headspace to limit mass loss from volatilization. The groundwater was pumped from the well two times during the testing to fill up the groundwater tedlar® bag. A constant flow was maintained using a Watson-Marlow qdos30 manual peristaltic pump with teflon tubing (OD 8 mm, ID 6 mm, Hounisen). Fe rods (99.95% Fe, D 12.7 mm, L 130 mm, GoodFellow) were used as cathodes. A cast Fe rod (D 12.7 mm, L 130 mm, Tasso A/S) was used as anode. Electrode compositions are given in Appendix II. A constant current was supplied using a Magna-Power SL800-3.2/380+LXI 0-800V, 0-3.2A, 0-2.6 kW (Metronic ApS) and three Arcol VRH320 wirewound slide rheostats in series (10kOhm, RS Components A/S). Fermentation locks (25-liter wine carboy, Brygladen) were used as water locks for automatic venting of gases generated. Gas stripping was

assessed using Dräger orsa sampling tubes 5 (Eurofins) above the fermentation locks. Silicone/PTFE septa (D 22 mm, thickness 3.2 mm, Mikrolab Aarhus A/S) allowed sampling of porewater.

2.2 Analytical methods

A WTW digital multimeter 3430 set KS2 (VWR) with Sentix 940 combined IDS pH probe (VWR) and Tetracon 925 conductivity probe (VWR) was used. Potential differences and currents were measured using Sagitta 60642 digital multimeter. Concentrations of Cl^- , NO_3^- , SO_4^{2-} and F^- were measured with IC. Concentrations of Ca, K, Mg, Na, Fe and Mn were measured with ICP. Quantification of volatile organic carbons (VOC), hydrocarbons, ionic species and metal elements as specified in Appendix I. Power consumption was recorded with a secondary electricity meter.

2.3 Experimental procedure

An acrylic box reactor with 15 sampling points was designed for this testing (Figure 1). Additional sampling ports for sampling of inlet solutions and effluent were installed. Groundwater was flowing through the reactor at a seepage velocity of 122 m/yr (11.6 ml/min). A constant current of 57 mA was applied across a three-electrode configuration of C – C – A, with the current split equally between the two cathodes. The cathodes were coated with 0.76 mg/cm² Pd according to the procedure described in Rajic et al. [6].

Once the reactor was saturated with the contaminated groundwater, a flow through the reactor was continued for one pore volume (PV) and monitored for VOC, hydrocarbons, ionic species, metal elements, pH and conductivity in every sampling port, inlet and effluent (Figure 1) as a reference background (control) without application of current. Current was then applied for 1 PV with concurrent monitoring of the system. The electrochemical testing continued for three days and was conducted at temperatures of 6-8 °C. A granular activated carbon filter was mounted downgradient the effluent sampling point to capture any residue contamination.

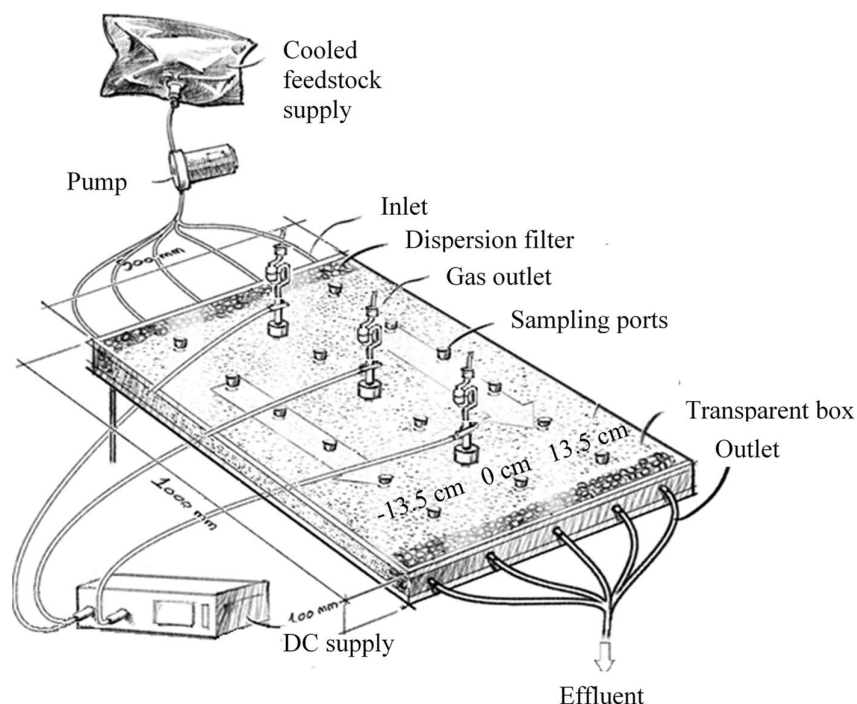


Figure 1. Illustration of the box electrochemical reactor with a C – C – A electrode configuration. Rheostats in series were mounted before the second cathode. Flow direction is indicated by arrows. Sampling ports are distributed in three parallel lines in the direction of groundwater flow, with a transverse spacing of 13.5 cm. The electrodes are positioned in the center line (0 cm).

3. Results and discussion

3.1 Changes in porewater composition

Monitored throughout the electrochemical zone, major changes in the characteristics of the groundwater were restricted to conductivity and concentrations of Cl^- , NO_3^- , SO_4^{2-} , F^- , Ca, K, Mg, Na, Fe and Mn.

The conductivity was lower throughout the box reactor during electrochemical application than pre-treatment (Figure 2) in agreement with observations in Appendix I. The decrease in conductivity indicated precipitation of groundwater species, which was verified by decreasing concentrations measured in the effluent of Cl^- (76%), NO_3^- (95%), SO_4^{2-} (79%), F^- (24%), Ca (5.4%), K (3.6%), Mg (7.5%) and Na (10%).

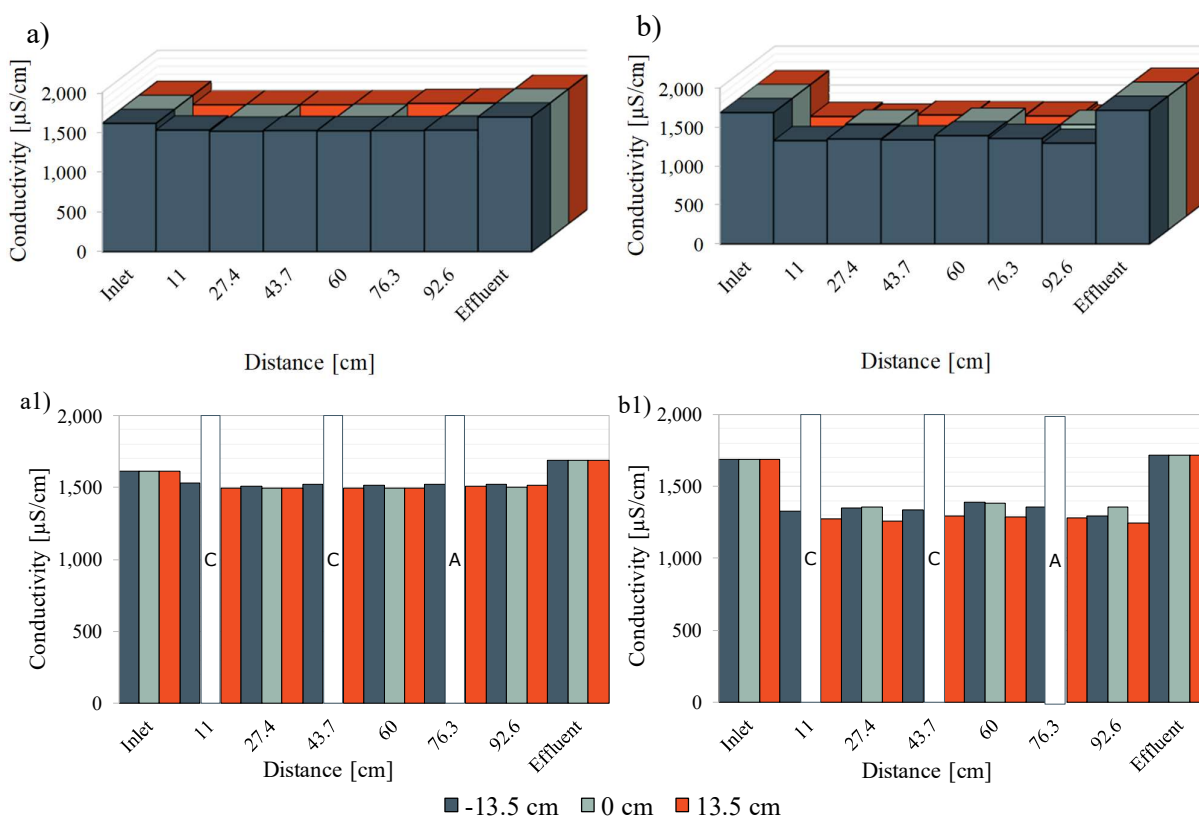


Figure 2. Development in conductivity a-a1) pre-electrochemical application and b-b1) post-electrochemical application. The two types of diagrams (a-a1 vs. b-b1) are illustrating the same data. Blank values (a-b) and white bars (a1-b1) indicate the positions of electrodes (no measurements). Sampling points (-13.5 cm, 0 cm and 13.5 cm) reflect the transverse locations in Figure 1. Inlet and effluent are based on one sample each.

The removals of Ca and Mg locally near the cathodes were more significant, but overall balanced by the sequence of different redox conditions, with dissolution near the downgradient anode. This supports the hypothesis of formation of Ca colloids with co-precipitation of Mg (Appendix I). In the reducing zone, primarily close to the first cathode, a major decrease in concentration of Cl^- , SO_4^{2-} , Ca and Mg was observed, while F^- increased. A decrease in concentration in the effluent compared to initial concentrations was found for Cl^- , NO_3^- , SO_4^{2-} , F^- , K, Na, Ca and Mg. On the contrary, considerably increased concentrations of Fe and Mn downgradient the anode were observed, which possibly originated from corrosion of the cast Fe anode (Appendix I-II). No significant change in concentration of Cl^- was observed near the anode. The decreasing concentrations measured in the effluent for Cl^- , NO_3^- , SO_4^{2-} and F^- may have been due to precipitation with Fe^{2+} and/or Mn^{2+} .

3.2 Contaminant removal

Within the electrochemical reactor, the aged contamination was transformed. In the dissolved phase, PCE, trichloroethylene (TCE), cis-dichloroethylene (cis-DCE) and trans-dichloroethylene (trans-DCE) was removed by 26%, 40%, 41% and 39%, respectively. A fraction of these removals was due to stripping of the volatile organic compounds, i.e. a phase transfer. Specifically, 11%, 7%, 2% and 5% of removals of PCE, TCE, cis-DCE and trans-DCE, respectively, in the dissolved phase was accounted for by volatilization. Thus, the electrochemically induced degradation was 15% (PCE), 33% (TCE), 39% (cis-DCE) and 34% (trans-DCE). No vinyl chloride, trichloromethane (chloroform), ethene or ethane was quantified above detection limits. The fact, that especially the intermediate vinyl chloride was not formed, is very positive, since this compound is considered more hazardous than the parent components.

The potential difference decreased over time from initially 35V to a stabilization at 18V (Figure 3). With an application of 57 mA throughout three days, the power consumption was 2.2 kWh, app. 47 kWh/m³ of water treated, 1430 kWh/kg TCE equivalents removed or 1.9 kWh/g cis-DCE equivalents removed. This power consumption is higher than removals reported [6,7], which possibly is related to the upscaling in this study, smaller electrode surface areas per volume of water and a lack of optimization of the box set-up related to efficient contaminant removal.

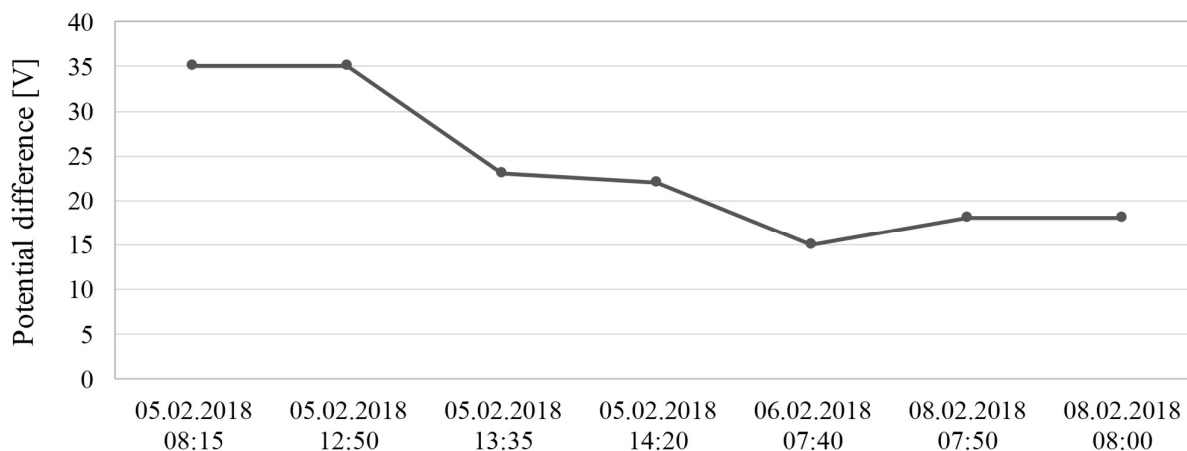


Figure 3. Development in potential difference over the electric field during three days of electrochemical treatment. Note, the horizontal date axis is showing a fixed interval between data points despite of varying time difference between the actual recordings of potential difference.

3.3 Observations

An hour after application of constant current, whitish cloud formations were observed on the outside of the uppermost part of cathode well screens, which was in line with the measured decrease in Ca concentration. The formations had strings directed towards the anode (Figure 4), maybe indicating the distribution of the electric field.



Figure 4. Cloud formation from the cathodes observed within the first hour of electrochemical application.

With constant current applied for 18 hours, black precipitates had deposited below the well screens of the cathodes, the white cloud formations had increased in thickness and whitish strings were hanging from the walls of the well screens (Figure 5a). Near the anode, a red coloration of the solution was observed from 60-100 cm of the reactor (Figure 5b), which corresponds well with the measured increase in Fe concentration due to corrosion of the cast Fe anode.

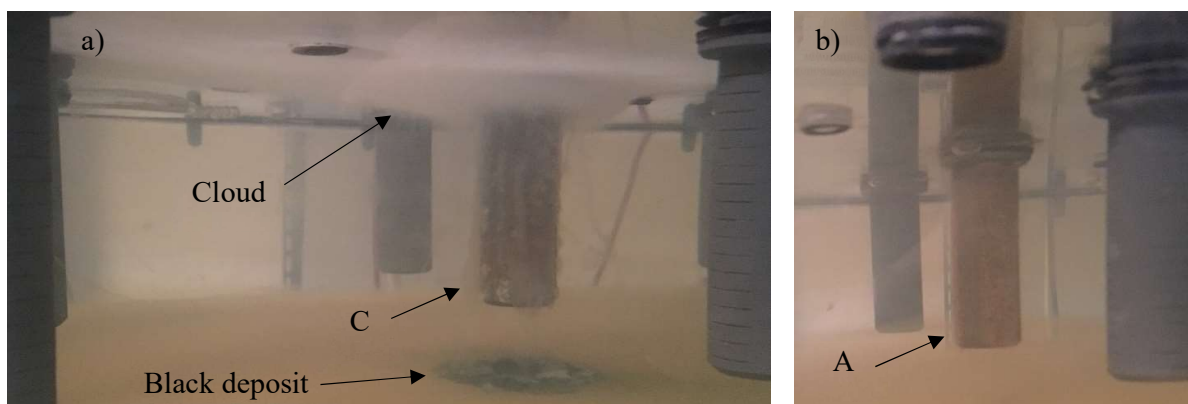
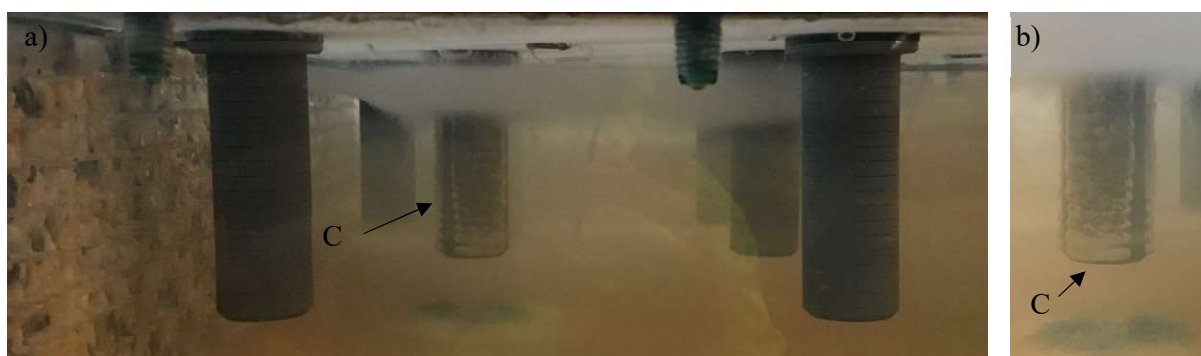


Figure 5. With application of electrochemical treatment for 18 hours, a) black deposits had formed below the cathodes (C), the cloud formations had thickened with white strings hanging from the cathode wells screens, and b) the solution was red in appearance around the anode (A).

After 67 hours of electrochemical treatment, the white clouds had thickened further to app. 2-3 cm and grown in diameter. The clouds had displaced downwards, now starting at 1 cm below the lid of the box (Figure 6a). White precipitates had deposited in the slits of the cathode well screens (Figure 6b). Above the clouds, a colorless liquid phase was stretching from the cathodes to the anode (Figure 6c). Downgradient the anode, the solution was homogeneously red in appearance and the red color had intensified (Figure 6d). A dark deposit was hanging from the bottom of the anode well screen. Between several of the monitoring wells, nets of a few mm in thickness had formed (Figure 6e-f), maybe indicating microbial growth, but this needs to be quantified. The dechlorinating microbial culture *Dehalococcoides* is detected in the groundwater well supplying the groundwater feedstock solution used in this study [8], which may benefit from the reducing conditions expected to establish within the reactor (Appendix II) [4,5,7,9]. The box reactor had started leaking after two days of operation from various fittings, indicating an increase in pressure within the reactor.



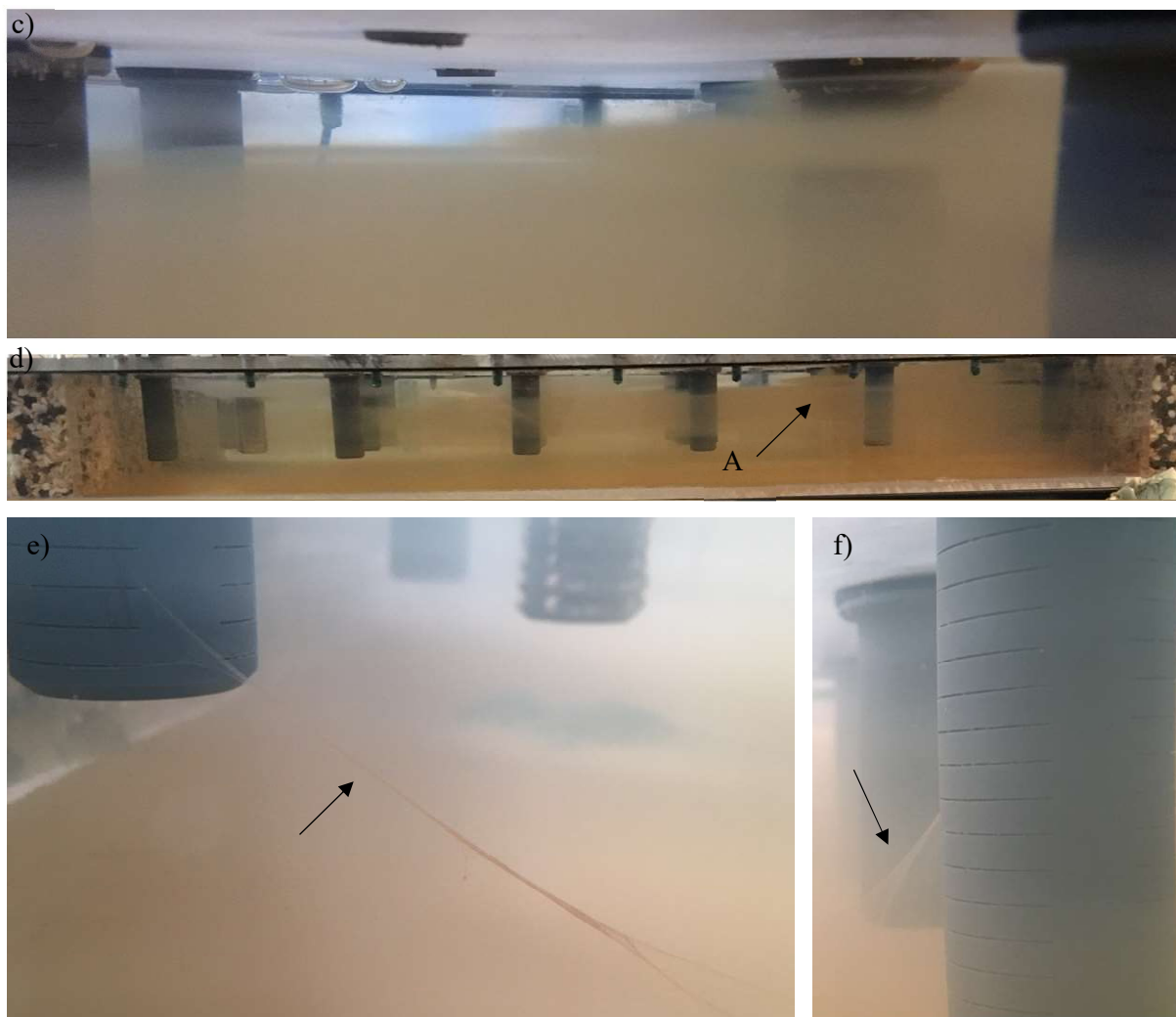


Figure 6. After 67 hours of electrochemical treatment, a) the cloud formations around the cathode wells screens had displaced downwards, b) white precipitates had accumulated within the cathode well screen slits, c) a colorless liquid phase was distributed above the cloud formations from the cathodes to the anode, d) the solution downgradient the anode had a homogenic and intensified shade of red and e-f) nets between monitoring wells had formed.

The white precipitates possibly containing Ca may not be a challenge to electrochemical application in field-realistic settings, whereas the Fe precipitates appear to clog the system (Appendix I-II). Hence, despite of the advantages of using Fe anodes, stable anodes may overall be more suitable (Appendix II, V).

No gas phase was accumulating outside of the well screens, but bubble formation was observed from all electrodes. Least gas formation was observed at the anode, which was expected due to corrosion of the cast Fe (Appendix II) [2,3,10].

4. Conclusion

A transparent box reactor comprising a three-electrode configuration of Fe electrodes was designed for visual assessment of precipitate formation during electrochemical transformation of an aged contamination of PCE in field-extracted groundwater. Observations included:

- Formation of white clouds around the cathodes with strings orientated towards the anode within the first hour of application. Over time, the clouds increased in size
- Black precipitates deposited below the cathodes
- Black precipitates formed at the anode well screen
- Red coloration of solution around the anode
- Formation of nets between monitoring wells

Sampling of the solution indicated precipitation of Ca and Mg in the reducing zone, possibly explaining the cloud formations observed. Further, an increase in Fe concentration in the effluent was measured, suggesting formation of Fe complexes, that could explain the red coloration observed in this zone. The net formation needs to be assessed, but could be indicative of microbial growth.

A transformation of the partially degraded aged contamination of PCE was observed for PCE (26%), TCE (40%), cis-DCE (41%) and trans-DCE (39%). Stripping of the contaminants to the vapor phase accounted for 11% (PCE), 7% (TCE), 2% (cis-DCE) and 5% (trans-DCE) of the measured removals. Thus, the electrochemically induced degradation was 15% (PCE), 33% (TCE), 39% (cis-DCE) and 34% (trans-DCE).

This study shows, that precipitates of groundwater species are formed within electrochemical zones, where especially Fe complexes appear to challenge the application. To overcome this challenge, it is suggested to apply stable anodes.

Acknowledgement

This work was funded by the Innovation Fund Denmark (grant number 5016-00165B), COWIfonden (grant number C-131.01), the Capital Region of Denmark (grant number 14002102), COWI A/S and Technical University of Denmark. The cast iron anode was kindly donated by Velamp A/S.

References

- [1] B.H. Hyldegaard, R. Jakobsen, E.B. Weeth, N.D. Overheu, D.B. Gent, L.M. Ottosen, Challenges in electrochemical remediation of chlorinated solvents in natural groundwater aquifer settings, *J. Hazard. Mater.* 368 (2019) 680–688. doi:10.1016/j.jhazmat.2018.12.064.
- [2] X. Mao, A. Ciblak, M. Amiri, A.N. Alshawabkeh, Redox Control for Electrochemical Dechlorination of Trichloroethylene in Bicarbonate Aqueous Media, *Environ. Sci. Technol.* 45 (2011) 6517–6523. doi:10.1021/es200943z.
- [3] N. Fallahpour, S. Yuan, L. Rajic, A.N. Alshawabkeh, Hydrodechlorination of TCE in a circulated electrolytic column at high flow rate, *Chemosphere.* 144 (2016) 59–64. doi:10.1016/j.chemosphere.2015.08.037.
- [4] F. Aulenta, A. Canosa, P. Reale, S. Rossetti, S. Panero, M. Majone, Microbial reductive dechlorination of trichloroethene to ethene with electrodes serving as electron donors without the external addition of redox mediators, *Biotechnol. Bioeng.* 103 (2009) 85–91. doi:10.1002/bit.22234.
- [5] F. Aulenta, L. Tocca, R. Verdini, P. Reale, M. Majone, Dechlorination of Trichloroethene in a Continuous-Flow Bioelectrochemical Reactor: Effect of Cathode Potential on Rate, Selectivity, and Electron Transfer Mechanisms, *Environ. Sci. Technol.* 45 (2011) 8444–8451. doi:10.1021/es202262y.
- [6] L. Rajic, N. Fallahpour, E. Podlaha, A.N. Alshawabkeh, The influence of cathode material on electrochemical degradation of trichloroethylene in aqueous solution, *Chemosphere.* 147 (2016) 98–104. doi:10.1016/j.chemosphere.2015.12.095.
- [7] F. Aulenta, R. Verdini, M. Zeppilli, G. Zanaroli, F. Fava, S. Rossetti, M. Majone, Electrochemical stimulation of microbial cis-dichloroethene (cis-DCE) oxidation by an ethene-assimilating culture, *N. Biotechnol.* 30 (2013) 749–755. doi:10.1016/j.nbt.2013.04.003.
- [8] A.A. Schiefler, D.J. Tobler, N.D. Overheu, N. Tuxen, Extent of natural attenuation of chlorinated ethenes at a contaminated site in Denmark, *Energy Procedia.* 146 (2018) 188–193. doi:10.1016/j.egypro.2018.07.024.
- [9] F. Aulenta, P. Reale, A. Canosa, S. Rossetti, S. Panero, M. Majone, Characterization of an electro-active biocathode capable of dechlorinating trichloroethene and cis-dichloroethene to ethene, *Biosens. Bioelectron.* 25 (2010) 1796–1802. doi:10.1016/j.bios.2009.12.033.
- [10] L. Rajic, N. Fallahpour, A.N. Alshawabkeh, Impact of electrode sequence on electrochemical removal of trichloroethylene from aqueous solution, *Appl. Catal. B Environ.* 174–175 (2015) 427–434. doi:10.1016/j.apcatb.2015.03.018.

SUPPORTING NOTE II

Galvanic abilities of electrodes installed in saturated sandy sediment

- background reference test for electrochemical transformation of chlorinated ethenes

Galvanic abilities of electrodes installed in saturated sandy sediment

- background reference test for electrochemical transformation of chlorinated ethenes

Abstract

Sorption, microbial activity and mass loss are possible mechanisms when working with field-extracted groundwater, sandy sediment and chlorinated ethenes. Therefore, background reference tests, i.e. controls with no current applied, are essential for verification of e.g. electrochemical transformation of chlorinated ethenes in natural aquifer settings. It was observed, that a galvanic potential developed between a palladized iron (Fe) electrode and two mixed metal oxide electrodes placed in a sandy sediment. The potential was 0.926 ± 0.013 V. Following, different changes were induced in the system. The Fe electrode corroded. The porewater composition and conductivity changed throughout the reactor and over time. Trichloromethane and ethane formed, and chlorinated ethene concentrations decreased in the aged contamination: tetrachloroethylene (3.7%), trichloroethylene (70%) and cis-dichloroethylene (63%). No gas evolution was observed, and pH remained steady. This study demonstrates the need for careful monitoring of control tests.

1. Introduction

Feasibility studies on electrochemical remediation of chlorinated ethenes must be conducted under near natural aquifer settings, e.g. using field-extracted groundwater and sandy sediment [1]. Due to the complexity of groundwater and geological matrices, it is important to compare test results against background references, i.e. controls without application of current. Such control tests can give indications of mass loss, sorption, microbial activity etc.

Metal electrode materials are conducting and if submerged into ionic solutions, a potential difference between the electrode and solution may arise. The system is said to be galvanic. A galvanic cell can generate a current between the electrodes [2,3]. Using electrodes of different metals and thereby electrode potentials may strengthen the galvanic cell properties. Locally, the electrodes may act bipolar, i.e. one electrode site becomes anodic polarized, an adjacent site cathodic [4,5]. If an adequate potential difference is generated, bipolarity may enhance chlorinated ethene removal due to e.g. enhanced contact between H_2 and O_2 from electrolysis at cathodic and anodic sites, respectively, to combine into the oxidant H_2O_2 [4].

The objective of this study is to perform a control experiment as a valid background reference for e.g. mass loss during electrochemical remediation of an aged contamination of chlorinated ethenes in field-extracted groundwater flowing through a sandy sediment.

2. Materials and methods

2.1 Materials

The chemicals and materials used are described in detail in Appendix V.

2.2 Analytical methods

The analytical procedures are described in detail in Appendix V.

2.3 Experimental procedure

The test was carried out as a control with no current applied, but with electrodes mounted in the reactor. The field-realistic parameters incorporated into the set-up included a sandy sediment and field-extracted groundwater according to Appendix V. Testing was conducted at room temperature of 22 °C. The experimental set-up is illustrated in Figure 1.

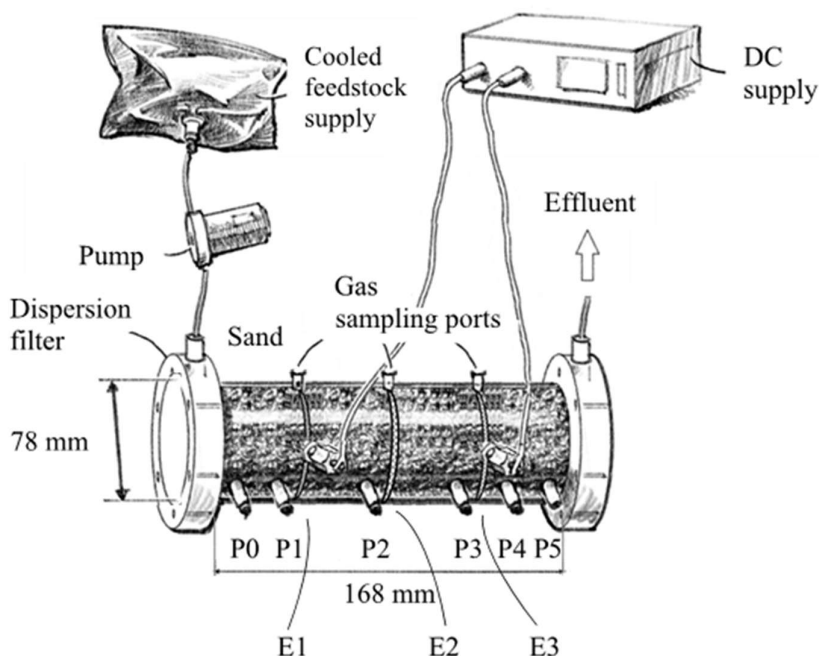


Figure 1. Illustration of the experimental set-up. Positions of electrodes (E1-E3), porewater sampling ports (P0-P5) and gas extraction sampling ports is shown.

3. Results and discussion

3.1 pH, conductivity and potential difference

With no application of direct current over the reactor, it was expected that only minor changes occurred throughout the reactor and over time. The pH remained steady on 7.5. The conductivity decreased downgradient the first electrode, increased beyond inlet level downgradient the second electrode and recovered inlet levels downgradient the third electrode. The conductivity fluctuated throughout the reactor in between 675 $\mu\text{S}/\text{cm}$ and 950 $\mu\text{S}/\text{cm}$. Over time, there was a tendency for these fluctuations to diminish. The fluctuating conductivity may have been a consequence of the potential difference establishing over the electrodes, having a measured weak electric field of $0.926 \pm 0.013\text{V}$. I.e., the reactor was galvanic. In previous studies (Appendix I, V), the conductivity was observed to increase near cathodes, while decrease near anodes, suggesting that E1 overall acted as anode, E2 as cathode, and E3 as anode. Bipolarity of each electrode was possible [4,5]. No gas evolution was observed. If the first electrode overall acted as an anode, it could explain a red coloring of the solution downgradient this specific electrode, which was composed of palladized iron (Fe). Ferrous ions are released during corrosion of Fe anodes [5,6] and may precipitate as ferric hydroxide, explaining the red color observed [7] (Appendix I).

3.2 Changes in porewater composition

Analysis of groundwater extracted throughout the reactor showed an increase in Cl^- downgradient the first electrode and a decrease downgradient the third electrode. Over time, the concentration of Cl^- increased from 0.9 mM to 1.77 mM, followed by a decrease and stabilization at 1 mM. Stoichiometrically, the release of Cl^- due to transformation of the chlorinated ethenes could not explain the observed increase in Cl^- . Release of Cl^- possibly adsorbed to the Fe electrode surface during palladization may contribute to the increase observed (Appendix II). SO_4^{2-} concentration in the porewater decreased downgradient the first electrode, increased downgradient the second electrode and decreased to initial levels downgradient the third electrode. Over time, the fluctuations of SO_4^{2-} and Cl^- measured throughout the reactor was levelling out and stabilized at inlet levels of 1 mM. The concentration of NO_3^- increased downgradient the first electrode and decreased to app. initial levels downgradient the third electrode. Over time, NO_3^- generally decreased throughout the reactor. Downgradient the galvanic zone, the concentrations of Ca, Na, and K decreased over time, while the concentrations of Mg and Mn increased.

3.3 Changes in dissolved contaminant composition

The composition of the aged contamination changed over the duration of the test (Figure 2 w. electrodes). The initial concentration of tetrachloroethylene (PCE) had been adjusted with 91% to cover mass loss in the tubing and e.g. sorption to the sandy sediment as conservatively defined in Appendix V. PCE, trichloroethylene (TCE) and cis-dichloroethylene (cis-DCE) concentrations decreased during the test by 3.7% (after the conservative adjustment), 70% and 63%, respectively, and over the course of the reactor. Trichloromethane (TCM), also known as chloroform, and ethane formed over the duration and course of the galvanic reactor. Ethane is a product of complete reductive dechlorination [8,9]. During electrochemical removal of the aged contamination in a similar set-up, ethane was not quantified above the detection limit in any of the tests conducted despite significant contaminant removal (Figure 2 w/o. electrodes, Appendix V). No mass loss of chloride was observed in this galvanic test besides the initial loss of PCE over the tubing, which had been corrected for.

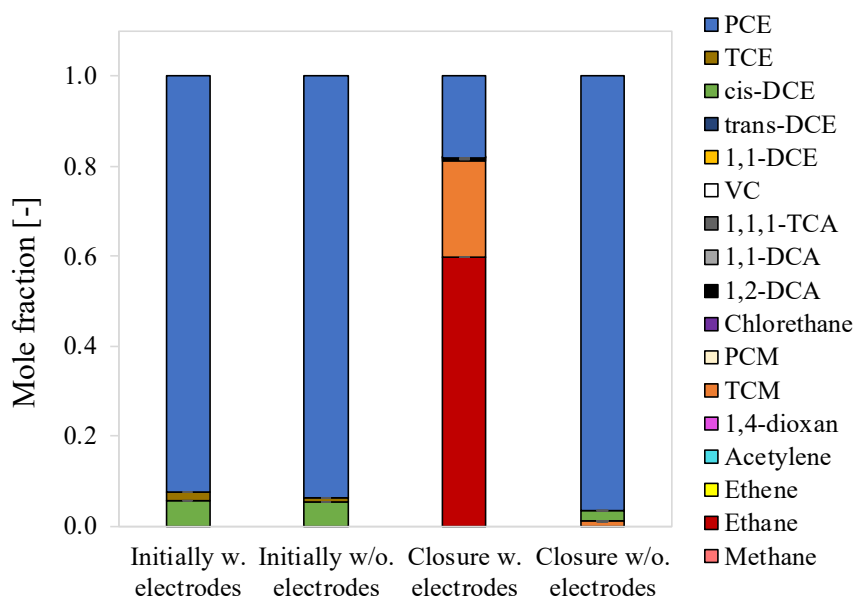


Figure 2. Composition of the porewater upgradient the electrodes at the initiation of the control test and downgradient the electrodes at the closing of the control test. The compositions in a similar test without (w/o.) electrodes is included for comparison (Appendix V).

TCM is quantified downgradient the first electrode. Over time, TCM concentration increased to a level of 1 μM followed by a decrease and stabilization at 0.5 μM . Stoichiometrically, complete conversion of PCE can explain the mass of TCM formed. This degradation pathway would require cleavage of PCE to carbon tetrachloride, which can be reduced to TCM [10,11]. However, in the

sandy sediment, this may not be the only mechanism explaining the formation of TCM. Oxidation of organic matter in the sandy sediment in presence of Cl^- [12,13], and the combination of photolysis and oxidation of chlorinated ethenes by H_2O_2 [14,15] may form TCM, as discussed in Appendix V.

Ethane was quantified above detection limit from downgradient the first electrode (Figure 3). Ethane was analyzed for at the end of the test only, because previous work by author studying this field-extracted groundwater and sandy sediment showed no formation of ethane or ethene without application of direct current (Appendix I) or even with application of a direct current (Appendix II, V, Supporting note I).

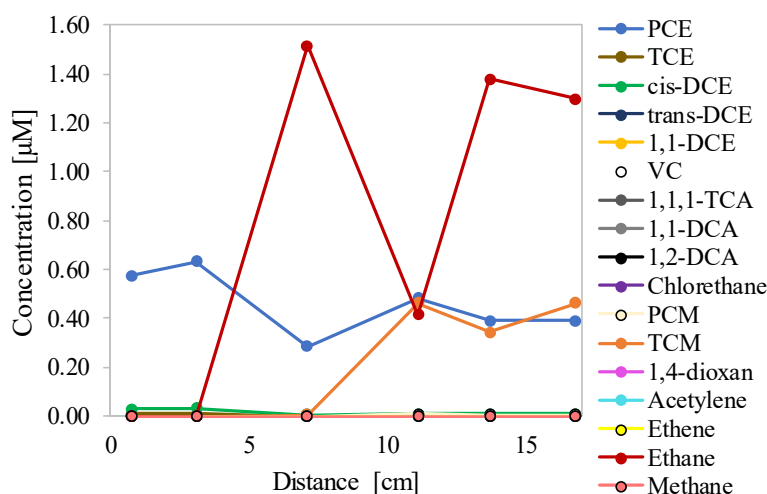


Figure 3. Contaminant development throughout the galvanic system measured at the end of the test. Electrodes are positioned at 4.4 cm, 8.4 cm and 12.8 cm.

Stoichiometrically, the initial concentrations of PCE measured within the reactor are adequate in explaining the mass of ethane measured. Abiotic reduction of PCE, TCE and cis-DCE have standard reduction potentials of 0.43V, 0.42V and 0.31V vs. standard hydrogen electrode (SHE), respectively and Gibbs free energies <0 [16]. Hence, PCE, TCE and cis-DCE can be spontaneously reduced at potentials $<0.42\text{V}$ vs. SHE. The standard oxidation potential of TCE on MMO is 0.54V vs. SHE (0.3V vs. saturated calomel electrode) [17], i.e. TCE can be oxidized at potentials $>0.54\text{V}$ vs. SHE. The specific potentials of the electrodes within the galvanic reactor were not measured. However, the overall potential difference measured was above the electric potentials required for abiotic oxidation. I.e., abiotic transformation of PCE could not to be disregarded. Another transformation mechanism could be stimulation of the microbial culture *Dehalococcoides (Dhc)* within the electrochemical reactor (Supporting note I), introducing biotic reduction of the chlorinated ethenes [18–22]. *Dhc*

previously has been detected in the groundwater at the site of extraction [23]. Whether the potential of the galvanic system was sufficient in driving abiotic and/or biotic transformation of the chlorinated ethenes needs to be quantified. Thirdly, ethane could have formed through a multistep reaction starting with reduction of CO₂ (Appendix I).

Hydrogen peroxide (H₂O₂) was not quantified above detection limit within the reactor, but formation could occur (Appendix V), with concurrent consumption due to contaminant transformation and/or decomposition explaining the lack of detection [24]. The standard reduction potential of O₂ to H₂O₂ is 0.695V vs. SHE [25]. As an indicator of the potentials established within the galvanic reactor, the standard reduction potential of Fe²⁺ to Fe⁰ is -0.44V [25]. Corrosion was observed, wherefore the half-cell reaction related to Fe must be reversed, having a potential of 0.44V. If the inevitable coupled reduction reaction allowing Fe corrosion was reduction of PCE and TCE, the resulting overall cell potential would be 0.43V + 0.44V = 0.87V if ignoring other possible redox reactions in the system. This can be compared against the measured potential difference of 0.926±0.013V.

With the observed galvanic abilities of passive electrochemical reactors, it is suggested to always measure the potential difference of control experiments used as references, as an indicator of galvanic processes. If changes in e.g. conductivity, contaminant composition or groundwater composition is observed, it may be necessary to conduct control reference tests with dismounted electrodes to prevent galvanic processes (Figure 2 w/o. electrodes, Appendix V).

4. Conclusion

An experiment without application of a direct current was carried out as a background reference for mass loss, sorption etc. during electrochemical remediation of an aged chlorinated ethene contamination in field-extracted groundwater flowing through a sandy sediment. However, the presence of three electrodes was able to create a galvanic cell with a weak electric field of 0.926±0.013V. Observed and measured system responses include:

- Red coloring of solution downgradient the Fe electrode (first electrode), suggesting corrosion (oxidation) and Fe(III) hydroxide formation
- Chlorinated ethene removal over the galvanic reactor: PCE (3.7%), TCE (70%) and cis-DCE (63%)
- TCM formation over the course of the reactor with decreasing concentrations over time

- Ethane formation over the course of the reactor
- Conductivity and concentration of SO_4^{2-} decreased downgradient the first electrode, increased downgradient the second electrode and decreased to initial levels downgradient the third electrode
- Concentrations of Cl^- and NO_3^- increased downgradient the first electrode and decreased downgradient the third electrode
- Concentrations of Ca, Na, and K decreased over time downgradient the galvanic reactor
- Concentrations of Mg and Mn increased over time downgradient the galvanic reactor

The pH was stable over time and over the course of the reactor and no gas evolution was observed. The standard potentials of the electrodes within the galvanic reactor were not measured, but a comparison of standard potentials for corrosion of Fe with those of reduction and oxidation of chlorinated ethenes suggested that reduction was a possibility. Hence, potential differences should always be measured during control testing as an indication of the galvanic abilities of the system. Dismounting of electrodes during control testing may be a precautionary measure.

Acknowledgement

This work was funded by the Innovation Fund Denmark (grant number 5016-00165B), COWIfonden (grant number C-131.01), the Capital Region of Denmark (grant number 14002102), COWI A/S and Technical University of Denmark. A special thanks to Professor Akram Alshawabkeh, Northeastern University, for access to the acrylic column and associated fitted electrodes for customization to comply with the lab work requirements of this study. The sandy sediment was kindly donated by Nymølle Stenindustrier A/S.

References

- [1] B.H. Hyldegaard, R. Jakobsen, E.B. Weeth, N.D. Overheu, D.B. Gent, L.M. Ottosen, Challenges in electrochemical remediation of chlorinated solvents in natural groundwater aquifer settings, *J. Hazard. Mater.* 368 (2019) 680–688. doi:10.1016/j.jhazmat.2018.12.064.
- [2] E. Mattsson, Basic electrochemical concepts, in: E. Mattsson (Ed.), *Basic Corros. Technol. Sci. Eng.*, 2nd ed., The Chameleon Press, Ltd., Wandsworth, 2001: pp. 15–28.
- [3] S.S. Zumdahl, Electrochemistry, in: R.B. Schwartz, C.L. Brooks, A. Galvin (Eds.), *Chem. Princ.*, 6th ed., Houghton Mifflin Company, Boston, Ma, 2009: pp. 472–520.
- [4] L. Rajic, R. Nazari, N. Fallahpour, A.N. Alshawabkeh, Electrochemical degradation of trichloroethylene in aqueous solution by bipolar graphite electrodes, *J. Environ. Chem. Eng.* 4 (2016) 197–202. doi:10.1016/j.jece.2015.10.030.

- [5] L. Rajic, N. Fallahpour, A.N. Alshawabkeh, Impact of electrode sequence on electrochemical removal of trichloroethylene from aqueous solution, *Appl. Catal. B Environ.* 174–175 (2015) 427–434. doi:10.1016/j.apcatb.2015.03.018.
- [6] X. Mao, A. Ciblak, K. Baek, M. Amiri, R. Loch-Caruso, A.N. Alshawabkeh, Optimization of electrochemical dechlorination of trichloroethylene in reducing electrolytes, *Water Res.* 46 (2012) 1847–1857. doi:10.1016/j.watres.2012.01.002.
- [7] P. Sarin, V.L. Snoeyink, J. Bebee, K.K. Jim, M.A. Beckett, W.M. Kriven, J.A. Clement, Iron release from corroded iron pipes in drinking water distribution systems: Effect of dissolved oxygen, *Water Res.* 38 (2004) 1259–1269. doi:10.1016/j.watres.2003.11.022.
- [8] T.M. Vogel, C.S. Criddle, P.L. McCarty, Transformation of halogenated aliphatic compounds, *Environ. Sci. Technol.* 21 (1987) 722–736. doi:10.1021/es00162a001.
- [9] L.M. Ottosen, T.H. Larsen, P.E. Jensen, G.M. Kirkelund, H. Kern-Jespersen, N. Tuxen, B.H. Hyldegaard, Electrokinetics applied in remediation of subsurface soil contaminated with chlorinated ethenes – A review, *Chemosphere.* 235 (2019) 113–125. doi:10.1016/j.chemosphere.2019.06.075.
- [10] V. Sáez, M.D. Esclapez Vicente, Á.J. Frías-Ferrer, P. Bonete, J. González-García, Electrochemical degradation of perchloroethylene in aqueous media: An approach to different strategies, *Water Res.* 43 (2009) 2169–2178. doi:10.1016/j.watres.2009.02.019.
- [11] V.M. Molina, V. Montiel, M. Domínguez, A. Aldaz, Electrolytic synthesis of chloroform from carbon tetrachloride in mild conditions. Laboratory approach, *Electrochem. Commun.* 5 (2003) 246–252. doi:10.1016/S1388-2481(03)00038-9.
- [12] Y. Zhao, H. wei Yang, S. ting Liu, S. Tang, X. mao Wang, Y.F. Xie, Effects of metal ions on disinfection byproduct formation during chlorination of natural organic matter and surrogates, *Chemosphere.* 144 (2016) 1074–1082. doi:10.1016/j.chemosphere.2015.09.095.
- [13] C.I. Chaidou, V.I. Georgakilas, C. Stalikas, M. Saraçi, E.S. Lahaniatis, Formation of chloroform by aqueous chlorination of organic compounds, *Chemosphere.* 39 (1999) 587–594. doi:10.1016/S0045-6535(99)00124-1.
- [14] S. Dobaradaran, H. Lutze, A.H. Mahvi, T.C. Schmidt, Transformation efficiency and formation of transformation products during photochemical degradation of TCE and PCE at micromolar concentrations, *J. Environ. Heal. Sci. Eng.* 12 (2014) 1–10. doi:10.1186/2052-336X-12-16.
- [15] D. Alibegic, S. Tsuneda, A. Hirata, Kinetics of tetrachloroethylene (PCE) gas degradation and by products formation during UV/H₂O₂ treatment in UV-bubble column reactor, *Chem. Eng. Sci.* 56 (2001) 6195–6203. doi:10.1016/S0009-2509(01)00217-2.
- [16] T.H. Wiedemeier, H.S. Rifai, C.J. Newell, J.T. Wilson, Overview of intrinsic bioremediation, in: T.H. Wiedemeier, H.S. Rifai, C.J. Newell, J.T. Wilson (Eds.), *Nat. Attenuation Fuels Chlorinated Solvents Subsurf.*, John Wiley & Sons, Inc., 1999: pp. 162–188. doi:10.1016/S0169-7722(99)00099-6.
- [17] P. Lakshminathiraj, G. Bhaskar Raju, Y. Sakai, Y. Takuma, A. Yamasaki, S. Kato, T. Kojima, Studies on electrochemical detoxification of trichloroethene (TCE) on Ti/IrO₂-Ta₂O₅ electrode from aqueous solution, *Chem. Eng. J.* 198–199 (2012) 211–218. doi:10.1016/j.cej.2012.05.092.
- [18] S.T. Lohner, D. Becker, K.M. Mangold, A. Tiehm, Sequential reductive and oxidative biodegradation of chloroethenes stimulated in a coupled bioelectro-process, *Environ. Sci. Technol.* 45 (2011) 6491–6497. doi:10.1021/es200801r.
- [19] F. Aulenta, A. Canosa, P. Reale, S. Rossetti, S. Panero, M. Majone, Microbial reductive dechlorination of trichloroethene to ethene with electrodes serving as electron donors without the external addition of redox mediators, *Biotechnol. Bioeng.* 103 (2009) 85–91. doi:10.1002/bit.22234.
- [20] A. Tiehm, S.T. Lohner, T. Augenstein, Effects of direct electric current and electrode reactions on vinyl chloride degrading microorganisms, *Electrochim. Acta.* 54 (2009) 3453–3459. doi:10.1016/j.electacta.2009.01.002.
- [21] F. Aulenta, L. Tocca, R. Verdini, P. Reale, M. Majone, Dechlorination of Trichloroethene in a Continuous-Flow Bioelectrochemical Reactor: Effect of Cathode Potential on Rate, Selectivity, and Electron Transfer Mechanisms, *Environ. Sci. Technol.* 45 (2011) 8444–8451. doi:10.1021/es202262y.
- [22] R. Verdini, F. Aulenta, F. de Tora, A. Lai, M. Majone, Relative contribution of set cathode potential and external mass transport on TCE dechlorination in a continuous-flow bioelectrochemical reactor, *Chemosphere.* 136 (2015) 72–78. doi:10.1016/j.chemosphere.2015.03.092.
- [23] A.A. Schiefler, D.J. Tobler, N.D. Overheu, N. Tuxen, Extent of natural attenuation of chlorinated ethenes at a contaminated site in Denmark, *Energy Procedia.* 146 (2018) 188–193. doi:10.1016/j.egypro.2018.07.024.
- [24] W. Zhou, L. Rajic, X. Meng, R. Nazari, Y. Zhao, Y. Wang, J. Gao, Y. Qin, A.N. Alshawabkeh, Efficient H₂O₂ electrogeneration at graphite felt modified via electrode polarity reversal: Utilization for organic pollutants degradation, *Chem. Eng. J.* 364 (2019) 428–439. doi:10.1016/j.cej.2019.01.175.
- [25] P. Vanýsek, Electrochemical series, in: D.R. Lide (Ed.), *CRC Handb. Chem. Phys.*, 85th ed., CRC Press LLC, Boca Raton, FL, 2005: pp. 8:23-8:33.

AWARDS

ELITE RESEARCH TRAVEL GRANT 2018

"The Elite Research travel grant helps very talented PhD students to perform longer-term studies in some of the best research environments in the world." (The Danish Ministry for Higher Education and Science). DTU nominated me for this prestigious research award with the words "In relation to chemistry, geology and hydrology in groundwater aquifers, there is no precedent for Bente's research. Already during the first year of her study, Bente has developed two advanced laboratory set-ups... Bente has acted at the highest professional and creative level within the interdisciplinary research. Bente has shown that her knowledge is alive and can be used for resolute practical solutions, which gives a continuous progression in her research. Bente is outstandingly skilled and has a promising future as a researcher." Thanks to the Danish Ministry for Higher Education and Science for hosting a very successful event and for the award. This achievement is thanks to excellent project settings, which I am very fortunate to be a part of.

Media coverage regarding the granting of the award:

- <http://www.byg.dtu.dk/nyheder/nyhed?id=AF849D53-78E1-4C94-A204-9CC5B3EF5BDF>
- <https://ufm.dk/forskning-og-innovation/forskningsformidling/eliteforsk/prismodtagere/prismodtagere-2018/eliteforsk-rejsesestipendierne-2018/bente-hojlund-hyldegaard>
- <http://www.dtu.dk/nyheder/2018/02/tre-dtu-forskere-modtager-eliteforsk-stipendiater?id=06566e00-d85d-4e0e-a231-8bae9f31143b>
- <https://sn.dk/Soroe/Pris-til-ung-og-lokal-forsker/artikel/728525>
- <https://sn.dk/Soroe/Forskertalent-vil-redde-grundvandet/artikel/730391>
- <https://www.linkedin.com/feed/update/urn:li:activity:6387253399468982273/>
- <https://www.linkedin.com/feed/update/urn:li:activity:6375044729083695104/>
- [https://www.linkedin.com/feed/update/urn:li:activity:6375269284196728832/?commentUrn=urn%3A%3Acomment%3A\(activity%3A6375269284196728832%2C6376183937861058560\)](https://www.linkedin.com/feed/update/urn:li:activity:6375269284196728832/?commentUrn=urn%3A%3Acomment%3A(activity%3A6375269284196728832%2C6376183937861058560))
- <https://theworldnews.net/dk-news/pris-til-ung-og-lokal-forsker>



Søren Pind (left), Minister of Higher Education and Science, Peter Lund Madsen (right), master of ceremony, and me (middle).

BATTELLE PALM PITCH 2018

A pitch event for up-and-coming scientists and engineers at the 'Eleventh International Conference on the Remediation of Chlorinated and Recalcitrant Compounds 2018' with more than 1,000 presentations in 80 breakout sessions and 1800 participants. I pitched my work on 'Electrochemical zone for degradation of chlorinated solvents in aquifers' for which I was recognized as first runner-up. It was a great challenge to narrow down my research to a 90 seconds pitch and I will like to acknowledge Battelle for giving me this opportunity and for the award.

Postings regarding the granting of the award:

- <https://www.linkedin.com/feed/update/urn:li:activity:639017777479401474>



Katie Kucharzyk (left), organizer of the pitch event and me (right).

PRESENTER AWARD, ELECTROCHEMICAL SCIENCE & TECHNOLOGY CONFERENCE 2017

My presentation entitled 'Electrochemically induced reduction and oxidation of chlorinated solvents in groundwater' was elected as best presentation given by PhD fellows and PostDocs at the Electrochemical Science and Technology Conference 2017 (arranged by the Danish Electrochemical Society). Thanks to Danish Electrochemical Society for hosting a very successful conference and for the award.

Postings regarding the granting of the award:

- <http://www.electrochemistry.dk/>
- <https://www.linkedin.com/feed/update/urn:li:activity:6345537433244880896/>

CONFERENCE CONTRIBUTIONS

Design of electrochemical zones for remediation of chlorinated solvents in natural groundwater aquifer settings

Bente Højlund Hansen^{ab*}, Rasmus Jakobsen^c, Eline Begtrup Weeth^a, Niels Døssing Overheu^d, David B. Gent^e, Lisbeth M. Ottosen^b

^a COWI A/S, Department of Waste and Contaminated Sites, DK-2800 Kongens Lyngby, Denmark

^b Technical University of Denmark, Department of Civil Engineering, DK-2800 Kongens Lyngby, Denmark

^c GEUS, Department of Geochemistry, DK-1350 Copenhagen K, Denmark

^d Capital Region of Denmark, Centre for Regional Development, DK-3400 Hillerød, Denmark

^e US Army Corps of Engineers, Engineer Research and Development Center, 39180 Mississippi, United States

*Corresponding author: behd@cowi.com

Chlorinated solvents threatens the quality of groundwater. The widespread contamination by chlorinated solvents is a relic from the past with extensive use of tetrachloroethene (PCE) and trichloroethene (TCE) in e.g. dry-cleaning facilities and metal processing. The chlorinated solvents and their chlorinated degradation products are acute toxic and carcinogenic. Furthermore, the compound's high solubility, volatility and low sorption to sediments challenge the current treatment systems. Thus, optimized means of protecting the groundwater from this group of contaminants is important. Pump-and-treat (P&T) systems are commonly used to keep plumes from reaching water supply wells. However, these treatment facilities are long-term solutions with substantial operation and maintenance requirements.

It is known that i) fast electrochemical reduction of chlorinated solvents near the electrodes can be obtained [1] and ii) reactants can be generated, which can subsequently reduce or oxidize the chlorinated solvents [2]. Thus, without addition of e.g. substrate or generation of waste products like deactivated carbon. Effort has so far mainly been on the influence from electrode materials and configurations [3,4], and the influence of system parameters such as current density, flow rate etc. [5,6]. For example, a system configured with two cathodes and a downstream anode has shown to enhance the removal rates of TCE with achieved removals of 89 % [4]. Further enhancements can be obtained by coating of the cathodes with Pd [4,7].

We propose, as an alternative to P&T, establishment of an electrochemical zone for *in situ* degradation of PCE and degradation products. The focus of this study is on intelligent use and combination of the different electrochemical processes to optimize the electrochemical zone for complete degradation of the chlorinated solvents in natural groundwater settings. Testing in natural groundwater settings is vital for proving the methods applicability. However, so far no studies on electrochemical remediation of chlorinated solvents have been performed under constant current with field extracted contaminated groundwater and unrefined sand as aquifer material.

This study has taken these challenges and developed a system for assessment and optimization of electrochemical zones in an undivided 1D experimental set-up targeting plume control (see Figure 1). The 1D-column set-up allows for assessment of the influence from single parameters, e.g. current density, flow and electrode material.

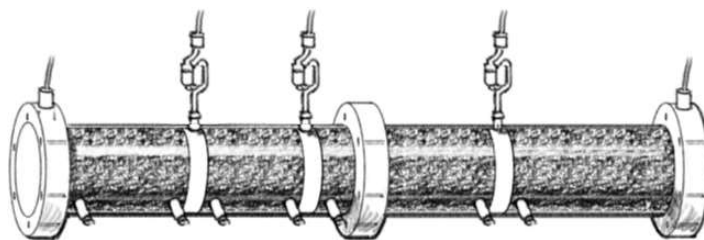


Figure 1. Illustration of the 1D-column set-up designed for tests on electrochemical zones for degradation of chlorinated solvents in plumes.

The set-up replicates natural conditions through flow-through of natural groundwater with an aged contamination of PCE in a sandy aquifer material. Common seepage velocities are applied and the sum of chlorinated solvents in the groundwater at the test site is around 185 $\mu\text{g/l}$.

Acknowledgement

The Innovation Fund Denmark, COWifonden and the Capital Region of Denmark are acknowledged for funding this project.

References

- [1] Wang, J. and Farrell, J. (2003). Investigating the Role of Atomic Hydrogen on Chloroethene Reactions with Iron Using Tafel Analysis and Electrochemical Impedance Spectroscopy, *Environ. Sci. Technol.*, vol. 37, pp. 3891-3896.
- [2] Yuan, S., Mao, X. and Alshawabkeh, A.N. (2012). Efficient Degradation of TCE in Groundwater Using Pd and Electro-generated H_2 and O_2 : A Shift in Pathway from Hydrodechlorination to Oxidation in the Presence of Ferrous Ions, *Environ. Sci. Technol.*, vol. 46, pp. 3398-3405.
- [3] Mao, X., Yuan, S., Fallahpour, N., Ciblak, A., Howard, J., Padilla, I., Loch-Caruso, R. and Alshawabkeh, A.N. (2012). Electrochemically Induced Dual Reactive Barriers for Transformation of TCE and Mixture of Contaminants in Groundwater, *Environ. Sci. Technol.*, vol. 46, pp. 12003-12011.
- [4] Rajic, L., Fallahpour, N. and Alshawabkeh, A.N. (2015). Impact of electrode sequence on electrochemical removal of trichloroethylene from aqueous solution, *Applied Catalysis B: Environmental*, vol. 174-175, pp. 427-434.
- [5] Mao, X., Ciblak, A., Baek, K., Amiri, M., Loch-Caruso, R. and Alshawabkeh, A.N. (2012). Optimization of electrochemical dechlorination of trichloroethylene in reducing electrolytes, *Water Research*, vol. 46, pp. 1847-1857.
- [6] Sáez, V., Esclapez, M.D, Tudela, I., Bonete, P. and González-García, J. (2010). Electrochemical Degradation of Perchloroethylene in Aqueous Media: Influence of Electrochemical Operational Variables in the Viability of the Process, *Ind. Eng. Chem. Res.*, vol. 49, pp. 4123-4131.
- [7] Rajic, L., Fallahpour, N., Podlaha, E. and Alshawabkeh, A. (2016). The influence of cathode material on electrochemical degradation of trichloroethylene in aqueous solution, *Chemosphere*, vol. 147, pp. 98-104.

ELECTROCHEMICALLY INDUCED REDUCTION AND OXIDATION OF CHLORINATED SOLVENTS IN GROUNDWATER

Bente H. Hyldegaard^{1,5}, Eline B. Weeth¹, Rasmus Jakobsen², Niels D. Overheu³, David B. Gent⁴, Lisbeth M. Ottosen⁵

¹*COWI A/S, Denmark, Denmark, behd@cowi.com/ebwe@cowi.com*

²*GEUS, Denmark, raj@geus.dk*

³*Capital Region of Denmark, Denmark, niels.doessing.overheu@regionh.dk*

⁴*U.S. Army Corps of Engineers, USA, David.B.Gent@erdc.dren.mil*

⁵*DTU Civil Engineering, Denmark, benho@byg.dtu.dk/lo@byg.dtu.dk*

Widespread contamination of chlorinated solvents threatens the quality of groundwater based on extensive use in the past for e.g. dry-cleaning and metal processing. The chlorinated solvents and their chlorinated degradation products are acute toxic and carcinogenic. Furthermore, the compound's properties challenge the current treatment systems. Thus, optimized means of protecting the groundwater from this group of contaminants is important. We propose, as an alternative method for remediation, establishment of electrochemical zones for in situ reduction and oxidation of chlorinated solvents and degradation products.

It is known that i) fast electrochemical reduction of chlorinated solvents near the electrodes can be obtained and ii) reactants can be generated, which can subsequently reduce or oxidize the chlorinated solvents. Effort has mainly been on the influence of electrode materials and configurations, and of the system parameters such as current density, flow rate etc. So far no studies on electrochemical remediation of chlorinated solvents have been performed under constant current with field extracted contaminated groundwater and unrefined sand as aquifer material.

This study has taken these challenges and developed systems for assessment and optimization of electrochemical zones in 1D and 2D experimental set-ups targeting plume control. The set-ups allow for assessment of the influence of single parameters, e.g. current density and flow rate, as well as power consumption, lateral dispersion of generated reactants, electrode configuration, material and spacing. For this conference, focus will be on the electrochemical aspects of the method: Electroless plating of cathodes, selective corrosion of anodes, electrocatalytic hydrodechlorination, competing electrochemically induced reduction and oxidation reactions in the complex saturated geochemical settings, polymerisation of methane, electrokinetically enhanced volatilisation of contaminants, and electrocatalysed formation of minerals possibly with reactive properties.

BATTELLE 2018 (Poster and pitch presentation)11th International Conference on Remediation of Chlorinated and Recalcitrant Compounds (USA)

Design and assessment of electrochemical zones for remediation of chlorinated solvents in natural groundwater aquifer settings

Bente H. Hyldegaard (behd@cowi.com) and Eline B. Weeth (COWI A/S, Lyngby, Denmark)

Rasmus Jakobsen (GEUS, Copenhagen, Denmark)

Niels D. Overheu (Capital Region of Denmark, Hillerød, Denmark)

David B. Gent (US Army Corps of Engineers, Vicksburg, MS, USA)

Lisbeth M. Ottosen (Technical University of Denmark, Lyngby, Denmark)

Background/objectives. Widespread contamination of chlorinated solvents threatens the quality of groundwater based on extensive use in the past for e.g. dry-cleaning and metal processing. The chlorinated solvents and their chlorinated degradation products are acute toxic and carcinogenic. Furthermore, the compound's properties challenge the current treatment systems. Pump-and-treat (P&T) systems are commonly used to keep plumes from reaching water supply wells. However, these are long-term solutions with substantial operation and maintenance costs. Thus, optimized means of protecting the groundwater from this group of contaminants is important. We propose, as an alternative to P&T, establishment of an electrochemical zone for *in situ* degradation of chlorinated solvents and degradation products.

Approach/Activities. It is known, that i) fast electrochemical reduction of chlorinated solvents near the electrodes can be obtained and ii) reactants can be generated and subsequently reduce or oxidize the chlorinated solvents, i.e. no need for addition of e.g. substrates. Furthermore, no waste products like deactivated carbon are generated. Studies have so far mainly focused on the influence from electrode materials and configurations, and the influence of system parameters such as current density, flow rate etc. in spiked, synthetic liquid phases only. The focus of this study is on intelligent use and combination of the different electrochemical processes to optimize the electrochemical zone for complete degradation of the chlorinated solvents in natural groundwater settings. Testing in natural groundwater settings is vital for proving the methods applicability. However, so far no studies on electrochemical remediation of chlorinated solvents have been performed under constant current with field extracted contaminated groundwater and unrefined sand as aquifer material.

This study has taken these challenges and developed systems for assessment and optimization of electrochemical zones in 1D and 2D experimental set-ups targeting plume control in field realistic designs. The 2D-box set-up allows for assessment of the influence of single parameters, e.g. current density, flow and electrode material as well as power consumption, lateral dispersion of generated reactants, electrode configuration and spacing. The set-up replicates site conditions through flow-through of natural groundwater with an aged contamination of PCE in a sandy aquifer material at common groundwater flow rates.

Results/Lessons Learned. Initial 1D-column tests revealed a high electrical resistance in the sandy geology, which inhibited the current distribution. Despite the low current level applied, contaminant degradation was observed. The 2D-box set-up has been further developed to overcome the challenges experienced in the column tests. Data expected to be available includes degradation efficiency, induced changes in geochemistry, influence of current density, flow rate and electrode composition on the degradation, and the power consumption of the bench scale electrochemical remediation in near natural settings.

Design and assessment of electrochemical zones for remediation of chlorinated solvents in natural groundwater aquifer settings

Bente H. Hydegaard, COWI & DTU; Eline Weeth, COWI; Rasmus Jakobsen, GEUS; Niels Overheu, Capital Region of Denmark; David Gent, US Army Corps of Engineers; Lisbeth Ottosen, DTU

I Project objectives

- Optimization of electrochemical zone(s) for complete degradation of the harmful chlorinated solvents and their chlorinated degradation products as a precautionary measure


II Motivation

- Chlorinated solvents threatens the quality of groundwater and cause health risks [1]. Consequently, extraction wells for drinking water are closed
- The compounds' properties challenge the current treatment systems
- Commonly used pump-and-treat systems for hydraulic containment are long-term solutions with substantial operation and maintenance costs
- Optimized means of protecting the groundwater from these contaminants are requested. We propose, establishment of electrochemical zones for *in situ* degradation of chlorinated solvents and degradation products.

IV State of the art

- | Reduction | Half-cell reaction [5] | E° [V] |
|-----------|---|--------|
| PCE | $C_2Cl_4 + H^+ + 2e^- \rightarrow C_2HCl_3 + Cl^-$ | 0.43 |
| TCE | $C_2HCl_3 + H^+ + 2e^- \rightarrow C_2H_2Cl_2 + Cl^-$ | 0.42 |
| Cis-DCE | $C_2H_2Cl_2 + H^+ + 2e^- \rightarrow C_2H_3Cl + Cl^-$ | 0.31 |
| VC | $C_2H_3Cl + H^+ + 2e^- \rightarrow C_2H_4 + Cl^-$ | 0.38 |
-
- | Oxidation | Half-cell reaction [5] | E° [V] |
|-----------|---|--------|
| DCE | $C_2H_2Cl_2 + 4H_2O \rightarrow 2CO_2 + 10H^+ + 8e^- + 2Cl^-$ | 0.70 |
| VC | $C_2H_3Cl + 4H_2O \rightarrow 2CO_2 + 11H^+ + 10e^- + Cl^-$ | 0.50 |
- Focus has been on the influence from electrode materials [6, 7, 9] and configurations [7, 8], and of system parameters such as current density [6, 7, 8, 9, 10], flow rate [6, 7] etc. in spiked, synthetic liquid phases
 - Knowledge gaps between state of the art and field implementation:
 - influence of naturally occurring geochemistry and aged contamination at natural groundwater temperatures

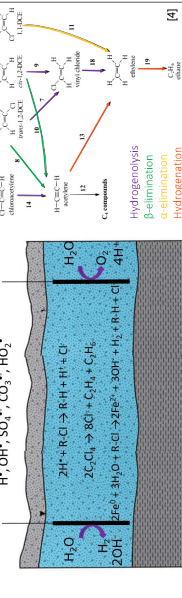
VI The field realistic design

- The field realistic parameters
- | Sampled groundwater | Conc. | Sampled groundwater | Conc. |
|-----------------------------|-------|--------------------------------------|-------|
| PCE [$\mu g/l$] | 40 | Ca ²⁺ [mg/l] | 370 |
| TCE [$\mu g/l$] | 30 | K ⁺ [mg/l] | 4 |
| Cis-1,2-DCE [$\mu g/l$] | 70 | Mg ²⁺ [mg/l] | 30 |
| Trans-1,2-DCE [$\mu g/l$] | 1 | Na ⁺ [mg/l] | 25 |
| VC [$\mu g/l$] | 0.1 | Cl ⁻ [mg/l] | 45 |
| pH [-] | 6.9 | NO ₃ ⁻ [mg/l] | 4.0 |
| Conductivity [mS/cm] | 1.7 | SO ₄ ²⁻ [mg/l] | 400 |
- 

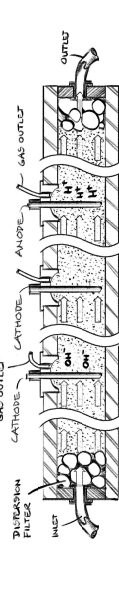
IX Acknowledgement

- This project and conference attendance is funded by
- 

III Relevant chemical processes

- Reactants can be generated and subsequently reduce or oxidize the chlorinated solvents [3] and fast electrochemical reduction of chlorinated solvents near the electrodes can be obtained [2].
- 

V Method

- We have designed 1D and 2D experimental set-ups targeting electrochemical plume control in field realistic designs
 - allows for assessment of single parameters; current density, flow and electrode material, and power consumption, lateral dispersion of reactants, electrode configuration and spacing
 - replicates site conditions: Flow-through of natural groundwater with an aged contamination of PCE in a sandy aquifer material at common groundwater flow rates and temperatures
- 

VII Challenges and opportunities

- Contaminant fate when no current is applied is unexpected; upon test completion, dissolved and gaseous fractions are low. When current is applied, these fractions are high in proportion.
- Alterations in redox conditions induce e.g. deposition and eventually clogging of the pore spaces in the geological matrix. One design solution may be short-term polarity reversal.
- Present geochemistry competes with dechlorination for electrons, e.g. reduction of carbon dioxide to methane followed by polymerization to ethane and oxidative dehydrogenation to ethylene [11]. These hydrocarbons may interfere with the resulting mass balances of dechlorination.
- Some precipitates formed may improve the abiotic dechlorination of chlorinated ethylenes, e.g. magnetite and green rust [12].
- The reduced conditions in the proximity of cathodes visually appear to enhance microbial growth. Dependent on the microbial culture, biodegradation of the chlorinated ethylenes may establish [13].

IX References

[1] B. H. Hydegaard, D. Gent, L. Ottosen, and N. Overheu, "Design and assessment of electrochemical zones for remediation of chlorinated solvents in natural groundwater aquifer settings," in *Proceedings of the 11th International Conference on Electrochemical Remediation Technologies (ELECTROREM 2019)*, vol. 1, pp. 1-10, 2019.

[2] J. L. Korte, "Electrochemical remediation of chlorinated solvents," in *Electrochemical Remediation of Contaminated Soils and Groundwater*, pp. 1-10, 2019.

[3] J. L. Korte, "Electrochemical remediation of chlorinated solvents," in *Electrochemical Remediation of Contaminated Soils and Groundwater*, pp. 1-10, 2019.

[4] J. L. Korte, "Electrochemical remediation of chlorinated solvents," in *Electrochemical Remediation of Contaminated Soils and Groundwater*, pp. 1-10, 2019.

[5] J. L. Korte, "Electrochemical remediation of chlorinated solvents," in *Electrochemical Remediation of Contaminated Soils and Groundwater*, pp. 1-10, 2019.

[6] J. L. Korte, "Electrochemical remediation of chlorinated solvents," in *Electrochemical Remediation of Contaminated Soils and Groundwater*, pp. 1-10, 2019.

[7] J. L. Korte, "Electrochemical remediation of chlorinated solvents," in *Electrochemical Remediation of Contaminated Soils and Groundwater*, pp. 1-10, 2019.

[8] J. L. Korte, "Electrochemical remediation of chlorinated solvents," in *Electrochemical Remediation of Contaminated Soils and Groundwater*, pp. 1-10, 2019.

[9] J. L. Korte, "Electrochemical remediation of chlorinated solvents," in *Electrochemical Remediation of Contaminated Soils and Groundwater*, pp. 1-10, 2019.

[10] J. L. Korte, "Electrochemical remediation of chlorinated solvents," in *Electrochemical Remediation of Contaminated Soils and Groundwater*, pp. 1-10, 2019.

[11] J. L. Korte, "Electrochemical remediation of chlorinated solvents," in *Electrochemical Remediation of Contaminated Soils and Groundwater*, pp. 1-10, 2019.

[12] J. L. Korte, "Electrochemical remediation of chlorinated solvents," in *Electrochemical Remediation of Contaminated Soils and Groundwater*, pp. 1-10, 2019.

[13] J. L. Korte, "Electrochemical remediation of chlorinated solvents," in *Electrochemical Remediation of Contaminated Soils and Groundwater*, pp. 1-10, 2019.

REMTEC 2019 (Poster and pitch presentation)
Remediation Technology Summit (USA)

Electrochemistry as an efficient remedy for tetrachloroethylene plumes

**Bente Højlund Hansen^{ab*}, Eline Begtrup Weeth^a, Rasmus Jakobsen^c, Niels Døssing Overheu^d,
David B. Gent^e, Lisbeth M. Ottosen^b**

^a COWI A/S, Department of Waste and Contaminated Sites, DK-2800 Kongens Lyngby, Denmark

^b Technical University of Denmark, Department of Civil Engineering, DK-2800 Kongens Lyngby, Denmark

^c GEUS, Department of Geochemistry, DK-1350 Copenhagen K, Denmark

^d Capital Region of Denmark, Centre for Regional Development, DK-3400 Hillerød, Denmark

^e US Army Corps of Engineers, Engineer Research and Development Center, 39180 Mississippi, United States

*Corresponding author: behd@cowi.com

Chlorinated ethenes are more frequently detected above regulatory levels in groundwater aquifers and current remedies are insufficient. With electrochemical remediation, i) fast reduction of chlorinated ethenes near the electrodes can be obtained and ii) reactants can be generated, which can subsequently reduce or oxidize the chlorinated ethenes. This study aims at filling in the major knowledge gaps that exist between state-of-the-art and application of electrochemistry for in situ remediation of high-permeability zones at chlorinated ethene contaminated sites.

A stepwise approach to assessing the significance of natural hydrogeochemistry at common groundwater temperatures on the electrochemical transformation of tetrachloroethylene is applied using a column reactor being adapted to field-settings. Degradation pathways, air stripping and power consumption are amongst the parameters addressed.

Electrochemistry is gaining increasing attention for remediation of contaminated sites, but the method needs to be significantly matured. This applied research brings valuable and relevant insight to the method towards field-demonstration.

KJUL & CO
TASK FORCE ENGINEERING

* COWI & Technical University of Denmark, Parallelvej 2, 2800 Kgs. Lyngby, Denmark. Phone: +45 56 40 87 70. E-mail: behd@cowi.com

Investigation of electrochemistry as a remedy for tetrachloroethylene plumes

Bente Højlund Hyldegaard^{1,2}; Akram Alshawabkeh³; Eline B. Weeth¹; Rasmus Jakobsen⁴; Niels D. Overheu⁵; David B. Gent⁶; Lisbeth M. Ottosen²

¹COWI; ²Technical University of Denmark; ³Northeastern University; ⁴GEUS; ⁵Capital Region of Denmark; ⁶US Army Corps of Engineers

Chlorinated ethene contamination of the subsurface is extensive and harmful. Effort has been put into remediation of the low-permeable zones, where electrokinetics in combination with more traditional remedies have shown to overcome some of the challenges experienced. With a more frequent detection of chlorinated ethenes above the regulatory levels in groundwater aquifers, attempts are now being made to adapt the promising mechanisms of electrokinetics towards remediation of high-permeable zones. Electrochemical remediation is one alternative for in-situ degradation of chlorinated ethene plumes, where i) fast electrochemical reduction of chlorinated ethenes near the electrodes can be obtained [1] and ii) reactants can be generated, which can subsequently reduce or oxidize the chlorinated ethenes [2]. Focus has been on electrochemical degradation of trichloroethylene in simplified laboratory set-ups. Hence, it is necessary to assess the potential of electrochemical remediation of tetrachloroethylene (PCE) to cover the full range of chlorinated ethenes detected at contaminated sites, and to incorporate field-site characteristics in the assessment. This study aims at filling in some of the knowledge gaps that exist on application of electrokinetics for remediation of high-permeability zones at chlorinated ethene contaminated sites.

The performance of electrochemical remediation of PCE is evaluated using a flow-through column reactor with a three-electrode configuration. The significance of electrode configuration and spacing, current intensity and catalyst concentration is assessed. In addition, the influence of a porous matrix, flow rate and orientation of the reactor is examined to simulate field conditions and field-realistic designs. The two-dimensional distribution of the electric field in a sandy geology and the influence of the current intensity on this distribution is assessed in a box set-up. The column and box set-ups are furthermore used for investigation of changes in hydrogeochemistry prompted by the electric field applied.

In the initial screening of electrochemical remediation of PCE in a flow-through reactor, 86% removal was obtained. The results showed, that a 50% increase in catalyst concentration on the cathode improved the removal with 36%-point, while a 60% increase in electrode spacing enhanced the removal with 13%-point due to extension of the redox zones. An inert porous matrix was found to enhance PCE removal with 24%-point compared to a fully water-filled reactor and the horizontal orientation accounted for another 9-16% increase in removal. The observed trends are promising when considering the installation and cost of field-implementations.

- [1] Wang, J., Farrell, J. (2003). Investigating the Role of Atomic Hydrogen on Chloroethene Reactions with Iron Using Tafel Analysis and Electrochemical Impedance Spectroscopy, *Environ. Sci. Technol.* 37, 3891-3896.
- [2] Yuan, S., Mao, X., Alshawabkeh, A.N. (2012). Efficient Degradation of TCE in Groundwater Using Pd and Electro-generated H₂ and O₂: A Shift in Pathway from Hydrodechlorination to Oxidation in the Presence of Ferrous Ions, *Environ. Sci. Technol.* 46, 3398-3405.

Harmful chlorinated ethenes are contaminating the groundwater and if used for drinking water, these contaminants constitute a health risk. Protection of the drinking water resource from chlorinated ethenes by establishment of electrochemical zones was investigated. To evaluate the potential of application of electrochemical remediation, three electrochemical flow-through reactors were designed. These reactors were used in the assessment of influence of various design and field-realistic parameters on the electrochemical degradation of the chlorinated ethenes. Also, the electrochemically induced changes in the natural hydrogeochemistry were investigated. The findings were used to mature the electrochemical method towards in situ field-application. Low contaminant concentrations were reached with the electrochemical method in complex field-realistic systems. This research demonstrates innovative aspects in the challenging field of remediation of sites contaminated with chlorinated ethenes as well as a potential of upscaling the method towards field-implementation.

DTU Civil Engineering

Brovej 118
2800 Kongens Lyngby
Tel. 45251700

www.byg.dtu.dk

87-7877-522-1